

EFFECT OF COSOLVENTS AND IONS ON
THE STABILITY OF AMINO ACIDS,
PEPTIDES AND SELF-ASSEMBLED
PEPTIDE-BASED NANOTUBES

Thesis

Submitted in partial fulfilment of the requirements for the
degree of

DOCTOR OF PHILOSOPHY

by

DILIP.H.N

(165025CY16F01)



DEPARTMENT OF CHEMISTRY
NATIONAL INSTITUTE OF TECHNOLOGY KARNATAKA,
SURATHKAL, MANGALURU – 575025
JULY, 2021

DECLARATION

I hereby declare that the Research Thesis entitled “**Effect of Cosolvents and Ions on the Stability of Amino acids, Peptides and Self-assembled Peptide-based Nanotubes**” which is being submitted to the National Institute of Technology Karnataka, Surathkal in partial fulfilment of the requirements for the award of the degree of **Doctor of Philosophy** in Chemistry is a *bonafide report of the research work carried out by me*. The material contained in this Research Thesis has not been submitted to any University or Institution for the award of any degree.

Dilip.H.N

Reg.No. 165025CY16F01

Department of Chemistry

Place: NITK, Surathkal

Date: 11/08/2021

CERTIFICATE

This is to *certify* that the Research Thesis entitled “**Effect of Cosolvents and Ions on the Stability of Amino acids, Peptides and Self-assembled Peptide-based Nanotubes**” submitted by **Dilip.H.N (Register Number: 165025CY16F01)** as the record of the research work carried out by him, is *accepted as the Research Thesis submission* in partial fulfilment of the requirements for the award of degree of **Doctor of Philosophy**.

Dr. Debashree Chakraborty
Research Guide

Chairman - DRPC
Date: 11/08/2021

This thesis is dedicated to my beloved Parents

ACKNOWLEDGEMENTS

I express my deep sense of gratitude to my research supervisor Dr. Debashree Chakraborty, Assistant Professor, Department of Chemistry, NITK, for giving me an opportunity to pursue my research work under her valuable guidance. This thesis would not have been possible without her supervision and persistence.

I genuinely acknowledge NITK, Surathkal for providing the research fellowship, laboratory facilities and financial support necessary for the completion of my doctoral research work.

My sincere gratitude is due towards my RPAC members, Dr. Ambar Chitharanjan Hegde of Chemistry Department and Dr. Keyur Raval of Chemical Engineering for their timely assessment and evaluation of my research progress. Their valuable inputs at various stages of my work have contributed immensely in giving the final shape to my research work.

I am grateful to the present Head of the Department, Dr. Arun M. Isloor and former Heads of the Department, Dr. D. Krishna Bhat and Dr. B. Ramachandra Bhat for providing the administrative facilities and infrastructure. I am also thankful to other faculties of our department Dr. A. Vasudeva Adhikari, Dr. A. Nithyananda Shetty, Dr. D. Udayakumar, Dr. Darshak R. Trivedi, Dr. Sib Sankar Mal, Dr. Beneesh P.B., Dr. Saikat Dutta, Dr. Vijayendra S. Shetti, Dr. Lakshmi Vellanki along with faculty of Computer Science & Engineering department Dr. Basavaraj Talawar for their assistance and moral support.

I sincerely thank all my lab members- Bratin, Pushyraga, Omkar for their constant help and support at every stage of my research work. I would like to extend my deep sense of appreciation and hearty thanks to all my seniors and colleagues within and outside the department for their valuable help at each and every stage during this journey and for cherishable moments. I owe a deep sense of gratitude and also would like to specially thank all my other seniors, friends, professionals and well-wishers within the country and abroad who have genuinely helped and guided me in tough times during this entire course of research work.

I am grateful to all the non-teaching staffs of our department for their timely cooperation and help during my research.

I am highly indebted to my beloved parents and my brother for their everlasting faith in me which has been the backbone of my hard work and patience. Finally, I extend my sincere thanks to all those who have contributed directly or indirectly towards the completion of this work.

Thank you.

Dilip.H.N.

ABSTRACT

There lies a major challenge in molecular biophysics towards understanding the various biophysical processes and molecular dynamics (MD) simulations have been an imperative tool in elucidating it at the molecular level. In many biological processes, water plays a crucial role as a basic solvent. The existence of biological water in the vicinity of biomolecules has profound implications and is particularly important for the structural and biological functions of the biomolecules. The functioning of these biomolecules emerges from the delicate balance between various interactions of biomolecules with the solvent environment. This balance can be modulated by the addition of ions and small molecules known as cosolvents. Molecular-level understanding of how these cosolvents affect the solvation shell near the biomolecules is important for understanding the factors affecting the stability of proteins.

The presence of both hydrophilic and hydrophobic moieties in amino acids facilitates its use as surfactant-like peptides which can be designed into well-defined nanostructures. These peptide nanostructures have wide applications in the bio-medical field. The water molecules near these nanostructures behave differently from the structural and dynamic point of view.

In this context, the present research work is focused on investigating the effect of cosolvents and ions on the solvation structure of amino acids and peptides which results in the stability/de-stability of proteins. Studies were done on water molecules present near the interface and bulk region of these biomolecules and peptide nanotubes.

Keywords: MD simulation, amino acids, peptides, surfactant-like peptide nanotubes, biomolecular solvation, water, osmolytes, ions.

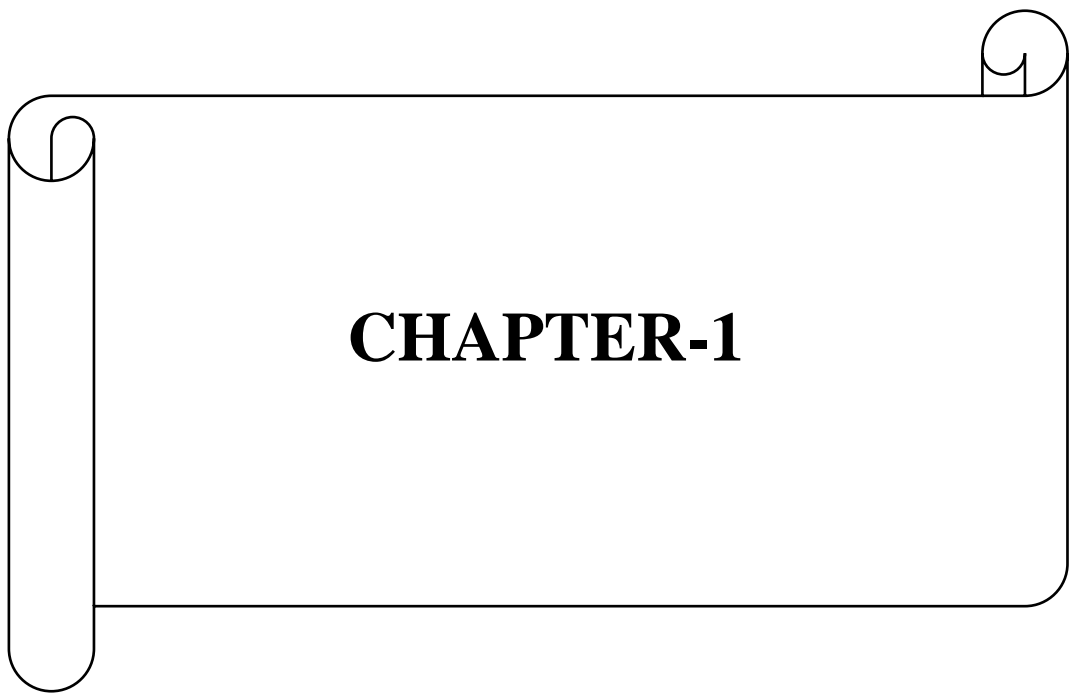
INDEX

CONTENTS	Page No.
CHAPTER 1 - INTRODUCTION	
1.1 PERSPECTIVE OF MOLECULAR DYNAMICS SIMULATIONS	01
1.2 THEORETICAL BACKGROUND	
1.2.1 Integrator Algorithms	05
1.2.2 Force Fields, Inter-atomic Interactions and Water Models	05
1.2.3 Periodic Boundary Conditions and Ewald's Summation	06
1.2.4 Thermostats and Barostats	06
1.3 SIMULATION OF BIOMOLECULES	07
1.4 SOLVATION OF BIOMOLECULES	07
1.5 AMINO ACIDS, PEPTIDES AND ITS CLASSIFICATION	08
1.6 EFFECTS OF COSOLVENTS ON AQUEOUS SOLUTION OF BIOMOLECULES	12
1.7 REVIEWS FROM LITERATURES SUPPORTING THE PRESENT WORK	16
1.8 SCOPE AND OBJECTIVES OF THE PRESENT WORK	23
CHAPTER 2 - INFLUENCE OF OSMOLYTES AND IONS ON THE HYDROPHOBIC GROUP OF GLYCINE AMINO ACID	
2.1 INTRODUCTION	25
2.2 COMPUTATIONAL METHODOLOGY	29
2.3. RESULTS AND DISCUSSION	
2.3.1 Radial Distribution Functions	31
2.3.2 Spatial Distribution Functions	37

2.3.3 Number of Hydrogen-bonded Water Molecules	38
2.3.4 Orientation Profile	41
2.3.5 Potential Mean Force	44
2.3.6 Hydrogen Bond Dynamics	47
2.4. SUMMARY AND CONCLUSIONS	49
CHAPTER 3 - ALANINE AND ITS HYDRATION IN PRESENCE OF UREA AND TMAO	
3.1 INTRODUCTION	51
3.2 COMPUTATIONAL METHODOLOGY	54
3.3. RESULTS AND DISCUSSION	
3.3.1 Radial Distribution Functions	57
3.3.2 Spatial Distribution Functions	63
3.3.3 Number of Hydrogen-bonded Water Molecules	64
3.3.4 Orientation Profile	66
3.3.5 Potential Mean Force	67
3.3.6 Kirkwood-Buff Integrals	69
3.3.7 Preferential Binding Coefficient	71
3.3.8 Hydrogen Bond Dynamics	73
3.4. SUMMARY AND CONCLUSIONS	74
CHAPTER 4 - SOLVATION STRUCTURE OF N-METHYL ACETAMIDE AND ACETAMIDE IN PRESENCE OF OSMOLYTES	
4.1 INTRODUCTION	77
4.2 COMPUTATIONAL METHODOLOGY	79
4.3. RESULTS AND DISCUSSION	

4.3.1 Radial Distribution Functions	82
4.3.2 Spatial Distribution Functions	84
4.3.3 Number of Hydrogen-bonded Water Molecules	86
4.3.4 Orientation Profile	88
4.3.5 Potential Mean Force	90
4.3.6 Preferential Binding Coefficient	96
4.3.7 Hydrogen Bond Dynamics	98
4.4. SUMMARY AND CONCLUSIONS	99
CHAPTER 5 - STRUCTURAL AND DYNAMIC PROPERTIES OF WATER IN PRE-ASSEMBLED PEPTIDE-BASED NANOTUBES: EFFECT OF TUBE LENGTH AND CHARGE REGULATION	
5.1 INTRODUCTION	101
5.2 COMPUTATIONAL METHODOLOGY	105
5.3. RESULTS AND DISCUSSION	
5.3.1 Radial Distribution Functions	113
5.3.2 Density Profile Distributions	115
5.3.3 Number of Hydrogen Bonds	116
5.3.4 Translational Tetrahedral Order Parameter	120
5.3.5 Orientation Profile	121
5.3.6 Hydrogen Bond Dynamics	123
5.4. SUMMARY AND CONCLUSIONS	126
CHAPTER 6 - SUMMARY AND CONCLUSIONS	
6.1 SUMMARY	129
6.2 CONCLUSIONS	130

REFERENCES	133
LIST OF PUBLICATIONS AND CONFERENCES ATTENDED	165
BIODATA	167



CHAPTER-1

CHAPTER 1

INTRODUCTION

Abstract: *This introductory chapter presents the significance of present research work on molecular dynamics simulations of amino acids and peptides in the presence of cosolvents (osmolytes and ions). It includes a general introduction and theory of molecular dynamics simulations. It also gives a brief classification and details of amino acids, peptides, its solvation effects with its importance in biological, medicinal fields and its applications along with a concise literature survey.*

1.1 PERSPECTIVE OF MOLECULAR DYNAMICS SIMULATIONS

“Everything that living things do can be reduced to wiggling and jiggling of atoms.”

- Richard Feynman (1963)

Molecular Dynamics (MD) simulations method is one of the most prominent tools in the theoretical study of biomolecules. It is a computer simulation technique in which the time evolution properties of a system of interacting particles are calculated by integrating their equations of motion. The potential energies and forces between the particles are calculated using inter-atomic potentials. The corresponding macroscopic properties of the system are calculated by averaging and sampling the long trajectories sufficiently.

MD simulation techniques can be used in two different perspectives. Firstly, it can be used to interpret the experimental results if the properties of the experimental results can be reproduced by simulation models. Secondly, and most importantly it can give possible observations and mechanism of a physical process which is hard to observe experimentally. Computer simulations play a pivotal role in providing essentially exact results for problems in dynamics, statistical mechanics. These results obtained from computer simulations can be compared with that of experimental results. In Figure 1.1 the role of computer simulations is illustrated. Computer simulations can be used to test an underlying model, its prediction with the experimental fact and eventually, if a good model is developed, it helps the simulator to pitch insights to the experimentalists by assisting them in the interpretation of results. It can be used for understanding unknown facts which are not accessible or described by the experiments. Due to this interconnecting act, the simulations protocols that are conducted and

analyzed, are often termed as “computer experiments”. Simulations provide a direct route of understanding of the microscopic details of a system to the macroscopic properties of interest in the experiments.

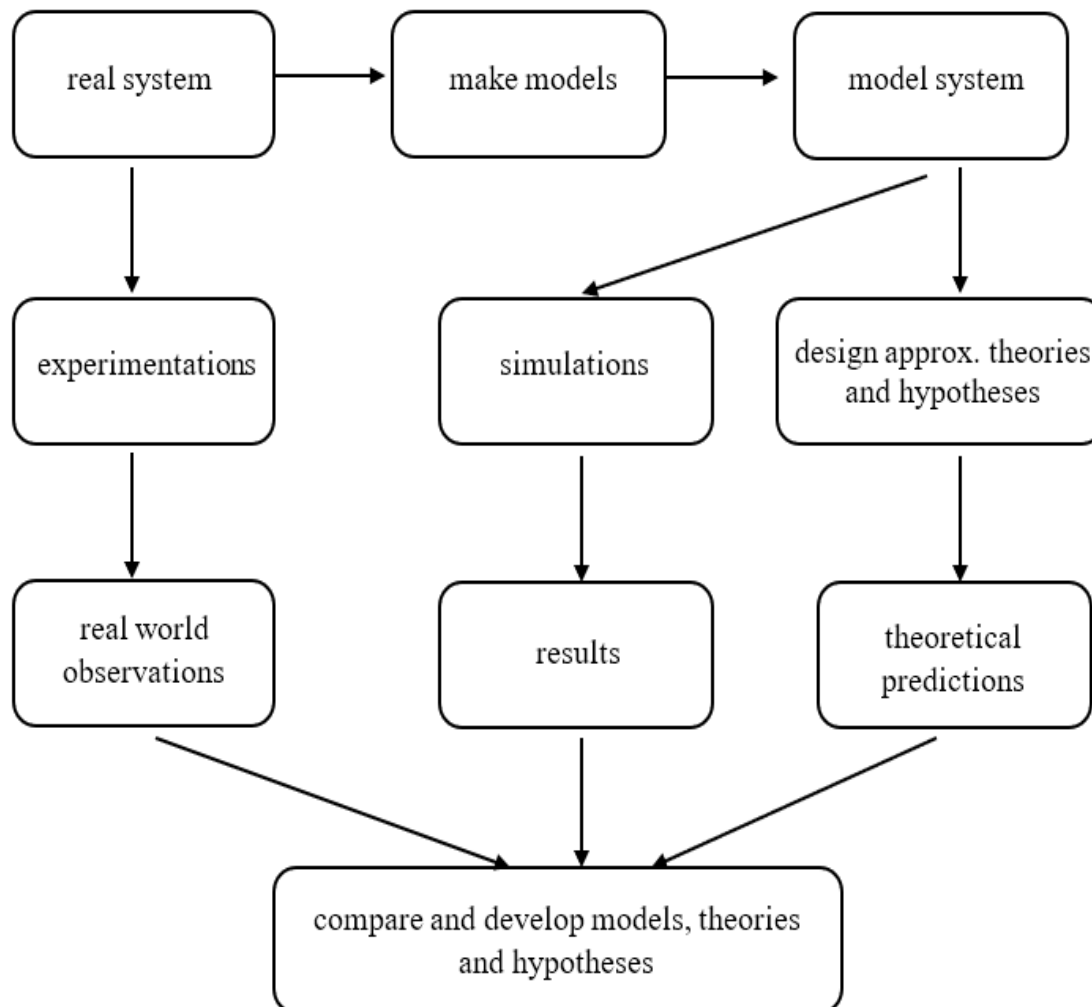


Figure 1.1: The connection between experiment, theory and computer simulation (Source: Computer Simulation of Liquids-Allen and Tildesley 1987).

The earliest of these computations was first introduced by Alder and Wainwright in the late 1950's (Alder and Wainwright 1959, 1960) for the interaction studies of hard spheres. Rahman carried out the first simulation using a realistic potential for liquid argon (Rahman 1964). Since then, step by step foundation was led to MD simulations (Allen and Tildesley 1989; Verlet 1967, 1968). The first MD simulation on liquid water with revised potential was done by Stillinger and Rahman in 1974 (Stillinger and Rahman 1974a; b). These simulations were extended to polyatomic molecules such as hydrocarbons and even proteins (McCammon and Karplus 1977). In the literature today, one can routinely find MD simulations of protein-DNA complexes, solvated

proteins, lipid systems etc., addressing the diverse issues such as protein folding, thermodynamics of protein-ligand binding and many more. The general simulation technique covers a range of time scale from femtoseconds to milliseconds, from atoms to macromolecular aggregates. A number of new specialized simulation techniques have been incorporated such as mixed quantum mechanical-molecular simulations (QM/MM techniques), which are being employed to study problems of biological processes in bigger systems for example enzymatic reactions, protein-ligand interactions (Elstner et al. 2003; Senn and Thiel 2007a; b; Vidossich and Magistrato 2014). Extensive use of MD simulation techniques is also used in interpretation of experimental procedures such as X-ray crystallography and NMR structure determination.

1.2 THEORETICAL BACKGROUND

“It is nice to know that the computer understands the problem. But I would like to understand it, too.”
- Eugene Wigner

In MD simulation technique the time evolution of a set of atoms is followed by integrating Newton’s equation of motion which follows the laws of classical mechanics, and most notably Newton’s second law:

$$\mathbf{F}_i = m_i \mathbf{a}_i \quad (1.1)$$

where, m_i is the mass of the atom, $\mathbf{a}_i = \frac{d^2\mathbf{r}_i}{dt^2}$ is the acceleration and \mathbf{F}_i is the force acting upon it, due to the interaction with other atoms for each atom i in a system consisting of N atoms.

The particle’s acceleration is equal to the force acting on it divided by its mass. The velocities and the positions of particles are updated by integrating the above equation over short time steps as time evolves. The forces of interactions between the particles are modeled by force fields or through quantum chemical calculations which constitute set of parameters and potential functions.

1.2.1 Integrator Algorithms

The force in terms of the gradient of the potential energy is expressed as,

$$\mathbf{F}_i = -\nabla_i V \quad (1.2)$$

From the above equations 1.1 and 1.2,

$$-\frac{dV}{dr_i} = m_i \frac{d^2 r_i}{dt^2} \quad (1.3)$$

A direct solution to equation (1.3) is given by Verlet algorithm (Allen and Tildesley 1989).

$$\mathbf{r}(t + \delta t) = 2\mathbf{r}(t) - \mathbf{r}(t - \delta t) + \mathbf{a}(t)\delta t^2 \quad (1.4)$$

The Verlet integration algorithm uses accelerations at time t and the positions from time $t-\delta t$ to calculate new positions at time $t+\delta t$ given by Taylor expansion series.

To improve the algorithm, certain modifications to Verlet integrator have been done by integration over half time step. The other two integrators which have been developed are leap-frog and velocity-Verlet algorithms (Allen and Tildesley 1989).

The leap-frog method, produces the position r at integer time steps and the velocity v at half integer time steps so that r and v jump over each other like leapfrog

$$\mathbf{r}(t + \delta t) = \mathbf{r}(t) + \mathbf{v}\left(t + \frac{1}{2}\delta t\right)\delta t \quad (1.5)$$

$$\mathbf{v}\left(t + \frac{1}{2}\delta t\right) = \mathbf{v}\left(t - \frac{1}{2}\delta t\right) + \mathbf{a}(t)\delta t \quad (1.6)$$

The velocity at integer time step is obtained as an average so that the kinetic energy can be evaluated at the same instant as other physical quantities.

$$\mathbf{v}(t) = \frac{1}{2}[\mathbf{v}\left(t + \frac{1}{2}\delta t\right) + \mathbf{v}\left(t - \frac{1}{2}\delta t\right)] \quad (1.7)$$

The velocity-Verlet algorithm gives both position \mathbf{r} and velocity \mathbf{v} at integer time steps, through the intermediate velocity at half integer time step

$$\mathbf{r}(t + \delta t) = \mathbf{r}(t) + \mathbf{v}(t)\delta t + \frac{1}{2}\mathbf{a}(t)\delta t^2 \quad (1.8)$$

$$\mathbf{v}(t + \delta t) = \mathbf{v}(t) + \frac{1}{2}[\mathbf{a}(t) + \mathbf{a}(t + \delta t)]\delta t \quad (1.9)$$

This algorithm requires storage of $\mathbf{r}(t)$, $\mathbf{v}(t)$ and $\mathbf{a}(t)$. The implementation is done in two stages-

$$\mathbf{v}\left(t + \frac{1}{2}\delta t\right) = \mathbf{v}\left(t + \frac{1}{2}\delta t\right) + \mathbf{a}(t)\delta t \quad (1.10)$$

$$\mathbf{v}(t + \delta t) = \mathbf{v}\left(t + \frac{1}{2}\delta t\right) + \frac{1}{2}\mathbf{a}[t + (t + \delta t)]\delta t \quad (1.11)$$

First, the velocities at half integer time steps are updated and then the positions, forces and velocities at time $t+\delta t$ are computed.

1.2.2 Force Fields, Inter-atomic Interactions and Water Models

A force field (energy functions or inter-atomic potentials) refers to a set of predefined potential functions and parameters that calculates the potential energy of a system. The potential energy can be decomposed into two terms; bonded and non-bonded. Bonded term consists of contributions from angles, bonds, dihedral angles and improper dihedral angles. Non-bonded terms constitute the electrostatic and non-electrostatic forces of interactions.

The general form for the total energy in a force field is given by

$$E_{\text{total}} = E_{\text{bonded}} + E_{\text{non-bonded}} \quad (1.12)$$

where, $E_{\text{bonded}} = E_{\text{bond}} + E_{\text{angle}} + E_{\text{dihedral}}$ and $E_{\text{non-bonded}} = E_{\text{non-electrostatic}} + E_{\text{electrostatic}}$

Bonded interactions occur between atoms that are interlinked through bonds. The angle bending and bond stretching are usually approximated by harmonic functions with a potential minimum at their reference bond length and angle. Conformations of the molecules are determined by the dihedral angles and the rotations of these angles have much lower frequencies compared to the frequencies corresponding to the vibrations of bonds.

Non-bonded interactions between a pair of atoms are described by the sum of electrostatic and van der Waal's potentials. The electrostatic potential is modelled by the coulombic interactions which is given by

$$V_c(r_{ij}) = \frac{q_i q_j}{4\pi\epsilon_0 r_{ij}} \quad (1.13)$$

where, r_{ij} represents the distance between two atoms having charges q_i and q_j and ϵ_0 represent the dielectric constant.

The van der Waal's interaction is modelled by the L-J potential which is given by

$$V_{LJ}(r_{ij}) = 4\epsilon_{ij} \left[\left(\frac{\sigma}{r_{ij}} \right)^{12} - \left(\frac{\sigma}{r_{ij}} \right)^6 \right] \quad (1.14)$$

where r_{ij} is the distance between a pair of atoms i and j , ϵ is the depth of the potential well, σ is the finite distance at which the inter-particle potential is zero.

Many force-fields have been modeled for treating different kinds of systems of various degrees of complexities. Some examples of the force fields are- AMBER (Assisted Model Building with Energy Refinement) (Cornell et al. 1995), CHARMM

(Chemistry at HARvard Macromolecular Mechanics) (Best et al. 2012), GROMOS (GRoningen MOlecular Simulation program package), OPLS (Optimized Potentials for Liquid Simulations) (Jorgensen and Tirado-Rives 1988).

Different water models are tailored for various force fields. Many simulations and theoretical investigations on the water structure of different models have been developed with varying the parameters such as charges and interactions. They are classified based on number of interacting sites and flexibility. Most commonly used are SPC (Simple Point Charge) (Berendsen et al. 1981), SPC/E (Simple Point Charge-Extended) (Berendsen et al. 1987), TIP3P, TIP4P (Transferable Intermolecular Potentials) (Jorgensen and Madura 1983) water models. SPC and its extended version SPC/E are widely used due to their simplicity and computational efficiency.

1.2.3 Periodic Boundary Conditions and Ewald's Summation

Periodic boundary conditions (PBC) are applied to bridge the gap between microscopic system and macroscopic world, which allows replicating the unit cell of the system in three dimensions with its periodic images to reasonably model an infinite system. The primary and the image cells have the same number, position and momentum of atoms. The system is considered as one-unit cell of an infinite periodic lattice and its electrostatic long-range interactions potentials can be expressed by Ewald summation (Ewald 1921). This summation method has reasonable speed and accuracy in computation. To calculate the total coulombic interaction accurately, this method requires charge neutrality of the molecular system. In order to improve the performance of the conventional Ewald summation, the Particle Mesh Ewald (PME) method (Darden et al. 1993; Essmann et al. 1995) was developed. This PME method has been widely used in large-scale MD simulations due to its higher efficiency.

1.2.4 Thermostats and Barostats

Integrating the equations of motion of an isolated system through any of the integrator algorithms will lead to conservation of energy which is within the accuracy of the algorithms which gives rise to NVE or microcanonical ensemble, where the number of particles (N), volume of the simulation box (V) and energy (E) remains constant during simulation. This is not suitable in majority of experiments which encompasses pressure and temperature parameters. Hence modifications in the integrators are needed which

includes the influence of external pressure and temperature by introducing barostats and thermostats by which isothermal-isobaric (NPT) ensembles or canonical (NVT) ensembles are generated.

Berendsen thermostat gives reasonable temperature coupling scheme which slowly corrects the temperature T to the prescribed value T_0 (Berendsen 1999). This coupling is adopted due to its ease in implementation and simplicity. Though this coupling scheme is simple and effective, there is a need of more accurate coupling algorithms which can generate the correct ensembles for small systems (Berendsen et al. 1984; Fogarty et al. 2010; Gao et al. 2016). In such cases, the extended-ensemble coupling methods are better choices, namely the Parrinello-Rahman barostat (Nosé and Klein 1983; Parrinello and Rahman 1981) and Nosé-Hoover thermostat (Hoover 1985; Nosé 1984).

1.3 SIMULATION OF BIOMOLECULES

Simulation approaches are notably relevant for the studies of structural and dynamics aspects of biomolecular systems. MD simulation techniques have gained enormous attention since they overcome the experimental limitations of biomolecular workings at spatial and temporal resolution by serving as a computational microscope. It is one of the significant tools which is used to study the properties of biomolecules such as amino acids, peptides, proteins and their interactions with solvents, cosolvents, ions in full atomistic detail and in fine timescales (femtoseconds) resolutions. This constitutes simulations, a powerful tool for the studies of the biomolecular dynamics.

1.4 SOLVATION OF BIOMOLECULES

Study of solvation of biomolecules is of great importance for understanding the biochemical processes and the factors effecting it. The structural and functional properties of biomolecules are modified due to their interactions with the water molecules which consequently internally alter the water-water interactions. Aqueous solutions of biomolecules show variations in their physical and chemical properties due to change in external or internal conditions of the systems. There lie many challenges in understanding the complexity of the aqueous biological systems along with their dependencies on the chemical compositions. Results reported from various

experimental studies on the stability of biomolecules in different concentration of aqueous salt solutions and in various chemical environments (Baldwin 1996; Collins 1995; Dill and Shortle 1991; Hofmeister 1888a) often fail to give molecular level understanding of the mechanisms which underlie behind some processes. Simulations of biomolecules can provide physical explanations about these biological processes.

1.5 AMINO ACIDS, PEPTIDES AND ITS CLASSIFICATION

Amino acids are the basic building blocks of proteins. A better understanding of their properties gives greater insights on the properties of larger biomolecules such as peptides and proteins. Several important functions of peptides and proteins depend on the structure and chemical behaviour of the amino acids. Studying their physical and chemical properties as individual entities has attracted a lot of attention especially in aqueous media and also in presence of other cosolvents or ions. This helps in understanding the solvent effect on the stability and folding process of larger biomolecules.

Amino acids have viable importance in biological systems. These molecules are amphoteric (can act either as an acid or as a base) in nature. They possess both acidic carboxylic acid group and basic amine group within the same molecule and hence can afford the basic linkages leading to formation of complex peptides and proteins. All the 20 amino acids that appear in genetic code, comprise of at least one amino group ($-NH_2$), one carbon atom (C) attached to a carboxyl group ($-COOH$) and some groups of atoms (R) which give unique characters to amino acids. In aqueous solutions they occur in zwitterionic form. The general structure of amino acid is given in Figure 1.2.

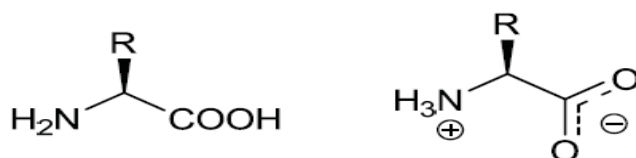


Figure 1.2: General structure of amino acid (left) and its zwitterionic form (right).

Peptides are formed through the linking of two or more amino acids forming peptide bonds. Peptide bonds are formed between molecules when the carboxylate group of one amino acid bonds to the amino group of the other amino acid as shown in Figure 1.3. Proteins are essentially very large peptides formed by joining many amino acids.



Figure 1.3: General mechanism of peptide bond formation between amino acids.

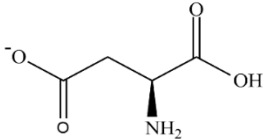
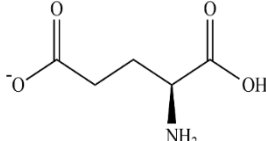
As it is discussed, amino acids contain more than one group, based on that their properties they can be differentiated as ‘hydrophobic’ and ‘hydrophilic’ molecules.

- Hydrophobic amino acids:- These water-hating molecules can be further divided according to the presence of aliphatic or aromatic side chains.
- Hydrophilic amino acids:- These water-loving molecules are surrounded by water. They participate in hydrogen bonding with water molecules and also with their side chains or with other biomolecules. Some of these carry a charge at typical biological pH's (pH=7). For example, arginine, lysine are positively charged; glutamate, aspartate are negatively charged; other polar amino acids such as, serine, glutamine, asparagine, histidine, threonine and tyrosine are neutral.

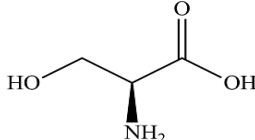
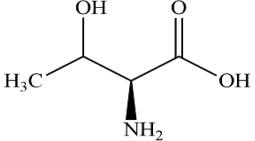
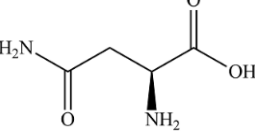
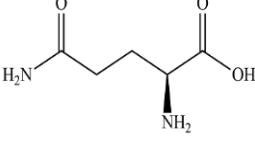
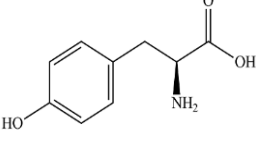
Amino acids can also be classified based on the presence of charged and uncharged side chains.

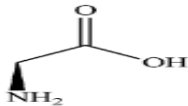
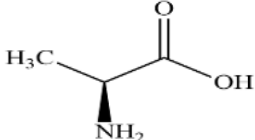
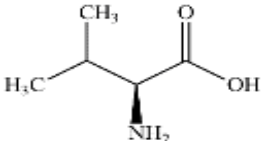
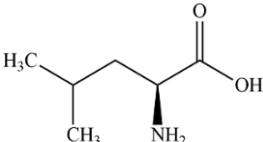
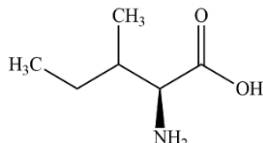
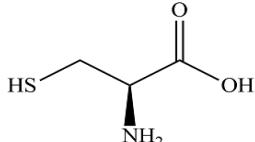
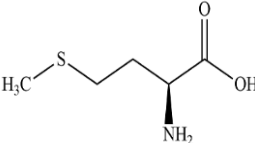
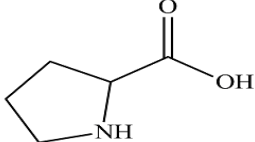
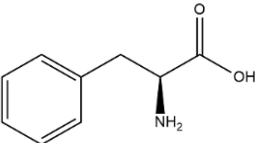
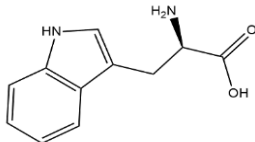
➤ Amino acids with charged side chains

Basic Side Chains			
Name	Abbreviations		Structural Representation
Lysine	Lys	K	
Arginine	Arg	R	
Histidine	His	H	

Acidic Side Chains			
Name	Abbreviations		Structural Representation
Aspartic Acid	Asp	D	
Glutamic Acid	Glu	E	

➤ Amino acids with uncharged side chains

Polar Side Chains			
Name	Abbreviations		Structural Representation
Serine	Ser	S	
Threonine	Thr	T	
Asparagine	Asn	N	
Glutamine	Gln	Q	
Tyrosine	Tyr	Y	

Non-Polar Side Chains			
Name	Abbreviations		Structural Representation
Glycine	Gly	G	
Alanine	Ala	A	
Valine	Val	V	
Leucine	Leu	L	
Isoleucine	Ile	I	
Cystine	Cys	C	
Methionine	Met	M	
Proline	Pro	P	
Phenylalanine	Phe	F	
Tryptophan	Trp	W	

Peptides are further subdivided into oligopeptides and polypeptides. Oligopeptides comprises of few amino acid residues (e.g., 2 to 20) and polypeptides comprises of higher molecular weight peptides. Peptides include many antibiotics, hormones and other substances that involve in the biological functions of the living beings.

1.6 EFFECTS OF COSOLVENTS ON AQUEOUS SOLUTION OF BIOMOLECULES

Water is undoubtedly the most familiar liquid to humanity. It is also a liquid that continues to be the subject of intense study due to its anomalies (Brovchenko and Oleinikova 2008; Chaplin 2001) making it a complex liquid. The dynamics of water around biomolecules is non-uniform and complex (Frank and Evans 1945). Hydration plays an active role in biological processes such as ligand binding, protein folding, maintenance of structural integrity of biomolecules. The role of water in influencing the structure and function of biomolecules and their dependency on the chemical compositions of solutions are often challenging which are not yet completely understood. Vast studies have been done on the peculiar properties of the hydration layer via numerous techniques such as neutron scattering (Fenimore et al. 2004; Svergun et al. 1998), THz spectroscopy (Born et al. 2009), NMR (Bryant 1996; Halle 2004), time-resolved fluorescence (Pal et al. 2002; Zhang et al. 2007) and also in simulations (Chakraborty et al. 2015; Pizzitutti et al. 2007; Priyadarshini et al. 2020; Schröder et al. 2006; Tarek and Tobias 2000; Xu and Berne 2001).

Biomolecules naturally exists in the environment of aqueous saline solutions. Salt solutions and electrolytes dissolve in water and dissociate into ions which affect the electrostatic interactions (Collins 2004; Collins et al. 2007; Shao et al. 2011) or charge-charge interactions (Debye and Hückel 1923) of the solution. Interactions between biomolecules and ions in aqueous solutions plays a pivotal role in many biochemical and biophysical processes such as salting-in and salting-out, enzymatic activity, protein crystallization etc. The properties of the solvation layer are affected by the concentration and nature of both cation and anion of the electrolyte, as well as the structural characteristics of biomolecules. The solvation structure altered in the presence of ions, indirectly affects the solubility of the biomolecules. Factors affecting the solubility of biomolecular species are: concentration of electrolyte in biomolecular

solutions (Kamali-Ardakani, et al. 2001), ionic strengths (Held et al. 2011), polarity of the solvents (Dolui et al. 2008), temperatures (Ferreira et al. 2009; Romero and Oviedo 2013), acidity or alkalinity of the media (Lu et al. 2006; Pradhan and Vera 1998) and ionic interactions (Hassan 2005; Tomé et al. 2012). These can alter the thermodynamics of solvation significantly. Both the solubility and thermodynamics of solvation of these biomolecules in aqueous solutions play an important role in many biochemical and biophysical processes such as enzymatic activity, protein crystallization etc. The addition of salts changes the solubility and the orientation of the biomolecules. These changes in turn affects the hydrophobic interactions and various dipole-dipole interactions between solute-solute, solute-solvent and solvent-solvent, thereby modifying the structure of proteins (Drabik et al. 2001; Friedman 2011; Friedman et al. 2005).

Cosolvents are small molecules which alters the solubility and stability of the system when added in limited quantities to aqueous biomolecular solutions. These includes alcohols, osmolyte protectants (e.g., trimethylamine-N-oxide), protein denaturants (e.g., urea, guanidinium chloride), ions or electrolytes etc. They modulate the functions and stability of biomolecules by interfering their hydrophobic, hydrophilic interactions and aqueous solubility in the system. In aqueous media, concentrations of these cosolvents strongly change the microscopic (diffusion constant, kinetic energy, hydrogen bond dynamics etc.) and macroscopic (density, viscosity, volume etc.) properties of the solution. Many cosolvents are found to aggregate, misfold, stabilize or disaggregate proteins depending on their interactions and binding with various groups of a protein which includes hydrophobic side chains of amino acid residues and peptide backbones (Auton et al. 2011; Li et al. 2011; Liu and Bolen 1995; Moeser and Horinek 2014; Tanford 1962). They also influence the thermodynamic stability of amino acids and peptides (Cacace et al. 1997; Collins and Washabaugh 1985; Robinson and Jencks 1965; Von Hippel 1969). The cells of environmentally stressed organisms accumulate small, soluble organic molecules in order to compensate for stress factors such as high temperature, dehydration and osmotic pressure (Yancey 2005) which are termed as osmolytes. Under harsh environmental conditions, these osmolytes tends to protect native proteins from denaturation and increase thermodynamic stability of folded proteins (Yancey et al. 1982a). They have also been useful in decreasing the damage to biomolecules at lower temperatures and stabilizing

native protein structures during freezing. Some amino acids also act as natural osmolytes (Yancey 2001) by stabilizing the proteins such as proline (Arakawa and Timasheff 1985; Kar and Kishore 2007; Wang and Bolen 1996). The influence of commonly available osmolytes especially trimethylamine-*N*-oxide (TMAO) [(CH₃)₃NO] and urea [(NH₂)₂CO] have attracted attention due to their importance in many biological processes. Osmolytes such as glycerol, betaine, sugars, TMAO plays an important role in stabilizing the folded state of proteins and are described as osmoprotectants (Auton and Bolen 2004; Kumar and Kishore 2014; Vagenende et al. 2009). Conversely, guanidinium chloride and urea favour the unfolded states and are described as denaturants (Lim et al. 2009; Stumpe and Grubmüller 2007). Certain marine creatures have adapted to life in saline water and high pressures with the help of osmolytes to maintain buoyancy and cellular volume (Withers et al. 1994; Yancey et al. 1982b). TMAO, betaine act as protective osmolytes by counteracting the denaturing effects of urea (Barton et al. 1999). The functioning, stability and activity of biomolecules are strongly affected by the presence of osmolytes and hence they are of great biological relevance (Canchi and García 2013). Osmolytes differ in their nature depending on the conditions of solvent, temperature, pH, solute concentrations and also on the presence of other osmolytes. The behaviours of osmolytes are different in dilute and in concentrated solutions. They also vary from one protein to another. For e.g., at pH lower than pK_a for lysozyme, glycine betaine denatures α -lactoalbumin (Singh et al. 2009) and TMAO which is generally a stabiliser of protein, denatures prion protein at room temperature and also acts as a destabilizer at low pH (Granata et al. 2006).

Presence of both hydrophobic and hydrophilic moieties in the amino acids facilitates its use as surfactant-like peptides (SLP's). Peptide-based surfactants deserves particular consideration these days due to their environment friendly, low toxicity, antimicrobial activity and excellent emulsifying properties. Different combination of amino acids in the formation of peptides affects the morphology of the nanostructures formed due to different physiochemical properties of the resultant peptides (Ghosh et al. 2012; Goldberger et al. 2011; Makovitzki et al. 2008; da Silva et al. 2016; Xu et al. 2010b; Zhao et al. 2010). The shape and size of the aggregates depends on the ionic strength, temperature, surfactant concentration, charge and also on the nature of the solvent. Solvent as a medium can strongly influence the self-assembly of surfactant-like peptides (SLP's) via the specific intermolecular interactions between solute and

solvent. Its ability to dissolve solutes, viscosity, polarity and hydrogen bonding effect can affect the chirality and formation of the nanostructures. The formation of chiral nanostructures of glutamide amphiphiles are triggered due to the addition of water in trace amount to organic solvents (Liu et al. 2014). Upon addition of water, nanofibrous structures evolved into helical nanostructures in polar solvents; whereas helical tube structures are found to produce in nonpolar solvents. Based on the solvent polarity, diverse nanostructures (nanofibers, microtubes) can be obtained. Various nanostructures such as microtube, nanotube, nanotwist and nanofiber were obtained in presence of solvents DMSO, DMF, chloroform and toluene respectively (Jin et al. 2013). Simplest peptide, diphenylalanine which is capable of forming self-assembly complexes, tends to form nanotube, long fibrils and microcrystals in pure water, toluene and ethanol respectively (Kim et al. 2010; Zhu et al. 2010). The supramolecular self-assembly is therefore, found to be dominated by solvent-driven morphological transitions in mixtures of cosolvents (Mao et al. 2014).

Peptide-based nanostructures exhibit distinct behaviours under varying conditions such as pH, temperature and electrolytes which affects the process of self-assembly. This is because the changes in hydrogen bonds due to pH fluctuations or addition of electrolytes which influences the peptide structures (Khandogin et al. 2006; Toksoz et al. 2011). Peptide amphiphiles (PA's) of different charge are reported to self-assembled into nanofibers over a wide range of pH (Cote et al. 2014; Niece et al. 2003). The positive, negative and oppositely charged PA's are self-assembled in basic, acidic and neutral pH respectively. The formation of PA's are also dependent on the weak noncovalent interactions such as van der Waals interactions, hydrophobic and electrostatic interactions (Cavalli et al. 2010; Fu et al. 2013; Hamley 2011; Ulijn and Smith 2008). These peptide-based self-assembly provides a novel and powerful bottom-up approach for the fabrication of materials with well-defined nanostructures and unique functions. The self-assembly mechanisms have not yet elucidated completely but the driving forces responsible for establishing the intermolecular connections have been studied (Qiu et al. 2018). These forces enable the formation of nanoscale assemblies and larger aggregates. Understanding of molecular-level description of these nanostructures along with their intermolecular interactions with the effect of the solvent have become important to design and model the nanostructures of choice and of biological importance. In this respect, MD simulation becomes an important tool to

understand this molecular nature of the forces and their resultant behaviour.

1.7 REVIEWS FROM LITERATURES DONE ON SYSTEMS STUDIED IN THE WORK

In this section, a brief review of the literature on the MD simulations studies of aqueous amino acids and peptides in presence of cosolvents (osmolytes and ions) along with work on studies of surfactant-like peptide (SLP) based nanostructures have been discussed.

The following literatures are regarding the studies of aqueous amino acids and effects of ions on these solutions. Campo *et.al.* studied the structural modifications of aqueous zwitterionic glycine, the simplest amino acid, with increase in NaCl salt concentration via MD simulation (Campo 2006). This amino acid showed hydrophilic character at infinite dilution through establishing six hydrogen bonds with surrounding water molecules forming a strong hydration layer. Increase in concentrations of glycine leads to more compact hydration shell of water molecules and decreases the water molecules bound to glycine. Chlorine ion binds to the amine group whereas sodium ion binds to the carboxyl group of amino acid. The addition of ions alters the regular water-water orientational correlation. The diffusion coefficient of solute and number of water-water hydrogen bonds decreases with increase in concentration of the ions. The solvation shells and interfacial water molecules in aqueous solution of glycine amino acid were studied by Jian Sun and his group (Sun et al. 2010) via *ab initio* molecular dynamics. Structural aspects of the different solvation shells of the zwitterion and their impact on the infrared spectrum were analyzed. It was found that the average number of water molecules around the ammonium group was three, whereas; the carboxylate group were solvated asymmetrically, with total of 4.4 water molecules in the first shell.

Mason *et. al.* examined the interactions of ammonium functionalities in aqueous amino acids with iodide and fluoride ions through MD simulations (Mason et al. 2010). The systems considered was ammonium ion (NH_4^+), glycine ammonium group (Gly-NH_3^+) and alkyl ammonium side chain of lysine (Lys-NH_3^+). Iodide showed a constant affinity for all three ammonium moieties, whereas the interaction of fluoride ions showed the following order- $\text{NH}_4^+ > \text{Lys-NH}_3^+ > \text{Gly-NH}_3^+$.

Heyda and his group investigated the ion-specific interactions between basic amino acids (lysine, arginine, histidine) and halides (F^- , Cl^- , Br^- , I^-) in aqueous solutions

(Heyda et al. 2009). The affinity of fluoride towards positively charged groups follows the order guanidinium>imidazolium>ammonium. Larger ions such as iodide, bromide and chloride are weakly attracted towards nonpolar regions of amino acids. Both polarizable and nonpolarizable force fields show the same ion-specific behaviour in the vicinity of basic amino acids.

Hassan investigated the effect of salts on the intermolecular interactions of amino acids side chains through MD simulations (Hassan 2005). Potentials of mean forces were calculated for NaCl salt in 0-2 M concentration range at 298 K. The addition of salt may either increase or decrease the strength of interactions depending on the nature of interacting molecules. Their results show that a critical balance of solvent forces operates on the solutes in the concentration range studied. The changes observed in the solvent forces occur when regions of high solvent density develop between the solutes as they dissociate. Contributions from both bulk and interfacial interactions plays a significant role in the intermolecular potentials. At higher salt concentrations the contributions from interfacial interactions determine the outcomes of stabilization. The significance of these conclusions on the mechanisms of protein association or dissociation processes have also been discussed.

The effect of ions on the structure of water has been studied by Hribar and his group (Hribar et al. 2002). Ion-water pair distribution was studied considering different cations and anions such as (Li^+ , Na^+ , Cs^+ , F^- , Cl^- , I^-). Monte Carlo (MC) simulations were carried with the incorporation of the MB (Mercedes Benz) water model. The results show that the interactions of water and ions are governed by charge densities. A fine balance between hydrogen bonding and electrostatic force determines the water structure. Smaller ions (kosmotropes) cause strong electrostatic ordering of nearby waters molecules due to high charge densities whereas the surrounding water molecules are largely hydrogen-bonded in case of larger ions (chaotropes) due to low charge densities.

Tomé *et al.* (Tomé et al. 2010) studied the solubility of amino acids such as alanine, isoleucine, valine and 2-aminodecanoic acid in the presence of aqueous inorganic salt solutions of NaClO_4 , Na_2SO_4 , NaCl , NaNO_3 and KCl . The radial distribution functions and coordination numbers show significant interactions of ClO_4^- with the apolar part of the amino acids, which is missing in presence of SO_4^{2-} ions. With increase in amino acid side chains, the preference of perchlorate ion for apolar moieties

and the lyophobicity of the sulphate ion increases linearly which results in stronger induced salting-in and salting-out effects by these ions respectively. Chloride ion showed the least significant interactions. This molecular-level mechanism helps in understanding the stability and solubility behaviour of the biomolecules in saline environments. They also studied the effect of the polyvalent cations on the solubility of these amino acids (Tomé et al. 2015). Their results indicate that the solubility of amino acids (salting-in) is affected by the polyvalent cations. The strongly hydrated polyvalent cations form charged complexes with the amino acids rather than establishing direct interactions with the nonpolar moieties; whereas weakly hydrated singly charged cations do not interact with the nonpolar moieties of amino acids and are neither capable of complex formation since they are ruled by mechanism by which salting-out anions operate.

They further investigated the interactions between ionic liquids and zwitterionic amino acids in aqueous media (Tomé et al. 2009). The influence of ionic liquid, 1-butyl-3-methylimidazolium with aqueous amino acids in presence of tricyanomethane was studied to find the preferential interactions between these three compounds. The effects of salting-in and salting-out were explained in terms direct or indirect (water-mediated) interactions of the ionic liquid and the amino acids.

Next, literatures on the study of peptides in presence of different cosolvents are discussed. The role of water in influencing the structural properties of N-methylacetamide (NMA) as a model peptide has been studied by Susan Allison and his co-workers (Allison et al. 2006) via classical MD simulations with varying concentration at 308 K. Their results show a significant change in water structures in aqueous NMA as compared to pure water. In lower concentrations, the water molecules form string-like networks with one donated and one accepted hydrogen bonds instead of the ideal four-coordinated network structure. At higher concentrations, water molecules form linear clusters. The addition of water molecules to pure NMA tends to break the latter's linear intermolecular hydrogen-bonds and forms 'bridged' hydrogen-bonds between NMA molecules.

Chowdhuri and his group (Pattanayak and Chowdhuri 2011) studied the effect of ionic and neutral solutes on the structure and dynamics of aqueous NMA environment. Simulations were carried out with compositions varying from pure water to pure NMA. Their results showed the preference of water molecules towards the ions

compared to NMA, irrespective of the size and charge of the ions. On the other hand, methyl groups of NMA were solvated more by the neutral solutes. The self-diffusion coefficient of solvent molecules decreased initially and then increased with increase in the ion compositions. Water molecules diffused faster compared to NMA molecules in all compositions due to the smaller size of the former. Further, they investigated the effects of alcohol (methanol) and organic molecule (dimethyl sulfoxide (DMSO)) on the hydrogen bonding structure and dynamics of NMA (Chand and Chowdhuri 2016; Pattanayak and Chowdhuri 2014). Methyl-methyl interactions between NMA molecules was found to exist even at lower concentrations of the cosolvents. The dynamic properties such as hydrogen-bond lifetimes and structural-relaxation times between the donor-acceptor moieties was reported to increase with the increase in cosolvent concentrations.

The effects of chaotrope cosolvent dimethyl sulfoxide (DMSO) and kosmotrope cosolvent glycerol on the structure and dynamics of N-acetyl-leucine-methyl amide (NALMA) were studied by Johnson and his group (Johnson et al. 2010). The results reveal that the water structure near the peptide interface shows an increase in hydration number in presence of glycerol whereas the hydration number decreases in presence of DMSO solution. The water dynamics is slower in presence of cosolvents as compared to the aqueous peptide solution. Glycerol keeps the protein structure hydrated and reproduces the dynamic signatures observed in aqueous peptide solution, on the other hand, DMSO restricts the accessibility of water near the hydrophobic regions of the peptide surface which results in disruption of dynamic properties of water.

Lei *et al.* investigated the structure and hydrogen bonding properties of aqueous N,N-dimethylformamide (DMF) solutions with varying concentrations by MD simulations (Lei et al. 2003). DMF enhances the water structure in dilute concentrations by tending to coalesce with water clusters through strong O-H...O hydrogen bonds, but further increase in concentrations leads to disruption of the tetrahedral structure of water. At low concentration, the hydration of the C-H group of DMF occurs through the weak C-H...O hydrogen bonds to bring on the change in the polarization of DMF solutes as well as surrounding water molecules.

The effects of the osmolytes as cosolvents on the structural and functional properties of biomolecules have been studied in vast detail. Soyoung Lee and his co-workers (Lee et al. 2010) carried out volumetric studies of urea interactions with protein

groups. The partial molar volumes and adiabatic compressibilities of N-acetyl amino acid, methyl amides, oligoglycines, N-acetyl amino acid amides and N-acetyl amino acids at different concentrations of urea ranging from 0M to 8M were investigated. Results were analyzed in terms of statistical thermodynamic formalism and equilibrium constants. It was found that urea molecules bind with each of the functionalities by replacing two molecules of water. The obtained results support the direct interaction mechanism in which the protein denaturation by urea is done via favourable solute-cosolvent interactions.

Stumpe and Grubmüller studied the interactions of urea with all 20 amino acids (Stumpe and Grubmüller 2007). Amino acids except ASP and GLU showed higher preferential interaction with water than urea. In general, urea preferentially solvates aromatic and polar residues as well as peptide backbones. It was found that protein-water and water-water hydrogen bonds were stronger compared to protein-urea hydrogen bonds. Their results implicate that the denaturation power of urea lies in the fine balance between its two features. First, its polar nature which is capable of forming weak hydrogen bonds with the protein backbone and second its apolar nature which is enough to solvate non-polar groups. Thus, the denaturation of protein by urea is done through interfacing between water and buried parts of the native protein.

Hua *et. al.* investigated the denaturation mechanism of hen lysozyme protein by urea by all-atom MD dynamics simulations of (Hua et al. 2008). The urea-induced denaturation proceeds through a 2-stage process which includes structural and kinetic stage. In the structural stage, the water molecules are displaced by urea within the first solvation shell of the protein. This results in higher binding of urea molecules with protein surface through greater favourable interactions and the formation of stronger hydrogen bonds with the peptide backbone. In the kinetic stage, the exposed polar, hydrophobic and charged residues are solvated by water and urea. Since, there is a large increase in the accessible surface area of hydrophobic residues during the unfolding process, dramatic changes in the interaction energies of the protein and the water molecules were observed. This study supports the direct interaction mechanism of urea denaturation through stronger dispersion interaction with protein as compared to water.

Molecular basis of chemical denaturation of chymotrypsin inhibitor 2 by urea at 8M concentration and 60°C was investigated by Bennion and his group (Bennion and Daggett 2003). Under these conditions, the unfolding of protein took place rapidly,

whereas in pure water the native structure was retained. The overall unfolding process by urea was found to be similar to the thermal denaturation of proteins observed in simulations above the protein's T_m of 75°C. Denatured structures at high temperature and in urea contained the same native residual helical structure, but complete disruption of the β -sheets was observed. The structure and dynamics of water were altered by urea resulting in enhancement of the solvation of the hydrophobic groups. Since, urea weakens the structure of water, the latter becomes free and competes with intra-protein interactions. The non-native conformations are stabilized by indirect interaction of urea with the peptide backbone and the polar residues. These results suggest that the denaturation of proteins is possible via both direct and indirect mechanisms.

Zou *et. al.* studied the thermodynamics of interaction between TMAO and protein functional groups (Zou et al. 2002). Free energy of the amide unit (-CONH-) when transferred from water to 1 M TMAO was found to be large and positive, indicating an unfavourable interaction between the amide unit and the TMAO solution which is enthalpic in nature. Favourable interactions were observed between TMAO and apolar groups. Their simulations result showed enhancement in the water structure by TMAO with respect to the formation of stronger hydrogen bonds, increase in number of hydrogen bonds per water molecule. Based on these findings they suggest that the stabilization of proteins by TMAO is via enhancement of water structure.

To study the mechanistic counteraction effects of urea by TMAO, Meersman and his group (Meersman et al. 2009) carried out isotopic substitution neutron-scattering measurements on aqueous solutions of TMAO and 1:1 TMAO-urea at a solute mole fraction of 0.05. The obtained results were compared with the results obtained with isosteric tert-butanol, along with spectroscopic data and the MD simulations. In aqueous solution, the oxygen atom of TMAO is strongly hydrogen-bonded on an average of two to three water molecules which suggests stronger hydrogen-bond network as compared to pure water. In mixed urea-TMAO solutions, the oxygen atom of TMAO forms hydrogen bonds with urea counteracting the effect of urea at 2:1 ratio of urea:TMAO.

The influence of osmolytes, urea and TMAO on the hydrophobic interactions of aqueous neopentane solutions were studied by Patey and his group (Paul and Patey 2007b, 2008) employing MD simulations. The addition of TMAO completely destroys the hydrophobic attraction between neopentane pairs in aqueous and its ternary

solutions. TMAO replaces water molecules from the first solvation shell of neopentane and hence acts as a simple surfactant. The elimination of hydrophobic attraction is likely due to surfactant like influence of TMAO. Their results emphasize on the fact that TMAO do not counteract the denaturing effect of urea on proteins by enhancing hydrophobic attraction among the nonpolar groups.

The applications of amino acids and peptides in various forms of nanostructures by mimicking the traditional surfactants have been addressed by many researchers. Andrade *et al.* reported the pre-organized SLP nanofibers using both NVT and NPT ensembles with amino acids linked in two different primary sequences NH₂-G₃A₃V₃I₃K₃-COOH and NH₂-K₃I₃V₃A₃G₃-COOH (Andrade et al. 2020). Analysis of coulombic and vdW interactions, hydrogen bonds and the role of each amino acid group on the stability of nanofibers were reported in this study. These nanofibers maintained their diameters despite of having significant volume of water molecules inside these nanostructures, indicating that these nanostructures behave like hydrogels which have various biotechnology applications. Self-assembly of peptides into cylindrical nanoscale fibers in aqueous solutions can be used to promote the growth of blood vessels, for regeneration of bone and cartilage tissues, to heal critical wounds, and other functions.

The structural and energetic properties of A_NK nanostructures have been investigated by Colherinhas and his group (Colherinhas and Fileti 2014a) via MD simulations. Self-assembled A₃K membrane, A₆K nanotube and A₉K nanorod were considered for the studies. Two different configurations were observed with A₃K membranes- namely, A₃K_C which had peptides tilted relative to the normal membrane plane and A₃K_T where the peptides were interlocked. A₆K and A₉K nanostructures have properties of hydrogels. Stable nanotube and nanorod structures were preferentially formed by A₆K and A₉K peptides respectively.

The regulation of size and charge on the self-assembled nanostructures of peptide amphiphiles (PA's) were investigated by Zaldivar and his co-workers (Zaldivar et al. 2019). Combinations of experimental (TEM, AFM), acid-base titrations and theoretical modelling studies were carried out on molecular structures of C₁₆K₂ and C₁₆K₃. A good agreement was shown between experimental data and theoretical predictions for the size of the nano assemblies and pH-dependent morphologies. Two important effects were associated with the mechanism of charge regulation. First, the

ionic strength which leads to aggregation with salt concentrations and second, the aggregation number which decreases with increase in charge per PA due to increase in electrostatic repulsions and increase in steric repulsions.

Nagai *et al.* investigated the dynamic behaviour of A₆D and A₆K nanotubes (Nagai *et al.* 2007). Dynamic light scattering method was used to determine the critical aggregation concentration (CAC) of the self-assemblies and Atomic Force Microscopic (AFM) studies were done to observe the nanostructures. Small vesicles or micelles are formed below the CAC. Structural transitions of assemblies occur above the CAC of SLP in both aqueous and phosphate buffered saline (PBS) solutions with increase in peptide concentration. The changes in the diameter of assemblies can be related to packing densities of the vesicle tubes.

von Maltzahn *et al.* designed a new type of surfactant peptide to mimic the cationic lipid systems properties (von Maltzahn *et al.* 2003). They constitute a cationic hydrophilic head with lysine or histidine and hydrophobic tail with six valine, leucine or alanine residues. Two distinct structural populations with average diameters of 50 nm (>95%) and 100-200 nm (<5%) was observed by dynamic light scattering at pH below the pI values of the peptides. The visualization of the samples done by electron microscopy revealed the presence of nanovesicles and nanotubes. These structures were absent above the pI. These cationic surfactant peptides have many applications such as the delivery of several small water-insoluble molecules, carriers for encapsulation.

Santoso *et al.* examined the self-assembly of SLP's with varying glycine tails forming nanovesicles and nanotubes (Santoso *et al.* 2002). SLP's containing 4-10 glycine as hydrophobic tails component and aspartic acids as the hydrophilic head component were studied. As the length of hydrophobic tail increases, these nanostructures become more polydisperse in nature due to increased flexibility of the longer glycine tails. The structures have dimensions in the range of 40-80 nm in size as revealed by dynamic light scattering method. These unique structures can serve as bridges for constructing diverse nanodevices and encapsulate rudimentary enzymes for the prebiotic molecular evolution studies.

1.8 SCOPE AND OBJECTIVES OF THE PRESENT WORK

From the literature survey, it is evident that many studies have been done to study the mechanism of denaturation by urea, stabilization by TMAO, counteracting effects of

urea by TMAO in a mixed urea-TMAO mixture, effects of ions on the solvation structure of water in presence of biomolecules. Both urea and concentrated salt solutions are found to denature protein solutions; whereas TMAO stabilizes it. Therefore, it would be interesting to study and explain the stabilization and destabilization of proteins by cosolvents and ions by a common theory. In this thesis, the effect of cosolvents (ions and osmolytes) on the solvation structure, dynamics and hydrophobicity of the amino acids and peptides has been investigated. Also, the hydration structure and dynamics of water molecules present inside and outside the hydrophobic core of self-assembled SLP based nanostructures having different length and pore size in presence of ions is studied to have an overview of the basic forces stabilizing them.

Based on the above-mentioned facts and thorough literature survey, the following main objectives have been intended in the research work.

- To investigate the effect of cosolvents on the different sub-units of amino acids and peptides to explain the elementary forces responsible for protein stability.
- To study the structural properties of cosolvents and water molecules near the interface and bulk of biomolecules.
- To evaluate the effect of cosolvents on the thermodynamic properties of aqueous amino acids and peptides through Potential Mean Force (PMF) and Kirkwood-Buff (KB) Integrals.
- To study the preferential binding coefficient of water, cosolvents with biomolecules and relate them with the stability of proteins.
- To examine the influence of cosolvents on the hydrogen bond dynamics of the aqueous biomolecules.
- To study the structural and dynamics properties of water molecules inside and outside the pore of SLP nanotubes with varying core size and tube length.
- To investigate the effect of charge and ion size on the structural and dynamic properties of peptide-water and water-water interactions in the pre-assembled SLP nanotubes.



CHAPTER-2

CHAPTER 2

INFLUENCE OF OSMOLYTES AND IONS ON THE HYDROPHOBIC GROUP OF GLYCINE AMINO ACID

Abstract: *This chapter includes classical molecular dynamics simulations to study the effect of cosolvents and ions on the solvation structure of zwitterionic glycine in liquid water. Simulations were carried out for 2 M and 1 M concentrations of urea, TMAO, KCl and LiCl solutions to observe the changes in liquid structure of water near the glycine molecule. Investigations on the structural and dynamic properties near the interface and bulk water molecules are calculated through radial distribution functions, spatial distribution functions, number of hydrogen bonds, potential of mean force, orientation profile and hydrogen bond dynamics.*

2.1 INTRODUCTION

Water is a dynamic and unquestionably a complex liquid. It consists of micro-domains which results in anomalous properties due to its existence of high-density water (HDW, density 1.2 g/ml) and low-density water (LDW, density 0.91 g/ml) (Mishima and Stanley 1998; Nilsson and Pettersson 2015; Poole et al. 1992; Vedamuthu et al. 1994; Wallqvist and Åstrand 1995; Woutersen 1997). These micro-domains can be induced due to the presence of hydrophobic and hydrophilic group in the protein moieties (Schoenborn 1995; Teeter 1991). Since proteins have both hydrophobic and hydrophilic moieties, they can easily modify the structure of the adjacent solvent layer which in turn changes the properties of the biomolecules. The dynamics of water around biomolecules is complex and non-uniform (Nucci et al. 2011). The surface water near the protein molecules mainly gets perturbed compared to the bulk due to the changes in the hydrogen bonding network. The associated distortions and loss of tetrahedral symmetry of the interfacial water molecules in turn affect the dynamic properties. It was observed that there is a decrease in entropy and enthalpy when water was mixed with hydrophobic molecules due to enhanced ordering of the solvation water (Frank and Evans 1945). Direct experimental proof of enhanced ordering is very difficult to get as important details of dynamic behaviour is masked by both time-averaged and spatially averaged measurements.

The dynamics of water is not only changed due to the presence of biomolecules, it is also affected by the presence of the cosolvents and ions (Cacace et al. 1997; Collins and Washabaugh 1985; Robinson and Jencks 1965; Timasheff and Fasman 1969; Von Hippel 1969). Aqueous salt solutions are natural environments for functioning of biomolecules. Protein solubility can be changed by the addition of salts to the solution (Robinson and Jencks 1965). Salts can affect the electrostatic interactions in a solution through charge-charge interactions (Debye and Hückel 1923) or by binding the charged groups and neutralizing it (Collins 2004). They can also influence the solubility of amino acids and proteins by altering the overall liquid water structure. Therefore, functionalities of protein molecules are affected by the concentration of salts.

Ions differ widely in their effects on the local structure of water (Cappa et al. 2006; Chakraborty and Chandra 2011; Chowdhuri and Chandra 2003; Näslund et al. 2005). Setschenow constants provide useful information about salting-in and salting-out behaviour of salt ions (Hofmeister 1888b). The behaviour of ions in solutions in general is discussed in terms of kosmotropic (water structure-making) or chaotropic (water structure-breaking) behaviour. It is known fact that small ions tend to cause “salting-out” i.e., reduction of hydrophobic solubilities; whereas large ions tend to cause “salting-in” i.e. increase in nonpolar solubilities (Dill et al. 2005; Shinto et al. 2005). This is explained by the fact that smaller ions have higher charge density which leads to strong electrostatic field which makes the water molecules to be firmly held in their solvation shell. As a result, the exchange of water molecules with the neighbouring shell becomes less probable which reduces the hydrophobic solubilities. They also exert strong orientational effects on water molecules within their first solvation shell. In case of larger ions, there is easy exchange of the water molecules with the neighbouring shells.

The different effects of the ions on local structure of water are also mirrored, in terms of their different Hofmeister effects. An exception to this trend is seen in case of salts containing lithium ion (Hyde et al. 2017; Randall and Failey 1927). Lithium ion being the smallest ion in the group I cations is expected to have the most salting out effect. But it has been reported in many cases that lithium ion has more salting-in property in comparison to sodium or potassium ion (Hyde et al. 2017; Randall and Failey 1927). This anomalous behaviour of lithium ion indicates that consideration of the charge densities only to describe their Hofmeister effects is not sufficient (Collins

2004). Many molecular dynamic simulation studies have been reported on aqueous solution of ions focussing mainly on the calculation of the hydration thermodynamics of the constituent ions (Åqvist 1990; Chandrasekhar et al. 1984; Grossfield et al. 2003; Rashin and Honig 1985) and structure of their hydration shell structures (Chandrasekhar et al. 1984; Chowdhuri and Chandra 2001; Dill et al. 2005; Du et al. 2007; Grossfield 2005; Guàrdia et al. 2006a; Hribar et al. 2002; Jensen and Jorgensen 2006; Kalra et al. 2001; Obst and Bradaczek 1996; Patra and Karttunen 2004; Rajamani et al. 2004). Recent studies quantified the extent in which salt concentration strengthens the hydrophobic interaction (Ghosh et al. 2005; Jönsson et al. 2006; Kalra et al. 2001; Mancera 1999; Thomas and Elcock 2007). Therefore, it would be interesting to observe the sensitivity of biological processes in presence of different ions and their changes with the concentration of ions (Brooks and Nilsson 1993; Carta and Tola 1996; Kohn et al. 1997; Lee et al. 2002; Robinson and Jencks 1965; Von Hippel 1969).

Changing the conditions of the solutions affect the thermodynamics of proteins by altering their structural aspects (Brooks and Nilsson 1993; Kohn et al. 1997). Presence of alcohols, urea and guanidine hydrochloride are found to denature the proteins; while addition of certain amino acids, sucrose, Trimethylamine N-oxide (TMAO) stabilises it. Urea is found to denature protein by direct (Auton et al. 2007; Auton and Bolen 2005; Bolen and Rose 2008; Lee et al. 2010) and indirect mechanism (Dill 1990; Frank and Franks 1968). It alters the structure of water molecules (Caballero-Herrera et al. 2005; Daggett 2006; Mountain and Thirumalai 2003) and thereby encourages the hydrophobic hydration. It can also directly interact with the polar groups of the protein favouring the denatured state. According to the ‘two-stage denaturation process (Hua et al. 2008; Samanta et al. 2014), denaturation begins with preferential solvation of protein molecule by urea and expulsion of water from the protein solvation shell. TMAO on the other hand, is known to be excluded from the protein surface for entropy effect (Canchi et al. 2012; Courtenay et al. 2000; Lin and Timasheff 1994). Its effects on the structure of water lead to stabilization of proteins (Wei et al. 2010; Zou et al. 2002). Several experiments support the formation of immobile water (Hunger et al. 2012; Panuszko et al. 2009; Rezus and Bakker 2007, 2009) in presence of TMAO which is supported by the simulations (Laage et al. 2009; Larini and Shea 2013). There are also some studies done on the mixture of urea and TMAO in protein aqueous solutions to study the stabilization effect of TMAO to the

protein molecules in presence of urea (Canchi and García 2013; Paul and Patey 2007a; Sahle et al. 2016). But the studies of the effect of hydrophobic hydration in presence of these molecules have not been given much importance.

Protein water-exposed interface undergoes a lot of topological disorder and chemical heterogeneity due to presence of hydrophilic and hydrophobic sites. There have been many studies done on the effects of ions on the solvation structure of water, mechanism of urea denaturation on protein, TMAO stabilization, urea and TMAO mixture effect on protein but no systematic study on the role of stabilizing and destabilizing effect of cosolvents on biomolecules. Both urea and concentrated salt solutions are found to denature the protein. Therefore, it would be interesting to see whether there is a common factor between these cosolvents that can explain the reasons leading to the destabilization on the biomolecules and also if it is different from the TMAO effect on the biomolecule. Further, it would be interesting to spot some interesting behaviour of lithium salts which can explain the anomalous behaviour of lithium solutes with respect to other salts (Hyde et al. 2017; Randall and Failey 1927; Thomas and Elcock 2007).

In view of this, a comprehensive set of MD simulations of aqueous glycine in presence of urea, TMAO, KCl, and LiCl at different concentrations has been presented. The main aim is to see the effect of cosolvents towards the solvation structure of glycine and calculation of the forces that stabilizes and destabilizes a protein molecule. To study this process, a simple and small amino acid, glycine was selected for its simplicity in having one $-NH_2$ group, one $-COOH$ unit and a hydrophobic part. The hydrophobic group is surrounded by hydrophilic groups. Glycine forms zwitterionic state in aqueous solution and in crystalline state (Albrecht and Corey 1939; Jönsson and Kvik 1972; Tortonda et al. 1996) whereas; neutral form in the gaseous phase (Bonaccorsi et al. 1984; Ding and Krogh-Jespersen 1992). Some theoretical studies using ab initio methods have been reported regarding the study of the internal structure of glycine and its interaction with water molecules and ions (Chaudhari et al. 2004; Jensen 1992; Jensen and Gordon 1995; Leung and Rempe 2005; Tuñón et al. 2000; Wong et al. 2002). In order to study the effects of cosolvents and ions in more details, simulations in different water models namely, SPC and SPC/E using different thermostat and system size were performed. From this study an overview of basic elementary molecular mechanism that are responsible for protein stabilization can be obtained.

2.2 COMPUTATIONAL METHODOLOGY

In the present work, glycine, urea, TMAO, KCl, LiCl and water molecules are characterized by multi-site interaction models. In these models, the interaction between atomic sites of two molecules is expressed as

$$u(r_{ij}) = 4\varepsilon_{ij}\left[\left(\frac{\sigma_{ij}}{r_{ij}}\right)^{12} - \left(\frac{\sigma_{ij}}{r_{ij}}\right)^6\right] + \frac{q_i q_j}{r_{ij}} \quad (2.1)$$

where, r_{ij} is the distance between sites i and j of different molecules, q_{ij} is the charge of i^{th} atom and the Lennard-Jones parameter (LJ) ε_{ij} and σ_{ij} are obtained by using combination rules $\sigma_{ij} = (\sigma_i + \sigma_j)/2$ and $\varepsilon_{ij} = \sqrt{\varepsilon_i \varepsilon_j}$, where σ_i and ε_i are the Lennard-Jones diameter and well-depth parameter for i^{th} atom. For water, the simple point charge (SPC) model (Berendsen et al. 1981) and the extended simple point charge model (SPC/E) model (Berendsen et al. 1987) were employed. The values for the potential parameters for glycine, urea, TMAO, KCl, LiCl and water molecules are taken from CHARMM36 FF (Klauda et al. 2010). The corresponding potential parameters for the amino acid, cosolvents and water molecules are given in Table 2.1.

Classical molecular dynamics have been carried out in a cubic box comprising a total of 512 and 1024 particles, including zwitterionic glycine, co-solvent and water molecules for SPC and SPC/E water models respectively. The compositions of each solvent mixture in four different solvent systems of varying concentrations are given in Table 2.2. Simulations were performed using the GROMACS (v2016.5) simulation package (Berendsen et al. 1995; Van Der Spoel et al. 2005). The equations of motions were integrated using the leapfrog algorithm with time step of 10^{-15} s (1 fs) along with minimum image conventions and periodic boundary conditions in all three directions (Allen and Tildesley 1989).

The minimum image conventions for calculation of the short-range Lennard-Jones interactions were employed and the particle mesh Ewald (PME) sum to treat the long-range electrostatic interactions (Darden et al. 1993; Essmann et al. 1995). Modified Berendsen thermostat ($\tau_T = 0.1$ ps) (Berendsen et al. 1984) and Velocity-rescale ($\tau_T = 0.1$ ps) (Bussi et al. 2007) thermostat was used for SPC and SPC/E water models respectively along with Parrinello-Rahman barostat ($\tau_P = 2.0$ ps) (Parrinello and Rahman 1980) to keep the temperature and pressure constant. All the bonds were constrained using the LINCS algorithm (Hess et al. 1997).

Table 2.1: Values of Lennard-Jones and electrostatic interaction potential parameters for glycine, urea, TMAO and water. e represents the magnitude of electronic charge.

Name	Atom	σ (Å)	ϵ (kJ/mol)	Charge (e)
Glycine	N	3.29	0.8368	-0.30
	H	0.40	0.1924	0.33
	C $_{\alpha}$	3.58	0.2343	0.13
	H $_{\alpha}$	2.38	0.1171	0.09
	C	3.56	0.2928	0.34
	O	3.02	0.5020	-0.67
Urea	C	3.56	0.2928	0.60
	O	3.02	0.5020	-0.58
	N	3.29	0.8368	-0.69
	H	0.40	0.1924	0.34
TMAO	N	3.29	0.8368	-0.83
	O	3.11	0.5020	-0.37
	C	3.94	0.3221	-0.35
	H	1.24	0.1924	0.25
Water (SPC)	O	3.16	0.6501	-0.82
	H	---	---	0.41
Water (SPC/E)	O	3.16	0.6502	-0.84
	H	---	---	0.42

Glycine molecule was centered in the box and co-solvents, water molecules were inserted with random orientations for all systems. Each system was equilibrated in NVT ensemble for 2 ns, followed by NPT ensemble for 2 ns in order to obtain the appropriate box length corresponding to 1 atm pressure at the end of simulation. Finally, simulations were run for another 50 ns and 30 ns for the calculation of structural and dynamic quantities with 1fs time step using NPT ensemble for SPC and SPC/E water models respectively.

Table 2.2: The system details considered in the simulation. (N_{glycine} , $N_{\text{urea/TMAO/KCl/LiCl}}$, N_{water} are the number of glycine, urea, TMAO, KCl, LiCl and water molecules in the simulation box.) *

System	N_{glycine}	$N_{\text{urea/TMAO/KCl/LiCl}}$	N_{water}
1	1	---	511
2	1	10	501 (491)
3	1	19	492 (473)
4	1	40	983 (945)

* System 1 corresponds to pure aqueous glycine. System 2 corresponds to 1M, whereas systems 3 and 4 corresponds to 2M concentrations. SPC water model was used for systems 1,2,3 and SPC/E water model for system 4. Number of water molecules corresponding to KCl and LiCl salts systems are shown in parenthesis.

2.3. RESULTS AND DISCUSSION

The 3-dimensional representations of the amino acid used in this chapter.

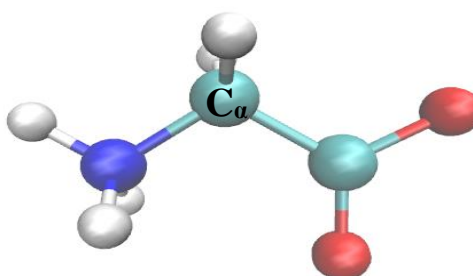


Figure 2.1. The 3-dimensional representation of glycine amino acid considered in this work.

2.3.1 Radial Distribution Functions

The structural arrangement of water molecules with the variation of solutes around the glycine molecule is calculated from the intermolecular O_w-O_w , $C_\alpha-O_w$, $C-O_w$, N_g-O_w and O_g-O_w radial distribution functions (RDF's). Figure 2.2 shows the effect of different cosolvents on the RDF of nitrogen of glycine with oxygen of water (N_g-O_w), carbonyl carbon of glycine with oxygens of water ($C-O_w$), carbonyl-oxygen of glycine with oxygens of water (O_g-O_w), carbonyl oxygen of glycine with cosolvents, hydrophobic carbon of glycine with oxygens of water ($C_\alpha-O_w$) and water oxygen-oxygen (O_w-O_w) at 2M solute concentrations in SPC water model. Similar trends in graphs were found with solute concentrations of 1M and 2M for SPC and SPC/E water

models respectively (Figures 2.4 and 2.5). The difference between SPC and SPC/E water molecules are in the partial charges. Therefore, qualitatively similar trends are obtained. In case of SPC water the effects were more pronounced.

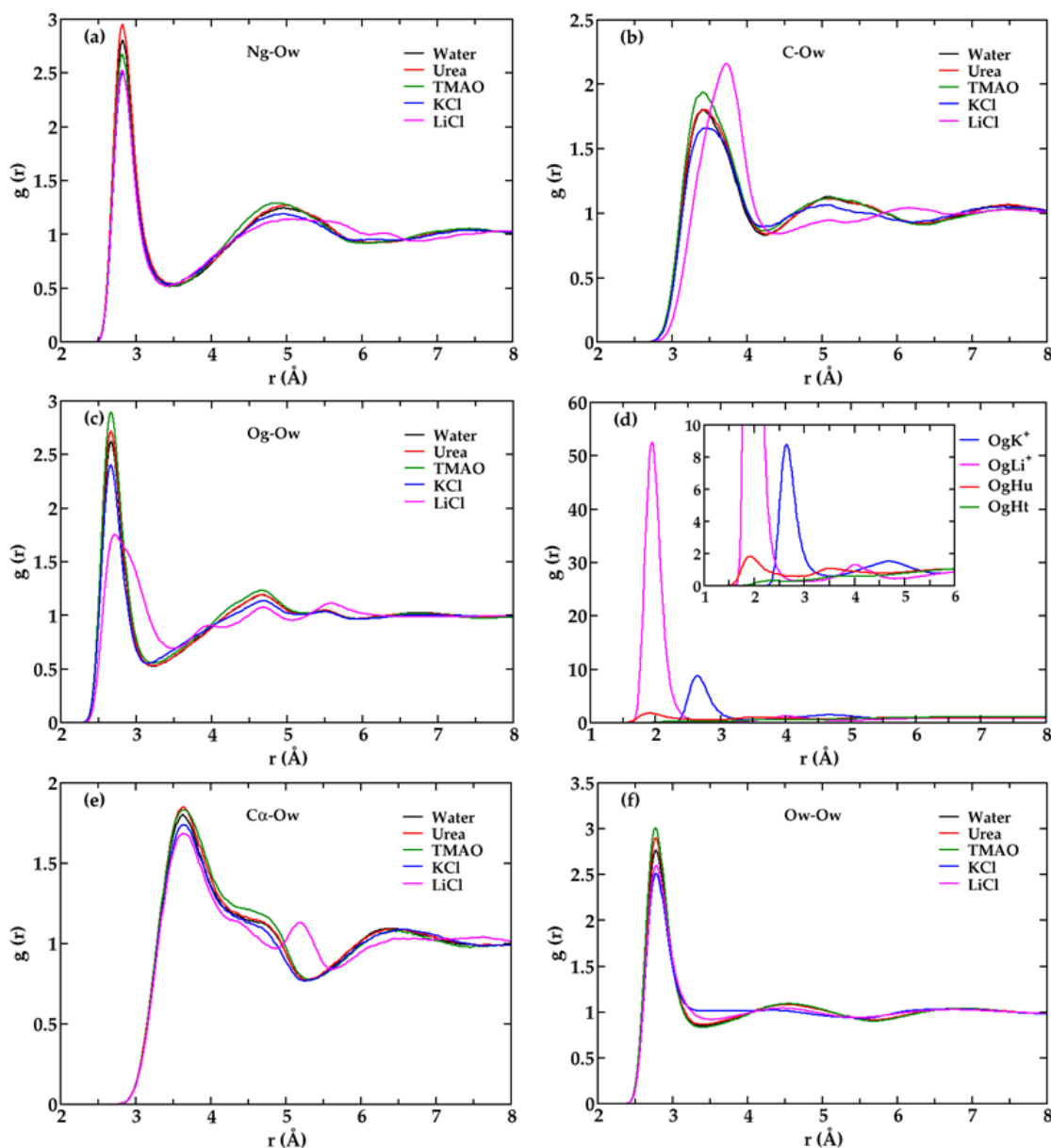


Figure 2.2. Radial Distribution functions $g(r)$ of aqueous glycine with different cosolvents for 2M concentration (a) N_g-O_w , (b) $C-O_w$, (c) O_g-O_w , (d) O_g with respect to positive ions, hydrogens of urea and TMAO, (e) $C_\alpha-O_w$ and (f) O_w-O_w for SPC water model.

It can be observed that the placement of first peak in case of N_g-O_w as shown in Figure 1(a) is same for all the co-solvent except for LiCl, where the minima is shifted

little towards lower distances. The height of the peak is more for urea, TMAO and least for LiCl and KCl, which shows that greater number of water molecules are bonded with the N-terminal of glycine is more in case of urea and least in case of ionic solutes. The second coordination shell of urea and pure glycine water remains almost same whereas the peak height increases slightly for TMAO and much disrupted in case of LiCl. This indicates that the second coordination shell is ordered more for TMAO but as moved towards the ionic salts there is loss in the tetrahedrality of water molecules. More well-defined peaks were observed for LiCl in case of SPC/E water model.

The hydration structure of the water molecules near the carbonyl carbon of glycine shown in Figure 2.2(b) is found to be more perturbed than the N-terminal in presence of ionic solutes and especially in case of LiCl. The position of the maxima and the minima of the first peak is found to be same for TMAO, urea, KCl and pure glycine water. However, the well-defined peak height is found to be more in case of TMAO which reduces in the order of TMAO > urea > KCl. This suggests that water molecules near the carbonyl carbon of glycine are more tetrahedrally ordered in case of TMAO. For LiCl, shifting of the first peak was observed towards higher distances. Significant disruption of the second and third solvation shells for LiCl were observed. Lithium ion has high charge density when compared with potassium ion, which significantly changes the structure of water.

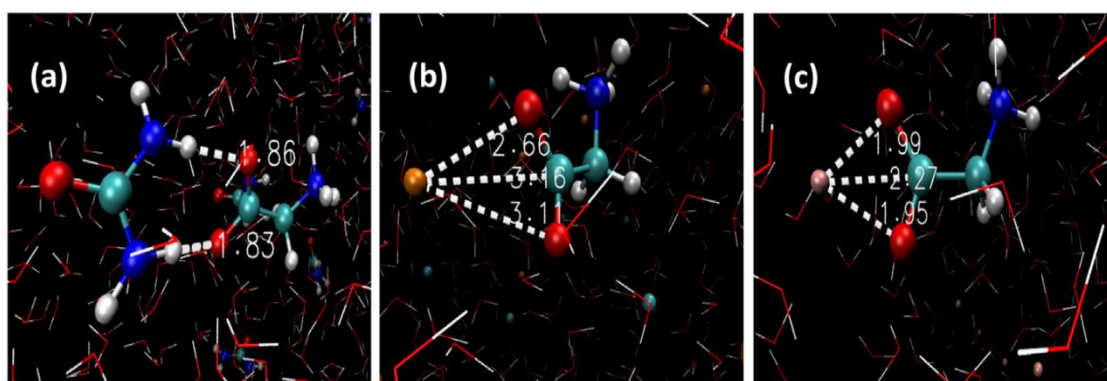


Figure 2.3. Snapshots from the simulations of aqueous glycine mixtures in presence of a) urea b) KCl c) LiCl at 2M concentration for SPC water model. Red, green, blue, white, orange and pink spheres represent oxygen, carbon, nitrogen, hydrogen, potassium and lithium atoms respectively. Water molecules are shown in line style.

The positions of the second and third maxima remain unchanged for TMAO, urea and glycine aqueous solution. However, change in the secondary solvation shell

structure for KCl was observed. The structure of the solvation shell for carbonyl oxygen in presence of LiCl shown in Figure 2.2(c) is somewhat different from the other three cosolvents. The cations have strong interactions with the carbonyl group compared to urea and TMAO as shown in Figure 2.2(d). In Figure 2.3, snapshots of the simulation trajectory of aqueous solutions of glycine in presence of urea, potassium and lithium salts are shown. The radial distribution functions of carboxylate oxygen (O_g)-cosolvent shown in Figure 2.2(d) clearly explains the strong association of the lithium cation towards the carbonyl group when compared with the potassium ions. It can be noted here that the first maxima of $O_g\text{-Li}^+$ is at 2 Å and that of $O_g\text{-O}_w$ in presence of LiCl is at 2.6 Å.

The peak height suggests that in case of LiCl, there is more probability of finding Li^+ ions near the surroundings of two carbonyl oxygen atoms than water molecules. This can be explained due to the fact that the positively charged lithium cation will be more attracted towards the carbonyl anion compared to water molecules. The lithium ion is then surrounded by water molecules which lead to shifting of the first solvation shell at higher distances, Figure 2.2(c). In case of potassium ion, there is lesser probability of finding K^+ ion near the two carbonyl oxygens molecules in comparison to lithium ion. The first maxima of $O_g\text{-K}^+$ and $O_g\text{-O}_w$ are nearly at same distance. Therefore, the changes in the solvation shell of carbonyl oxygen and water molecules ($O_g\text{-O}_w$) for KCl are found to be less pronounced compared LiCl. However, the second solvation shell of carbonyl carbon and water oxygen in case of KCl as shown in Figure 2.2(b) is seen to be disrupted. In case of urea, some probability of binding the hydrogen of urea with the carboxylate oxygen molecules was found at lower distances as shown in Figure 2.2(d), but due to the absence of strong electrostatic field, there is no strong hydration shell near the hydrophobic unit as it is found for LiCl.

The ionic association near the carbonyl oxygen of glycine changes the water density near the hydrophobic unit. It can be seen from Figure 2.2(e) that the position of the first maxima is same for all the cosolvents but there is significant difference in the placement of the first minima. The height of the first peak increases in case of TMAO in comparison to aqueous glycine but it decreases in case of the ionic solutes. Further, it can be seen that in case of TMAO, a small hump near the minima of first solvation shell is observed. The height of the hump decreases from TMAO > urea > KCl > LiCl. This means there is an increment in the density of water molecules near the first

solvation of the C_α in case of TMAO compared to aqueous glycine which reduces in case of the ionic solvents. For LiCl, a smaller hump at a distance of 5.4 Å can be noticed. The formation of smaller hump can be related to the presence of first hydration shell of Li^+ ion near the carbonyl oxygen which is missing in case of other cosolvents. Similar type of hump was noticed for SPC/E water model.

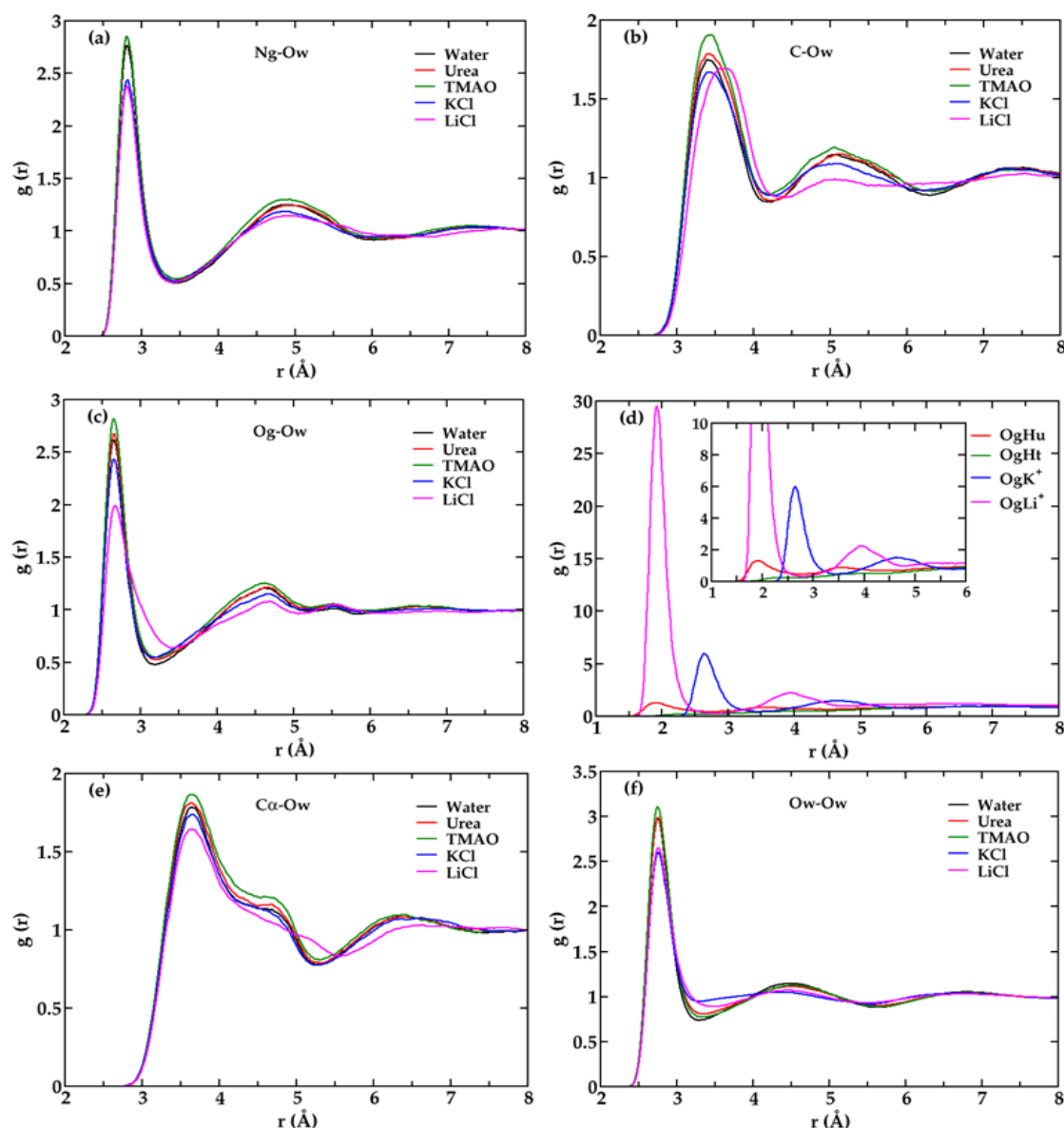


Figure 2.4: Radial Distribution functions $g(r)$ of aqueous glycine with different solutes for 2M concentration (a) N_g-O_w , (b) $C-O_w$, (c) O_g-O_w , (d) O_g with respect to positive ions, hydrogens of urea and TMAO (e) $C_\alpha-O_w$ and (f) O_w-O_w for SPC/E water model.

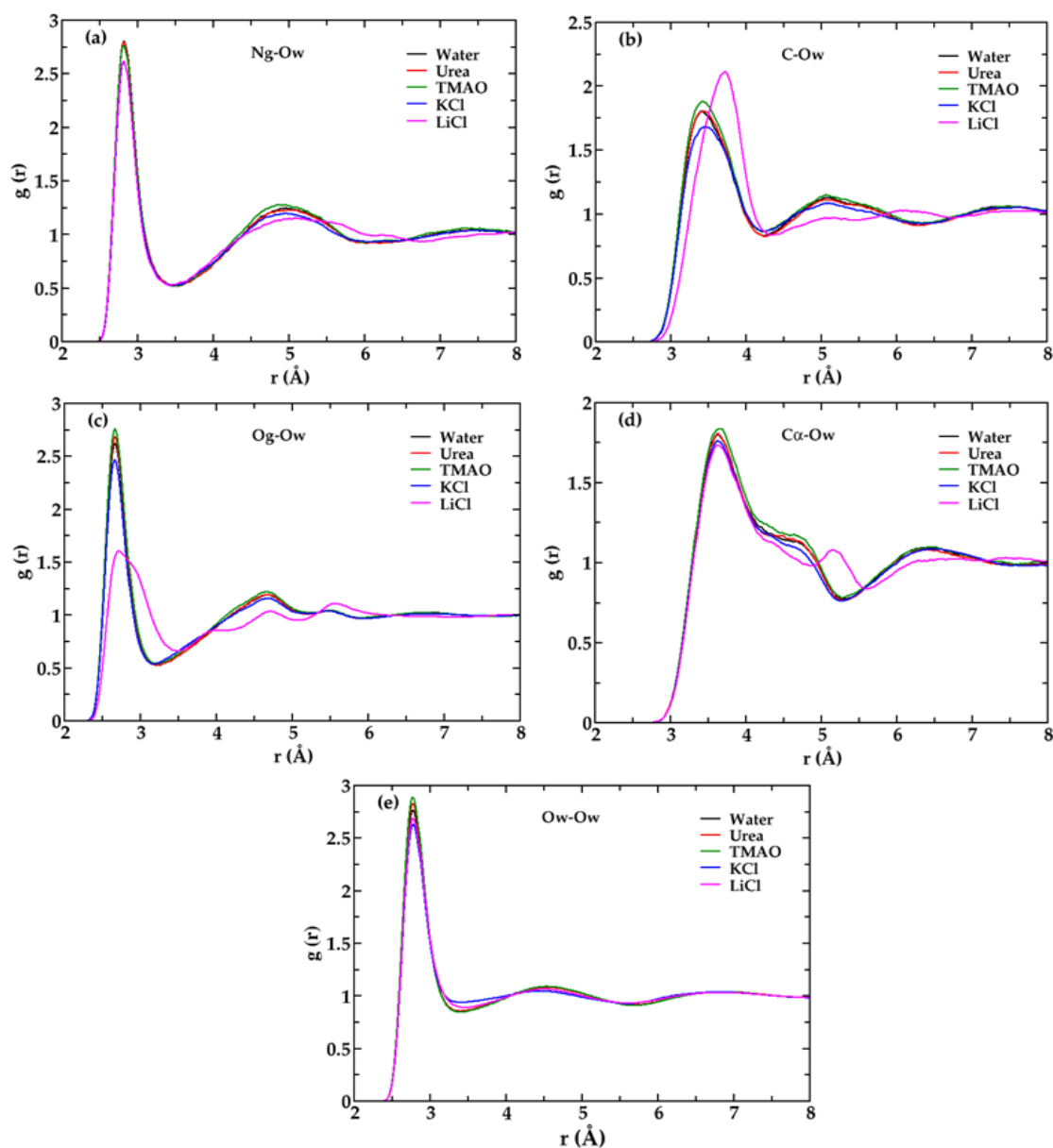


Figure 2.5: Radial Distribution functions $g(r)$ of aqueous glycine with different solutes for 1M concentration (a) N_g-O_w , (b) $C-O_w$, (c) O_g-O_w , (d) $C_\alpha-O_w$ and (e) O_w-O_w for SPC water model.

Finally, it would be interesting to see the changes in the RDF of the water oxygen-oxygen (O_w-O_w) as shown in Figure 2.2(f). The first peak of O_w-O_w RDF profile occurs at 2.80 \AA for all of the cosolvents. Variations in the peak height, minima positions and the peak maxima of the second and third solvation shells is observed for all the cases. Significant differences were observed in structure of water around the glycine molecule mainly for the ionic solutes. The distribution of the peak height of the first maxima clearly shows that the water molecules are more ordered in case of TMAO. Presence of ions promotes local structure in water molecules.

Therefore, in present scenario, the hydrophobic unit is more surrounded by water molecules in presence of TMAO and LiCl. In other words, it can be said that the hydrophobic part of glycine is more hydrophilic (water loving) in presence of TMAO than other cosolvents. Similar trend was observed at lower concentration of 1M. Now, it would be interesting to see whether this hydration of the hydrophobic unit gives an extra stabilization to the glycine water system in comparison to other cosolvents system. For more insights, spatial distribution functions have been plotted in the next section.

2.3.2 Spatial Distribution Functions

Spatial distribution functions (SDF's) of oxygen molecules around glycine for SPC water model in presence of different cosolvents at 2 M concentration by using the TRAVIS (Brehm and Kirchner 2011) software package was calculated. The calculated results of SDF's are shown in Figure 2.6.

Oxygen atom densities are shown up to 6 Å from the centre of glycine molecule. It can be seen that there are three main regions where the electron density cloud is mainly distributed. First, near the three hydrogens of the ammonia, second near the carboxylate ion and third near the hydrophobic unit. With the change in cosolvent, changes in the electron density were found mainly near the carboxylate ion and near the hydrophobic unit. The oxygen density near the amine hydrogens remains almost unchanged which correlates well with the RDF results.

The oxygen density is significantly more towards carbonyl group for all cases mainly due to strong hydrogen bond between the water molecules with carbonyl group. The SDF is found to be same for aqueous glycine and urea solution, so plots corresponding to urea have been included, TMAO, KCl and LiCl in Figure 2.6. It can be observed that there is an increment in the oxygen density in the region (I) near the hydrophobic unit for TMAO, which is very unique. This is related to the hump seen near the first minima of (C_{α} - O_w) RDF. Further, it can also be seen that there is a growth of a new water dense region in the region (II) near the carbonyl oxygen for the ions which increases from KCl to LiCl. This can be related to the small hump at 5.4 Å seen in the RDF of hydrophobic carbon of glycine with oxygen molecules of water (C_{α} - O_w) in case of LiCl.

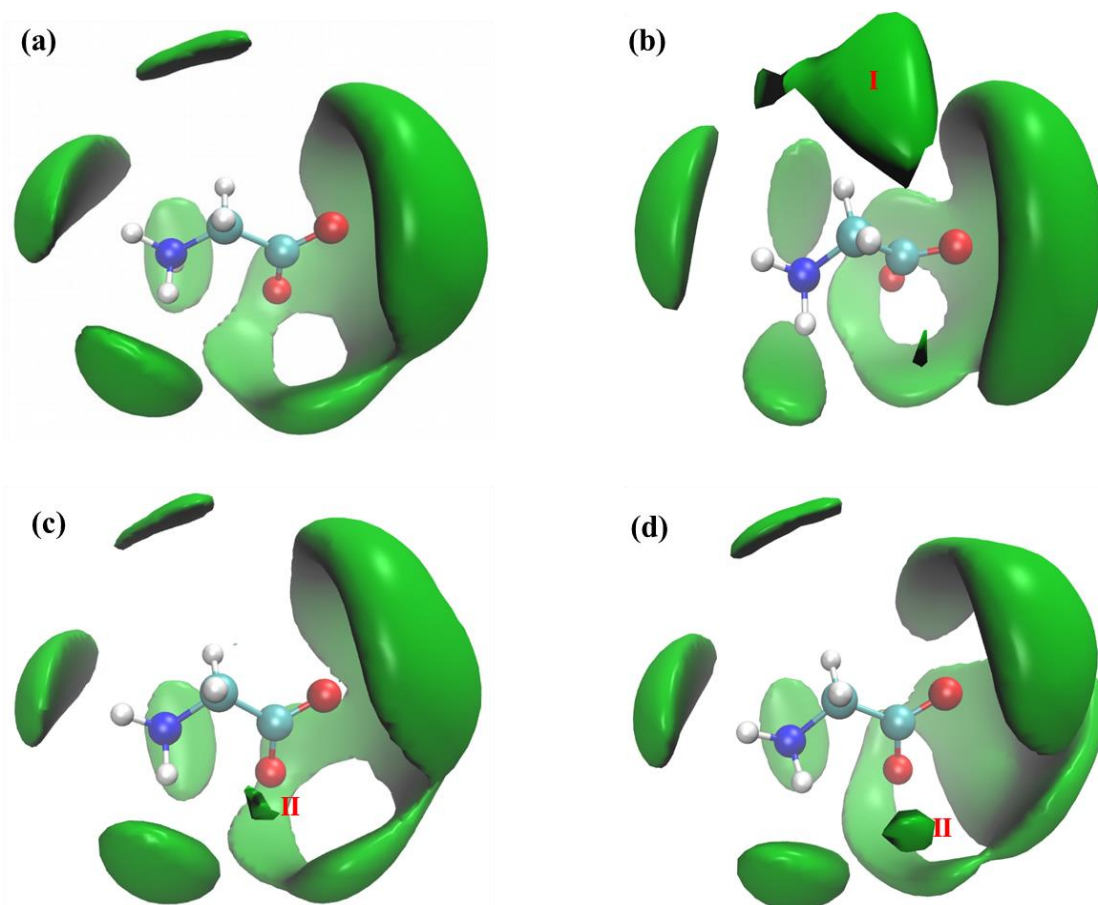


Figure 2.6: Spatial distribution functions of water oxygen around aqueous glycine amino acid in presence of different cosolvents (a) urea, (b) TMAO, (c) KCl and (d) LiCl at 2M concentration for SPC water model considering isovalues of 41.

2.3.3 Number of Hydrogen-bonded Water Molecules

Presence of cosolvents and ions changes the solvent structure near the glycine molecule significantly. Therefore, it would be interesting to see the distribution of water molecules near the interface of the amino acid. In Figure 2.7, the population of number of hydrogen bonded oxygen molecules near the C_{α} , carbonyl carbon and N-terminal with the variation of cosolvents at 2 M concentration for SPC water model have been plotted. The distance criteria considered for two oxygen-oxygen atoms to be hydrogen bonded is 3.25 Å. The interfacial water molecules within a distance of 5.6 Å from the C_{α} , 6.1 Å from carbonyl carbon and 3.5 Å from amine nitrogen of glycine were selected in the calculations based on the radial distribution functions. The fraction (f_n) of oxygen atoms of water molecules involving in total n number of water–water hydrogen bonds were computed and plotted.

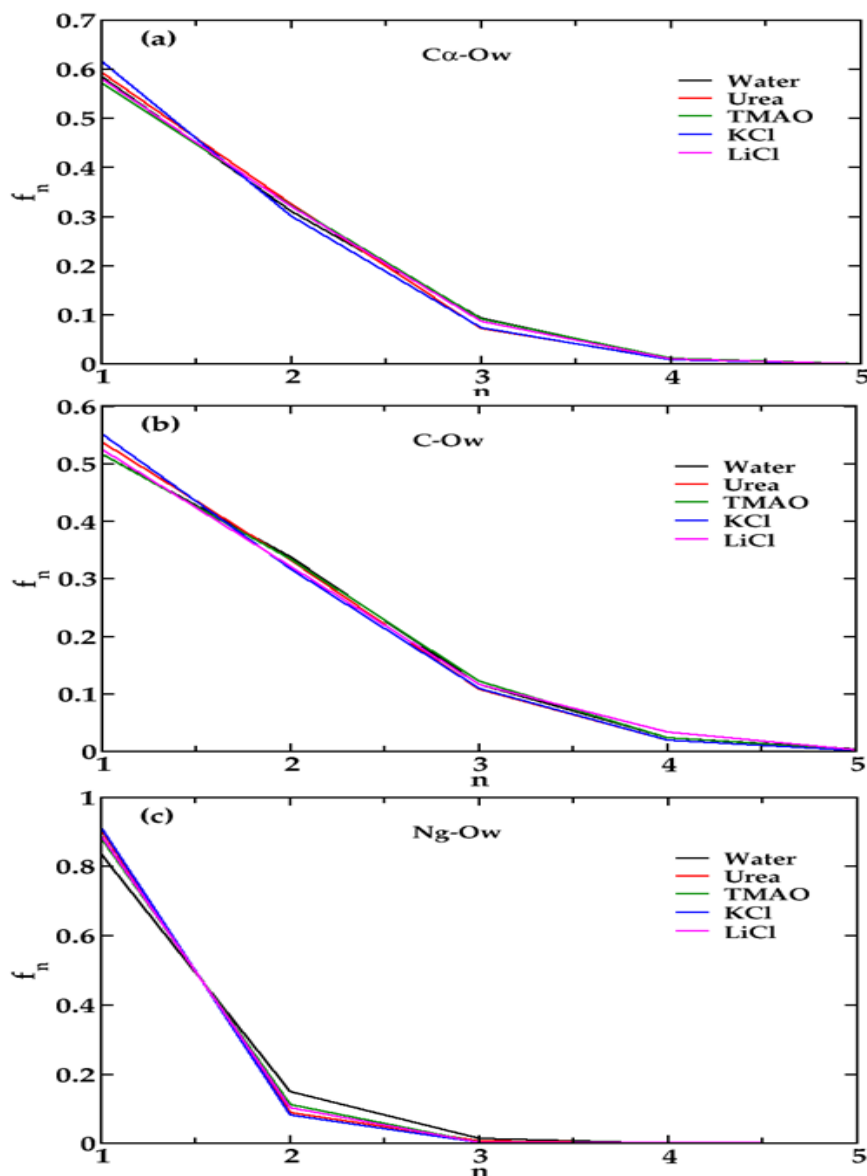


Figure 2.7: The fraction of water molecules having n number of hydrogen bonds within the distance (a) 5.6 Å from C_{α} (b) 6.1 Å from carbonyl carbon and (c) 3.5 Å from amine nitrogen of glycine at 2M solute concentration for SPC water model.

In all the cases it can be seen that the probability of occurrence of one or two number of hydrogen bonds are found to be more compared to three and four hydrogen bonds. In case of C_{α} and carbonyl carbon, the probability of three coordinated water molecules are found to be little more in presence of TMAO and LiCl in the solution, whereas presence of KCl and urea makes the probability of finding single coordinated water more. This indicates that TMAO and LiCl are found to have more ordered water molecules near the C_{α} of glycine compared to normal glycine water. Presence of KCl and urea in the solution was found to promote more broken type of hydrogen bonds.

Moreover, it can be noticed here that LiCl has more probability of having four coordinated water for carbonyl carbon than TMAO. This can be explained as, since the carbonyl oxygen molecules are more chelated by the Li^+ ion as in Figure 2.1(d), there is a probability of finding strongly bound hydration sphere of Li^+ ion. This makes the water molecules more ordered and four coordinated near the carbonyl oxygen. This hydration sphere is missing in case of TMAO and urea. For K^+ ion even though, there is a probability of finding such hydration sphere near the carbonyl oxygen, it is less likely to be found as in Figure 2.2 (d).

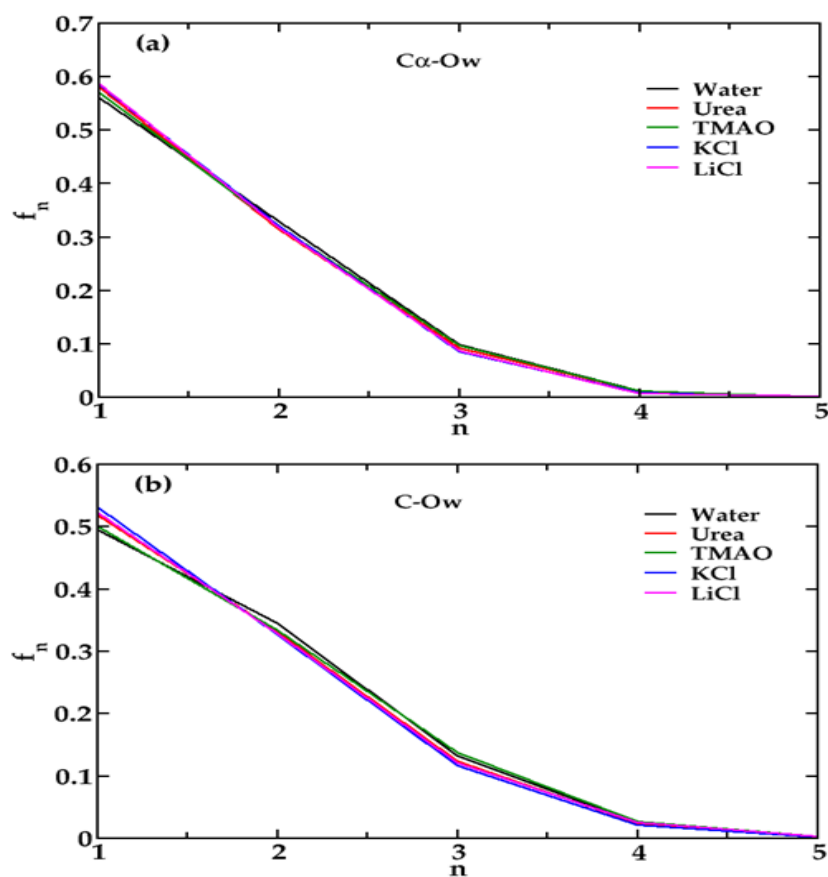


Figure 2.8: Fraction of water molecules having n number of hydrogen bonds within the distance (a) 5.6 Å from C_α (b) 6.1 Å from carbonyl carbon of glycine at 2M solute concentration for SPC/E water model.

The scenario is quite different near the N-terminal. All the cosolvents are found to have less ordered and broken hydrogen bonds in comparison to that of pure glycine water. This may be because the anions present in case of ionic cosolvents and the oxygen present in TMAO preferably replaces some water molecules near the $-\text{NH}_3$ group as observed in Figure 2.2(a) resulting to lesser number of hydrogen bonded water

molecules. For SPC/E water model more 3 and 4 number of hydrogen bonds were found in presence of TMAO near C_α and carbonyl carbon atoms. The rest of the cosolvents behaved in similar way.

2.3.4 Orientation Profile

As evident from the RDF, structures of water molecules are very much different near the C-terminal of glycine in presence of different cosolvents, therefore, it would be interesting to see the orientation profile of water molecules found near the interfaces. One of the important criteria to see the tetrahedrality of the water molecules is to calculate the $\langle O-O-O \rangle$ angle distribution. For tetrahedral water, the know ideal angle is 104.5° .

In Figure 2.9, the probability distribution of $\langle O-O-O \rangle$ angle of the bulk water and interfacial water molecules near the C_α and the carbonyl carbon at 2M concentration for SPC water model has been plotted. Water molecules up to a distance of 5.6 \AA from C_α and 6.1 \AA from carbonyl carbon were considered as interfacial water molecules. It can be seen that in all the cases a broad distribution of angles near 104.5° and a small peak near 50° is observed. These peaks are found to be shifted slightly towards the lower angles in case of ionic solutes. Therefore, it can be remarked here that as the cosolvent water hydrogen bond strength decreases compare to water-water hydrogen bond strength, the distribution of $\langle O-O-O \rangle$ angle is found to be shifted towards the higher angles. Similar trend in peak distribution were found for the interfacial water near C_α as in Figure 2.9(a) and carbonyl carbon as in Figure 2.9(b).

For LiCl, it is found that the distribution near 104.5° gets flat and broader. The peak height near 50° increases. The angle distribution of water molecules presents near the hump region of C_α carbon for all cosolvents, i.e., in the distance range of $4.2\text{-}5.6 \text{ \AA}$, corresponding to the shoulder of the first peak and rise of the second peak were also calculated. The distribution gets broader in the range of 104.5° for all the cosolvents except for LiCl. Significant different curve for LiCl near the interface was found and it is included in the Figure 2.9(a). It can be seen that there is clear emergence of two peaks in this region for LiCl. Water molecules near the minima of the first solvation shell of the hydrophobic unit in presence of LiCl show two distinct peaks, one at lower angles and the other at the higher angles.

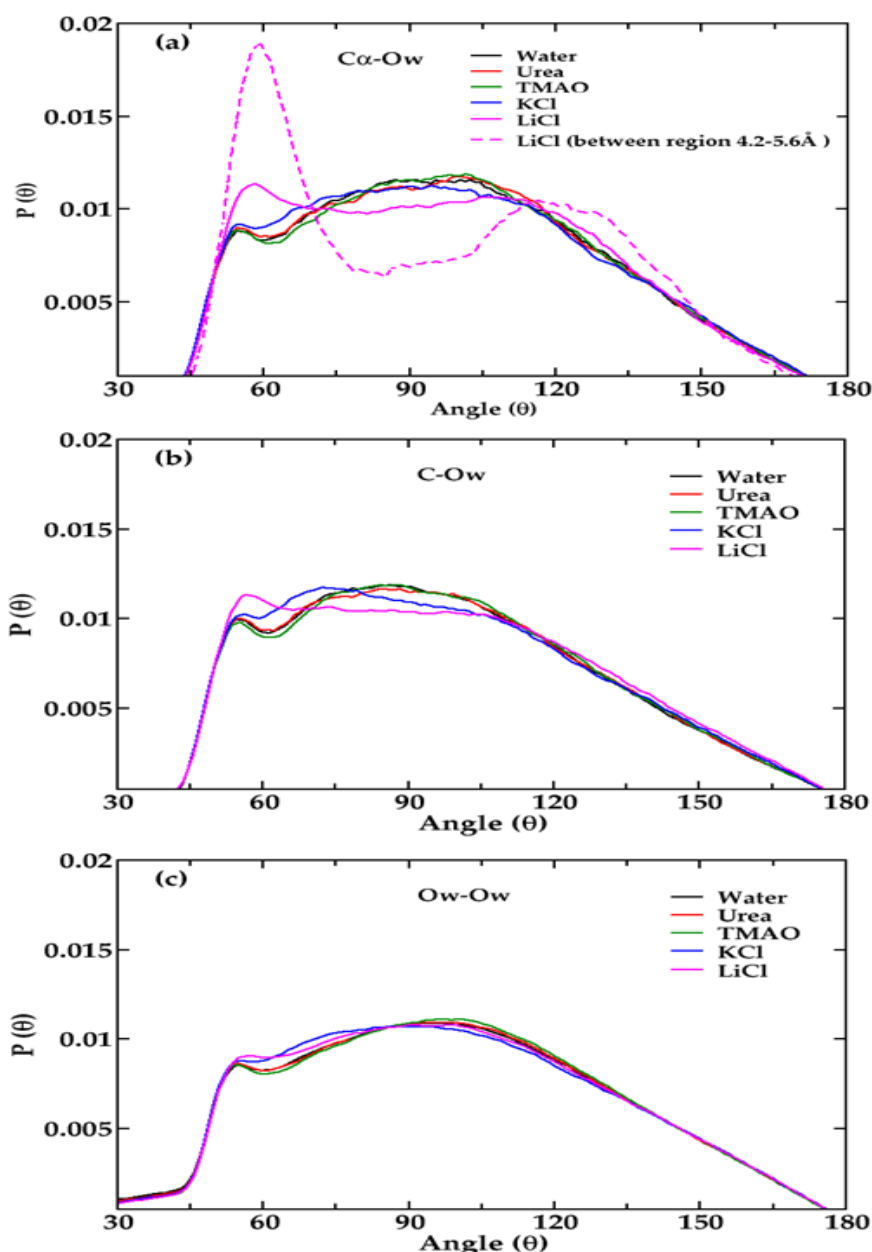


Figure 2.9: Probability distribution of $\langle \text{O-O-O} \rangle$ angle of oxygen atoms of water molecules which are within the distance (a) 5.6 \AA from C_α (b) 6.1 \AA from carbonyl carbon and (c) bulk O_w at 2M solute concentration for SPC water model.

This implies that the probability of observing linear hydrogen bonds in this region is very less. The higher charge density of Li^+ ion makes the hydrogen bond strength of water molecules within the first coordination shell of Li^+ much stronger than the hydrogen bond strength of water molecules which leads to the disruption of hydrogen bond network and breaking down of the tetrahedral structure to icosahedral structure (Prasad and Chakravarty 2017). The peaks shift from 50° to 60° and emergence of a new peak near 120° occurs. Similar type of behaviour is observed in

case of SPC/E water model as shown in Figure 2.10, except the peaks are broader for LiCl. This implies that tetrahedral structures of water molecules are less disturbed in presence of LiCl for SPC/E model as compared to SPC model. The angular distribution of SPC water model for 1M concentration is given in Figure 2.11,

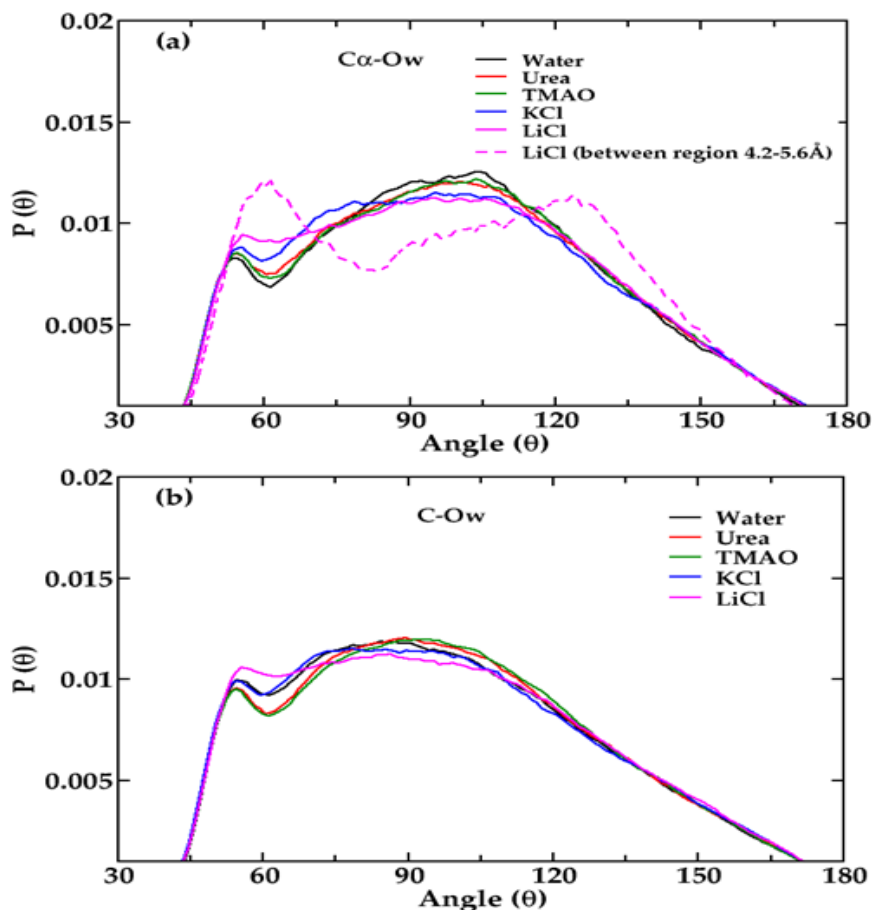


Figure 2.10: Probability distribution of $\langle O-O-O \rangle$ angle of oxygen atoms of water molecules which are within the distance (a) 5.6 Å from C_α (b) 6.1 Å from carbonyl carbon at 2M solute concentration for SPC/E water model.

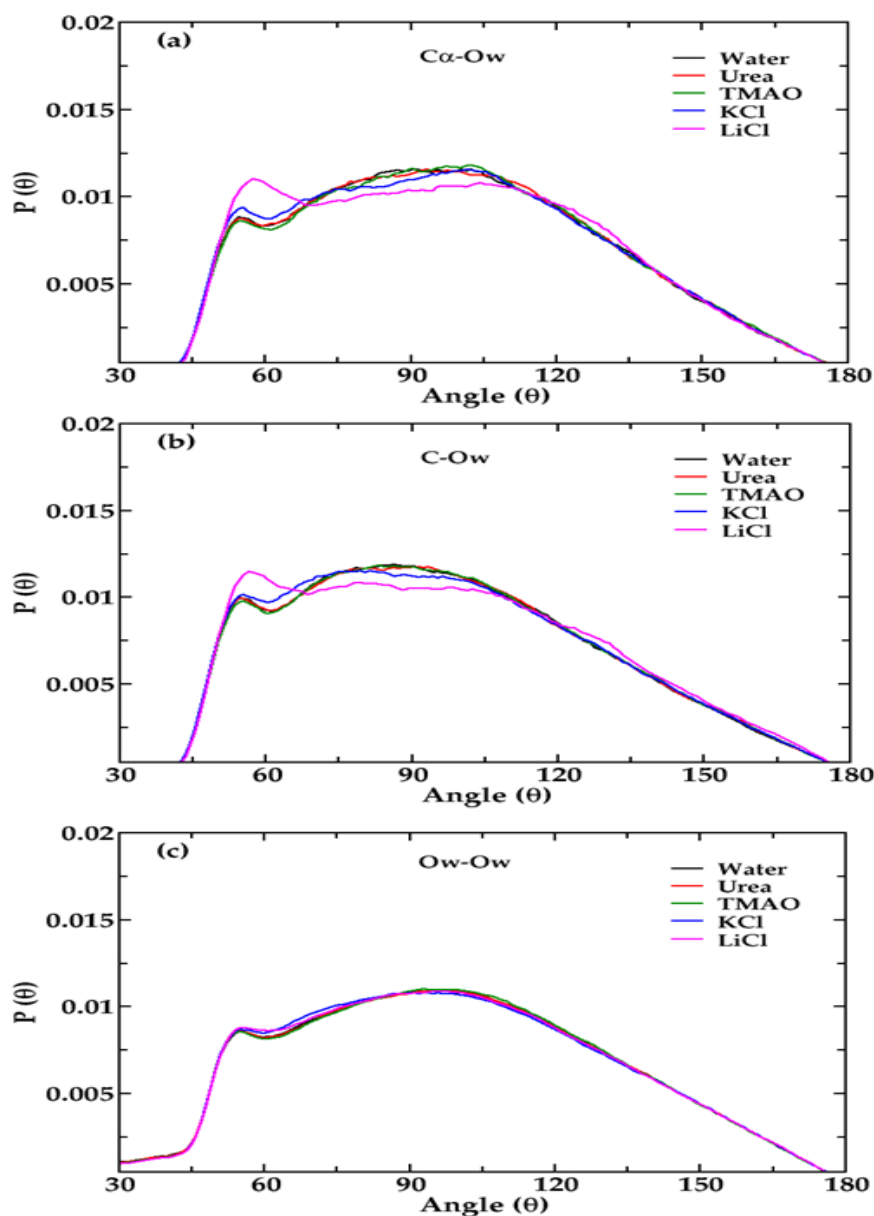


Figure 2.11: Probability distribution of $\langle \text{O-O-O} \rangle$ angle of oxygen atoms of water molecules which are within the distance (a) 5.6 \AA from C_α (b) 6.1 \AA from carbonyl carbon and (c) bulk O_w at 1M solute concentration for SPC water model.

2.3.5 Potential Mean Force

Determination of solvation free energies is one of the important criteria in the calculation of stabilizing forces. Solvation energies have profound influences in the conformational stability. From the calculations of solvent free energies, an overview of complex processes that determines the thermodynamics of the biological systems can be observed. Structuring of liquid around biomolecules adds up a contribution to the free energy cost due to increased free energy barrier along the potential of mean force

between the first and second solvation shells.

To calculate Potential Mean Force (PMF), glycine-water pair correlation functions, $g(r)$ was used, in the equation

$$W(r) = -k_B T \ln g(r) \quad (2.2)$$

where, k_B is the Boltzmann constant, T is the temperature and r is the inter-atomic separations.

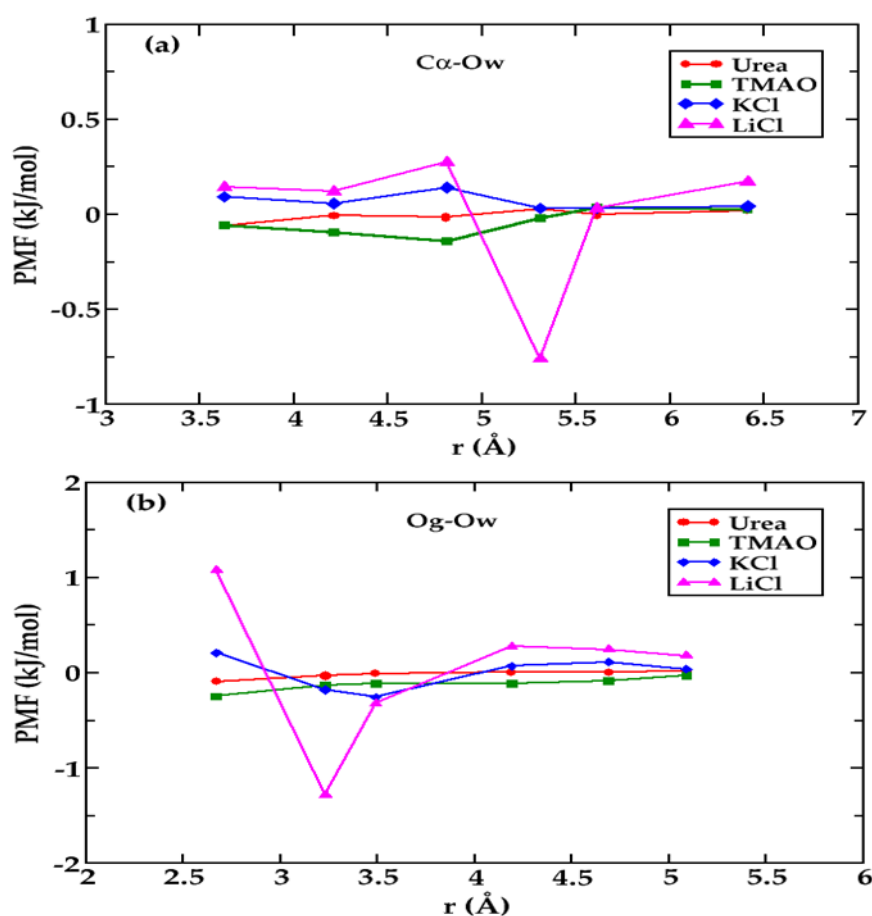


Figure 2.12: Potentials of Mean Force depicting relative free energies of interaction between (a) Hydrophobic carbon, C_α and (b) carbonyl oxygens, O_g of glycine with the oxygen sites of water molecules at different distances with respect to interaction energy of aqueous glycine water at 2M solute concentration for SPC water model.

The differences in PMF can be compared more prominently by converting the first minima and second maxima of the RDF's into free energies. Figure 2.12(a) and (b) shows the relative free energies of interaction between C_α of glycine with the water molecules and carbonyl oxygen with the water molecules at different distances with respect to the interaction energy of the aqueous glycine water respectively for SPC

water model. The concentration considered here is 2 M. A clear difference was found in the interaction of the water molecules with the glycine in presence of different cosolvents.

At smaller distances, maximum stabilization energy was found for water molecules near C_{α} of glycine in presence of TMAO. The stabilization energy decreases as moved towards the more charge dense species (urea > KCl > LiCl). This indicates that water molecules like to come closer to the hydrophobic unit in case of TMAO solution and prefer least in case of LiCl solution. This trend continues up to a distance of 4.8 Å, and then at 5.4 Å for LiCl, a sudden reversal in the trend is noticed. At this distance, the stabilization energy is more for LiCl which is even greater than TMAO and at around 5.8 Å, the stabilization energy becomes almost equal for all the cosolvents. At higher distances, again LiCl system becomes the most destabilized with respect to other cosolvents. It is also noted that from 5.4 Å, for all other cosolvents other than LiCl, the stabilization energy becomes almost equal. This stabilization energy gained around 5.4 Å by the LiCl solution can be attributed due to the carbonyl oxygen molecules which are bonded with the Li^{+} cation.

It would be more clarified when the relative free energies of interaction between carbonyl oxygen of glycine and the water molecules is observed as shown in Figure 2.12(b). Here also it can be clearly observed that the stabilization energy is more for TMAO solution at smaller distances but around 3.2 Å and 3.5 Å, LiCl solutions give more stabilization. The solution of ionic species, LiCl and KCl solutions are found to have more stabilizing energies than that of urea and TMAO in this region. The stabilization energy in this region is attributed due to the presence of strongly bound first hydration shell of the cations. Lithium being the most charge dense will have more compact hydration shell leading to the more stabilization energy than potassium ions. Therefore, it can be commented here that maximum hydrophobic solubility is mainly gained in presence of TMAO solution. Ionic solutions also contribute to the hydrophobic solubility due to the presence of strongly bound hydration shell arising due to the chelated ion-carboxylate ion. This contribution comes more from LiCl than KCl which may be the origin of anomalous property shown by lithium salts. So, the hydrophobic group of glycine is more hydrophilic in presence of TMAO and LiCl.

2.3.6 Hydrogen Bond Dynamics

Since interaction with water molecules is one of the main factors of protein stability, therefore it would be interesting to investigate the hydrogen bond strength of water molecules in presence of these cosolvents. Two water molecules are defined to be hydrogen bonded if the intermolecular hydrogen-oxygen distance is less than 2.45 Å. The hydrogen bond population variable $H(t)$ is calculated as follows: If two molecules remain continuously hydrogen bonded from time $t = 0$ to $t = t$ then $H(t) = 1$ or it is zero otherwise. The continuous correlation function $S_{HB}(t)$ is defined as (Chandra 2000; Luzar and Chandler 1996)

$$S_{HB}(t) = \frac{\langle h(0)H(t) \rangle}{\langle h(0)^2 \rangle} \quad (2.3)$$

where $\langle \dots \rangle$ denotes an average over all pairs of a given type. This function gives the probability that an initially hydrogen bonded pair remains bonded at all times up to t .

The associated integrated relaxation time τ_{HB} gives the average hydrogen bond lifetime of that particular pair type. Water-water (O_w-H_w), carbonyl oxygens of glycine-water hydrogen (O_g-H_w) and amine hydrogen of glycine-water oxygen ($H_{ng}-O_w$) hydrogen bond lifetimes are shown in Table 2.3.

In all cases, strongest hydrogen bond is found in TMAO solution (Bennion and Daggett 2004) followed by LiCl, then KCl and least for urea. In general, an increase in hydrogen bond lifetimes for SPC/E water model is observed compared to SPC water model. Hydrogen bond lifetimes increase as the concentration of the cosolvent is increased from 1 M to 2 M. The hydrophilic end of TMAO makes a strong hydrogen bond with water molecules and the presence of hydrophobic group blocks the approach of new water molecules. This reduces the exchange rate of water molecules leading to increased hydrogen bond lifetime of water molecules. Hydrogen bond lifetimes of amine-water and carbonyl-water are also found to increase in presence of TMAO.

Less change in water-water hydrogen bond lifetime was found in presence of urea. Urea fits well into the hydrogen bond network of water (Wei et al. 2010; Zou et al. 2002). The structure of TMAO is semi spherically symmetric whereas urea is not symmetric. This causes more disorder and disruption of hydrogen bond in the sphere of influence (Zou et al. 2002) in case of urea whereas for TMAO greater spatial ordering was found. Therefore, in case of urea faster cooperative hydrogen bond rearrangement

dynamics is observed which arises due to the possible disruption in the extended hydrogen bond layer around urea (Wei et al. 2010; Zou et al. 2002). This reduces the water-water hydrogen bond lifetime compare to the presence of TMAO. There is negligible change in hydrogen bond lifetime for carbonyl oxygens and water molecules (O_g-H_w) in presence of urea with the increase in cosolvent concentration.

Table 2.3: The lifetime (τ_{HB}) of glycine-water and water-water hydrogen bonds (in ps) in the presence of different cosolvents of 2M and 1M concentrations for SPC and 2M concentration for SPC/E water models. *

Species		GW	G UW	GTW	GKCIW	GLiCIW
SPC	O_w-H_w	0.91	0.95 (0.93)	1.18 (1.03)	0.99 (0.95)	1.03 (0.96)
	$H_{ng}-O_w$	0.92	0.96 (0.94)	1.20 (1.04)	1.02 (0.97)	1.05 (0.98)
	O_g-H_w	0.93	0.95 (0.95)	1.31 (1.18)	1.06 (0.99)	1.02 (1.03)
SPC/E	O_w-H_w	0.95	0.99	1.42	1.06	1.10
	$H_{ng}-O_w$	0.99	1.03	1.29	1.07	1.12
	O_g-H_w	0.94	0.98	1.31	1.04	1.07

*The lifetimes (τ_{HB}) of 1M solutions are given in parenthesis.

The lifetime of water-water hydrogen bonds increases in presence of ions due to the presence of strong hydration sphere around the ions. This result is in accordance with Soto et. al. (Rodríguez et al. 2003) where it has been reported to have an increase in the molar volume in presence of ions and a consequent increase of compressibility of glycine (Park and Fayer 2007; Urbic 2014). With increase in concentration of the ions this lifetime further increases due to greater number of ions and their electrostatic field of attraction. Lifetime also increases in case of amine-water hydrogen bond. However, it can be noticed here that negligible change in carbonyl oxygen-water lifetime was found with an increase in concentration especially for LiCl case. This further confirms the fact that Li^+ has a preference towards binding the carbonyl carbon which disrupts the water structure in lower concentrations. On further increase in the concentration, there is negligible change in the water structure. For KCl, some changes in the hydrogen bond lifetimes were observed.

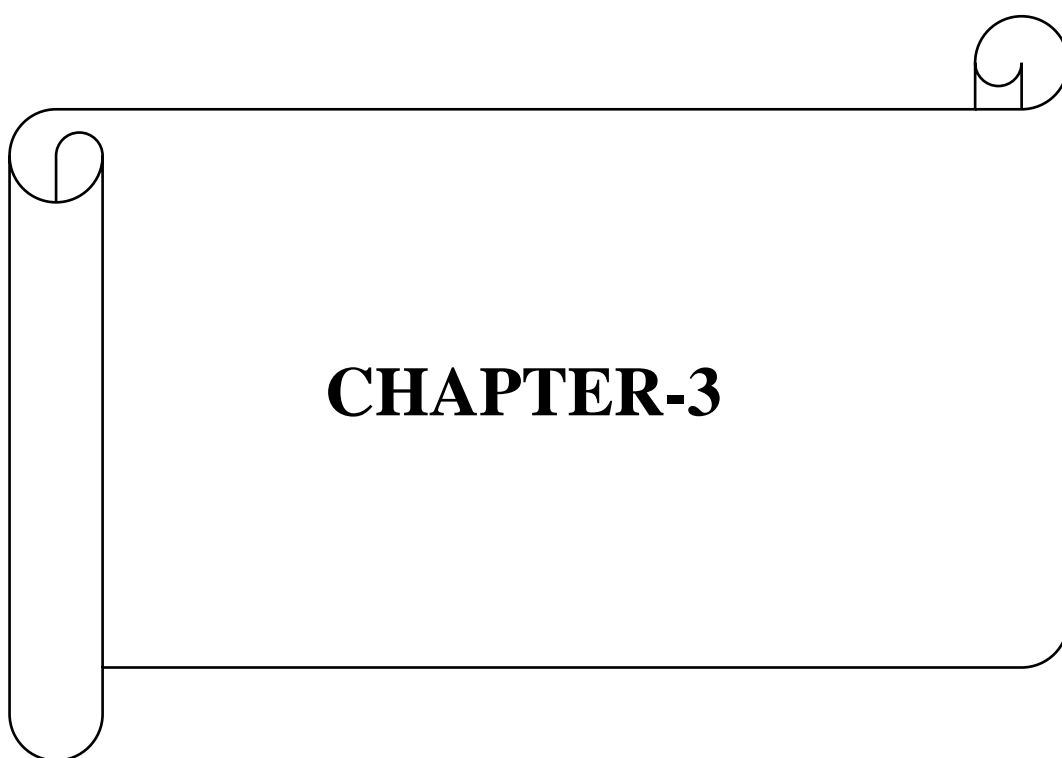
2.4. SUMMARY AND CONCLUSIONS

In this chapter, the structural and dynamic properties of urea, TMAO, KCl and LiCl solutions as a function of cosolvent concentration on zwitterionic glycine using MD simulations are investigated. The structural properties are studied in terms of radial distribution functions, spatial distribution functions and $\langle \text{O-O-O} \rangle$ angle distributions. The potential mean force and hydrogen bond dynamics for these systems at different concentrations are also calculated. TMAO was found to impart more tetrahedrality to the structure of water. The water structure near the N-terminal of glycine was found to be less disrupted than the C-terminal. A compact hydration shell was found for TMAO near the hydrophobic group of glycine which reduces when TMAO is replaced by more charge dense species. However, in ionic systems especially for LiCl, increment in the water density is observed near the hydrophobic unit at higher distances due to the presence of the first solvation shell of Li^+ ion bounded to the carboxylate group of the glycine. This water density actually found to give extra stability to glycine molecule.

When ions are incorporated in the solution, hydration structure around the glycine molecule is significantly modified. Both the ions interfere the first hydration sphere of glycine. Lithium ions showed preference towards binding with carboxylate ions, which displaces water from the first hydration shell of the carboxylate oxygen. This leads to decrease in the hydration number and number of hydrogen bonds near carboxylate ion. The water structure near the carboxylate ion is strongly modified by LiCl giving rise to two extreme peaks in the angular distribution of $\langle \text{O-O-O} \rangle$ near 60° and 120° . These peaks suggest that tetrahedral structures of water molecules are highly disrupted near the C-terminal. Further, the hydrogen bond strength of the water molecules near the surface of glycine are calculated. Addition of the cosolvents found to increase the hydrogen bond strength of water compared to that of pure glycine water. The water-water hydrogen bond strength increases in presence of TMAO whereas, urea showed similar strength of hydrogen bond as that of aqueous glycine. Incorporation of ions increases the hydrogen bond lifetime at the interfaces due to strong electrostatic field.

Finally, to conclude it is found that the hydrophobic hydration plays a role in the protein stability. TMAO which is known to stabilize protein structures are found to form a hydration shell near the hydrophobic unit. The formation of another hydration

shell was observed in case of LiCl due to the presence of the carboxylate group. These hydration shells were found to give some extra stability and have higher hydrogen bond lifetimes. The presence of these hydration shells near the hydrophobic unit is termed as the “Hydrophilicity behaviour of the hydrophobic group”. The anomalous behaviour of lithium ion in comparison to other group I cations can be explained on the basis on the extra stability gained due to the presence of the hydration layer in comparison to the potassium ion. The result also stresses out the fact that the hydrophobic solubility can be attributed as one of the reasons for protein stability. In the next chapter, such effects on another amino acid having more hydrophobic groups are investigated.



CHAPTER-3

CHAPTER 3

ALANINE AND ITS HYDRATION IN PRESENCE OF UREA AND TMAO

Abstract: *This chapter includes classical molecular dynamics simulations to study the effects of two naturally occurring osmolytes, urea and trimethylamine-N-oxide (TMAO) on the solvation structure of hydrophobic moiety of alanine and glycine amino acids. Simulations were carried out at 1M, 2M and 3 M concentration of urea and TMAO and at mixed concentration of 2:1 M ratio of urea:TMAO solutions to observe the changes in water structure near the amino acids due to the presence of cosolvents. The results are analyzed in terms of site-site radial distribution functions (RDF), spatial distribution functions (SDF), number of hydrogen bonds, orientation profile, potential mean force, Kirkwood-Buff (KB) integrals, preferential binding coefficient and hydrogen bond dynamics.*

3.1 INTRODUCTION

Alanine is one of the simplest amino acids like glycine; commonly found in the transmembrane proteins (Senes et al. 2000). The presence of water as hydration layer around the amino acids are crucial for their stability and functions in aqueous solutions. Free energy measurements suggest that the protein backbone plays a key role in governing the scale of protein and the sidechains plays a minor role (Liu and Bolen 1995). The penalty of hydrophobic interactions by transferring a non-polar molecule to water can be reduced or increased based on the model parameters used in the simulation studies (Ganguly et al. 2016; Rodríguez-Ropero et al. 2016; Su et al. 2018). Stability of the proteins results due to fine balance between the protein-water interactions and intramolecular interactions of the functional groups. This stability can be profoundly modulated by the addition of cosolvents (Canchi et al. 2012; Hu et al. 2009; Teng and Ichiye 2019).

Osmolytes such as urea, TMAO effects the stability of biomolecules through direct or indirect mechanism (Canchi and García 2013). TMAO, a naturally occurring amphiphilic osmoprotectant, stabilizes the biomolecules whereas urea destabilizes it (Bennion and Daggett 2004). Mixture of osmolytes that exists in the cells of several organisms, suggests that they have influence on the stability of proteins. At a biologically relevant ratio of 2:1 molar of urea-TMAO ternary

mixture, the denaturing effects of urea is counteracted by TMAO (Bennion and Daggett 2004; Lin and Timasheff 1994; Meersman et al. 2009; Wang and Bolen 1997; Yancey and Somero 1979). It is found that in mixture each osmolytes have insignificant effects on each other and their interactions with the protein molecules are independent of the other's presence (Lin and Timasheff 1994). This ratio is generally found in the tissues of sea creatures in order to maintain the osmotic pressure with the environment (Lin and Timasheff 1994; Yancey and Somero 1980).

Studies proposed both direct and indirect pathways for protein denaturation by urea (Bennion and Daggett 2003; Caballero-Herrera et al. 2005; Daggett 2006; Wei et al. 2010). In the "indirect" process, urea alters the structure of water, acting as a structure breaker which enhances the protein hydration, in contrast; the "direct" mechanism hypothesizes direct interactions with the protein molecule with urea through strong interactions with the sidechains or backbone. Both of these possible pathways contribute towards the denaturation of proteins and are not mutually exclusive. The stabilization of proteins by TMAO is proposed through exclusion of TMAO molecules from the vicinity of protein surfaces or by strengthening the surrounding water structure and hydrogen bond (HB) network (Hunger et al. 2012; Zou et al. 2002). Stabilization also occurs due to direct interactions of the TMAO molecules with the proteins, affecting their stability and structure (Auton et al. 2008; Auton and Bolen 2005; Bolen and Baskakov 2001; Courtenay et al. 2000). Another unique stabilization pathway of TMAO is due to its hydrophilic fragment (Baskakov and Bolen 1998).

All these studies have been done considering only urea-water (Berteotti et al. 2011; Caballero-Herrera et al. 2005; Caffisch and Karplus 1999; Kleinjung and Fraternali 2012; Stumpe and Grubmüller 2007, 2008) or TMAO-water systems (Athawale et al. 2005; Canchi et al. 2012; Cho et al. 2011; Ma et al. 2014; Mondal et al. 2013; Schneck et al. 2013; Su et al. 2017; Teng and Ichiye 2019) . Very few simulation studies have been done where both the effect of urea, TMAO have been considered to explain the stability of the proteins (Paul and Patey 2007a, 2008; Wei et al. 2010; Zou et al. 2002).

Counteraction of the deleterious effects of urea on protein denaturation by TMAO are done through enhancement of water-urea and water-water interactions or through osmolyte-induced conformational changes on protein-water interactions

(Meersman et al. 2009; Wei et al. 2010). TMAO is also found to induce structural modification of water network and water-water interactions (Bennion and Daggett 2004; Daggett 2006). Another proposed mechanism is that TMAO tends to enhance the hydrophobic attraction among nonpolar groups leading to stabilization of the folded states (Mondal et al. 2013; Paul and Patey 2008). However, a conclusive pathway that accounts for the stabilization ability of TMAO and also its counteraction effects on urea remains elusive (Ganguly et al. 2016) and it is highly dependent on the model parameters (Borgohain and Paul 2016; Ganguly et al. 2016; Teng and Ichiye 2019). It is said that urea mainly interacts with the protein backbone and TMAO is excluded from the vicinity of protein due to entropy effect.

In the previous chapter, it is evident that there is an enhancement in the protein stability in presence of cosolvent TMAO due to formation of an extra hydration shell near hydrophobic unit of glycine. Therefore, it would be interesting to find out whether such effect is also visible near the hydrophobic groups in case of alanine that have contributions in imparting stability to the proteins and how the scenario is different in case of urea and the 2:1 M ratio of urea-TMAO ternary mixture. The objective of this present work is to explore the molecular pathway by which proteins gets stabilized in the presence of TMAO and have opposing effects in presence of urea.

Since, proteins are big molecules, presence of more than one factor such as intermolecular hydrogen bonds, disulphide bonds, ion pairs etc., can make difference in showing their effect in protein stabilization. In view of this, simple amino acids alanine and glycine were chosen to consider the effect on the basic entities; i.e., amine, carboxylic and hydrophobic groups. Different solutions of aqueous alanine and glycine amino acids in urea, TMAO and its ternary mixture of urea: TMAO of 2:1 ratio was considered and compared to see the effect of hydrophobic group in explaining the stabilization and destabilization of proteins. MD simulations were carried out using CHARMM36 FF force field; which is used generally in the simulation of proteins to study these effects. It can be noted here that the studies of TMAO as cosolvents is mainly done with Kast (Kast et al. 2003), Neitz (Schneck et al. 2013), Gracia (Canchi et al. 2012) and Shea (Larini and Shea 2013) models and very few studies have done in CHARMM forcefield (Best et al. 2012; Klauda et al. 2010; Lee et al. 2016). As it is evident from the literature survey,

the behaviour of TMAO, urea towards the protein backbone is highly model dependent. Therefore, in this chapter the behaviour of these osmolytes in CHARMM forcefield is studied which is commonly used in studying protein dynamics and see whether it is possible to explain their opposing effects. In this chapter, the results for glycine have been incorporated and discussed to have a comparison with alanine wherever necessary.

3.2 COMPUTATIONAL METHODOLOGY

In order to gain detailed insights on the protein stability in presence of the osmolytes TMAO and urea as cosolvents, classical MD simulations of aqueous alanine and glycine amino acids in binary and ternary osmolyte solutions of urea and TMAO were performed. Alanine, glycine, urea, TMAO and water molecules are characterized by multi-site interaction models. Expression for interaction between inter-atomic sites in these models are given as:

$$u(r_{ij}) = 4\varepsilon_{ij} \left[\left(\frac{\sigma_{ij}}{r_{ij}} \right)^{12} - \left(\frac{\sigma_{ij}}{r_{ij}} \right)^6 \right] + \frac{q_i q_j}{r_{ij}} \quad (3.1)$$

where, r_{ij} is the inter-atomic distance between molecular sites i and j , q_{ij} is the charge of the site i^{th} atom. The LJ parameters ε_{ij} and σ_{ij} are obtained by using combination rules $\sigma_{ij} = (\sigma_i + \sigma_j)/2$ and $\varepsilon_{ij} = \sqrt{\varepsilon_i \varepsilon_j}$, where ε_i and σ_i are the well-depth and LJ diameter parameters for i^{th} atom. The force field parameters for alanine, glycine, urea and TMAO were taken from CHARMM36 FF (Klauda et al. 2010), SPC/E and SPC potential models were considered for water (Berendsen et al. 1981, 1987) which are summarized in Table 3.1.

Simulations were performed with a total of 1024 number of water molecules, zwitterionic alanine, glycine and osmolytes in cubic boxes at 298 K. In Table 3.2, the compositions of aqueous alanine and osmolyte mixtures of different concentrations are tabulated. Atomistic simulations were carried out with GROMACS (v2018.4) MD simulation package (Van Der Spoel et al. 2005). Lennard-Jones electrostatic interactions were treated with the particle mesh ewald (PME) summation method (Darden et al. 1993) with the nonbonded interaction space cut-off of 1.2 nm. Leapfrog algorithm was employed to integrate the equations of motions with integrating time step of 10^{-15} s (1 fs) beside minimum image conventions and periodic boundary conditions (PBC) applied in all spatial

directions. Parrinello-Rahman barostat ($\tau_P = 2.0$ ps) (Parrinello and Rahman 1980) and Velocity-rescale thermostat ($\tau_T = 0.1$ ps) (Bussi et al. 2007) were employed to keep the pressure and temperature constant respectively. LINCS algorithm was employed to keep the bond lengths constrained (Hess et al. 1997).

Table 3.1: The Lennard-Jones parameters and charges used in models for alanine, glycine, urea, TMAO and water. e represents the elementary charge.

Name	Atom	σ (Å)	ϵ (kJ/mol)	Charge (e)
Alanine	N	3.29	0.8360	-0.30
	H	0.40	0.1924	0.33
	C $_{\alpha}$	3.56	0.1338	0.21
	H $_{\alpha}$	2.35	0.0920	0.10
	C $_{\beta}$	3.63	0.3263	-0.27
	H $_{\beta}$	2.38	0.1004	0.09
	C	3.56	0.2928	0.34
	O	3.02	0.5020	-0.67
Urea	C	3.56	0.2928	0.60
	O	3.02	0.5020	-0.58
	N	3.29	0.8368	-0.69
	H	0.40	0.1924	0.34
TMAO	N	3.29	0.8368	-0.83
	O	3.11	0.5020	-0.37
	C	3.94	0.3221	-0.35
	H	1.24	0.1924	0.25

Table 3.2: The system details considered in the simulation. (N_{alanine} , N_{glycine} , N_{urea} , N_{TMAO} , N_{water} represents the corresponding number of alanine, glycine, Urea, TMAO and water molecules in the simulation box).

Sl.No	System	$N_{\text{glycine/alanine}}$	N_{urea}	N_{TMAO}	N_{water}
1	AW	15	0	0	1009
2	AUW (3M)	15	66	0	943
3	ATW (3M)	15	0	66	943
4	AUTW (6:3M)	15	132	66	811
5	GW	15	0	0	1009
6	GUW (3M)	15	66	0	943
7	GTW (3M)	15	0	66	943
8	GUTW (6:3M)	15	132	66	811
9	AUW (2M)	15	44	0	965
10	ATW (2M)	15	0	44	965
11	ATW (4:2M)	15	88	44	877
12	AUW (1M)	15	22	0	987
13	ATW (1M)	15	0	22	987
14	AUTW (2:1M)	15	44	22	943

Different numbers of osmolyte molecules with random orientations were placed in the starting configuration for all the systems rendering different concentrations. At first, each system was subjected to equilibration for 10 ns in the NVT ensemble. Subsequently, NPT ensemble was run for another 10 ns in order to attain an appropriate box length corresponding to 1 atm pressure. Finally, each simulation was run for further 50 ns using NPT ensemble (Allen and Tildesley 1989) and the results are reported.

3.3. RESULTS AND DISCUSSION

The 3-dimensional representations of the amino acid used in this chapter.

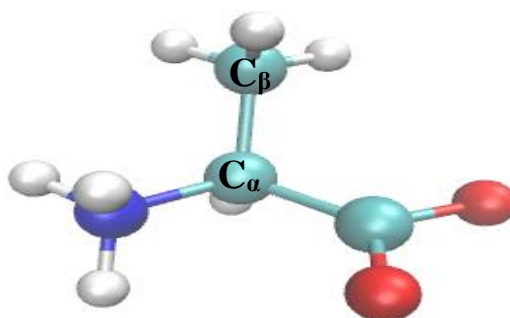


Figure 3.1. The 3-dimensional representation of alanine amino acid considered in this work.

3.3.1 Radial Distribution Functions

The influence of osmolytes on the local structural properties of aqueous alanine and glycine solutions are characterized by various intermolecular alanine-water, glycine-water pair correlation functions. The hydration pattern of water molecules in presence of osmolytes around the alanine molecules are calculated from the intermolecular N_a-O_w , $C-O_w$, $C_\alpha-O_w$, $C_\beta-O_w$, O_a-O_w and O_w-O_w radial distribution functions which are depicted in Figure.3.2.

In case of N_a-O_w (Figure.3.2(a)), the peak height is found to be highest for urea solution and least for TMAO, indicating that more tetrahedral water molecules are bonded to the first coordination shell of N-terminal of alanine in presence of urea, but the second coordination shell is found to be more well defined for TMAO and ternary mixture solutions compared to aqueous alanine-water and urea-water mixtures. This means collapse of the secondary solvation shell near the amine group of alanine in pure alanine-water and in presence of urea. The structural arrangement of water molecules near carbonyl carbon is shown in Figure.3.2(b). The peak height is found to be more in case of mixed urea-TMAO mixture which decreases in the order: mixed urea-TMAO>TMAO>urea.

In case of hydrophobic carbon ($C_\alpha-O_w$), shown in Figure.3.2(c), the first peak height of the ternary mixture and urea are found to be more than aqueous alanine solution and TMAO-water solutions which changes its trend in the second peak. TMAO-water solutions and ternary mixture is found to have bigger and broader second peaks compared to the urea-water solutions suggesting greater

hydration of the hydrophobic moiety and less tetrahedral water. The first peak of water molecules near C_α in presence of urea can be attributed due to the presence of more solvation shell near the amine group. The structural analysis of water molecules in this region can be seen in the subsequent sections.

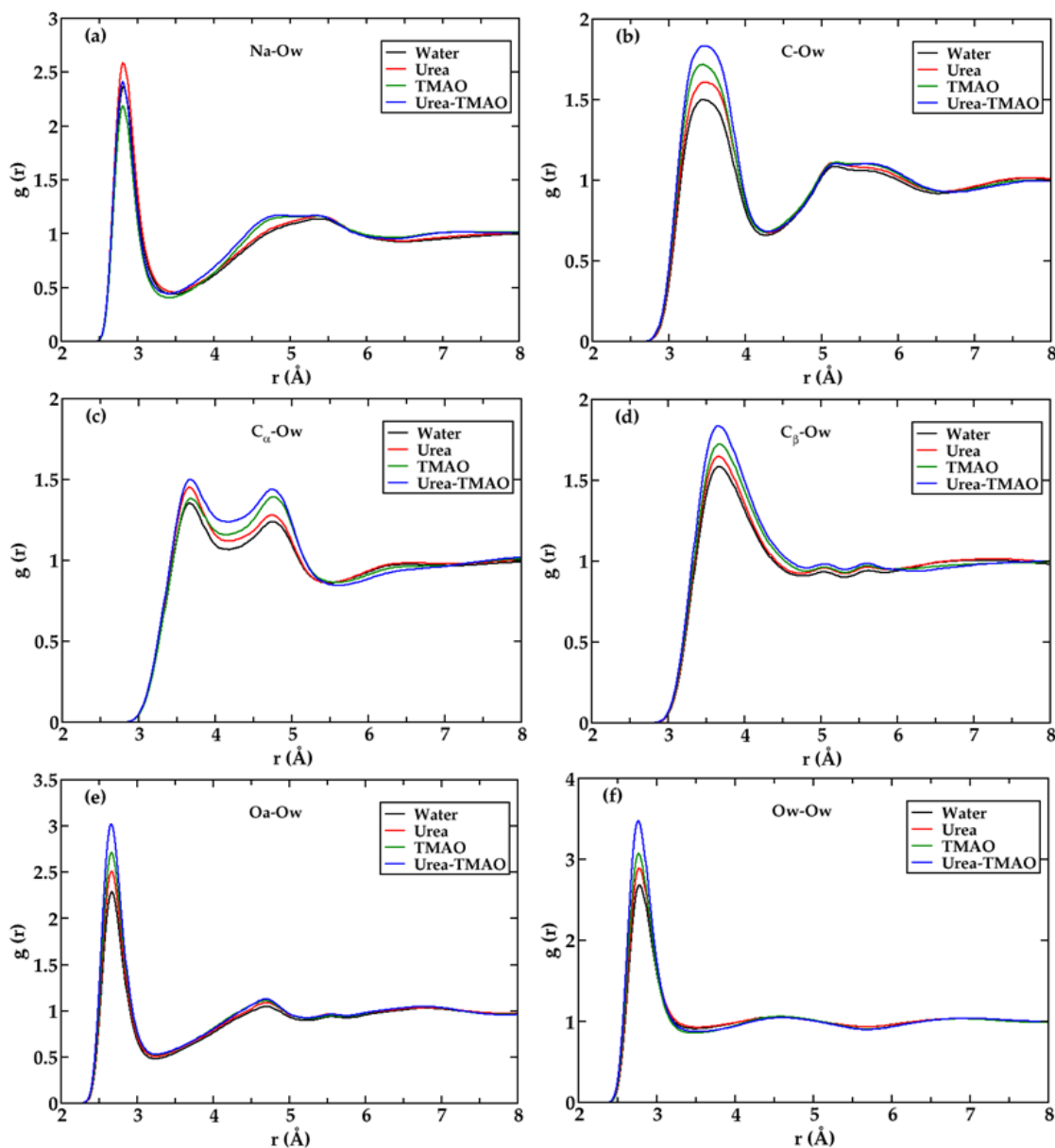


Figure 3.2: Site-site radial distribution functions $g(r)$ of aqueous alanine of different atoms (a) N_α - O_w , (b) C - O_w , (c) C_α - O_w (d) C_β - O_w , (e) O_α - O_w and (f) O_w - O_w in different osmolytes for systems 1-4 in SPC water model.

The positions of maxima of the first peak of C_β - O_w (Figure.3.2(d)) is found to be same for urea-water, TMAO-water and mixed urea-TMAO solutions. However, the peak is found to be bigger and broader for ternary mixture and

TMAO-water. The minima are slightly shifted towards higher distances. Figure.3.2(e) shows the radial distribution function of the carbonyl oxygen with oxygen of water (O_a-O_w). The increase in peak height of the first peak and shallow minima for ternary mixtures indicates rise in water density around carbonyl carbon compared to other cosolvents. Further, on careful observation of O_w-O_w RDF (Figure.3.2(f)), it is found that the second solvation shell is more well defined for TMAO and ternary mixture compared to aqueous alanine solution and urea-water solution. The RDF's consisting of glycine with 3M concentration are given in Figure 3.3. Similar graphs were obtained for alanine-osmolyte solutions of 3M concentration with SPC/E water model, 2M and 1M concentrations with SPC water model which are given in Figures 3.4, 3.5, 3.6 respectively

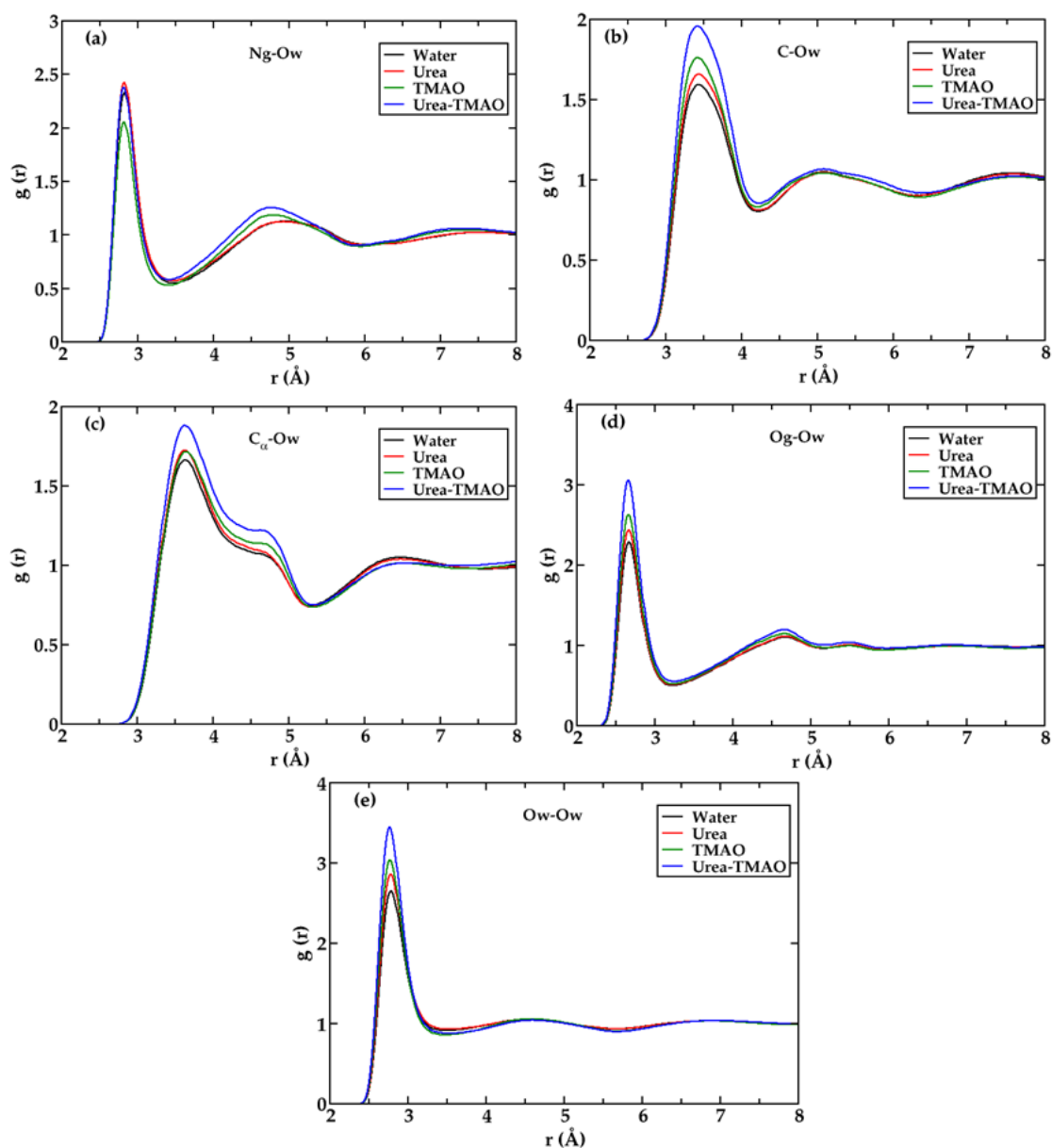


Figure 3.3: Site-site radial distribution functions $g(r)$ of aqueous glycine of different atoms (a) N_g-O_w , (b) $C-O_w$, (c) $C_\alpha-O_w$ (d) O_g-O_w and (e) O_w-O_w in different osmolytes for systems 5-8 in SPC water model.

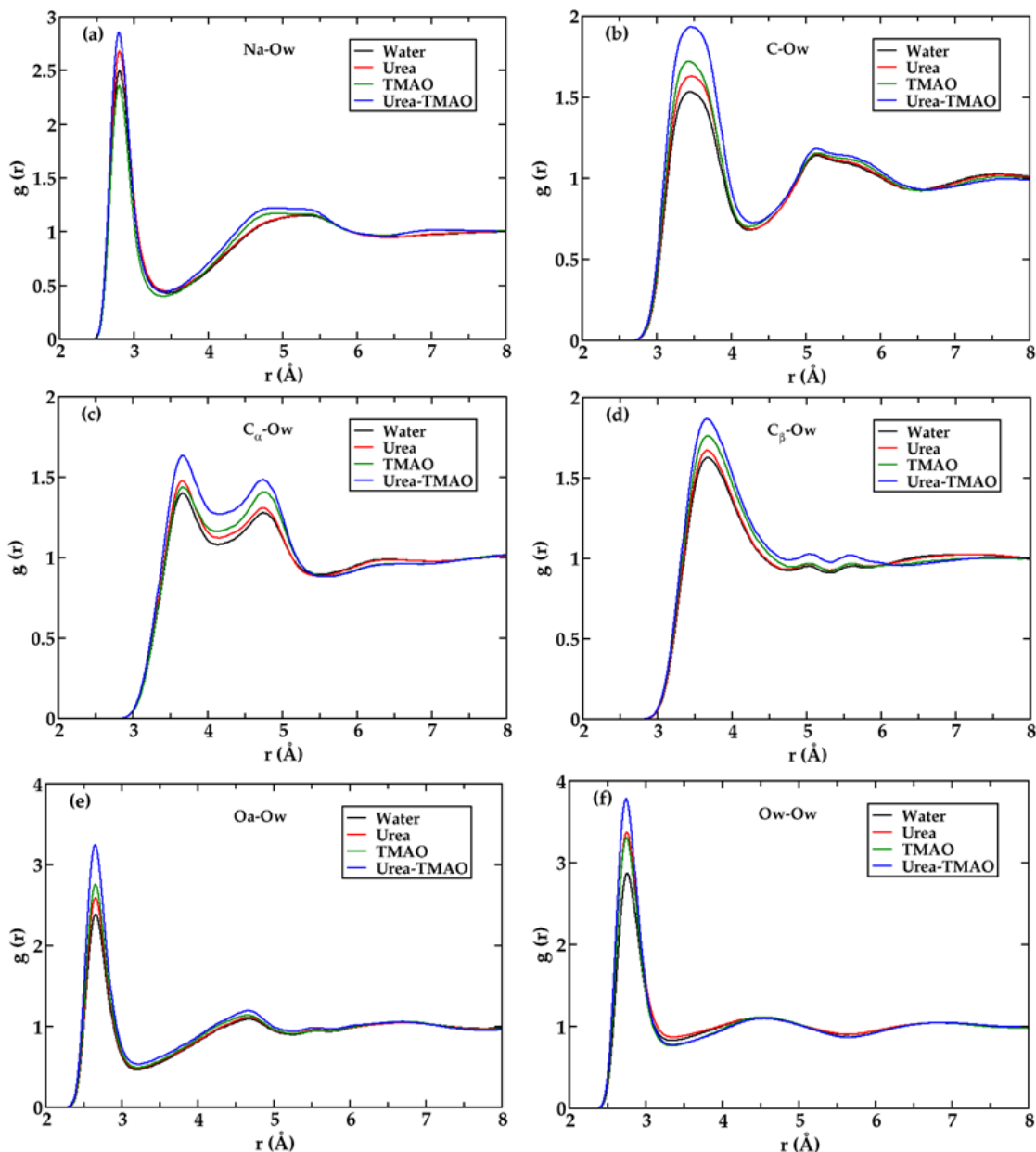


Figure 3.4: Site-site radial distribution functions $g(r)$ of aqueous alanine of different atoms (a) N_a - O_w , (b) C - O_w , (c) C_α - O_w (d) C_β - O_w , (e) O_a - O_w and (f) O_w - O_w in different osmolytes for systems 1-4 in SPC/E water model.

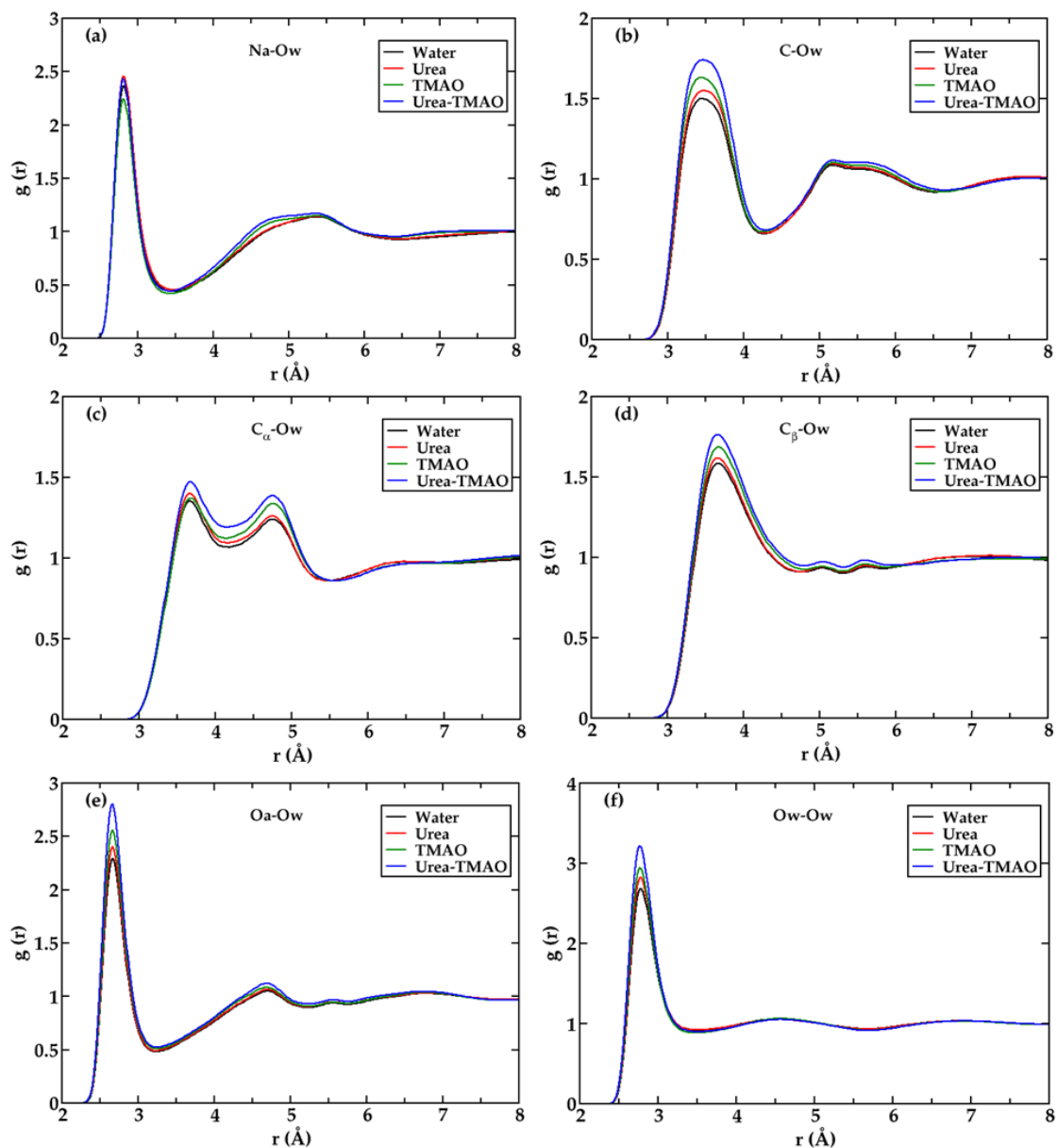


Figure 3.5: Site-site radial distribution functions $g(r)$ of aqueous alanine of different atoms (a) N_a-O_w , (b) $C-O_w$, (c) $C_\alpha-O_w$ (d) $C_\beta-O_w$, (e) $O_\alpha-O_w$ and (f) O_w-O_w in different osmolytes for systems 9-11 in SPC water model.

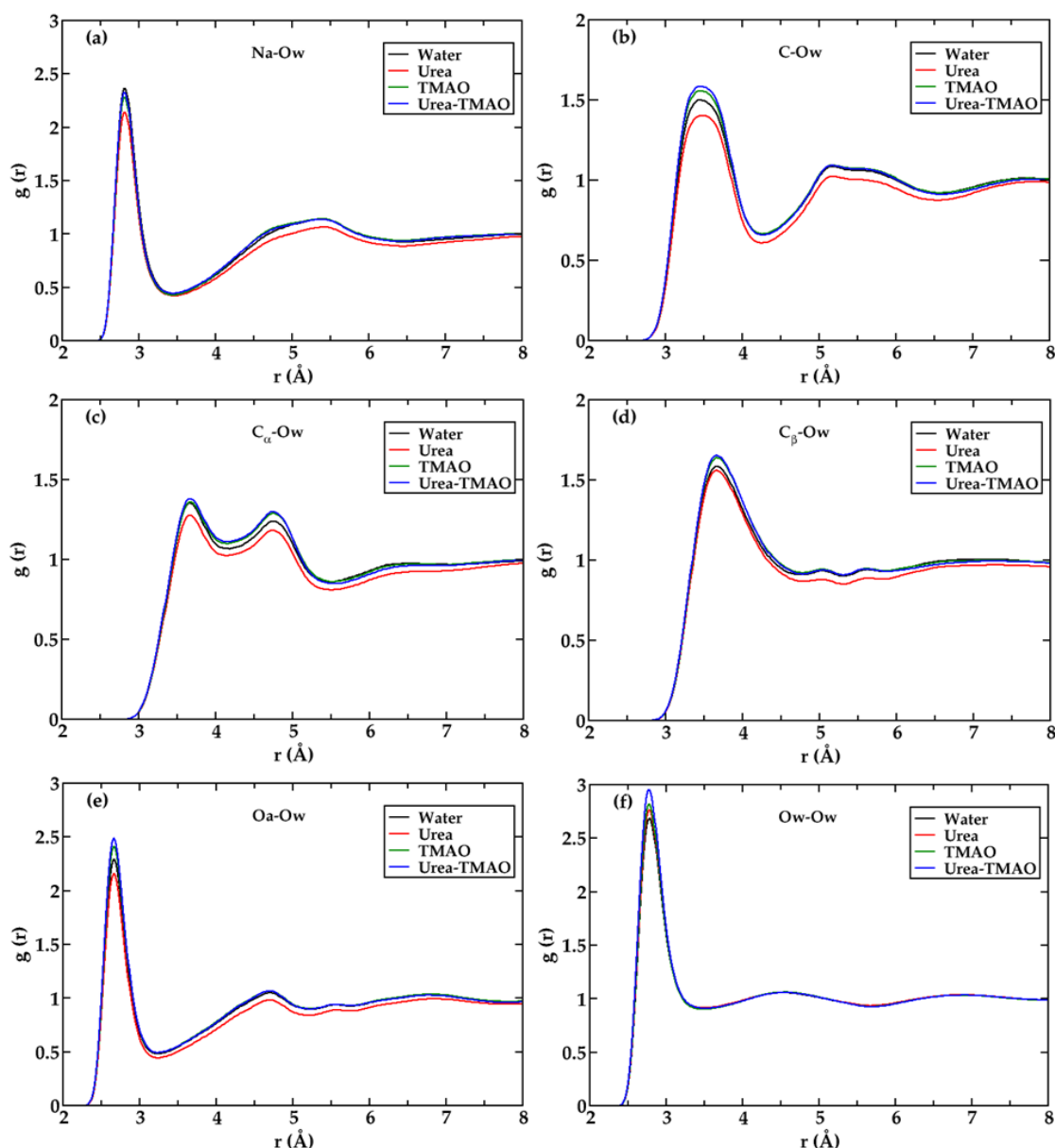


Figure 3.6: Site-site radial distribution functions $g(r)$ of aqueous alanine of different atoms (a) N_a-O_w , (b) $C-O_w$, (c) $C_\alpha-O_w$ (d) $C_\beta-O_w$, (e) O_a-O_w and (f) O_w-O_w in different osmolytes for systems 12-14 in SPC water model.

3.3.2 Spatial Distribution Functions

The spatial distribution functions (SDF's) of oxygen molecules around the central alanine molecule in presence of different osmolytes were calculated with the TRAVIS software package (Brehm and Kirchner 2011). The calculated SDF's of urea-water and TMAO-water are depicted in Figure.3.7. The water densities around the alanine molecule can be distributed in three main regions namely, near the amine group (region I), carbonyl group (region II) and near the hydrophobic unit (region III). It is clearly

visible that the water density near the hydrophobic region (C_α) of alanine i.e., region III is significantly more in case of TMAO than urea. This protective hydration shell near the hydrophobic unit in case of TMAO correlates well with the second solvation shell of $C_\alpha-O_w$ (Figure.3.2(c)) which is very unique.

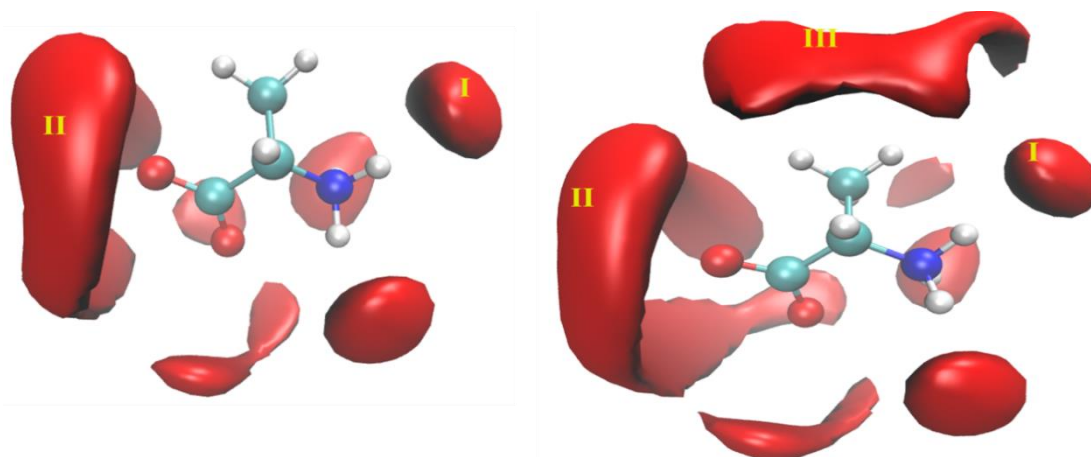


Figure 3.7: SDF of water oxygen around aqueous alanine in presence of osmolytes urea (left) and TMAO (right) considering same isovalues of 39.5.

In comparison with glycine as in previous chapter, it is seen that the water distribution near amine and carboxyl groups remains almost similar whereas, changes are observed near the hydrophobic region. In urea solutions, there is depletion of water molecules near the hydrophobic group with increase in methyl unit of amino acid, whereas the hydrophobic hydration is enhanced in the presence of TMAO solutions.

3.3.3 Number of Hydrogen-bonded Water Molecules

It has been already seen that the solvation structure near the alanine molecules are different in presence of different cosolvents. To gain further insights into the structure of water molecules near the interface of alanine, the fraction (f_n) of oxygen atoms of water molecules that engage in n number of water-water hydrogen bonds have been plotted in Figure.3.8. The distance criteria considered to be hydrogen bonded between two inter oxygen atoms is 3.25 Å. Only the interfacial water molecules were selected which are present within a distance 6.0 Å from amine nitrogen, 5.6 Å from the C_α , 6.1 Å from C_β and 6.6 Å from carbonyl carbon of alanine in the calculations (decided from the RDF's).

In all cases the probability of occurrence of lower coordinated (i.e., one or two coordinated) water molecules are found to be more compared to three and four coordinated water molecules. The effect of addition of osmolytes on the water-water hydrogen bond number is significant compared to aqueous alanine. The fraction of lower coordinated water molecules (f_1) increases with addition of osmolytes, whereas higher coordinated water molecules (f_3 , f_4 and f_5) show the opposite trend suggesting that water loses some of its identical nearest neighbours near the cosolvent surface. The comparatively large enhancement of one coordinated water molecules and the reduction of three, four and five coordinated water molecules can be related to the number of osmolytes/alanine that has been accommodated in the cavities of water molecules.

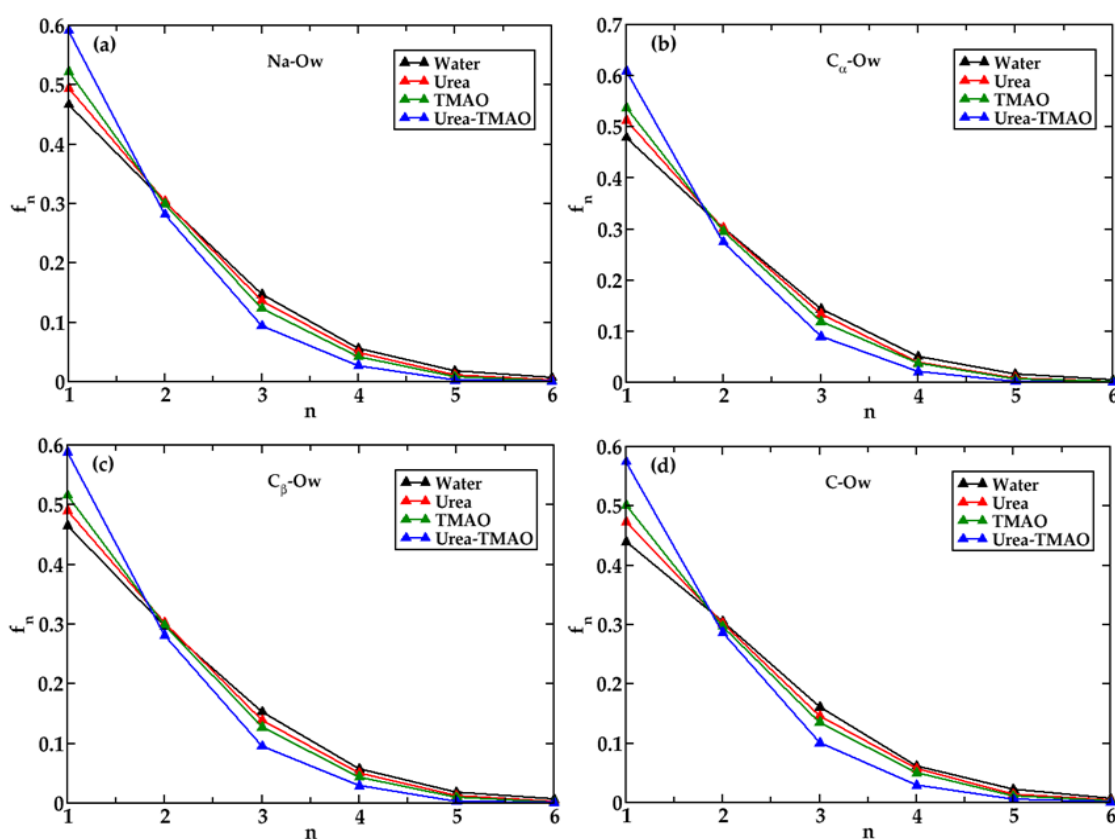


Figure 3.8: The fraction of water molecules having n number of hydrogen bonds within the distances (a) 6.0 Å from amine nitrogen (b) 5.6 Å from C_α (c) 6.1 Å from C_β and (d) 6.6 Å from carbonyl carbon of different alanine-osmolyte solutions.

The osmolytes/alanine preferably replaces water molecules resulting in lesser number of hydrogen bonded water molecules. This effect is more in presence of mixed urea-TMAO solutions which promotes more broken type of hydrogen bonds, then TMAO>Urea>pure alanine water. The trend is found to be similar near the N-terminal, C-terminal and the C_α carbon. Similar trend was found for glycine molecule.

3.3.4 Orientation Profile

To elucidate the tetrahedrality structure of water molecules, the angular distribution function θ_{OOO} of the interfacial water molecules near the interface of alanine has been calculated. In Figure.3.9, the probability distribution $P(\theta_{OOO})$ of the interfacial water molecules near the hydrophobic C_α , C_β and the hydrophilic carbonyl carbon has been plotted. Water molecules up to a distance of 5.6 Å from C_α , 6.1 Å from C_β and 6.6 Å from carbonyl carbon are considered as interfacial molecules for calculations.

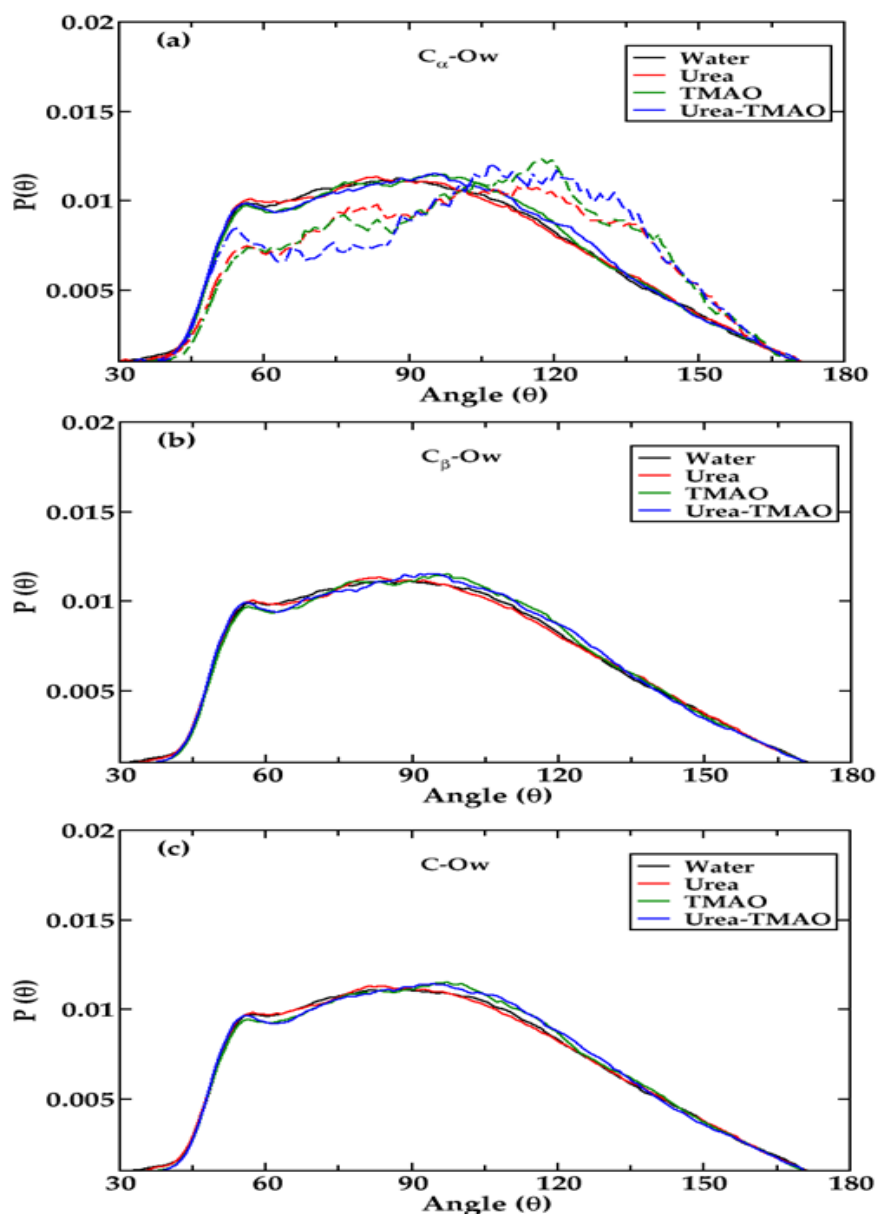


Figure 3.9: Normalized probability distribution of $\langle O-O-O$ angle of oxygen atoms of water molecules which are within the distance (a) 5.6 Å from C_α (b) 6.1 Å from C_β and (c) 6.6 Å from carbonyl carbon for systems 1-4. The dotted lines in (a) represent the region between 4.0 to 5.6 Å from C_α .

In all the cases, it is seen that there is a small peak near 50° and a broad distribution of angles near 104.5° . It is well known that the ideal angle for tetrahedral water is 104.5° . The peaks are found to shift slightly towards the higher angles in case of TMAO and mixed urea-TMAO solutions compared to urea solution and alanine water system. This can be related with the number of hydrogen bond distribution. TMAO and mixed urea-TMAO solutions showed more fraction of broken dimer and trimer water molecules than tetrahedral water. The shift of broad peak towards 120° is due to breaking of tetrahedral network of water at higher distances. The effect is however found to be prominent in case of the interfacial molecules near C_α .

The calculated probability distribution $P(\theta_{OOO})$ of water molecules present near the hump region of the C_α carbon for all the cosolvents, i.e., in the distance range of $4.2\text{--}5.6\text{ \AA}$, corresponding to the shoulder of the first peak and rise of the second peak is shown in Figure.3.9(a). The rise in the second peak seen in the RDF of $C_\alpha\text{-Ow}$ in presence of TMAO and in mixed urea-TMAO solutions mainly consists of more broken hydrogen bonds which contributes towards the higher angles.

3.3.5 Potential Mean Force

The Potentials Mean Force (PMF's) between alanine-water with the help of pair correlation functions, $g(r)$, were computed using the relation:

$$W(r) = -k_B T \ln g(r) \quad (3.2)$$

where r is the inter-atomic separations, k_B is the Boltzmann constant and T is the temperature.

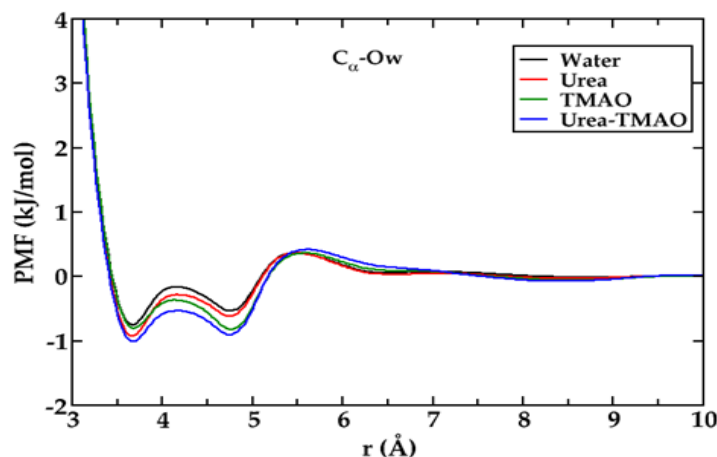


Figure 3.10: PMF depicting the free energies of interaction between hydrophobic carbon C_α of alanine with the water oxygen sites as a continuous function of distance for systems 1-4.

In Figure.3.10 the potentials of mean force are plotted as a continuous function of distance between hydrophobic carbon (C_α) of alanine and the water molecules. It can be seen that; urea is found to have less stabilization energy compared to the ternary mixture and TMAO. This can be related due to the presence of extra hydration shell noticed near the C_α of alanine indicating that the hydrophobic hydration has some contribution towards the stability of the biomolecules.

The entropic and enthalpic contributions in each PMF profile are depicted in Figure 3.10 which are calculated from the finite difference temperature derivative of the PMF or $\Delta G(r)$ at each inter cosolvent separation r (Pettitt and Rossky 1986; Smith and Haymet 1993),

$$-\Delta S(T) = \frac{\Delta G(T+\Delta T) - \Delta G(T-\Delta T)}{2\Delta T} \quad (3.3)$$

MD simulations at 278 K and 318 K were performed in the NPT ensemble to determine the entropic and enthalpic contributions. In this present study, values of T and ΔT are chosen to be 298 K and 20 K respectively. $H(r)$ i.e., enthalpic contribution is computed using the equation given below,

$$\Delta H(r) = \Delta G(r) + T\Delta S(r) \quad (3.4)$$

The entropic $-T\Delta S(r)$ and enthalpic $\Delta H(r)$ contributions to the PMF at 298 K for all the systems under study are shown along with the PMF's.

The entropic and enthalpic contributions to the PMF act in opposite directions to each other and the relative proportion of the two contributions depends on the inter-particle distances. Inter-particle pair state is determined by the balance between the stabilizing enthalpic contribution and the destabilizing entropic contribution. In case of alanine-water, the solvent assisted and solvent separated configurations, enthalpy and entropy contributions are quite significant in magnitude.

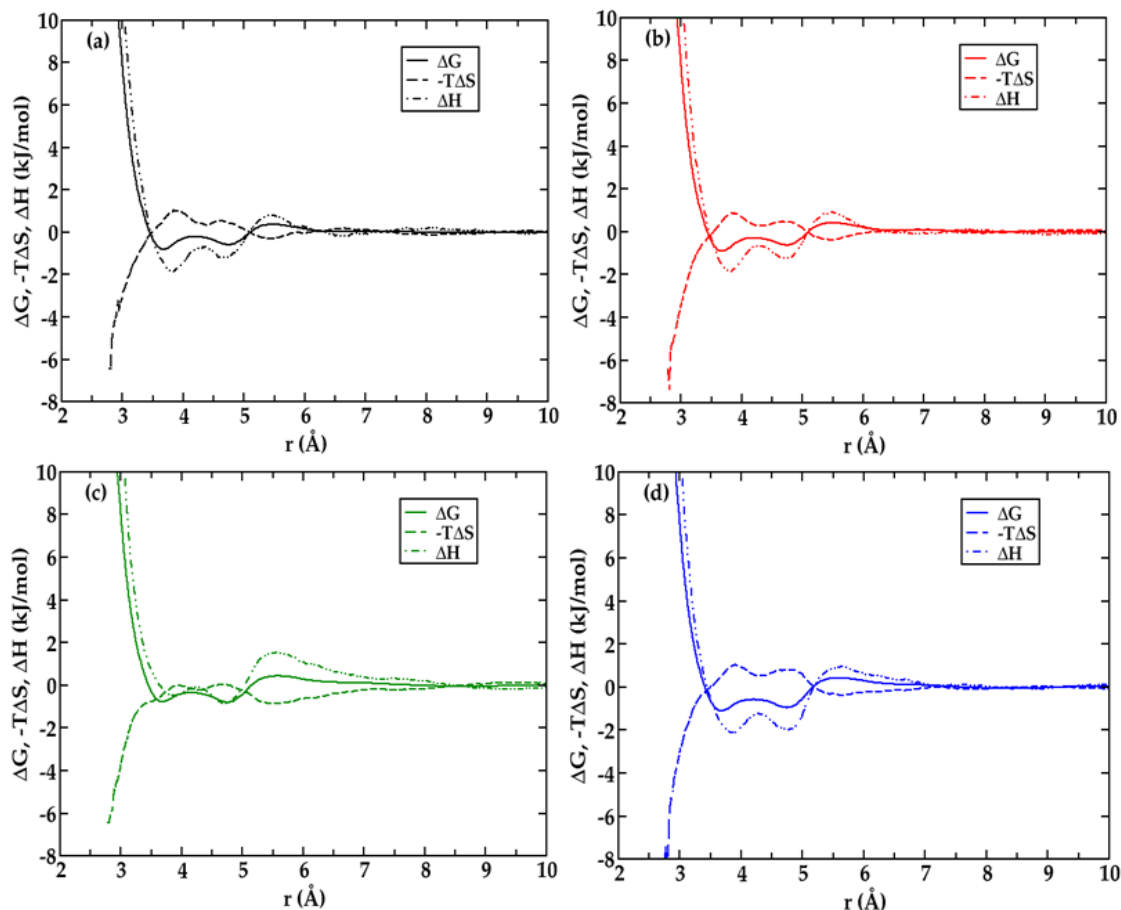


Figure 3.11: Entropic ($-T\Delta S(r)$) and enthalpic ($\Delta H(r)$) contributions to the PMF for alanine (C_{α} -Ow) in presence of different cosolvents a) water b) 3M urea c) 3M TMAO d) 6:3 M urea: TMAO mixtures.

3.3.6 Kirkwood-Buff Integrals

To have an overview of the solvation structure of the alanine molecule with the cosolvents and water, Kirkwood-Buff (KB) integrals (Ganguly et al. 2012; Newman 1994) between water-water, water-osmolytes and protein-osmolytes have been calculated. In this process, the structure of the solution can be related to the thermodynamic properties by using the pair correlation functions. The physical significance of the KB integrals can be viewed as a measure of mutual affinities between the interacting molecular species in a solution. This will give us information about the interactions between the protein-water, water-water and water-osmolytes. The KB integrals between solution components can be expressed using the equation:

$$G_{\alpha\beta} = 4\pi \int_0^{\infty} r^2 [g_{\alpha\beta}(r) - 1] dr \quad (3.3)$$

where, $g(r)$ is the radial distribution function, r is the inter-atomic separations.

A higher value of G_{ij} indicates an overall stronger interatomic attraction between the species i and j (either direct or mediated by other components).

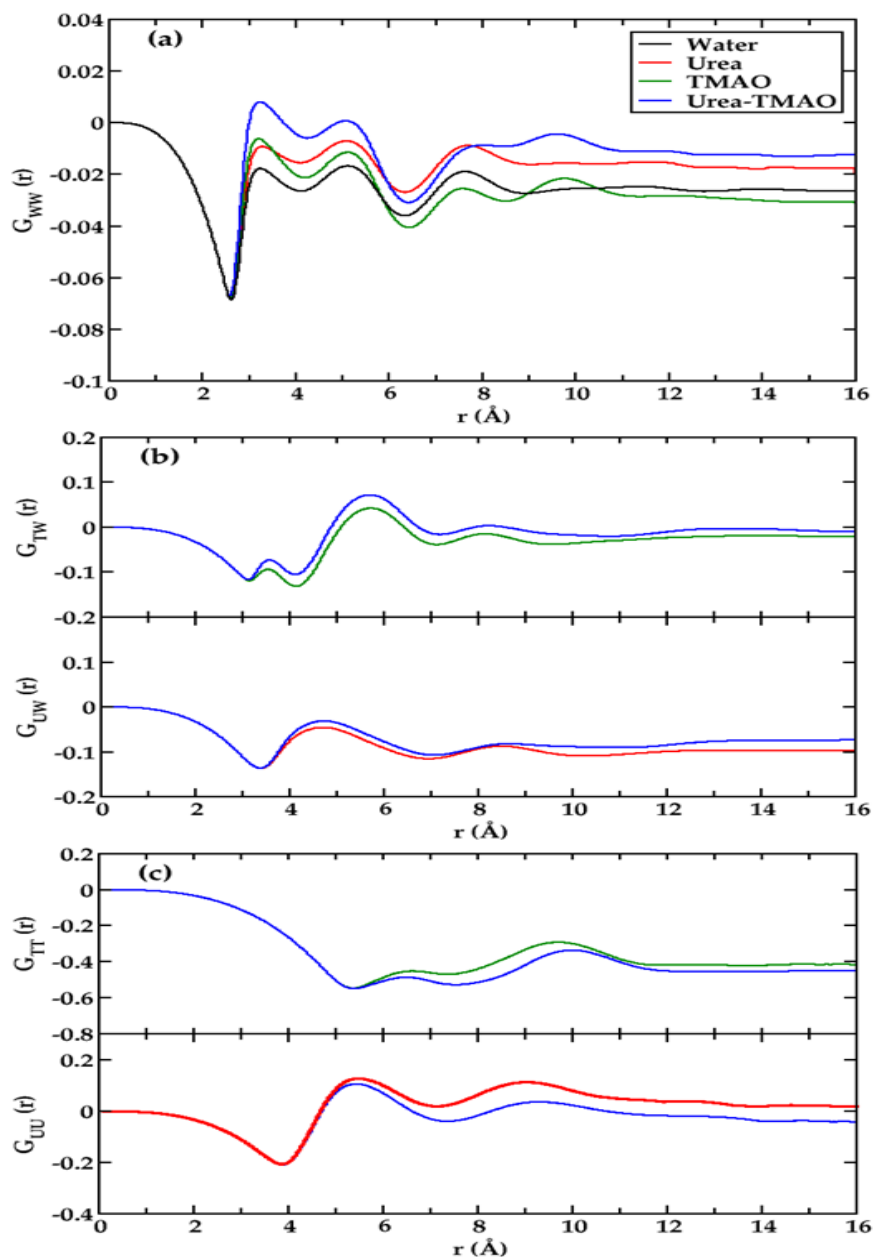


Figure 3.12: Kirkwood-Buff running integrals $G_{ij}(r)$ for (a) water-water (b) osmolyte-water and (c) osmolyte-osmolyte interactions for systems 1-4.

In Figure.3.12, the KB integrals with the correction factor applied in the tail region (Ganguly and van der Vegt 2013; Pierce et al. 2008) for water-water, water-osmolyte and for osmolyte-osmolyte interactions by taking centre of mass as a function of interatomic distance for systems 1-4 are shown. From the graph, (Figure.3.12(a)) it is clear that in the solution water-water association is more in case of ternary mixture. More water-water association is also found in presence of urea in comparison to

TMAO. Further, it can be seen that water-TMAO association is more favoured over water-urea association. From the Figures 3.12(b) and (c), it is clear that urea-urea like to associate more in comparison to TMAO-TMAO. This suggests that in urea-water-alanine system, urea like to aggregate with urea and water with water than urea-water combination.

In presence of TMAO, water-TMAO association is more favourable than water-water, which is again more favourable than TMAO-TMAO association. Similar trend is observed for urea and TMAO in the ternary mixture. Therefore, it can be commented here that water molecules interact with TMAO more favourably than urea molecules. Also, water likes to interact with water molecules in comparison to TMAO-TMAO interactions in a TMAO-water system.

3.3.7 Preferential Binding Coefficient

The stability of proteins being modulated in presence of osmolytes can be quantified via preferential solvation of water or osmolytes with the protein resulting due to the competition between protein-osmolyte and protein-water interactions. These interactions measure the net excess or deficit of species around a particle in a solution. In order to calculate these, the preferential binding coefficient (Pierce et al. 2008) $v_{\alpha\beta}$ between the amino acid-water, amino acid-urea and amino acid-TMAO has been calculated. If solvent water is denoted by subscript 1, amino acid by 2 and osmolyte by 3, then,

v_{21} preferential binding of water to protein, is given by

$$v_{21} = \rho_1(G_{21} - G_{23}) \quad (3.4)$$

v_{23} preferential binding of osmolytes to protein molecule, is given by

$$v_{23} = \rho_3(G_{23} - G_{21}) \quad (3.5)$$

where ρ_3 denotes the osmolyte and ρ_1 denotes the water number densities.

Figure 3.13 depicts the $v_{\alpha\beta}$ values for urea, TMAO and water around amino acids alanine and glycine as a function of distance. The preferential binding behaviour can be detected from the value $v_{\alpha\beta} > 1$ and preferential exclusion of the species can be detected from $v_{\alpha\beta} < 1$ region. It can be easily seen that the $v_{\alpha\beta}$ values for amino acid-water is more compared to amino acid-osmolytes. This suggests that water is preferentially favoured over other solvents near amino acids surface. Further, it can be noted that both TMAO and urea are excluded from the amino acids surface. The $v_{\alpha\beta}$

values for amino acid-TMAO is slightly lesser than that of amino acid-urea. The $v_{\alpha\beta}$ values for amino acid-water in presence of TMAO is found to be more compared to urea. This implies that water-amino acids interaction is more favoured in presence of TMAO solutions compared to that of urea solutions and both urea and TMAO are excluded from the amino acids surface. Therefore, the $G_{\alpha\beta}$ values of the solution and the $v_{\alpha\beta}$ values of the amino acids interface suggests that TMAO which is a stabilizing agent encourages protein hydration which is lacking in case of urea-water system. Also, there is an increment in the intermolecular (TMAO-water) interaction in presence of TMAO. In case of urea, favourable intramolecular (urea-urea, water-water) association was observed. It would be interesting to check the strength of the hydrogen bond lifetime in these solutions to further confirm the fact.

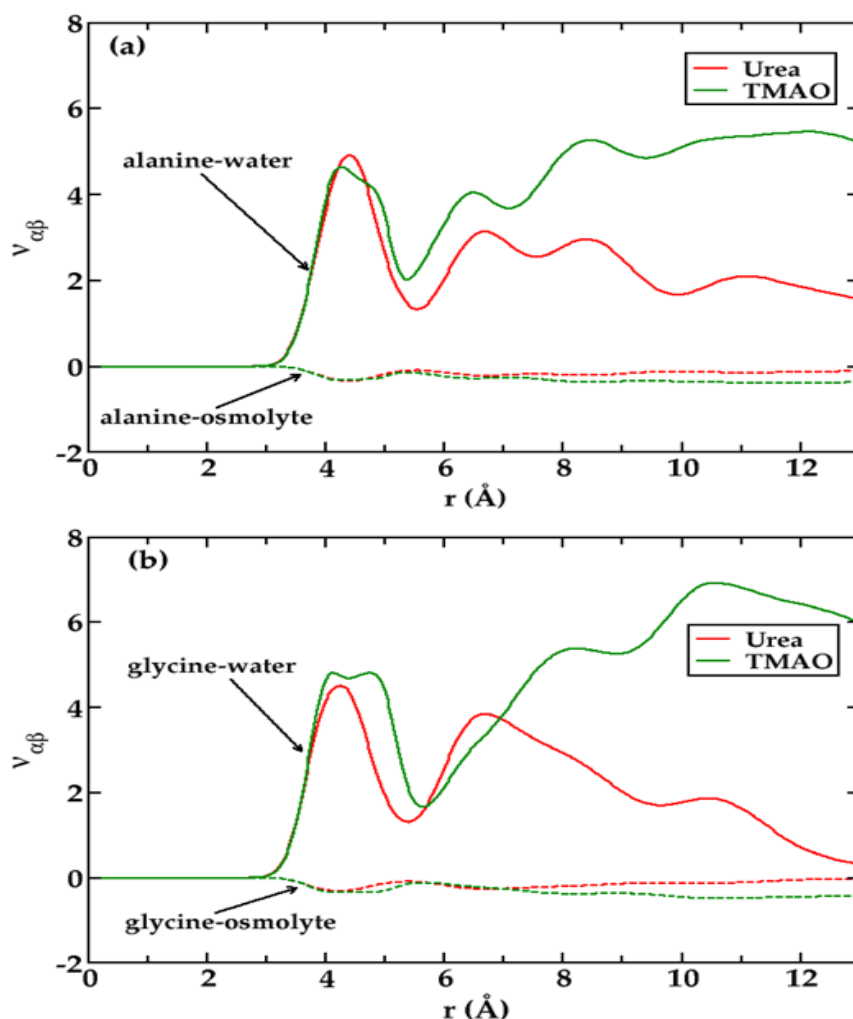


Figure 3.13: Preferential binding coefficients $v_{\alpha\beta}$ for (a) alanine-water, alanine-osmolytes and (b) glycine-water, glycine-osmolytes in 3M aqueous solutions of urea and TMAO as a function of distance.

3.3.8 Hydrogen Bond Dynamics

As evident in the previous section, water has an important role in the solvation structure of the protein molecule; it will be interesting to study the hydrogen bond dynamics of water molecules in different cosolvent systems. The distance between hydrogen bond donor and acceptor pairs are defined to be hydrogen bonded if the interatomic distance is $< 2.5 \text{ \AA}$. The average continuous lifetimes of hydrogen bond population is calculated as (Chandra 2000; Luzar and Chandler 1996; Rapaport 1983)

$$S_{HB}(t) = \frac{\langle h(0)H(t) \rangle}{\langle h(0)^2 \rangle} \quad (3.6)$$

where $\langle \dots \rangle$ denotes the average over all pairs of a given type. The population parameter $h(t) = 1$ if a particular hydrogen bond between two molecules exists from time $t=0$ to $t=t$ or zero otherwise. The hydrogen bond lifetime of water-water (O_w-H_w), alanine-water (O_w-H_{na} and O_a-H_w), urea-water (O_u-H_w), TMAO-water (O_t-H_w) and urea-TMAO (O_t-H_u) are given in Table 3.3.

It can be seen that addition of osmolytes increases the hydrogen bond lifetime of the system. The hydrogen bond lifetime is found to be more in presence of ternary urea-TMAO mixtures for all cases followed by TMAO, urea, aqueous alanine solutions. In general, SPC/E water model exhibits higher hydrogen bond lifetimes compared to SPC water model. Higher lifetimes between carbonyl oxygen and water were found when compared to amine-water interactions in all the cases indicating stronger interaction of the water molecules with the carbonyl group as compared to amine group. It is clearly evident from Table.3.3, that addition of TMAO increases the hydrogen bond lifetime of the solutions.

The stabilization of water hydrogen bonding network by TMAO has pivotal role in counteracting the denaturing effects of urea. The higher lifetime of TMAO-water (O_t-H_w) can be attributed due to significant partial charges located on the oxygen atom (Stirnemann et al. 2010). The TMAO-water hydrogen bond lifetime in ternary urea-TMAO mixture is found to be three times higher than water-water and water-urea hydrogen bond lifetime. The hydrogen bond lifetime of water-water and urea-water increases in the ternary mixture compared to normal urea-water system (Teng and Ichiye 2019). This strengthening of water hydrogen bonds in presence of TMAO can be related to the stability imparted to protein molecules.

Table 3.3: The lifetime (τ_{HB}) of hydrogen bonds (in ps) formed by alanine and glycine amino acids with water and osmolytes for SPC/E and SPC water models for systems 1-8. * Lifetimes for SPC/E water models are given in parenthesis.

Species	AW	AUW	ATW	AUTW
O _w -H _w	0.60 (0.89)	0.65 (0.94)	0.93 (1.42)	1.03 (1.60)
O _w -H _{na}	0.98 (1.19)	1.08 (1.31)	1.36 (1.76)	1.66 (1.80)
O _a -H _w	1.40 (1.70)	1.57 (1.99)	1.86 (2.50)	2.23 (2.97)
O _u -H _w	----	0.72 (0.89)	----	1.13 (1.43)
O _t -H _w	----	----	3.61 (5.13)	3.87 (5.72)
O _t -H _u	----	----	----	0.92 (0.91)
O _w -U _H	----	0.23 (0.25)	----	0.30 (0.32)
Species	GW	GUW	GTW	GUTW
O _w -H _w	0.60	0.64	0.91	1.04
O _w -H _{ng}	0.67	0.71	0.92	1.00
O _g -H _w	1.26	1.34	1.74	2.02
O _u -H _w	----	0.70	----	1.06
O _t -H _w	----	----	3.46	3.99
O _t -H _u	----	----	----	0.70
O _w -U _H	----	0.23	----	0.29

3.4. SUMMARY AND CONCLUSIONS

In this study, the effects of TMAO, urea and their ternary mixture on the solvation structure of alanine and glycine amino acids have been examined to explain the stability aspect of TMAO and denaturing effect of urea. Structural properties were studied in terms of radial distribution functions, spatial distribution functions, number of hydrogen bonds, <O-O-O angle distributions, potentials of mean force and kirkwood-buff integrals. It is found that in presence of TMAO, amino acids are solvated by water more in comparison to the aqueous and urea solutions.

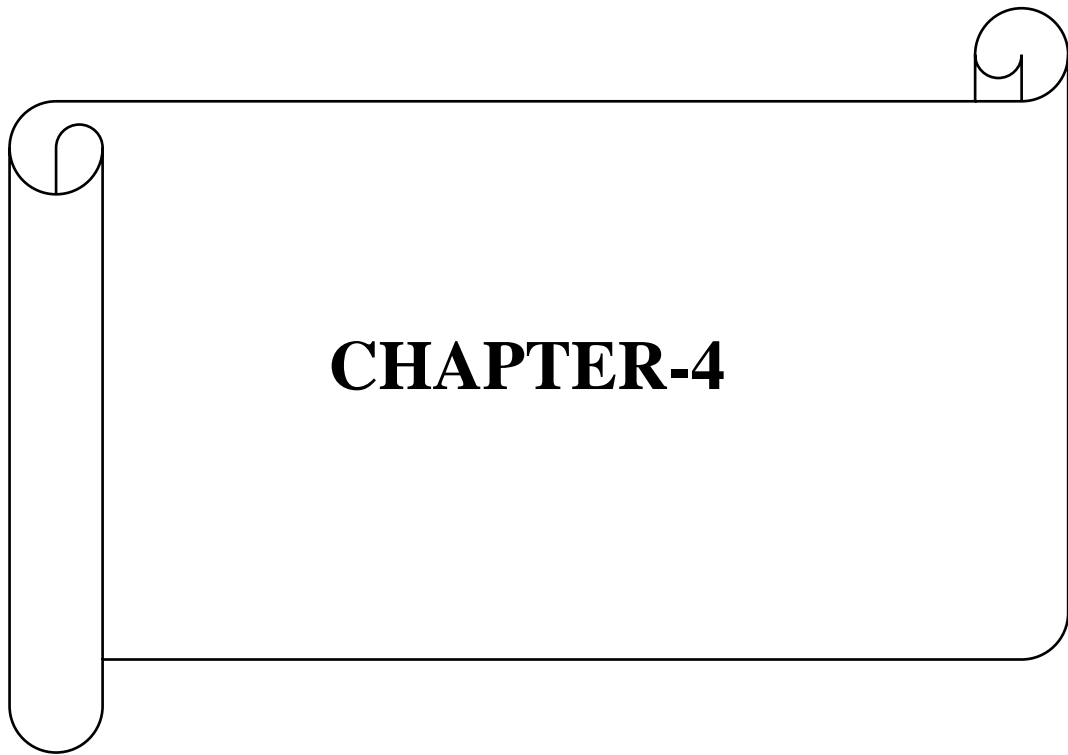
Specially, near the hydrophobic groups, an extra hydration shell is observed. This hydration shell results mainly from the strong hydration shell of the neighbouring polar groups i.e., the carbonyl carbon and the amine group of the biomolecule. The water molecules near the alanine interface mainly consists of broken hydrogen bonds which were found to increase on addition of osmolytes. This broken hydrogen bonds are mainly composed of dimer and trimer water molecules. This is also reflected in the $\langle \text{O-O-O} \rangle$ angle distribution. The $\langle \text{O-O-O} \rangle$ angle distribution shifts towards the higher angle due to the loss of tetrahedrality of the water molecules near the C_α carbon. It can be commented here that these effects were more visible in case of C_α carbon compared to the C_β carbon. Potentials of mean force showed that presence of these water molecules actually imparts stability to alanine.

To shed light on the solvation structure of the solution, KB integrals and preferential binding affinity, $\nu_{\alpha\beta}$ of the amino acids with water and cosolvents were examined. In urea solution, the urea-urea and water-water association is found to be more favoured than urea-water association; whereas in case of TMAO solutions, the water-water and TMAO-TMAO association is less favoured than water-TMAO interactions. Similar trend was found for ternary mixture of urea-TMAO. It is also found that near the alanine interface, water is preferentially favoured over the presence of other cosolvents.

The hydrogen bond strength near the surface of alanine are increased on addition of osmolytes. Addition of TMAO was found to increase the hydrogen bond lifetime of the system. The TMAO-water ($\text{O}_T\text{-H}_w$) bond was found to be the strongest bond due to the polar oxygen of TMAO. The water-TMAO interaction actually increases the corresponding hydrogen bond life time of water-water and water-urea life time in a ternary solution compared to normal water-urea and aqueous water-biomolecule system.

In conclusion, TMAO is found to impart stability to the biomolecules by increasing the hydration shell and strengthening the hydrogen bond network of the solution. In urea solution, this protective hydration shell is missing and less interaction between the solvent molecules and the protein is found. The extra hydration shell in presence of TMAO is strikingly observed more near the hydrophobic group of the biomolecules. Further, TMAO-water has the highest hydrogen bond lifetime which also increases the hydrogen bond lifetime of water-water and water-urea in case of ternary

mixture. This could be the possible reasons for the stability of proteins in presence of TMAO and also in ternary mixture. In the next chapter, peptides are considered as a system to study the solvation structure near the hydrophobic unit and how they add up to the stability of the system.



CHAPTER-4

CHAPTER 4

SOLVATION STRUCTURE OF N-METHYLACETAMIDE AND ACETAMIDE IN PRESENCE OF OSMOLYTES

Abstract: *This chapter includes MD simulations to study effects of osmolytes- urea and trimethylamine-N-oxide (TMAO) and its 2:1 M ratio of urea:TMAO solutions on the solvation structure of acetamide and N-methylacetamide (NMA). Simulations were carried out at 3 M concentration of urea and TMAO and at mixed concentration of 2:1 M ratio of urea:TMAO solutions to observe the changes in water structure near the amides sub-units in presence of cosolvents. The results are analyzed in terms of site-site radial distribution functions (RDF), spatial distribution functions (SDF), number of hydrogen bonds, orientation profile, potential mean force, preferential binding coefficient and hydrogen bond dynamics.*

4.1 INTRODUCTION

In the previous chapters, effects of cosolvents on simple amino acids and their relation with the stability has been investigated. In this present chapter, effects of osmolytes on amides (acetamide and N-methyl acetamide) have been investigated. Amides can be used as model systems for studying complex biomolecular systems which are analogous to the functional groups present in polypeptides and proteins (Greenberg et al. 2000; Zabicky 1970). The structures and properties of biological systems are determined by the molecular interactions of the functional groups. Therefore, understanding the interactions of these groups with each other and with the surrounding solvent molecules, will give information regarding the stability of the native structure of proteins (Akiyama 2002; Johnson et al. 2010; Pattanayak et al. 2014; Pattanayak and Chowdhuri 2011; Sitkoff and Case 1997). The microscopic description of the solute–solvent interactions in aqueous solutions of amides are of specific interest (Ludwig 2000), since they represent a suitable model for studying of both hydrophobic and hydrophilic interactions in peptides and proteins (Baker and Hubbard 1984; Kuntz and Kauzmann 1974; Yang et al. 2009).

In amide-water complexes, there are two major types of intermolecular hydrogen bonds which are $C=O\cdots H-O-H$ and $N-H\cdots OH_2$ (Hagler et al. 1974; Lii and Allinger 1998). Both these hydrogen bonds play important role in maintaining the

stabilities of the secondary and tertiary structures of proteins in aqueous medium and have been studied by *ab initio* molecular dynamics (Dixon et al. 1994; Mirkin and Krimm 1991; Radom and Riggs 1982) and molecular mechanics methods (Baudry and Smith 1994; Kang 2000; Langley and Allinger 2003). Methylation at carbonyl carbons or at the amide nitrogen atoms of formamide have various effects on its properties (Cordeiro et al. 2006; Eberhardt and Raines 1994; Panuszko et al. 2008). The weak C-H...O interactions exists widely in many biological systems such as peptides, nucleic acids and proteins which plays significant role in the stabilization of the complexes and in the activity of biological macromolecules (Lei et al. 2003; Musah et al. 1997; Sitkoff and Case 1997).

Aqueous acetamide mixture helps in understanding the degree of solvation and reaction rates of the amide group (Assarsson and Eirich 1968). N-methyl acetamide (NMA) on the other hand holds special status as an ideal model because of the presence of the peptide linkage containing a single peptide group (O=C-N-H) terminated by methyl moieties on the carbonyl carbon. Many studies on its structural details have been carried out (Allen et al. 1979; Allison et al. 2006; Drakenberg and Forsén 1971; Fillaux and Baron 1981). As it is evident from the previous chapters that there is a probability of finding an extra hydration shells near the C_α carbon of the amino acids in presence of TMAO which further gives some extra stabilization, a comparative study of acetamide and NMA will be interesting in this case where the hydrogen in acetamide is substituted by the methyl moiety near N atom in NMA to see the effect of the presence of extra methyl group to the stability of the amides and also their influence on the water structure around the amide molecule.

As pointed out earlier, TMAO plays significant role in the determination of protein folding and it helps to manage the environmental stress against the cellular components of proteins (Baskakov and Bolen 1998; Daggett 2006; Khan et al. 2011; Liu and Bolen 1995; Meersman et al. 2009; Wei et al. 2010; Yancey et al. 1982b; Yancey 2005; Zou et al. 2002). Osmolytes like urea, TMAO have contrasting actions (Bennion and Daggett 2003; Caballero-Herrera et al. 2005; Canchi and García 2013; Liao et al. 2017; Yancey and Somero 1979). In view of this, model peptide N-methyl acetamide (NMA) and acetamide were considered in this chapter to investigate the effect of cosolvents on the four subunits: amine group, carboxylic group, hydrophobic group and the amide linkage. Microscopic studies on these amides in aqueous solutions

of urea, TMAO and its ternary mixtures will give important insights into the understanding of several factors responsible for protein stability.

The main objective is to explore how the placement of hydrophobic (-CH₃) units near the nitrogen affects the structure of water near the amide moiety and whether there is presence of any extra hydration shell near the hydrophobic unit as observed in the previous chapters in presence of TMAO; if so, how it is stabilizing the molecule. These studies are done in presence of cosolvents like urea, TMAO and 2:1 M ratio of urea:TMAO ternary mixtures.

4.2 COMPUTATIONAL METHODOLOGY

MD simulations of acetamide and NMA in pure water as well as in aqueous binary and ternary osmolyte solutions of urea and TMAO were performed to gain insights on the protein stability in presence of cosolvents. All the biomolecules and osmolytes are characterized by multi-site interaction models. The expression for interaction between two atomic sites in these models is given as:

$$u(r_{ij}) = 4\varepsilon_{ij} \left[\left(\frac{\sigma_{ij}}{r_{ij}} \right)^{12} - \left(\frac{\sigma_{ij}}{r_{ij}} \right)^6 \right] + \frac{q_i q_j}{r_{ij}} \quad (4.1)$$

where, r_{ij} is the inter-atomic distance between molecular sites i and j , q_{ij} is the charge of the site i .

The LJ parameters ε_{ij} and σ_{ij} are obtained by using combination rules $\sigma_{ij} = (\sigma_i + \sigma_j)/2$ and $\varepsilon_{ij} = \sqrt{\varepsilon_i \varepsilon_j}$, where ε_i and σ_i are the well-depth and LJ diameter parameters for i^{th} atom. The force field parameters for NMA, acetamide, osmolytes were taken from CHARMM36 FF (Klauda et al. 2010), SPC/E potential model was considered for water (Berendsen et al. 1981, 1987) which are summarized in Table 4.1. Simulations were performed with a total of 1024 number of water molecules, acetamide, NMA and osmolytes in cubic boxes at 298 K. In Table 4.2, the compositions of aqueous acetamide, NMA with varying compositions of osmolytes are tabulated. Atomistic simulations were carried out with GROMACS (v2018.4) MD simulation package (Van Der Spoel et al. 2005). LJ interactions were treated with the particle mesh ewald (PME) summation method (Darden et al. 1993) with the nonbonded interaction space cut-off of 1.2 nm. LINCS algorithm was employed to keep the bond lengths constrained (Hess et al. 1997). Leapfrog algorithm was employed to integrate the equations of motions with integrating time step of 10^{-15} s

(1 fs) beside minimum image conventions and periodic boundary conditions (PBC) applied in all spatial directions. Parrinello-Rahman barostat ($\tau_P = 2.0$ ps) (Parrinello and Rahman 1980) and Velocity-rescale thermostat ($\tau_T = 0.1$ ps) (Bussi et al. 2007) were employed to keep the pressure and temperature constant respectively.

Table 4.1: The Lennard-Jones parameters and charges used in models for NMA and acetamide. e represents the elementary charge.

Name	Atom	σ (Å)	ϵ (kJ/mol)	Charge (e)
Acetamide	CH ₃	3.56	0.4602	0.55
	H(CH ₃)	2.38	0.100	0.09
	C	3.65	0.3260	-0.27
	O	3.02	0.502	-0.55
	N	3.29	0.8360	-0.62
	H(N)	0.40	0.1924	0.32
NMA	CH ₃ (C)	3.65	0.3263	-0.27
	H(CH ₃)	2.38	0.1000	0.09
	C	3.56	0.4602	0.51
	O	3.02	0.5020	-0.51
	N	3.29	0.8368	-0.47
	H(N)	0.40	0.1924	0.31
	CH ₃ (N)	3.65	0.3263	-0.11

Table 4.2: The system details considered in the simulation. (N_{Ace} , N_{NMA} , N_{urea} , N_{TMAO} , N_{water} represents the corresponding number of acetamide, NMA, urea, TMAO and water molecules respectively in the simulation box).

Sl. No	System	$N_{\text{Ace/NMA}}$	N_{urea}	N_{TMAO}	N_{water}
1	AceW	15	0	0	1009
2	AceUW (3M)	15	66	0	943
3	AceTW (3M)	15	0	66	943
4	AceUTW (6:3M)	15	132	66	811
5	NMAW	15	0	0	1009
6	NMAUW (3M)	15	66	0	943
7	NMATW (3M)	15	0	66	943
8	NMAUTW (6:3M)	15	132	66	811

All molecules were initially placed with random orientations with varying number of osmolytes and water molecules rendering different concentrations. Initially each system was equilibrated for 10 ns in canonical ensemble, followed by NPT ensemble for another 10 ns to obtain appropriate box size and pressure. Subsequently, production runs were carried out for further 50 ns using NPT ensemble (Allen and Tildesley 1989) and the results are reported.

4.3. RESULTS AND DISCUSSION

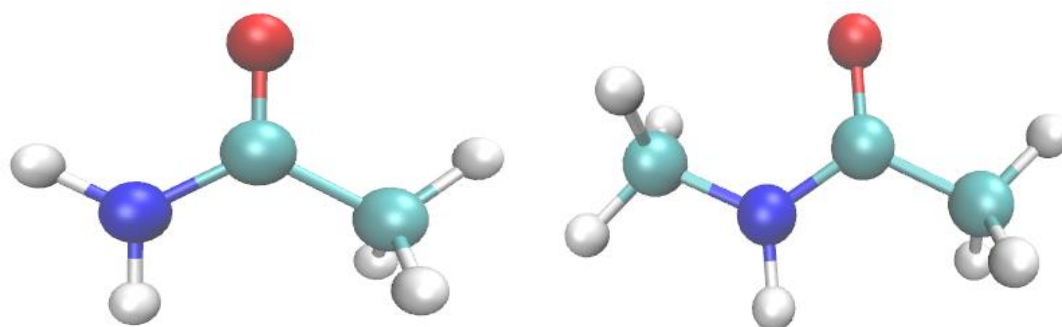


Figure 4.1. The 3-dimensional representation of acetamide (left) and N-methyl acetamide (right) considered in this work.

4.3.1 Radial Distribution Functions

The osmolytes induced changes on the local structural properties of aqueous amide solutions and its solvation behaviour are characterized by intermolecular amide-water pair correlation functions. The solvation structure of amides and the distribution of water molecules around it are shown through various site-site radial distribution functions.

In Figure 4.2, the site-site radial distribution functions $g(r)$ of nitrogen-water ($N-O_w$), carbonyl carbon-water ($C-O_w$), methyl carbon-water ($Me(C)-O_w$) and water-water (O_w-O_w) of acetamide in different osmolyte solutions are plotted. The enhancement of peak heights in presence of TMAO and ternary mixtures are seen in all the cases suggesting an improved hydration of acetamide moieties. A small hump near the minima of first solvation shell is observed both in case of C_α carbon ($Me(C)-O_w$) and near nitrogen atom ($N-O_w$).

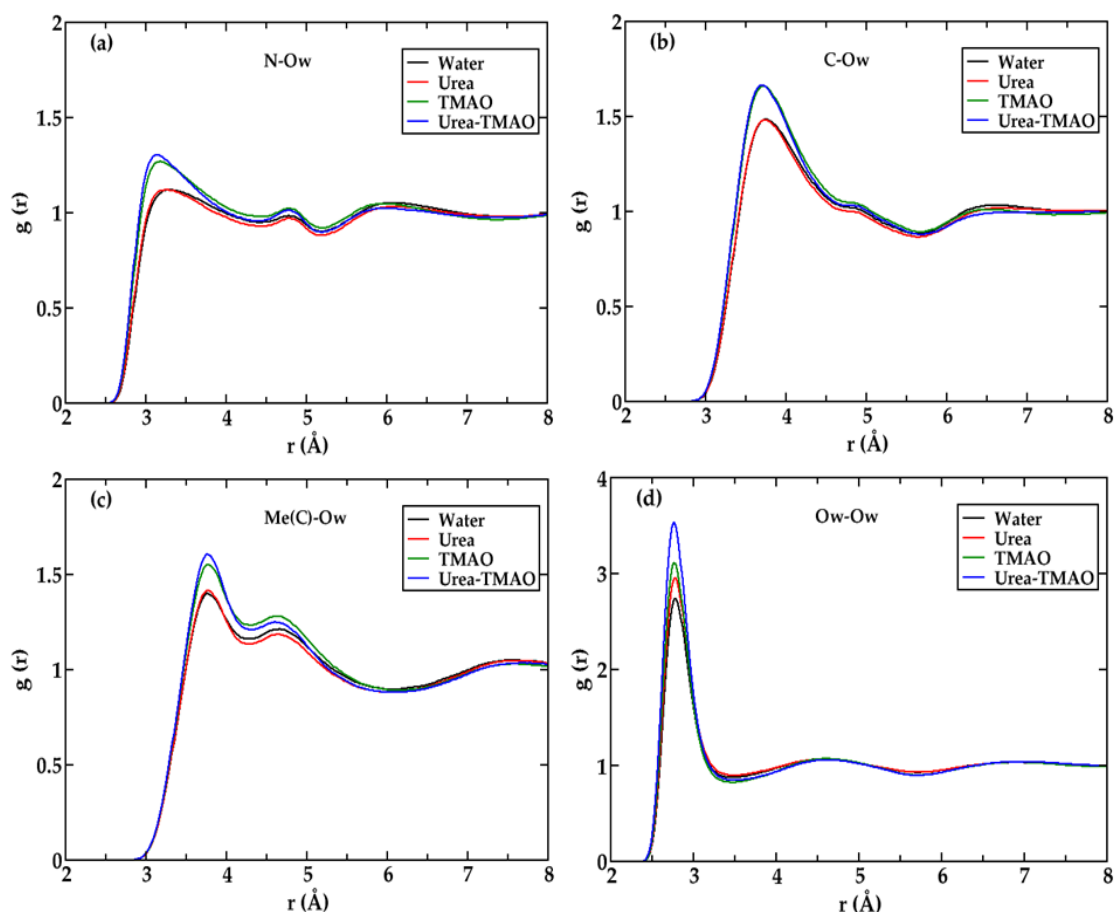


Figure 4.2: Site-site radial distribution functions $g(r)$ of aqueous acetamide of different atoms (a) $N-O_w$, (b) $C-O_w$, (c) $Me(C)-O_w$ (d) O_w-O_w in different osmolytes.

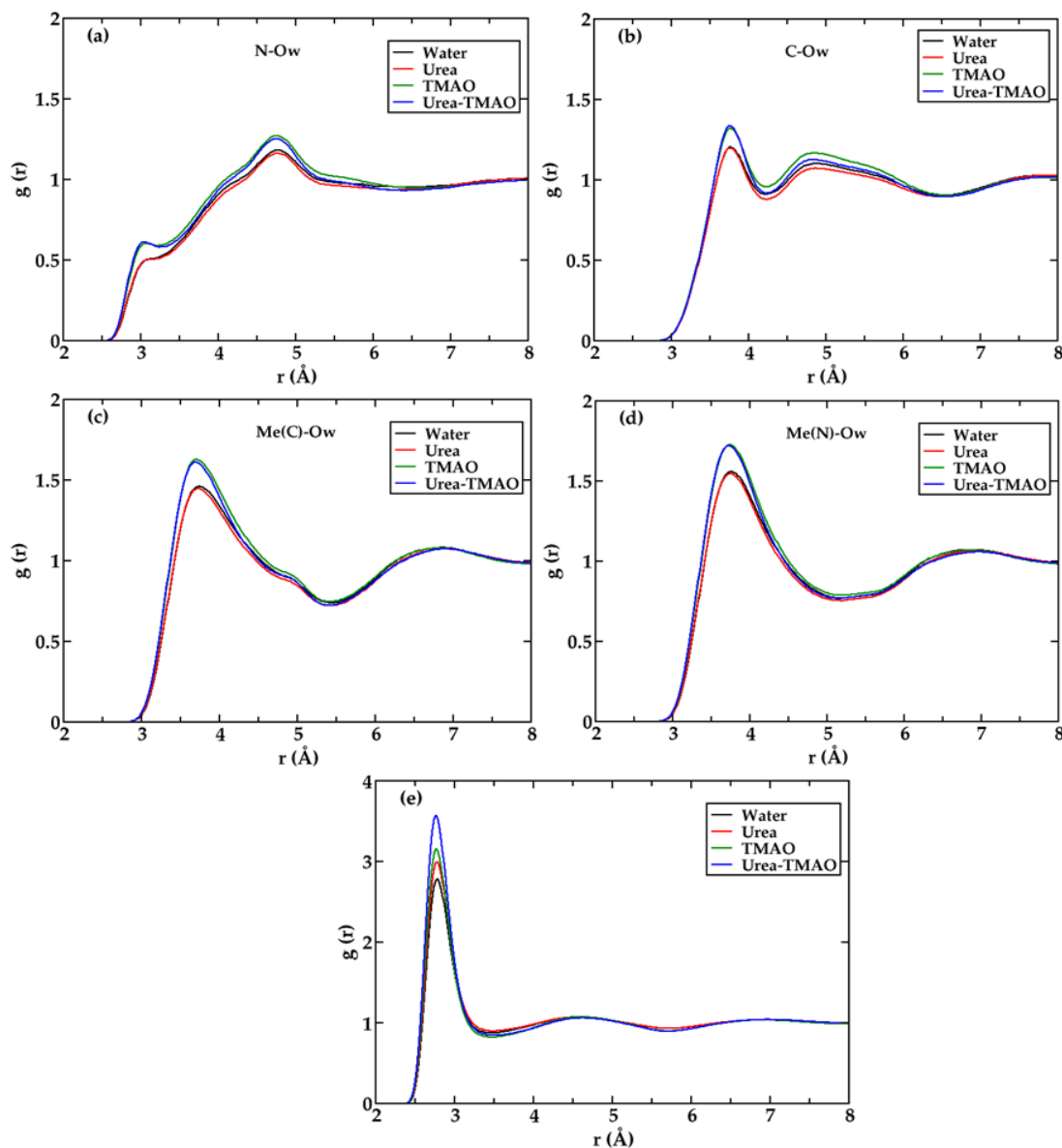


Figure 4.3: Site-site radial distribution functions of aqueous NMA of different atoms (a) N-O_w (b) C-O_w (c) Me(C)-O_w (d) Me(N)-O_w and (e) O_w-O_w in presence of different osmolytes.

In Figure.4.3, the intermolecular radial distribution functions of nitrogen-water (N-O_w), carbonyl carbon-water (C-O_w), methyl carbon attached to carbonyl carbon-water (Me(C)-O_w), methyl carbon attached to amide nitrogen-water (Me(N)-O_w) of NMA have been plotted. TMAO mixtures are found to enhance the peak heights of the radial distribution functions compared to urea and aqueous NMA solutions in all the cases suggesting an improved hydration of NMA moieties. The changes in water structure is most prominently seen near the amide and carbonyl groups. The first and second solvation shells of N-O_w and C-O_w are visibly more enhanced in case of ternary

mixture and TMAO solutions whereas; less peak height is seen in case of solutions of urea and aqueous NMA. The presence of methyl group attached to nitrogen atom makes the amide group more hydrophobic resulting in disruption of the first solvation shell. Typical behaviour of hydrophobic hydration is observed in presence of TMAO by both methyl groups of NMA.

Water solvation shells are found to be more well defined in case of acetamide compared to NMA. The absence of methyl group in acetamide, increases the hydration of amide group. The amide moiety in case of acetamide shows clear solvation shells indicating greater number of water molecules being surrounded near the amide nitrogen. There is relatively greater solvation near the carbonyl group. The addition of urea has very little effect on these intermolecular distribution functions which is similar in both aqueous acetamide and NMA solutions. Therefore, from the radial distribution functions it is evident that it is the neighbouring polar groups i.e. the carboxylic and amide group which actually make changes in the distribution of water near the biomolecules in presence of different cosolvents. It would be interesting to know about the spatial distribution of the hydration shell near these amide molecules.

4.3.2 Spatial Distribution Functions

In Figure 4.4 spatial distribution functions of water oxygen around acetamide in presence of osmolytes urea and TMAO are calculated. The water density is found to be concentrated in three main regions- near the hydrophobic unit (Region I), amide unit (Region II) and carbonyl unit (Region III). Acetamide is more solvated by water molecules in presence of TMAO as compared to urea.

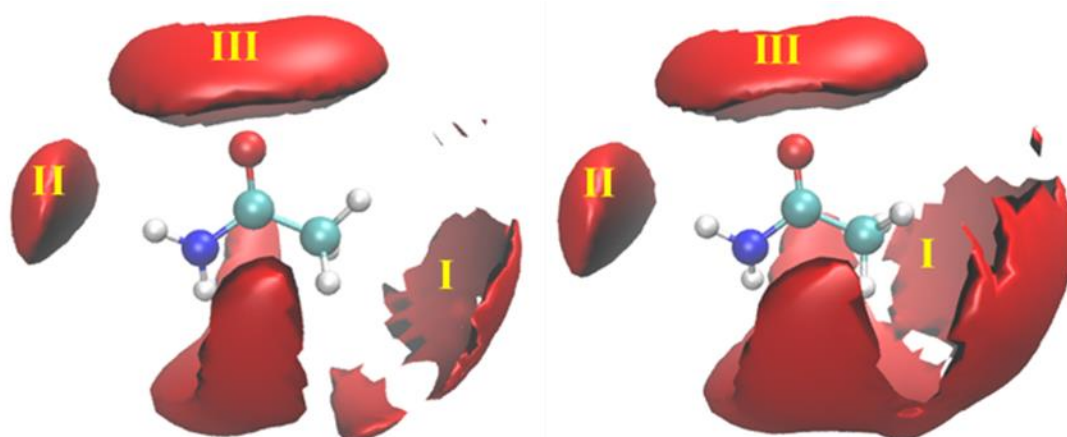


Figure 4.4: SDF of water oxygen around acetamide in presence of osmolytes urea (left) and TMAO (right) considering same isovalues of 39.5.

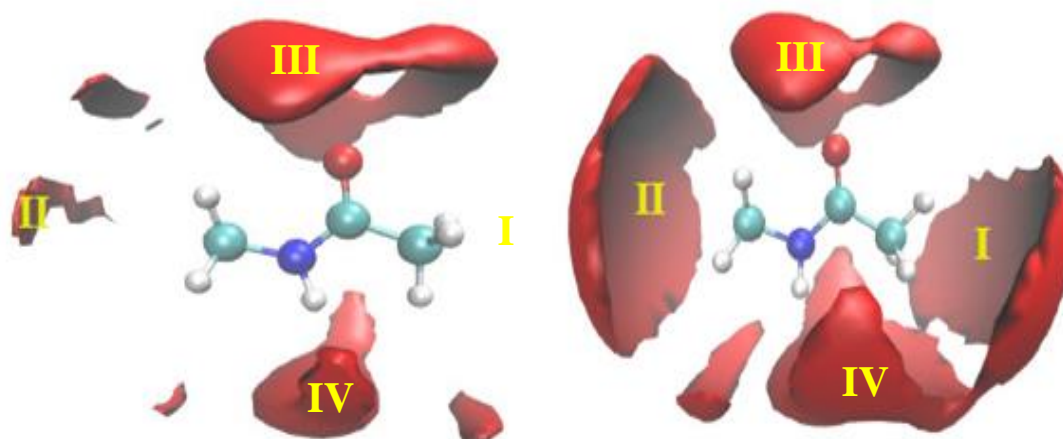


Figure 4.5: SDF of water oxygen around NMA in presence of osmolytes urea (left) and TMAO (right) considering same isovalues of 39.5.

The spatial distribution functions of oxygen molecules around the NMA molecule in presence of osmolytes urea and TMAO with same isovalues are calculated and depicted in Figure 4.5. The water density changes significantly in presence of different osmolytes. In both cases of aqueous acetamide and NMA solutions, TMAO increases the hydration of hydrophobic and amide groups significantly which leads to greater stability as compared to urea in which water density gets depleted from those regions. In case of NMA, there are four main regions where the water density is concentrated. Near the two hydrophobic units (Region I and II), carbonyl unit (Region III) and amide unit (Region IV). In urea solutions, the hydration layer is mainly found near the carbonyl and amide groups. Presence of water near the two hydrophobic units were found to be negligible. In presence of TMAO, there is considerable amount of increase in the water densities near the hydrophobic units making NMA molecules to be solvated more by water molecules in comparison to urea. The absence of methyl group in acetamide in comparison to NMA, increases the hydration near amide group in NMA (region II).

Now it will be interesting to see whether this extra solvation shell can be related to the stability of proteins in the subsequent sections.

4.3.3 Number of Hydrogen-bonded Water Molecules

To calculate the hydrogen bond properties of water molecules around acetamide and NMA, the fraction (f_n) of oxygen atoms of water molecules that engage in n number of water-water hydrogen bonds have been calculated and plotted in Figures 4.6 and 4.7 respectively. The distance criteria are considered same as discussed in the previous chapters. The distances are decided from the radial distribution functions plots.

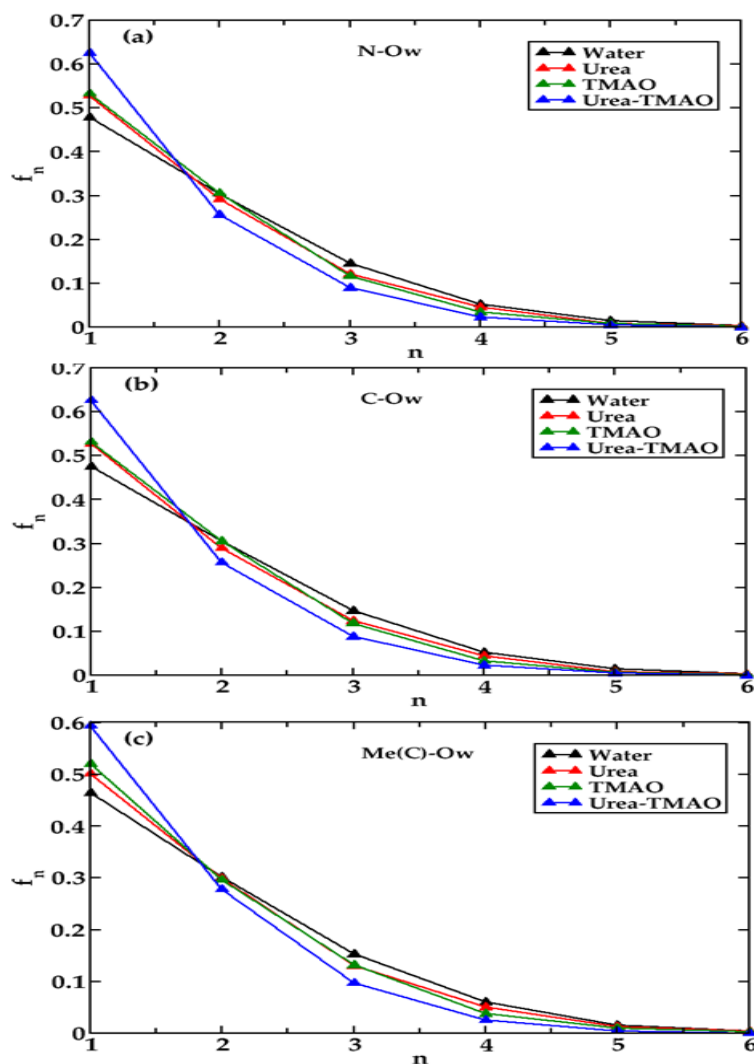


Figure 4.6: The fraction of water molecules having n number of hydrogen bonds considering oxygen-oxygen within the distances (a) 5.6 Å from amine nitrogen (b) 5.6 Å from carbonyl carbon (c) 6.0 Å from Me(C)-O_w for acetamide-osmolyte solutions.

In case of aqueous acetamide solutions, the interfacial water molecules which are present within a distance 5.6 Å from amide nitrogen, 5.6 Å from carbonyl carbon, 6.0 Å from Me(C)-O_w of acetamide are depicted in Figure 4.6 and that of NMA is shown in Figure 4.7. For NMA, interfacial water molecules which are present within a

distance 5.6 Å from amide nitrogen, 4.4 Å from carbonyl carbon, 5.6 Å from Me(C)-O_w, 5.6 Å from Me(N)-O_w of NMA were considered. In all cases the probability of occurrence of lower coordinated water molecules are found to be more compared to the higher coordinated water molecules. Addition of osmolytes increases the fraction of lower coordinated water molecules (f_1) and decreases the fraction of higher coordinated water molecules (f_3 , f_4 and f_5). Ternary mixture increases the fraction of single coordinated water molecules which are less ordered and results to mainly broken hydrogen bonds.

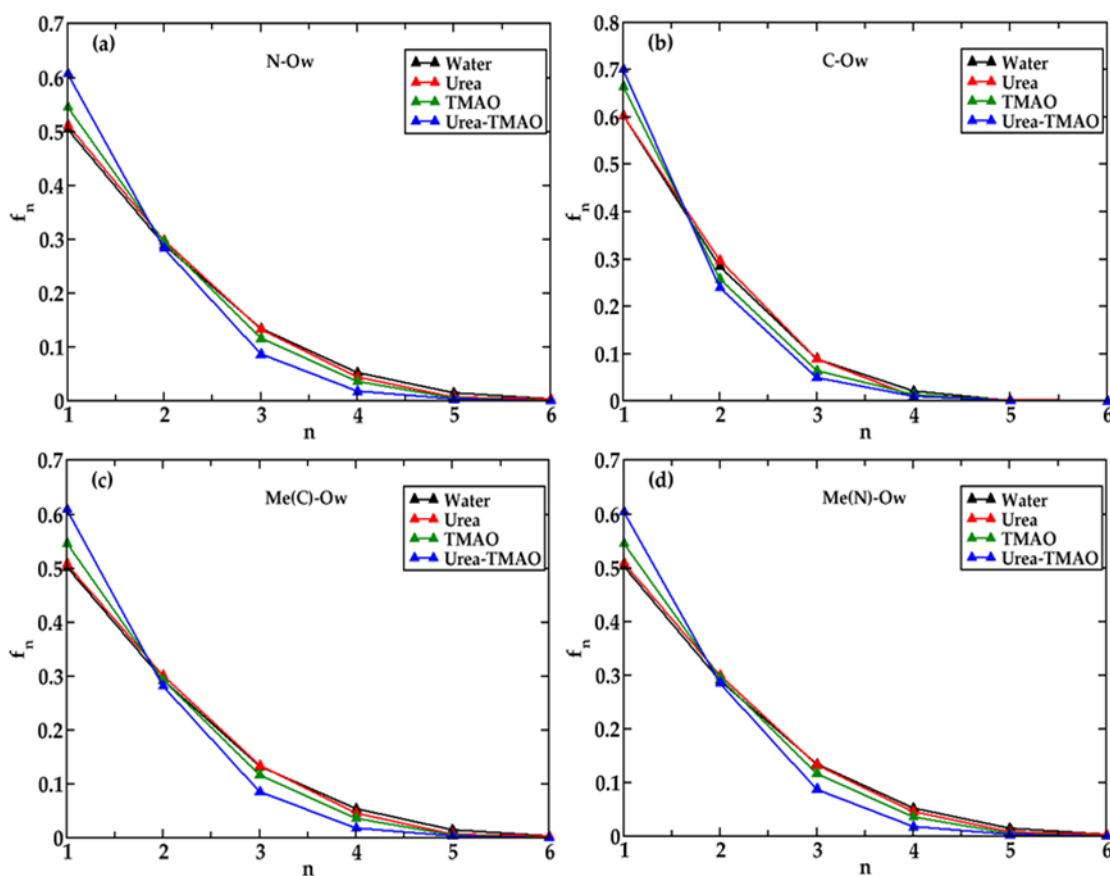


Figure 4.7: The fraction of water molecules having n number of hydrogen bonds considering oxygen-oxygen within the distances (a) 5.6 Å from amine nitrogen (b) 4.3 Å from carbonyl carbon (c) 5.6 Å from Me(C)-O_w (d) 5.6 Å from Me(N)-O_w for NMA-osmolyte solutions.

The effect of addition of osmolytes on the water-water hydrogen bond number is quite apparent. The neighbouring water molecules in a solvation shell of a water molecule are preferably replaced by the osmolytes molecules resulting in lesser number of hydrogen bonded water molecules. On addition of the osmolytes, the fraction of lower coordinated water molecules (f_1) is found to further increase a lot and the fraction

of higher coordinated water molecules (f3, f4 and f5) are found to decreased. The opposing effects of urea and TMAO on the hydrogen bonding nature of water molecules are distinctly observable. TMAO and 2:1 M urea: TMAO ternary mixture mainly increases the fraction of single coordinated water molecules in the solution which are less ordered and results to mainly broken hydrogen bonds. Ternary mixture of urea: TMAO solutions promotes maximum broken type of hydrogen bonds followed by the order TMAO > urea > aqueous NMA.

4.3.4 Orientation Profile

The tetrahedral orientation symmetry of water molecules near the interface is broken in the presence of cosolvents. To see this, the angular probability distribution function $P(\theta_{OOO})$ near the interface of acetamide and NMA are calculated and depicted in Figures 4.8 and 4.9 respectively. Water molecules up to a distance of 5.6 Å from amine nitrogen, 4.3 Å from carbonyl carbon, 5.6 Å from Me(C)-O_w, and 5.6 Å from Me(N)-O_w are considered as interfacial molecules for calculations.

In Figure 4.8, it is seen that in case of aqueous solutions of acetamide two distinct peaks are observed near 50° and 104.5° angles which have a small and broad distributions respectively. The curves are slightly shifted towards higher angles in solutions of TMAO and ternary mixtures as compared with urea and aqueous solutions which can be attributed to greater fraction of broken hydrogen bonds.

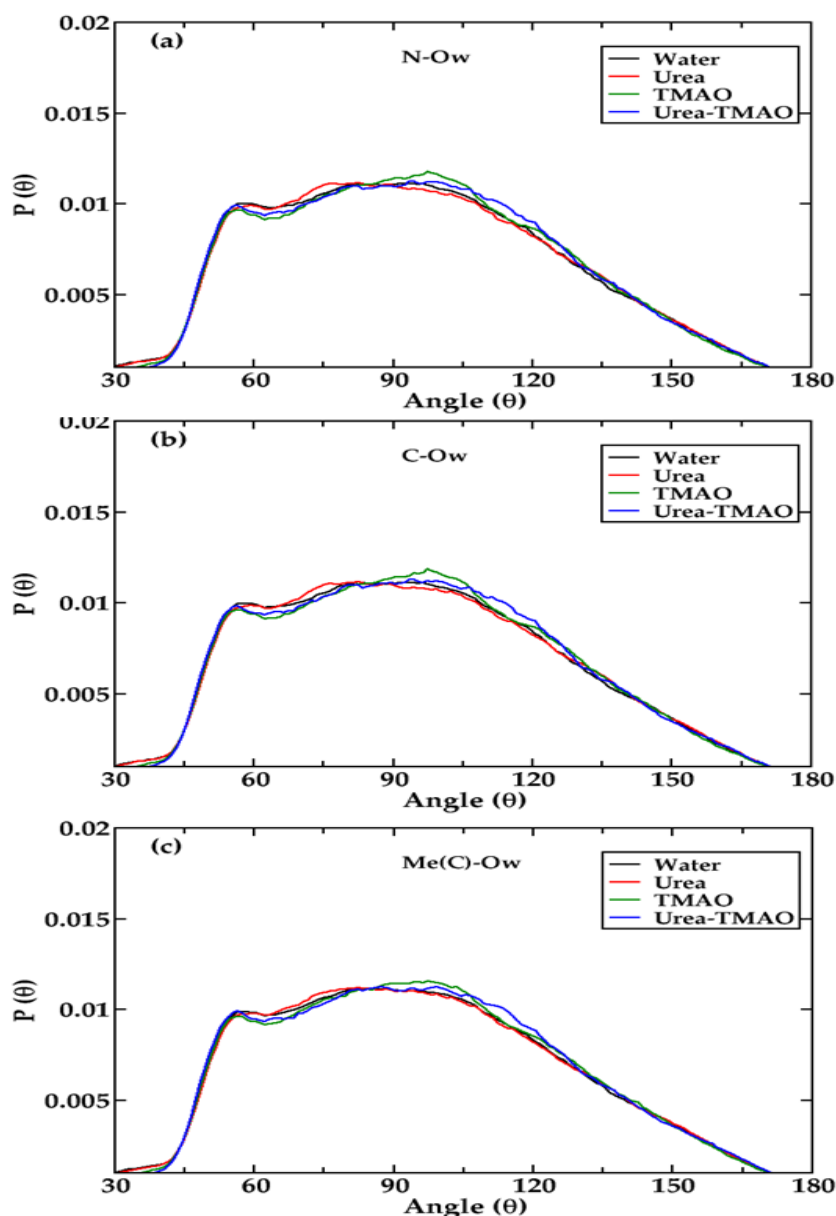


Figure 4.8: Normalized probability distribution of $\langle \text{O-O-O} \rangle$ angle of oxygen atoms of water molecules which are within the distance (a) 5.6 Å from amine nitrogen (b) 5.6 Å from carbonyl carbon (c) 6.0 Å from Me(C)-O_w for acetamide-osmolyte solutions.

In Figure 4.9, it is observed that for aqueous solution of NMA and urea, mainly a broad distribution with a small hump is observed but in case of TMAO and 2:1 M urea: TMAO ternary mixture, two distinct peaks are observed. One near 50° which is small and another near 104.5° angle which has a broad distribution. Solutions of TMAO and ternary mixtures curves are little bit shifted towards the higher angles in comparison to urea and aqueous solutions as seen in case of acetamide. This shifting is observed more in case of the hydrophobic units and near the amide nitrogen.

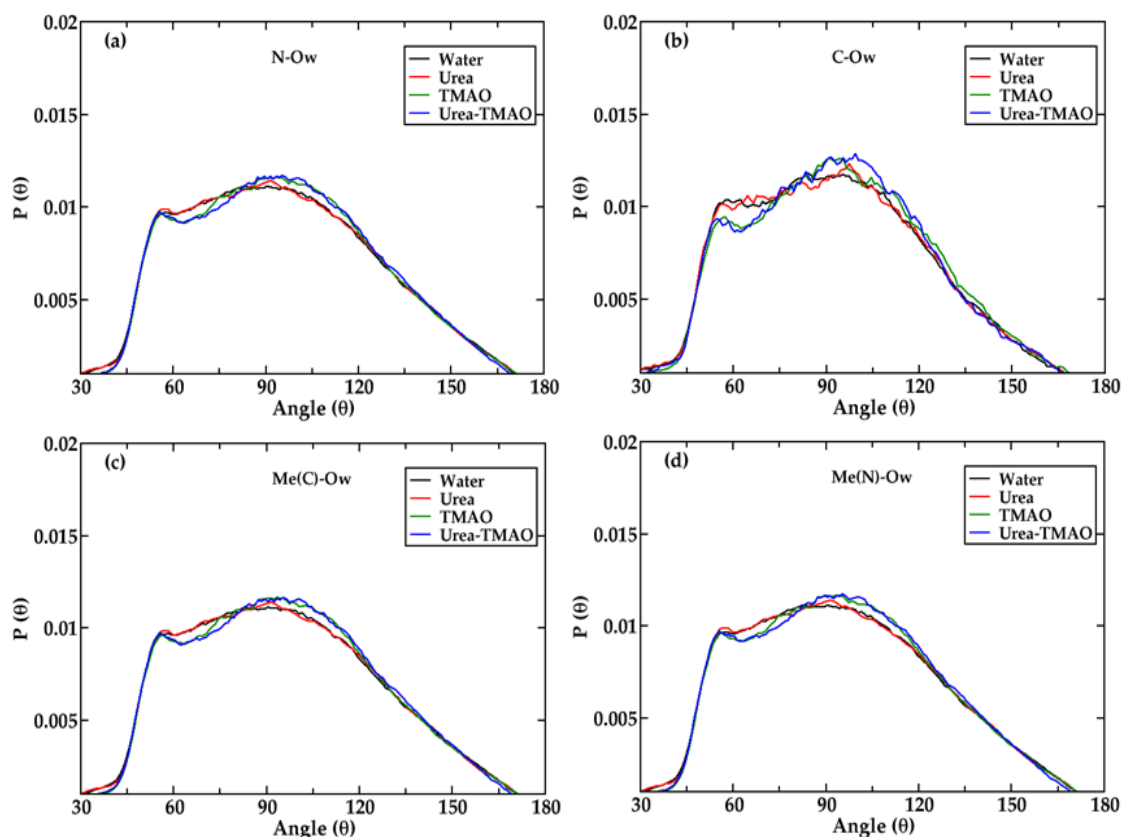


Figure 4.9: Normalized probability distribution of $\langle \text{O-O-O} \rangle$ angle of oxygen atoms of water molecules which are within the distance (a) 5.6 Å from amine nitrogen (b) 4.3 Å from carbonyl carbon (c) (c) 5.6 Å from Me(C)-O_w (d) 5.6 Å from Me(N)-O_w for NMA-osmolyte solutions.

4.3.5 Potential Mean Force

To calculate the potential of mean forces (PMF's), various inter-atomic amide-water pair correlation functions, $g(r)$, are used as shown in the following equation

$$W(r) = -k_B T \ln g(r) \quad (4.2)$$

where r is the inter-atomic separations, k_B is the Boltzmann constant and T is the temperature.

In Figure 4.10 the potentials of mean force are plotted as a continuous function of distance between nitrogen and carbonyl carbon of acetamide with water. In both the cases, the presence of urea is found to have less stabilization energy compared to TMAO and ternary mixture due to higher hydration shell noticed near the polar groups of acetamide.

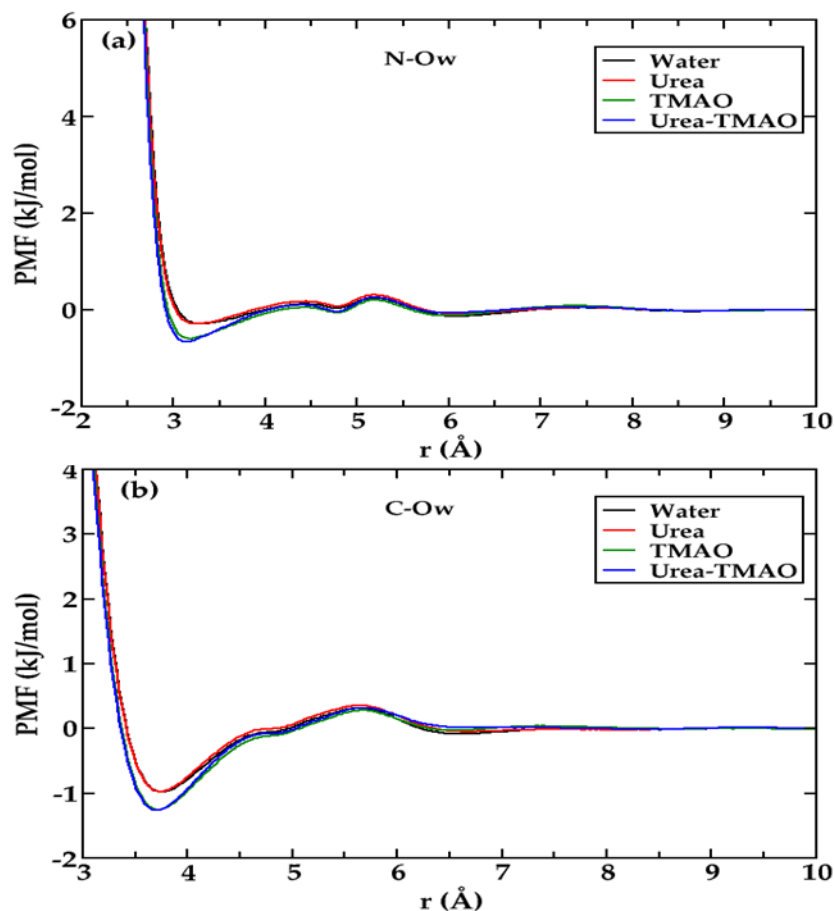


Figure 4.10: PMF depicting the free energies of interaction between (a) nitrogen of acetamide (b) carbonyl carbon of acetamide with the water oxygen sites as a continuous function of distance.

In Figure 4.11 the potentials of mean force are plotted as a continuous function of distance between nitrogen and carbonyl carbon of NMA with water. Greater stabilisation energy in presence of TMAO and the ternary mixture can be related to the presence of extra hydration shell noticed near the hydrophobic groups of NMA indicating that the hydrophobic hydration has some contribution towards the stability of biomolecules.

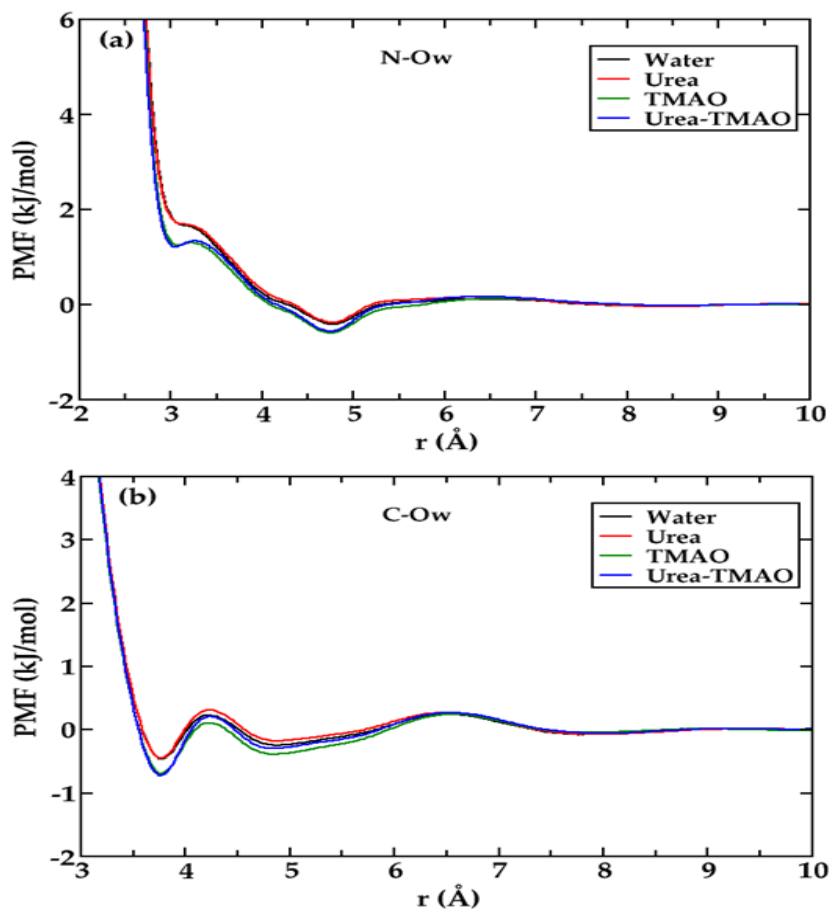


Figure 4.11: PMF depicting the free energies of interaction between (a) nitrogen of NMA and (b) carbonyl carbon of NMA with the water oxygen sites as a continuous function of distance.

Further, thermodynamic (entropy and enthalpy) contributions to PMF profiles of acetamide and NMA solutions have been calculated. The entropic contribution is calculated from the following equation (Keshri and Tembe 2017; Pettitt and Rossky 1986; Smith and Haymet 1993),

$$-\Delta S(T) = \frac{\Delta G(T+\Delta T) - \Delta G(T-\Delta T)}{2\Delta T} \quad (4.3)$$

In this study, the values of T and ΔT are chosen to be 298 K and 20 K respectively.

The enthalpic contribution is computed using the equation given below,

$$\Delta H(r) = \Delta G(r) + T\Delta S(r) \quad (4.4)$$

The entropic $-T\Delta S(r)$ and enthalpic $\Delta H(r)$ contributions to the PMF at 298 K for all the systems under study are shown along with the PMF's in Figures 4.12 to 4.15.

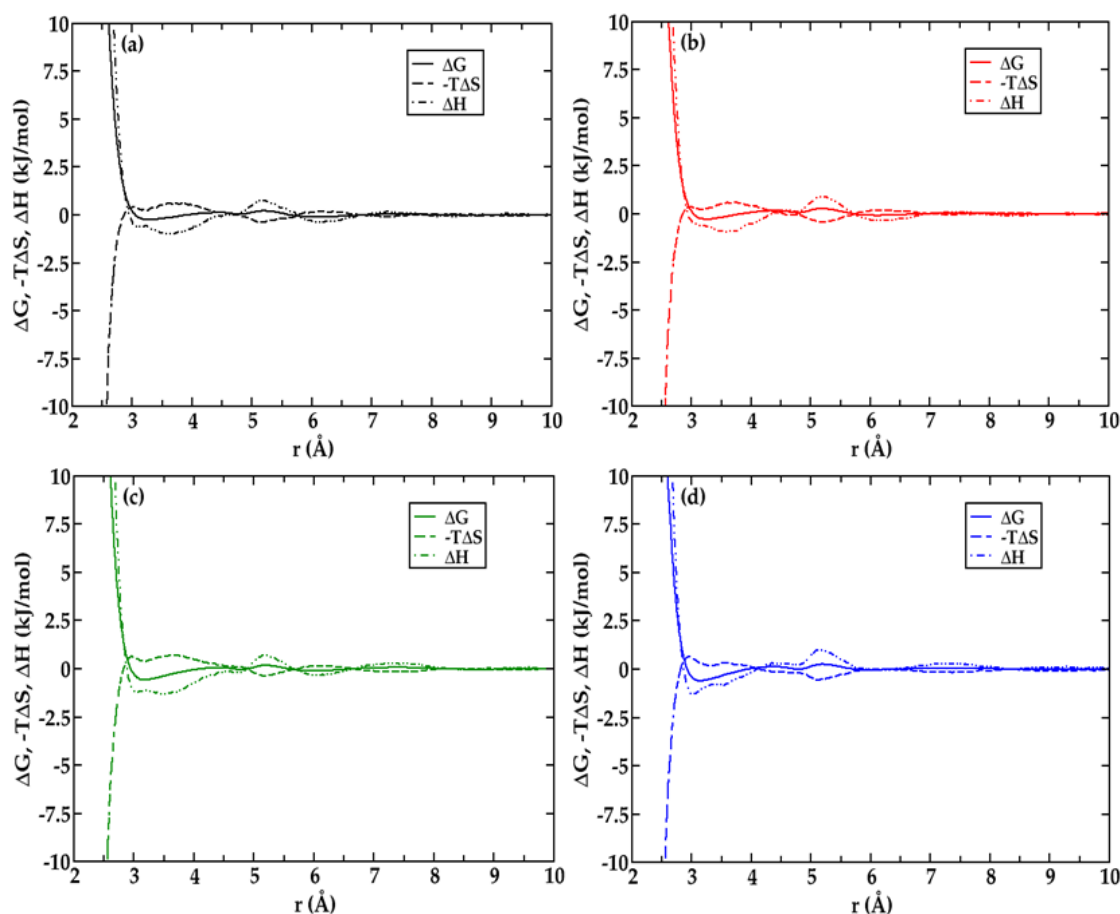


Figure 4.12: Entropic ($-T\Delta S(r)$) and enthalpic ($\Delta H(r)$) contributions to the PMF for acetamide (N-Ow) in presence of different cosolvents a) water b) 3M urea c) 3M TMAO d) 6:3 M urea: TMAO mixtures.

The entropic and enthalpic contributions act in opposite directions to each other. Inter-particle pair state is determined by the balance between stabilizing enthalpic and destabilizing entropic contributions. In all the cases, the contact configurations are stabilized by the favourable negative entropic contributions and destabilized by the unfavourable positive enthalpic contributions. In solvent assisted and solvent separated configurations, enthalpy and entropy contributions are quite close to each other in magnitude as compared to alanine in previous chapter. The solute-solvent stabilization of the solvent separated configurations in aqueous solutions is due to preferential intermolecular interactions between them.

The presence of methyl group attached to nitrogen in case of NMA, increases the entropic and enthalpic energetic changes at the contact configuration to relatively greater extent.

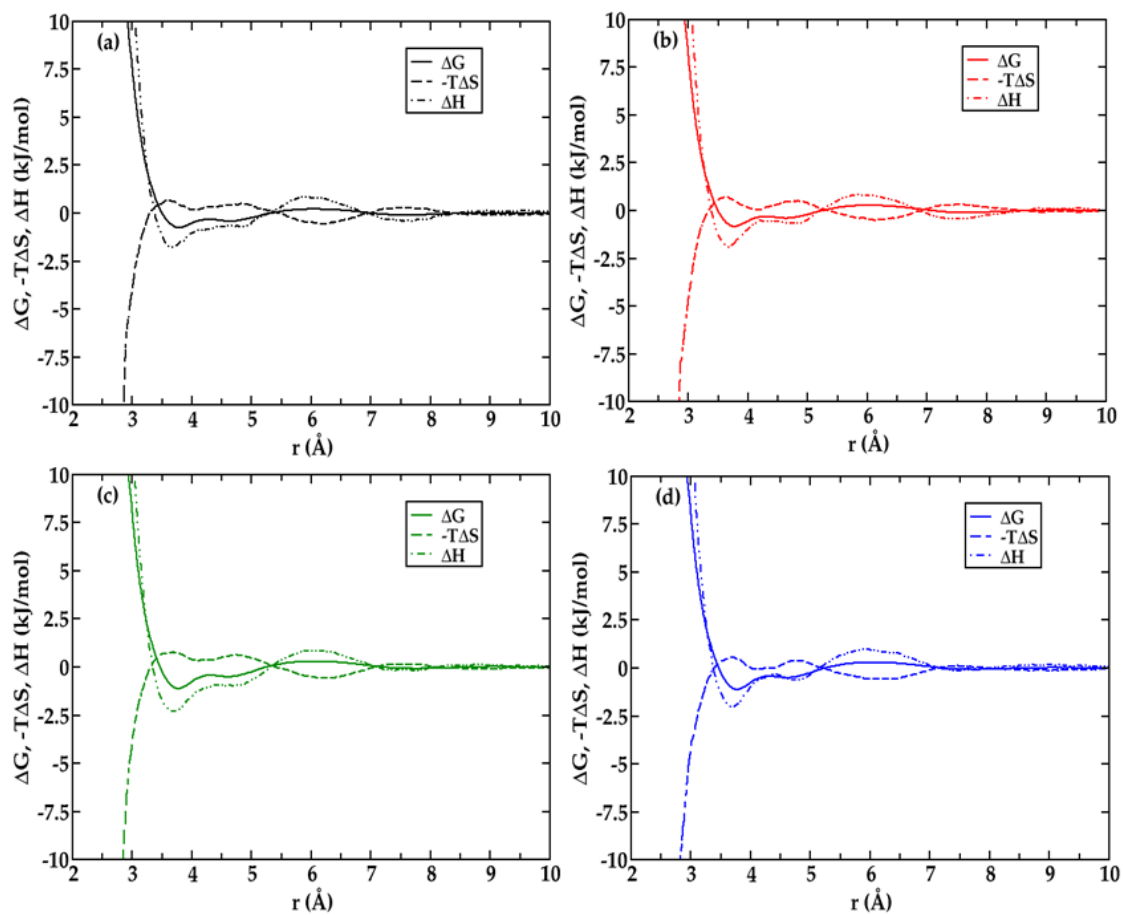


Figure 4.13: Entropic ($-T\Delta S(r)$) and enthalpic ($\Delta H(r)$) contributions to the PMF for acetamide (C-Ow) in presence of different cosolvents a) water b) 3M urea c) 3M TMAO d) 6:3 M urea: TMAO mixtures.

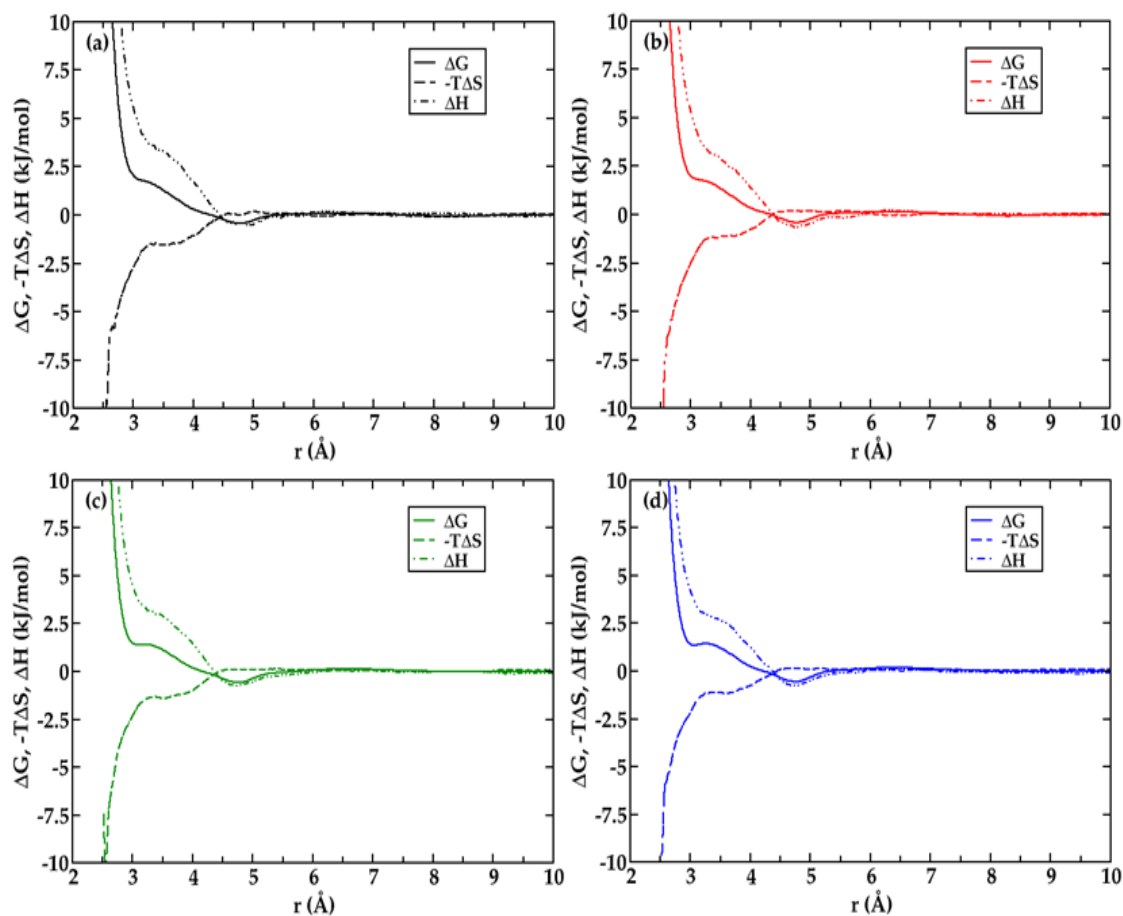


Figure 4.14: Entropic ($-T\Delta S(r)$) and enthalpic ($\Delta H(r)$) contributions to the PMF for NMA (N-Ow) in presence of different cosolvents a) water b) 3M urea c) 3M TMAO d) 6:3 M urea: TMAO mixtures.

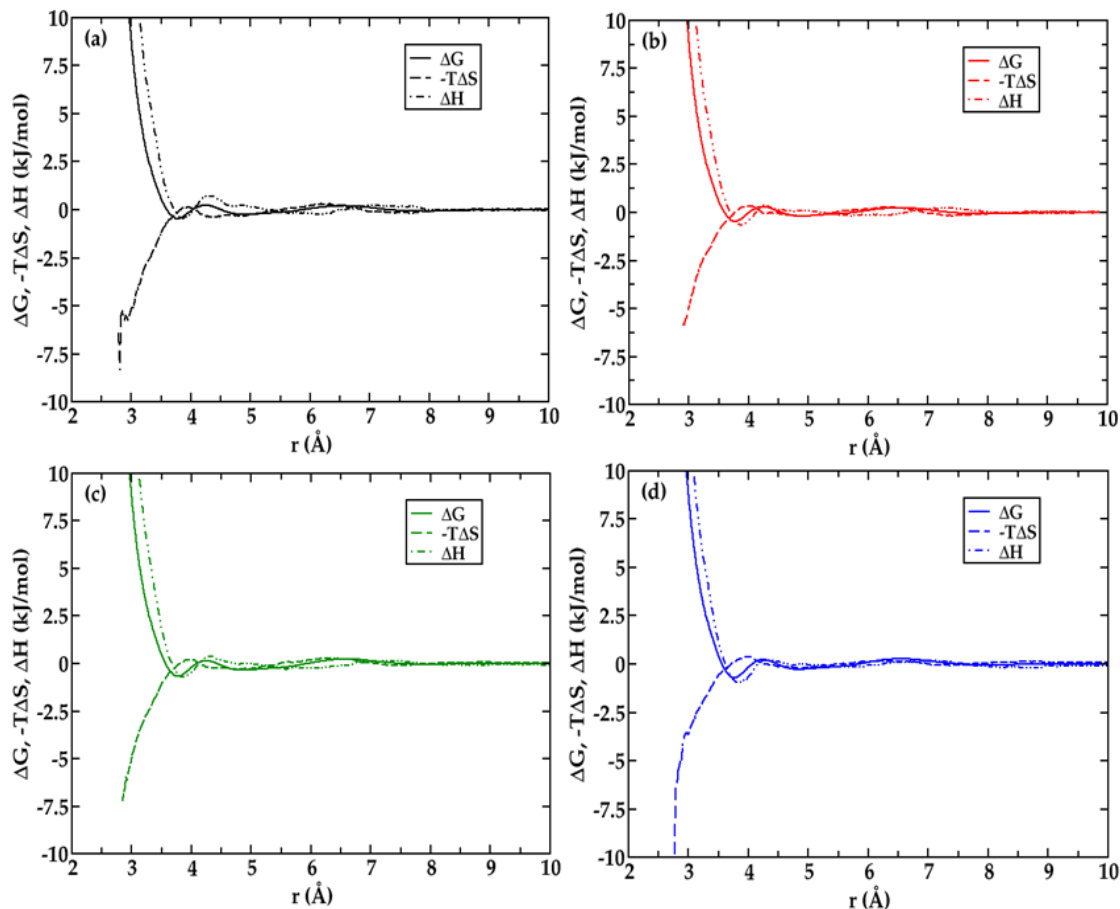


Figure 4.15: Entropic ($-T\Delta S(r)$) and enthalpic ($\Delta H(r)$) contributions to the PMF for NMA (C-Ow) in presence of different cosolvents a) water b) 3M urea c) 3M TMAO d) 6:3 M urea: TMAO mixtures.

4.3.6 Preferential Binding Coefficient

In order to calculate the net excess or deficit of species around amides in presence of osmolytes, preferential binding coefficients (Pierce et al. 2008) $v_{\alpha\beta}$ are calculated between the amide-water, amide-urea and amide-TMAO. If water, amide and osmolytes are denoted by subscripts 1, 2 and 3 respectively, then,

v_{21} preferential binding of water to protein, is given by

$$v_{21} = \rho_1(G_{21} - G_{23}) \quad (4.5)$$

v_{23} preferential binding of osmolytes to protein molecule, is given by

$$v_{23} = \rho_3(G_{23} - G_{21}) \quad (4.6)$$

where ρ_3 denotes the osmolyte and ρ_1 denotes the water number densities.

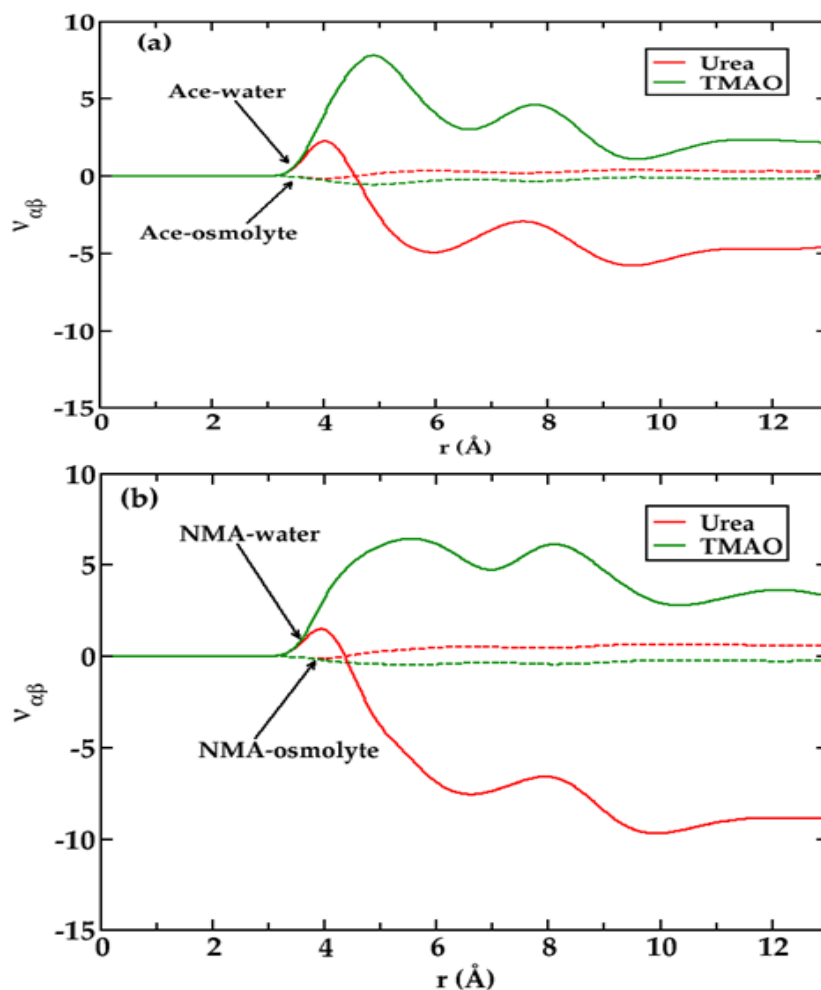


Figure 4.16: Preferential binding coefficients $v_{\alpha\beta}$ for (a) acetamide-water, acetamide-osmolytes and (b) NMA-water, NMA-osmolytes in 3M aqueous solutions of urea and TMAO as a function of distance.

Figure.4.16 depicts the $v_{\alpha\beta}$ values for urea, TMAO and water around acetamide and NMA as a function of distance. The preferential binding behaviour can be detected from the value $v_{\alpha\beta} > 1$ and preferential exclusion of the species can be detected from $v_{\alpha\beta} < 1$ region. The scenario is very much different for urea-water and TMAO-water solutions. In urea-water system, it is found that the preferential binding affinity for water is more in comparison to urea at lower r values. However, at larger r values > 4.35 Å water is excluded from amide surfaces and presence of urea is favoured. For TMAO-water system, water is favoured over the osmolyte near the amide surfaces. It can be correlated with the RDF and SDF results that in presence of urea, less water molecules were observed near the protein surface compared to TMAO solution.

4.3.7 Hydrogen Bond Dynamics

Presence of osmolytes influences the structure of water molecules which consecutively will influence the dynamics of the solution. To check this, hydrogen bond dynamics of amide–water and water–water molecules are calculated in presence of osmolytes and its ternary mixtures. The distance, angle criteria and parameter definitions are considered same as described in previous chapters. The average continuous lifetimes of hydrogen bond population is calculated as (Chandra 2000; Luzar and Chandler 1996; Rapaport 1983)

$$S_{HB}(t) = \frac{\langle h(0)H(t) \rangle}{\langle h(0)^2 \rangle} \quad (4.7)$$

where $\langle \dots \rangle$ denotes the average over all pairs of a given type. The hydrogen bond lifetimes of amide-water and water-water are given in Table 4.3.

Table 4.3: The lifetime (τ_{HB}) of hydrogen bonds (in ps) formed by acetamide and NMA with water in presence of osmolytes and its ternary mixtures.

Species	Ace-W	Ace-U-W	Ace-T-W	Ace-U-T-W
O _w -H _w	0.613	0.656	0.927	1.043
O _w -H _{N-Ace}	0.208	0.221	0.260	0.282
O _{Acet} -H _w	0.564	0.624	0.790	0.870
O _u -H _w	----	0.750	----	1.142
O _t -H _w	----	----	3.682	4.000
O _t -H _u	----	----	----	0.700
O _w -H _u	----	0.231	----	0.297
Species	NMA-W	NMA-U-W	NMA-T-W	NMA-U-T-W
O _w -H _w	0.623	0.665	0.949	1.062
O _w -H _{N-NMA}	0.307	0.323	0.363	0.390
O _{NMA} -H _w	0.579	0.611	0.815	0.876
O _u -H _w	----	0.741	----	1.069
O _t -H _w	----	----	3.667	3.995
O _t -H _u	----	----	----	0.700
O _w -H _u	----	0.229	----	0.296

It is seen that addition of osmolytes increases the hydrogen bond lifetime of the system. The hydrogen bond lifetime is found to be more in presence of ternary urea-TMAO mixtures for all the cases followed by TMAO, urea, aqueous amide solutions. Higher lifetimes between carbonyl oxygen and water are found when compared to amine-water interactions in all the cases indicating stronger interaction of water molecules with the carbonyl group as compared to amine group. It is clearly evident from Table.4.3, that addition of TMAO increases the hydrogen bond lifetime of the solutions as seen for the amino acid case. The stabilization of water hydrogen bonding network by TMAO has pivotal role in counteracting the denaturing effects of urea.

4.4. SUMMARY AND CONCLUSIONS

In this study, the effects of osmolytes urea, TMAO and their ternary mixtures on the solvation structures of acetamide and NMA were examined to explain the stability aspect of TMAO and denaturing effect of urea. Results were analyzed in terms of radial distribution functions, spatial distribution functions, number of hydrogen bonds, $\langle O-O \rangle$ angle distributions, potentials of mean force, preferential binding parameter and hydrogen bond dynamics.

It is found that in presence of TMAO, amides are solvated by water more in comparison to aqueous solution and urea. Specially, near the hydrophobic groups, an extra hydration shell is observed. As compared with the previous chapter of amino acids, this hydration shell results mainly from the strong hydration shell of neighbouring polar groups i.e. carbonyl carbon and amine groups of biomolecules. Water molecules near the amides interface mainly consists of broken hydrogen bonds which were found to increase on addition of osmolytes. This broken hydrogen bonds are mainly composed of dimer and trimer water molecules which are also reflected in the $\langle OOO \rangle$ angle distributions. Potentials of mean force showed that presence of these water molecules actually imparts stability to amides.

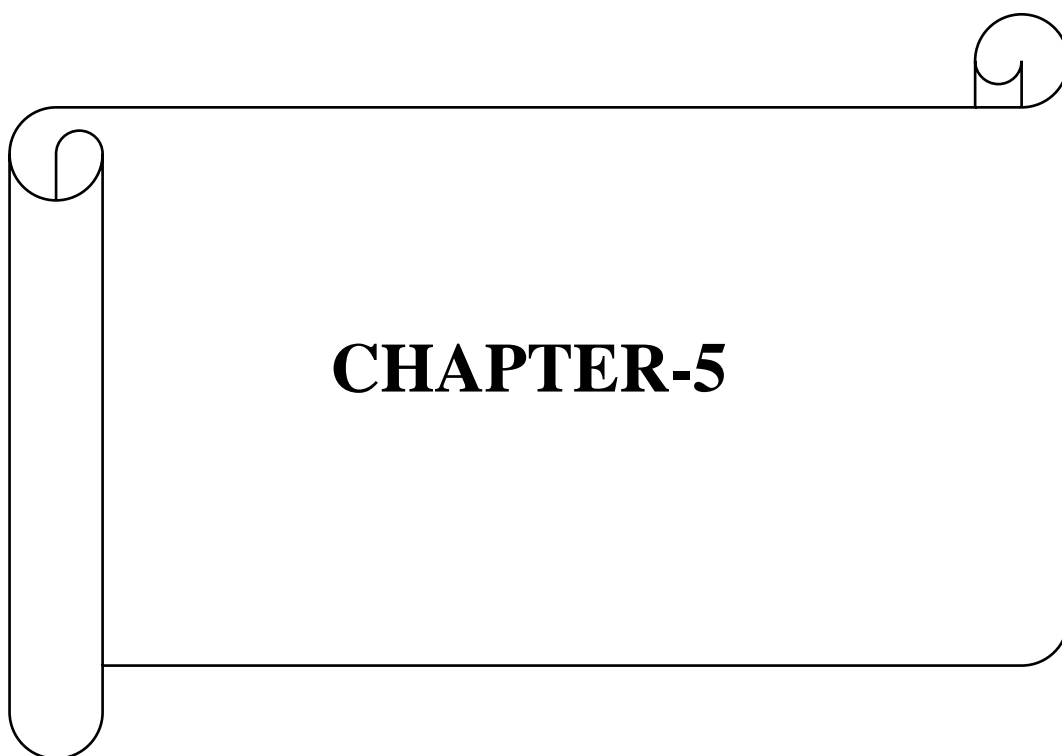
In solvation structure of the solution, preferential binding affinity, $v_{\alpha\beta}$ of amides with water and osmolytes were further examined. It is found that near the amide interface, water is preferentially favoured over the presence of other cosolvents up to smaller region of $r < 4.35 \text{ \AA}$. Amides are found to be less solvated with water in comparison to amino acids (in previous chapter) in aqueous urea system. This implies that urea molecules can come closer to amide more compared to amino acids. This can

be explained on the basis of the placement of the polar groups (-NH, -COO). In case of amino acids, the location of polar groups is near the end of backbone, which is present in the middle in case of amides. As a result, hydration of water is favoured up to a small distance ($r < 4.35 \text{ \AA}$) from the amides. This gives space to the urea molecule to approach the amides. Polar groups are found to be mainly responsible for the hydration of proteins. Preferential exclusion of TMAO was observed from the protein surface compared to urea near amide surfaces. In case of bigger proteins, consisting of more protein backbones and amide linkages this effect may be more visible. In case of ternary mixture of urea: TMAO, same trend was observed.

Hydrogen bond strength of water-water and water-amide molecules near the surface of amides increase on addition of osmolytes as observed in case of amino acids. The water-TMAO interaction actually increases the corresponding hydrogen bond lifetime of water-water and water-urea lifetime in ternary solutions compared to normal water-urea and aqueous water-biomolecule systems.

In conclusion, the position of subgroups i.e., amine, carbonyl and hydrophobic groups plays a key role in imparting the stability of proteins in presence of osmolytes. TMAO enhances the stability of biomolecules by hydrating the hydrophobic moiety and strengthening the hydrogen bond network of the solutions whereas urea destabilizes biomolecules by depleting the hydration shell and hindering the interactions between protein and solvent molecules. These could be the possible reasons for the stability of proteins in presence of TMAO and also in ternary mixture.

In the next chapter structural and dynamic properties of water in pre-assembled surfactant-like peptide-based nanotubes which are formed by joining the amino acids in the form of peptides have been studied.



CHAPTER-5

CHAPTER 5
STRUCTURAL AND DYNAMIC PROPERTIES OF WATER IN
SURFACTANT-LIKE PEPTIDE-BASED NANOTUBES: EFFECT OF
PORE SIZE, TUBE LENGTH AND CHARGE.

***Abstract:** This chapter includes atomistic molecular dynamics simulations carried out to study the structural and dynamic properties of water molecules around pre-assembled surfactant-like peptide (SLP) nanotubes in aqueous media. These SLPs can be thought as a class of biocompatible and biodegradable surfactants for biomedical applications. Glycine and lysine were taken as the constituents for composition of G₆K SLP nanotubes. Nanotubes considered were of different dimensions; such as 18x15 (number of peptides on the circumference x number of peptides layers), 18x12 and 16x12 for both charged and neutral analogues. The charged composition consists of protonated nitrogen in the lysine subunit and chlorine/bromine as counter ions. The structural and dynamic properties of water molecules and its interactions with peptides are analyzed in terms of site-site radial distribution functions, density profiles, number of hydrogen bonds, translational order parameter, orientation profile and hydrogen bond dynamics.*

5.1 INTRODUCTION

In previous chapters, effects of ions and osmolytes on the solvation structure and dynamics of aqueous amino acids and amides solutions have been investigated. In this chapter solvation structure and dynamics of water molecules in pre-assembled peptide nanotubes which are formed by joining amino acids has been studied. Living organisms are mainly composed of self-assembly of biological macromolecules/proteins which results in varieties of complexities and functionalities in them. These self-assembled biomolecules have well-defined molecular structure that performs many critical functions with high efficiency and precision. Misfolded proteins on the other hand, can lead to many human diseases (Dobson 2003). Keeping this in mind, many studies in the past two decades have been focusing on two main aspects (Chen and Zou 2019; Gazit 2007; Ghadiri et al. 1993; Hartgerink et al. 2001, 2002; Rad-Malekshahi et al. 2016; Reches and Gazit 2003; Zhang 2003; Zhao 2009). First on the principles and forces that govern the self-assembly of biomolecules and secondly to fabricate functional

nanostructures for targeted applications. In this respect, short peptides are good system to study as their smaller length have advantages in easy synthesis and structural stability. Moreover, it is easy to establish the structure-property relationship in these peptides which will be helpful in understanding the self-assembly of bigger systems. As a result, the self-assembly of smaller peptides have received lot of attention in current days (Cui et al. 2010; Fichman and Gazit 2014; Gazit 2007; Hamley 2011; Hosseinkhani et al. 2013; Loo et al. 2012; Ulijn and Smith 2008; Yan et al. 2010; Zhao et al. 2010; Zhao and Zhang 2006). The short peptides may include many different types of peptides such as peptide amphiphiles, hairpin peptides, SLPs (Baumann et al. 2008; Cui et al. 2010; Dehsorkhi et al. 2013; Ghadiri et al. 1993; Hamley 2011; Han et al. 2011; Hartgerink et al. 2001; Khoe et al. 2009; von Maltzahn et al. 2003; Nagai et al. 2007; Reches and Gazit 2003; Santoso et al. 2002; Wang et al. 2009; Xu et al. 2010a; Yan et al. 2010; Zhang et al. 1993; Zhao et al. 2010, 2013) and many more. Out of this SLP-based nanofibers have potential applications in growth of blood vessels in post-infarct therapies, cancer therapy, regenerative medicine, artificial trans-membrane channel, drug and gene delivery vehicles etc(Chen et al. 2010, 2011; Cui et al. 2010; Infante et al. 2004; Pinazo et al. 2016; Pinheiro and Faustino 2017; Qiu et al. 2018; Seroski and Hudalla 2018; Zasloff 2002). They deserve exceptional consideration due to their environment-friendly, low toxicity, antimicrobial activity and excellent emulsifying properties (Dehsorkhi et al. 2013; Dexter and Middelberg 2008; Greber et al. 2017; Infante et al. 2004; Morán et al. 2004; Pinazo et al. 2016).

The design and fabrication of peptide nanofibers have opened a platform of immense potential in the field of biomedical applications (Chen and Zou 2019; Fan et al. 2017; Lee et al. 2019). These nanofibers can be uniquely designed (Cui et al. 2010) by keeping their temperature reversible bio-active properties (Andrew Mackay and Chilkoti 2008; Dunshee et al. 2020; Huang et al. 2014) and stiffness (Adler-Abramovich and Gazit 2014; Pashuck et al. 2010). Temperature and solution pH are the two main factors that affect the self-assembly process and functions of these nanostructures. Temperature is found to have dual role in the stability of SLPs. An increase in temperature often leads to the unfolding of the secondary structure of peptides and therefore disrupting its function (Dexter 2010), but it is also seen that increasing the temperature helps to preferentially form the self-assembly of nanofibers composed of diphenylalanine (FF) molecules and transformed them to crystalline

structures (Huang et al. 2014). Another important factor affecting peptide stability is the solution pH whose values are mainly important for peptides with charged amino acids. They influence the self-assembly process leading to the formation of different nanostructures (Aggeli et al. 2003; Ghosh et al. 2012; Greber et al. 2017; Morán et al. 2004). By balancing the hydrogen bonding, hydrophobic, electrostatic and non-covalent interactions, the self-assembly morphology can be fine-tuned based on desired applications. Different combination of amino acids present in peptides also affects the morphology of the nanostructures formed in the self-assembly process (Ghosh et al. 2012; Goldberger et al. 2011; Makovitzki et al. 2008; da Silva et al. 2016; Xu et al. 2010b; Zhao et al. 2010).

SLPs can be easily designed and modified to form various nanostructures since they are usually consisting of two main parts: a hydrophilic head composed of one or two hydrophilic amino acids and a hydrophobic tail composed of many hydrophobic amino acids. The presence of both hydrophobic and hydrophilic moieties in amino acids facilitates its use as surfactant-like peptides. The hydrophobic core in SLPs can be used for encapsulating water-insoluble molecules/drugs and the hydrophilic end can be modified into some functional groups for cell-targeting (Chen et al. 2011; Wiradharma et al. 2009). By mimicking the structure of traditional surfactants, a large family of SLPs have been designed (Ghosh et al. 2012; Makovitzki et al. 2008; Xu et al. 2010b). SLPs have a major advantage over other self-assembling peptides due to their short length. Zhang *et. al.* pioneered the synthesis of SLP proteins and their applications in membrane protein stabilizations (Kiley et al. 2005; Koutsopoulos et al. 2012; von Maltzahn et al. 2003; Santoso et al. 2002; Vauthey et al. 2002). A wide range of studies on lysine-based surfactants have been done in recent years due to its lower toxicity in comparison with conventional surfactants. This lead to a considerable edge in their use in cosmetics and pharmaceutical applications (Sanchez et al. 2006; Vives et al. 1997, 1999). Zhao et al. experimentally investigated the association of SLPs antimicrobial activity with their nanostructure formation ability in A_NK peptides (Xu et al. 2009; Zhang 2012).

Molecular-level description of these nanostructures along with their intermolecular interactions with water plays a pivotal role in understanding their applications in the medical field. In view of this, combination of glycine as an inner pore and lysine as an outer pore was selected for constructing the nanotubes. Glycine

was chosen in contrast to other amino acids since it is hydrophobic and hence helps the nanostructures to have more fluidity and flexibility. Glycine is an achiral molecule with hydrogen on its side chain and is the simplest constituent among the 20 amino acids. The absence of a side chain in glycine reduces the steric hindrance and hence leads to higher degree of flexibility compared to other amino acids. This is also predicted from the Flory's model, which correlates between glycine content and chain flexibility (Brant and Flory 1965; Miller et al. 1967; Ulijn and Smith 2008). As the glycine tail becomes longer, the apparent structure becomes broader and flexible (Brant and Flory 1965). Despite its structural simplicity, glycine is present as a major building block unit in structural proteins besides all types of collagens (Ayad et al. 1998). It is also present as an inhibitory neurotransmitter in the central nervous system, as a buffering agent in analgesics and as recombinant silk proteins (Seroski and Hudalla 2018). Lysine, on the other hand, is found in humans and is required for growth, tissue repair and is also present in many forms in dietary supplements. It plays an extensive role in building muscle protein, calcium absorption and have many other antimicrobial properties (Chen et al. 2010; Sánchez et al. 2007).

In this chapter, atomistic molecular dynamics (MD) simulations of the solvated G₆K (charged and neutral) nanotubes were performed with varying lengths and pore size. Stable neutral SLPs nanotubes of G₆K peptides were simulated successfully in this work. The main aim here was to investigate the structural and dynamic properties of water molecules inside the hydrophobic core and outside these pre-assembled nanotubes with varying pore size, tube length and presence of charges. Although, some studies regarding neutral A₆H membrane (Andrade and Colherinhas 2020) and other nanostructures has been reported using molecular dynamics where the obtained results were comparable to experimental results (Andrade et al. 2019, 2020; Andrade and Colherinhas 2020; Colherinhas and Fileti 2014a; b), the structural and dynamic properties of water molecules present inside and outside the pore of the peptide nanotubes have not been addressed. The present work aims in investigating the structural and dynamic aspects of water hydrogen bonding environment near the SLP-based nanotubes. Water is used as the basic solvent for this purpose because water has very specific properties that are essentially related to life and biological molecules like nucleic acids and proteins. It is a fascinating liquid

with a large number of anomalous properties (Biswas et al. 2018; Priyadarshini et al. 2020) and is essentially involved in nearly all chemical and biological processes. Water confined within such nanoscopic microemulsions has been shown to have different dynamics from the bulk (Hanasaki and Nakatani 2006; Kayal and Chandra 2015; Paul et al. 2014; Rana and Chandra 2007, 2015; Souza et al. 2006). It is also said to play a key role in the self-assembly process of nanostructures and in maintaining it (Zelenovskiy et al. 2020). A significant volume of water has been found inside the peptide nanotubes indicating the hydrogel behaviour of these nanotubes (Caló and Khutoryanskiy 2015; Engels et al. 1995; Yang et al. 2012). Therefore, studies on the properties of water in relation with the structure and dynamics of hydrogen bond network around the hydrophobic and hydrophilic pore of SLP nanostructures will be of great biological interest.

5.2 COMPUTATIONAL METHODOLOGY AND SIMULATION PROTOCOLS

5.2.1 Simulation Setup

In the present work, SLP nanotubes were investigated with G₆K peptides which composed of six glycine residues with a charged and neutral lysine head group. The terminals of glycine and lysine are capped with acetyl and N-methyl amide groups respectively. The studied polypeptide primary sequences are depicted in Figure.5.1. All the systems were initially preassembled with a juxtaposition of smaller polypeptides in form of intertwined spiral rings as given in Figure.5.2. This kind of initial organization was done to set forth the formation of intermolecular hydrogen bonds which have a significant role in peptide nanostructuring (Xu et al. 2009). Chloride/bromide anions were added as counter ions to neutralize the charged systems and finally, all the SLP nanotubes were solvated with water. Each system was setup keeping a buffer space of 1 Å (considering upto the third solvation shell of water-water RDF) between the peptide and the box. The details of system setup, parameters and compositions of all the simulated systems are given in Table 5.1, 5.2 and 5.3 respectively.

MD simulations were carried out with GROMACS (v2018.4) MD simulation program suite (Berendsen et al. 1995; Van Der Spoel et al. 2005) at constant temperature 300 K. All the nanostructures were modelled using CHARMM36 force field (Klauda et al. 2010) to employ the nonbonded and bonded interactions in the system and SPC/E model was used for water (Berendsen et al. 1981, 1987). SPC/E

water model has been extensively and successfully used in MD simulations of aqueous systems. Of all the three-point water models, SPC/E most accurately reproduces the experimental values of liquid water and its parameterization is the best three-point water model to interpret the interfacial behaviour of water hence making it the most favourable water model (Kusalik and Svishchev 1994; Underwood and Greenwell 2018). It can be noted that use of different water models and force fields gives similar qualitative results (Dilip.H.N. and Chakraborty 2019, 2020). To see the effect of a bigger counter ion in the system, one extra system was simulated using the parameters of bromine from the OPLS-AA force field (Jorgensen et al. 1996) for comparison. The mixture of these two different forces does not pose any problem in this study and the only intention of using this force field is to see the effect of anion size on water structure.

The systems were equilibrated in NVT ensemble using Velocity-rescale thermostat (Bussi et al. 2007) followed by NPT ensemble using modified Berendsen followed by Parrinello-Rahman barostats (Berendsen et al. 1984; Parrinello and Rahman 1980) for 10 ns each, followed by production stage for further 100 ns using NPT ensemble. All the structural properties were calculated from the last 50ns of the trajectory and for the calculation of hydrogen bond dynamics another MD run of 1 ns with time step of 1 fs was performed. Leapfrog algorithm was employed to integrate the equations of motions with integrating time step of 2.0 fs beside minimum image conventions (Allen and Tildesley 1989) and periodic boundary conditions was applied in all spatial directions. LINCS algorithm was employed to keep the bond lengths constrained (Hess et al. 1997). Lennard-Jones electrostatic interactions with a cut-off distance of 1.2 nm was employed (Darden et al. 1993; Essmann et al. 1995). Particle mesh ewald summation method was used to treat the coulombic interactions beyond cut-off of 1.2 nm in accordance with CHARMM36 specifications. Visual Molecular Dynamics program was used for visual analysis and image rendering (Humphrey et al. 1996). The appropriate pressure and temperature for the systems were maintained via semi-isotropic Parrinello-Rahman and velocity rescaling schemes, with coupling constants of 2.0 and 1.0 ps, respectively (Parrinello and Rahman 1980, 1981).

5.2.2 System Details

Systems 1 and 2 consist of eighteen G₆K capped peptides (charged and neutral each) in one ring and then stacked fifteen layers of such rings and hence described as 18x15. Systems 3 and 4 consist of eighteen G₆K capped peptides (charged and neutral each) in one ring and then stacked twelve layers of such rings and hence described as 18x12. Systems 5 and 6 consist of sixteen G₆K capped peptides (charged and neutral each) in one ring and then stacked twelve layers of such rings and hence described as 16x12. Chloride ions were added to neutralize the charged systems. All the basic entities of G₆K peptides were in accordance with the CHARMM36 FF specifications.

Table 5.1: Average box lengths (x, y, z), diameters of the inner pore, SLP and lengths of the nanotubes simulated.

Sl. No	Nanotube G ₆ K	Box dimension (nm)			Diameter (Å)		Length (Å)
		x	y	z	Inner pore	SLP	
1	18x15-charged	7.500	7.500	8.000	19.30	64.84	49.00
2	18x15-neutral	7.500	7.500	8.000	19.25	65.20	49.00
3	18x12-charged	7.500	7.500	7.000	19.30	64.84	38.54
4	18x12-neutral	7.500	7.500	7.000	19.25	65.20	38.54
5	16x12-charged	7.000	7.000	7.000	13.66	60.21	38.51
6	16x12-neutral	7.000	7.000	7.000	13.61	59.81	38.51

18 and 16 G₆K peptides were arranged in the form of cone shape (tilted by 30°) in one layer and each cone was placed on another cone layer rotated by 20° forming a nanotube structure of desired layers. Gromacs commands `gmx translate` and `gmx rotate` were used to construct the initial structures of nanotubes. Initial arrangement of G₆K nanotube was to promote the formation of intermolecular hydrogen bonds which imparts stability to the structure of nanotubes.

Table 5.2: The Lennard-Jones parameters and charges used in models for acetyl, glycine, lysine, N-methyl amide of G₆K charged and neutral peptide, water, chloride ion and bromide ion. e represents the elementary charge. *

Name	Atom	σ (Å)	ϵ (kJ/mol)	Charge (e)
ACE	CH ₃ (C)	3.63	0.3263	-0.27
	H (CH ₃)	2.38	0.1000	0.09
	C	3.56	0.4602	0.51
	O	3.02	0.5020	-0.51
Glycine	C	3.56	0.2928	0.51
	C _{α}	3.58	0.2343	-0.02
	O	3.02	0.5020	-0.51
	N	3.29	0.8368	-0.47
	HN	0.40	0.1924	0.09
	H _{α}	2.38	0.1171	0.31
Lysine	N	3.29	0.8368	-0.47 (-0.47)
	HN	0.40	0.1924	0.31 (0.31)
	CA	3.56	0.1338	0.07 (0.07)
	HA	2.35	0.0920	0.09 (0.09)
	CB	3.58	0.2343	-0.18 (-0.18)
	CG	3.58	0.2343	-0.18 (-0.18)
	CD	3.58	0.2343	-0.18 (-0.18)
	CE	3.58	0.2343	0.21 (0.13)
	HB	2.38	0.1422	0.09 (0.09)
	HG	2.38	0.1422	0.09 (0.09)
	HD	2.38	0.1422	0.09 (0.09)
	HE	2.38	0.1422	0.05 (0.07)
	NZ	4.053	0.0836	-0.30 (-0.96)
	HZ	0.40	0.1924	0.33 (0.34)
	C	3.56	0.4602	0.51 (0.51)
	O	3.02	0.5020	-0.51 (-0.51)
NME	N	3.29	0.8368	-0.47
	HN	0.40	0.1924	0.31
	CH ₃ (C)	3.63	0.3263	-0.11
	H (CH ₃)	2.38	0.1000	0.09
Water (SPC/E)	O	3.16	0.6502	-0.84

	H	---	---	0.42
Chlorine	Cl	4.04	0.6276	-1
Bromine**	Br	4.62	0.3765	-1

*The charges (e) for neutral lysine are given in parenthesis.

**The parameters for bromine are taken from OPLS-AA force field.

Table 5.3: Composition of all the simulated nanostructures. *

Sl. No	System	No. of G ₆ K (atoms per G ₆ K)	No. of ions	No. of water Molecules	Total no. of atoms
1	18x15-charged	270 (76)	270	8768	47094
2	18x15-neutral	270 (75)	---	9023	47319
3	18x12-charged	216 (76)	216	8089	40899
4	18x12-neutral	216 (75)	---	8274	41022
5	16x12-charged	192 (76)	192	7049	35931
6	16x12-neutral	192 (75)	---	7220	36060

*The numbers in parentheses refers to the number of atoms in each peptide.

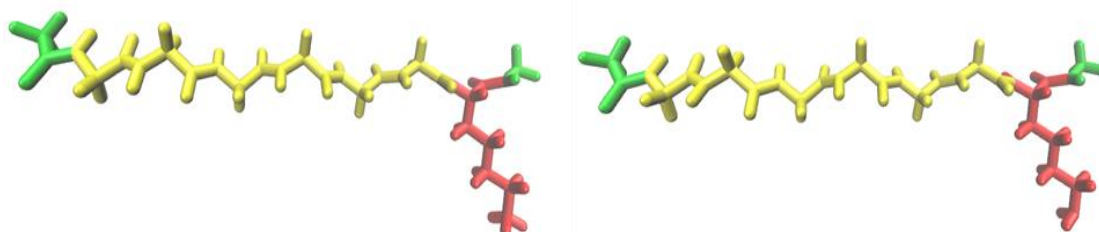


Figure 5.1: Charged (lysine unit having NH_3^+) (left) and neutral (lysine unit having NH_2) (right) G₆K peptide units investigated in this work. Glycine (G) in yellow, hydrophilic head lysine (K) in red, acetylated (CH_3CO) and amidated (NHCH_3) termini are shown in green. The terminals of glycine and lysine are capped with acetyl and N-methyl amide groups respectively.

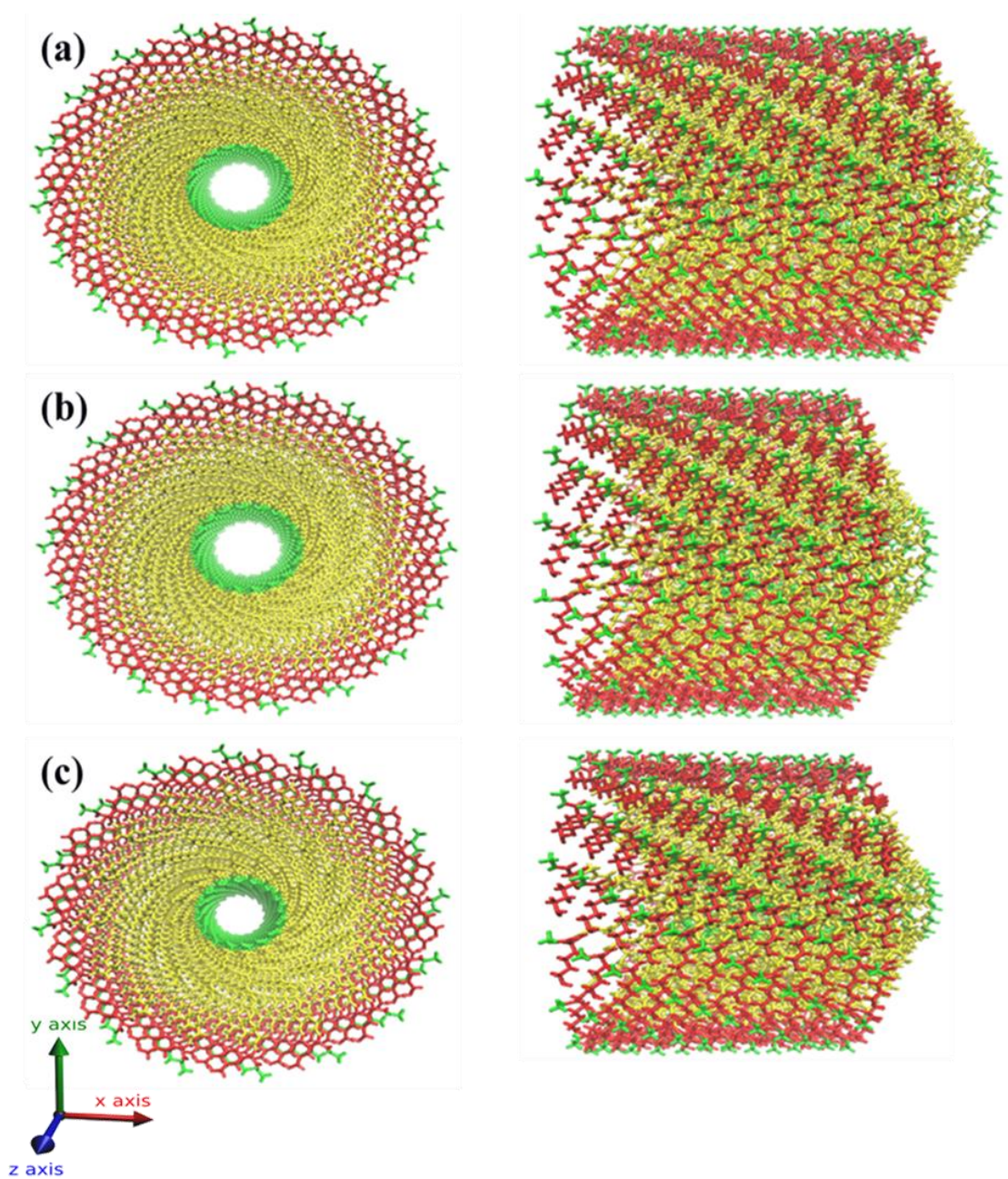


Figure 5.2: Lateral (left) and frontal (right) representations of G_6K nanotubes starting structures (a) 18x15 (b) 18x12 (c) 16x12 systems (water molecules omitted for clarity).

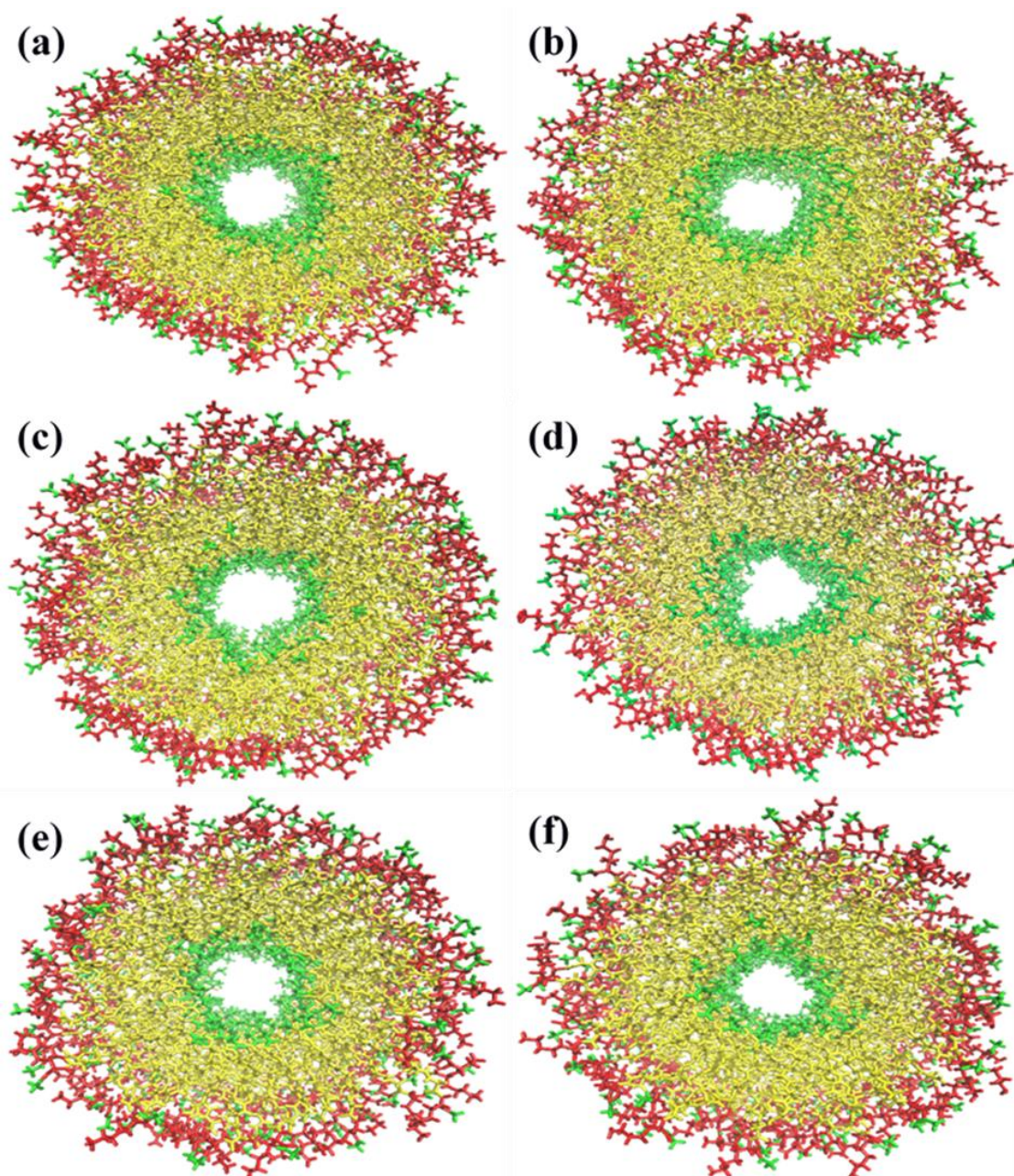


Figure 5.3: Nanotubes structures after NVT equilibration. (a) 18x15-charged (b)18x15-neutral (c) 18x12-charged (d) 18x12-neutral (e) 16x12-charged (f) 16x12-neutral.

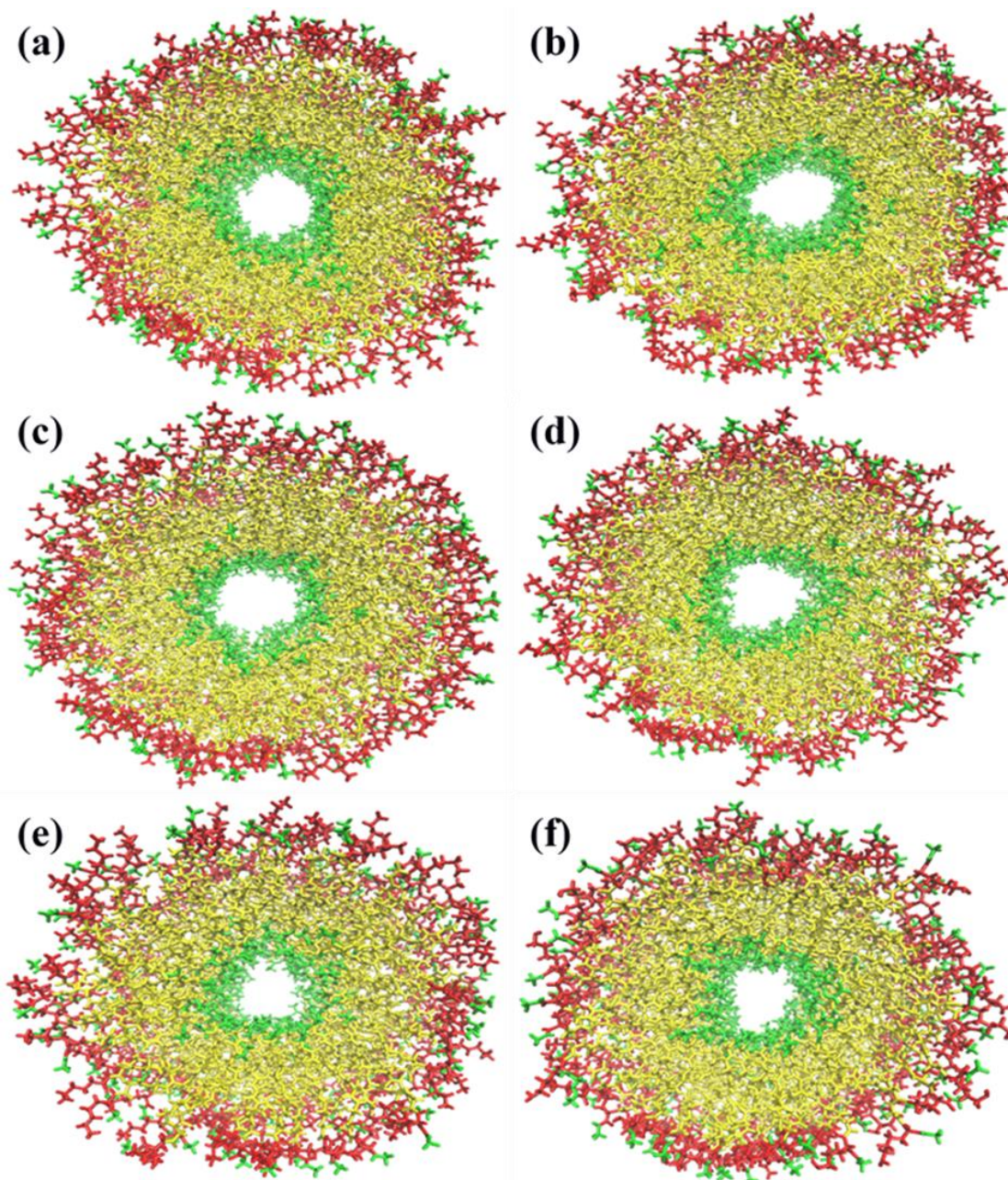


Figure 5.4: Nanotubes structures after NPT equilibration. (a) 18x15-charged (b)18x15-neutral (c) 18x12-charged (d) 18x12-neutral (e) 16x12-charged (f) 16x12-neutral.

5.3. RESULTS AND DISCUSSION

Final structures of all the simulated nanotubes and its corresponding water distributions are shown in Figure 5.5.

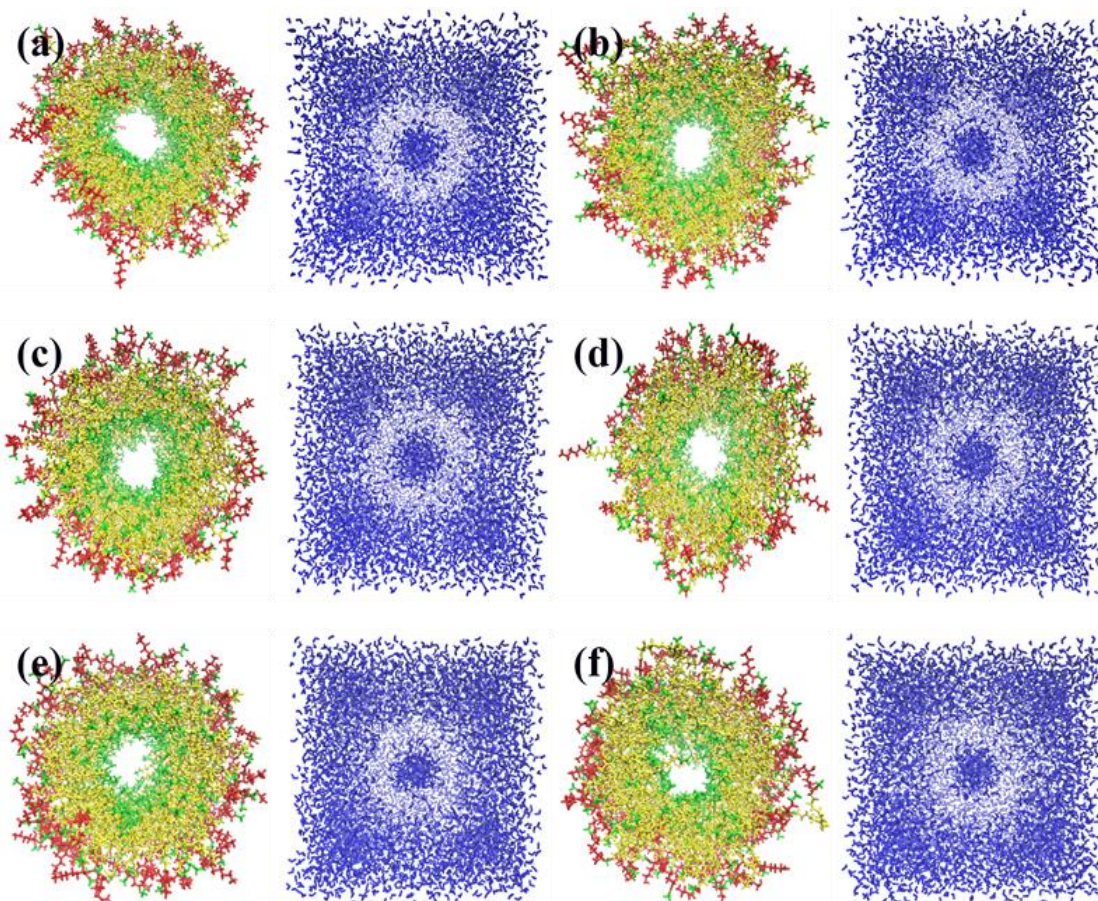


Figure 5.5: Lateral view representations of (a)18x15-charged (b)18x15-neutral (c)18x12-charged (d)18x12-neutral (e)16x12-charged (f)16x12-neutral G_6K nanotubes after the end of simulations (with water omitted) and its corresponding views of water distribution (with SLP omitted) in each nanotube systems are presented in blue colour.

5.3.1 Radial Distribution Functions

To study the structural properties of water molecules, present inside and outside the pore of SLPs, radial distribution functions (RDF) of the capped portion of peptides with water i.e. $COCH_3-O_w$ (methyl carbon of acetylated group with oxygen of water) and $NHCH_3-O_w$ (methyl carbon of amidated group with oxygen of water) are plotted in Figure 5.6. It can be seen that the positions of first peak maxima and minima of RDFs of acetyl-water and N-methyl amide-water remain same for all the six systems. The acetyl-water RDF shows the inner pore RDF and N-methyl amide-water shows the

outer pore RDF of the nanostructures with water molecules. The peak heights of the first and second solvation shells of acetyl-water RDF are found to be almost same for charged and neutral systems of 18x15 and 18x12. However, for 16x12 system, higher peak height for the charged system is observed compared to its neutral analogue due to the presence of the ions trapped inside the charged system which can be further confirmed from Figure 5.6(d). The RDFs can be well correlated with the density plots given in Figure 5.7. In case of N-methyl amide-water, peak heights for the charged systems are more compared to its neutral analogues. This may be due to the presence of positive charge over nitrogen atom of lysine group which is present outside the pore attracting more water molecules.

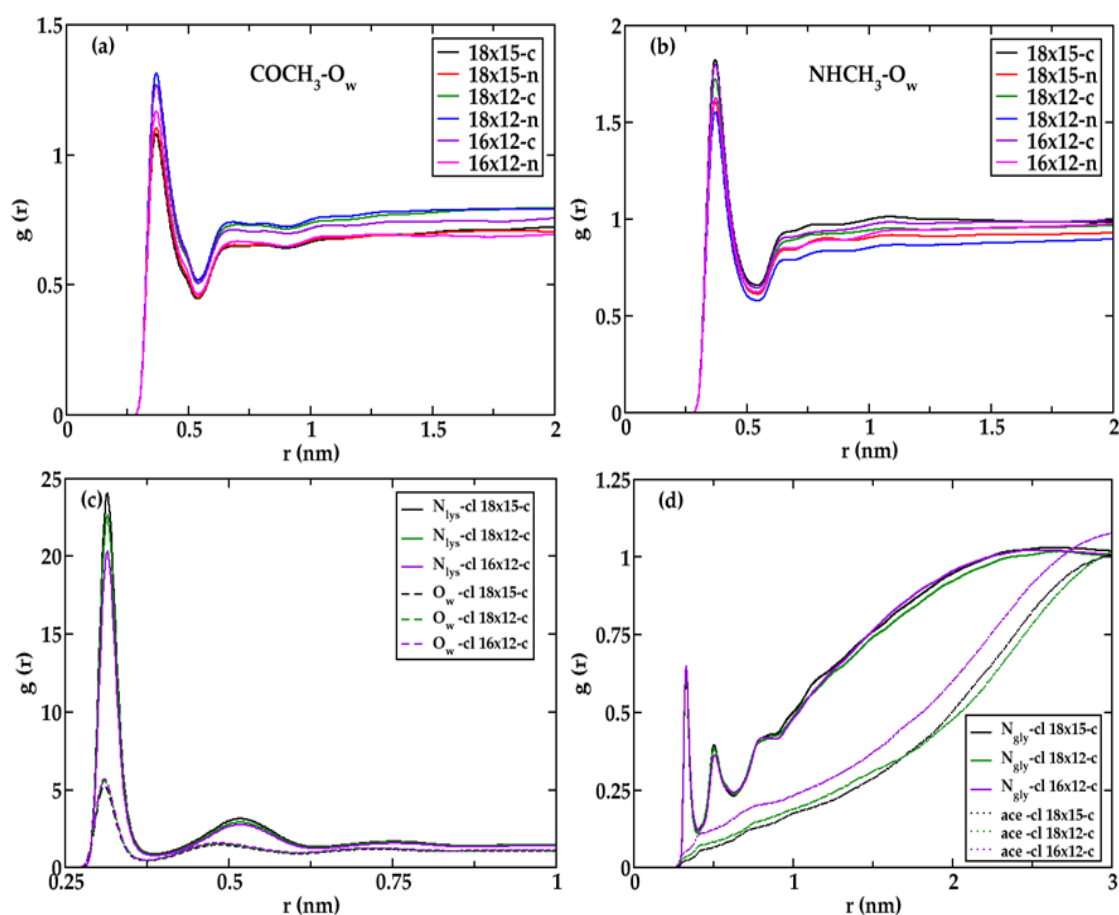


Figure 5.6: Various site-site radial distribution functions $g(r)$ of (a) $COCH_3-O_w$ and (b) $NHCH_3-O_w$ for different systems, (c) terminal nitrogen of lysine-chlorine (solid line), water-chlorine (dotted line) and (d) nitrogen of glycine-chlorine (solid line), acetyl-chlorine (dotted line) for charged systems.

Radial distribution functions of chloride ion with peptide and chloride ion with water molecules are plotted to check the distribution of ions in the charged nanotubes.

In Figure 5.6(c) and (d), various site-site interactions of terminal nitrogen of lysine-chlorine ($N_{\text{lys}}\text{-Cl}$), water-chlorine ($O_{\text{w}}\text{-Cl}$), nitrogen of glycine-chlorine ($N_{\text{gly}}\text{-Cl}$) and acetyl-chlorine ($\text{COCH}_3\text{-Cl}$) have been plotted. Chloride ions are more likely to be found near the lysine group (Figure 5.6(c)) as compared to water molecules in charged systems. Interestingly, greater probability of chloride ions trapped inside the nanotube of 16x12 charged system was observed. In case of 18x12, due to its higher pore/height ratio with respect to other nanotubes, probability of chloride ions getting trapped inside the nanotube is much less.

5.3.2 Density Profile

Next it will be interesting to study the density profile of water molecules with respect to x/y-axes and z-axis of SLP nanotubes. The nanotubes were stacked in the z-direction. In Figure 5.7, water density profiles of all nanotubes with respect to z-axis and x-axis (since density profiles with along x and y-axes will be almost same) have been plotted. Two types of water density profiles are observed. Along z-axis (Figure.5.7(a)), the density of water molecules initially decreases from 1000 kg.m^{-3} to around 430 kg.m^{-3} as the nanotube is encountered, then it slightly increases to around 570 kg.m^{-3} inside the pore (2.3 nm - 4.7 nm) and ultimately increases to the bulk density as it crosses the nanotube. The region of minima in z-axis gives information about the length of nanotube. It is found that the charged nanotubes have more water molecules inside the pore in contrast to their neutral analogues which decreases on approaching the nanotube walls in x/y axes. Maximum density is found for 18x15 systems which is quite obvious because of the bigger tube length and pore size.

Study of density profiles along x-axis shows the presence of two sharp minima. These two minima are due to presence of two walls of nanotube, where the density of water decreases. It is evident from Figure.5.7(b) that these nanotubes consist of water molecules even in-between the interpeptide planes due to the presence of polar groups. Water molecules inside the pores are heterogeneously distributed along the x/y plane. The two minima are more pronounced in case of charged systems which suggests that water molecules are more evenly distributed in neutral system compared to its charged analogue. The width of two minima gives an idea of the pore size width. To investigate further structural details of water molecules near these nanotubes, number of hydrogen

bonds, translational order parameter and angle distributions of $\langle \text{O-O-O} \rangle$ bonds have been calculated in subsequent sections.

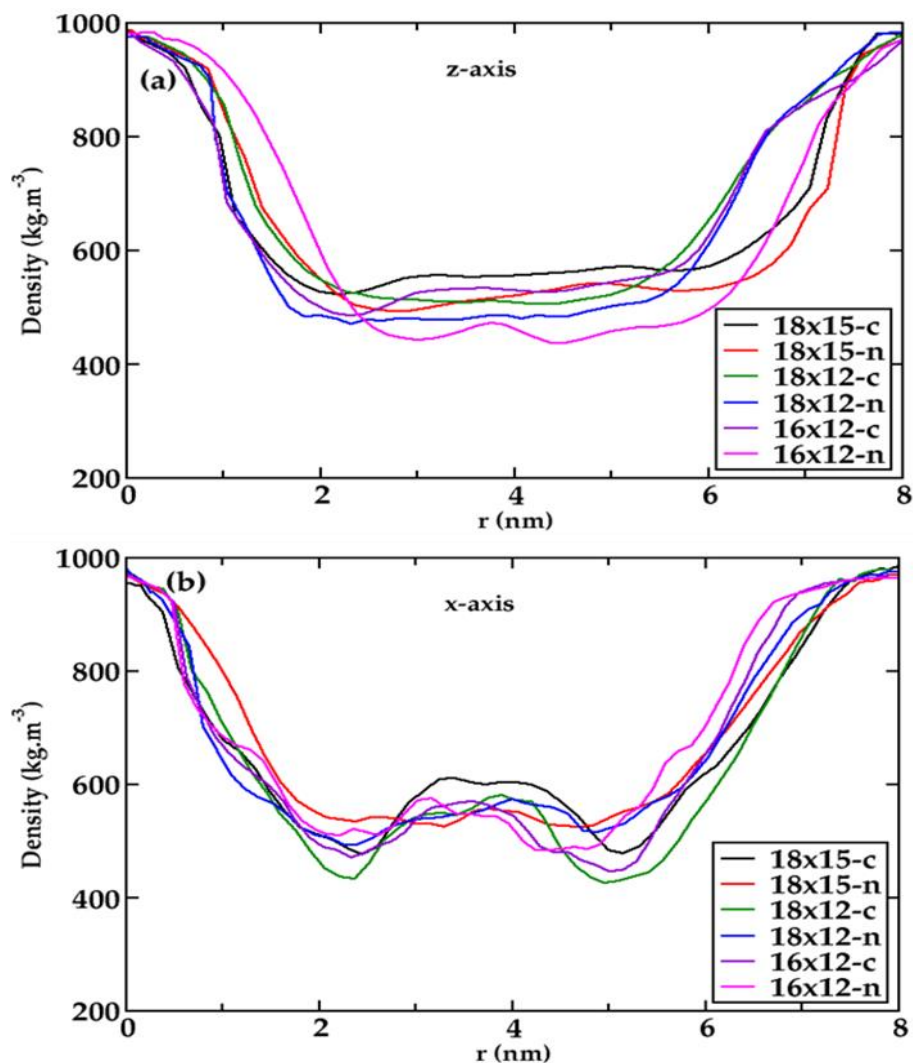


Figure 5.7: Water density profile (kg.m^{-3}) along the z and x directions computed for different systems.

5.3.3 Number of hydrogen bonds

In Figure 5.8, the number of hydrogen bonds with respect to capped acetyl and N-methyl amide groups have been plotted. Since the acetylated and amidated groups are present towards the inner and outer pore of nanotubes respectively, these distributions give information about the water network inside and outside the pore. Two oxygen atoms are considered to be hydrogen bonded if the interatomic distance is less than 3.25 \AA . Two cut-offs for our calculations were considered to see the distribution of the water molecules based on the placement of the solvation shells in RDF, one $0\text{-}5.6 \text{ \AA}$ and the other $5.3\text{-}10.0 \text{ \AA}$ from the acetyl and N-methyl amide groups of the nanostructures. The

fraction of water molecules (f_n) that engage in n number of water-water hydrogen bonds have been computed and plotted.

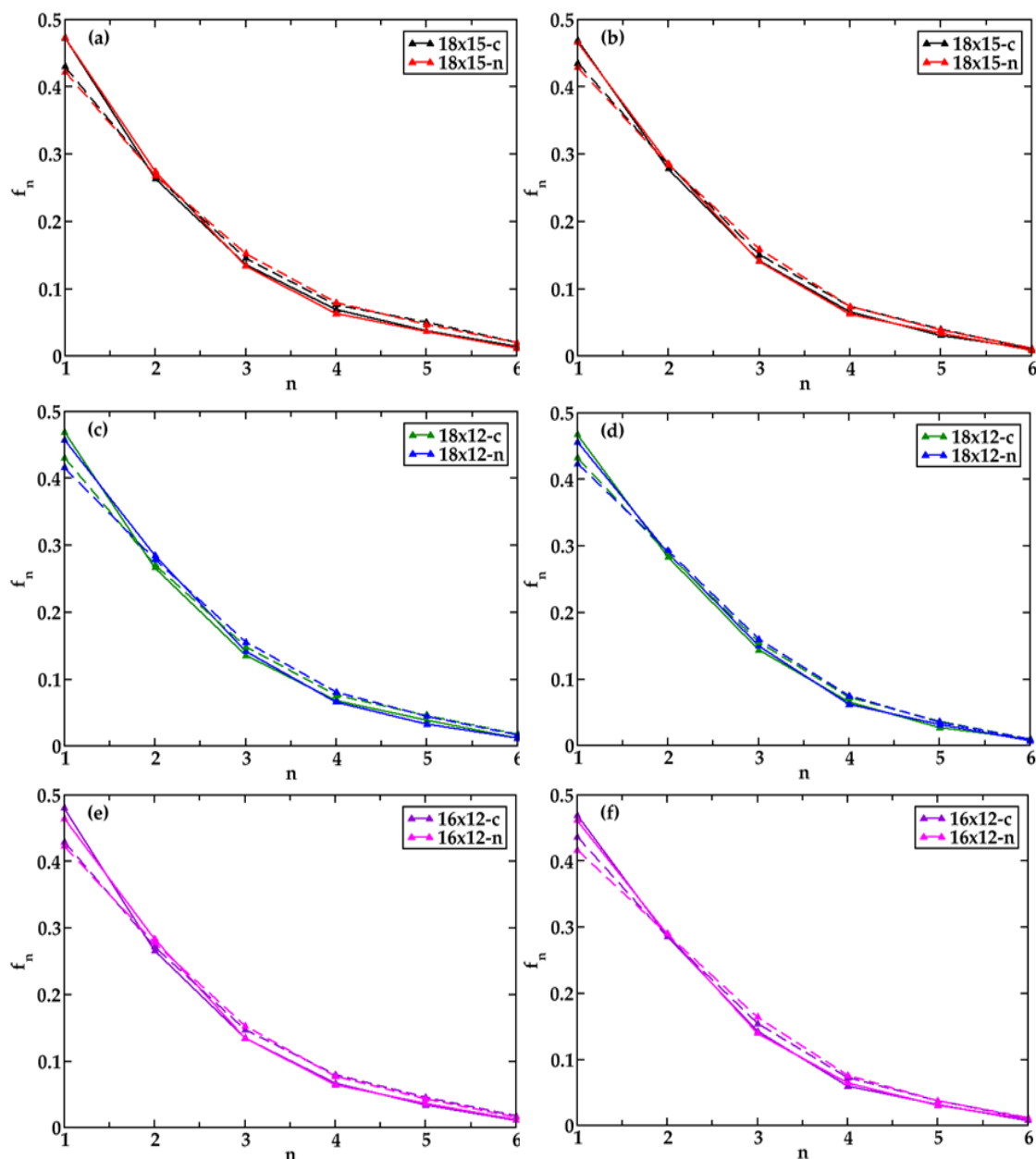


Figure 5.8: The fraction of water molecules (f_n) having n number of hydrogen bonds within the pore (a, c, e) and outside the pore (b, d, f) up to distance 5.6 Å (solid lines) and within distance 5.3-10.0 Å (broken lines) of acetyl and N-methyl amide groups.

Negligible difference was observed in the number of hydrogen bonds near the interfaces of inner and outer walls of the nanotube. In general, neutral systems have higher coordinated hydrogen bonds compared to its charged analogues (Figure.5.8 (a), (c) and (e)) and it is also found that neutral 18x12 systems have more fraction of higher coordinated hydrogen bonds compared to other systems (Figure. 5.9 (c) and (d)) which

indicates the presence of more tetrahedral water arrangement. This can be further confirmed from the translational order parameter (S_k values) given in Figure 5.13. In the inner pore, near 0-5.6 Å cut-off, charged 18x15 and 18x12 systems show more presence of higher coordinated hydrogen bonds compared to 16x12 systems (Figure.5.9 (a)).

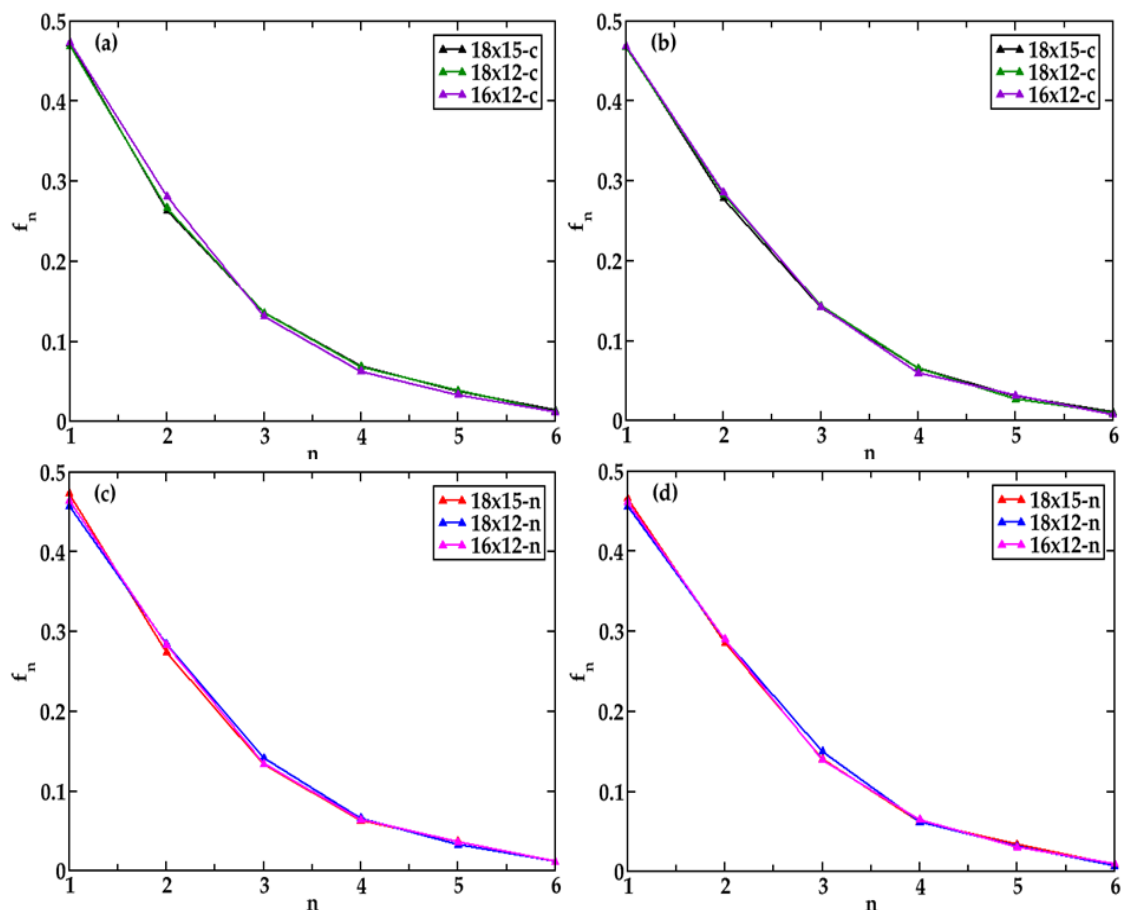


Figure 5.9: The fraction of water molecules having n number of hydrogen bonds within the pore (left) and outside the pore (right) for different systems up to distance 5.6 Å of acetyl and N-methyl amide groups.

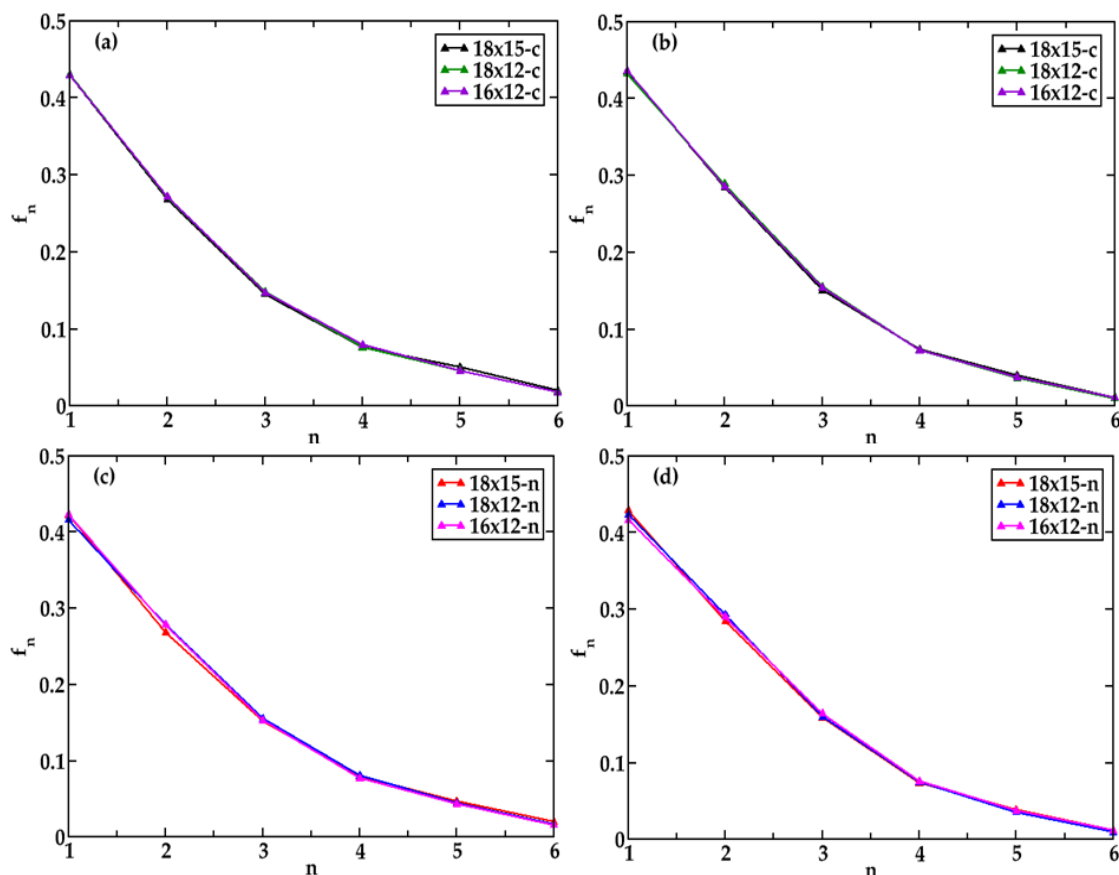


Figure 5.10: The fraction of water molecules having n number of hydrogen bonds within the pore (left) and outside the pore (right) for different systems within distance 5.3-10.0 Å of acetyl and N-methyl amide groups.

Fraction of water molecules having n number of hydrogen bonds within (left) and outside (right) the pores for system 5 and its bromine analogue are given in Figure 5.12.

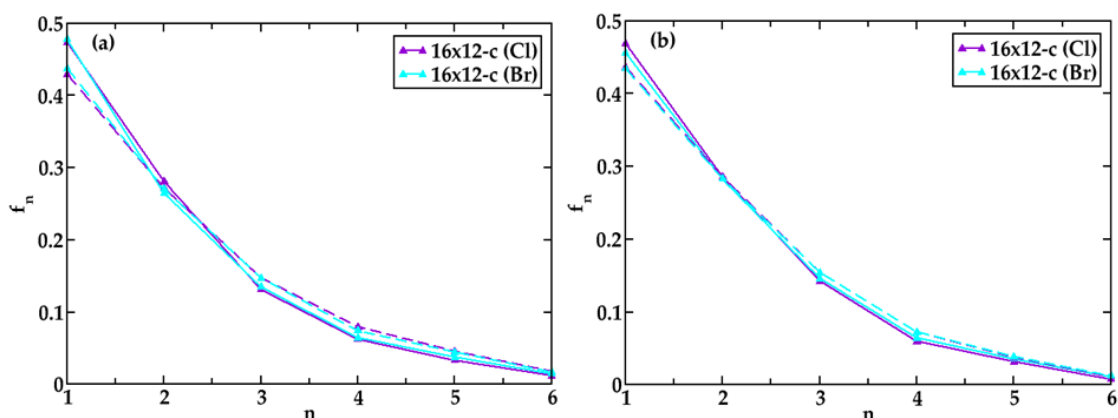


Figure 5.11: The fraction of water molecules having n number of hydrogen bonds within the pore (left) and outside the pore (right) for systems 5 and its bromine analogue up to distance 5.6 Å (solid lines) and within distance 5.3-10.0 Å (broken lines) of acetyl and N-methyl amide groups.

Further, the number of hydrogen bonds formed between each pair of SLPs, amino acid residues and peptide-water have been calculated which are depicted in Figure 5.12. It is seen that the number of hydrogen bonds formed by the donors and acceptors between SLP-SLP and peptide-peptide is more for neutral nanostructures. On the other hand, number of hydrogen bonds formed between SLP, peptides with water is higher in case of charged nanostructures indicating that SLP and peptides form higher hydrogen bonds with water in charged analogues. It will be useful to look at the translational order parameter of water molecules near these nanotubes.

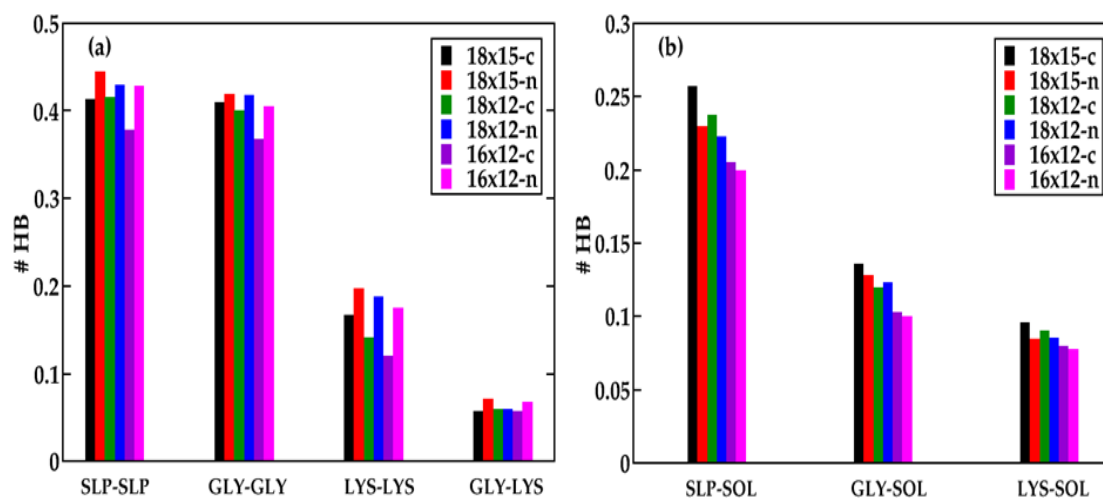


Figure 5.12: Number of hydrogen bonds formed per residue (a) among the residues and (b) between peptides and water molecules. Peptide is abbreviated as SLP, glycine residue as GLY, lysine residue as LYS and water as SOL.

5.3.4 Translational Tetrahedral Order S_k

The tetrahedral order distance part S_k was introduced by Chau and Hardwick (Chau and Hardwick 1998) to measure the radial distances between a central atom to peripheral atoms which is defined as

$$S_k = \frac{1}{3} \sum_{k=1}^4 \frac{(r_k - \bar{r})^2}{4\bar{r}^2} \quad (5.1)$$

where $1/3$ is a normalization factor, r_k is the radial distance from the central atom to the k^{th} peripheral atom, \bar{r} is the arithmetic mean of the four radial distances. S_k is 0 for a perfect tetrahedron and reaches a maximum value of 1 if the configuration deviates from tetrahedrality.

In Figure 5.13, the translational tetrahedral order parameter of water molecules in different nanotubes have been plotted. It can be seen that water molecules inside the

neutral nanotubes are more tetrahedral compared to its charged analogues. As the length of the tube is increased, tetrahedrality increases and it is found least in the case of 16x12 system due to smaller pore size.

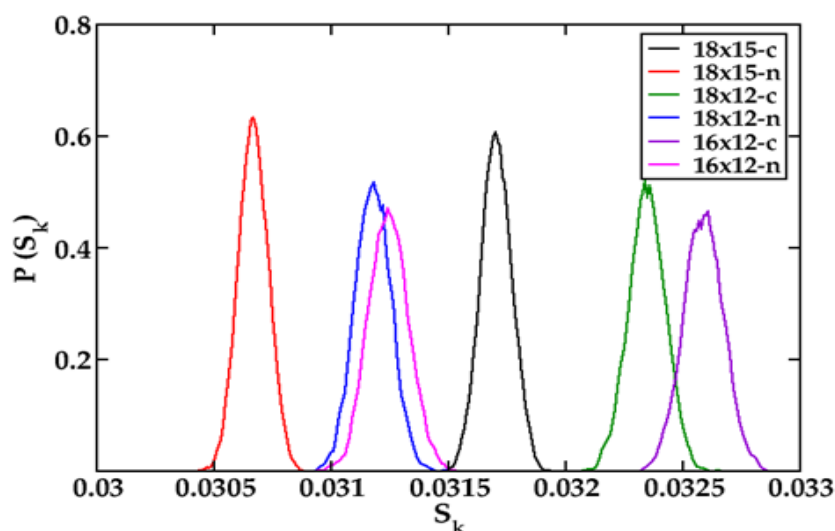


Figure 5.13: Normalized tetrahedral order (S_k) distribution of water molecules in different nanotubes.

5.3.5 Orientation Profile

Similar to the number of hydrogen bonds calculation, the orientation profiles of water molecules present inside and outside the pore have been calculated. To elucidate the tetrahedral structure of water molecules, the angular distribution function θ_{OOO} of water molecules inside and outside the pore of nanotubes have been calculated. Water molecules which are present up to 0-5.6 Å and 5.3-10.0 Å of acetyl and N-methyl amide groups are considered as interfacial molecules for calculations. In Figure 5.14, the probability distribution $P(\theta_{OOO})$ of interfacial water molecules inside and outside the pore present near the capped ends (acetyl and N-methyl amide) of nanotubes have been plotted.

Three distinct peaks are observed in the distribution profiles at 20-30°, 60° and 109° which corresponds to bent linear, icosahedral (Dilip.H.N. and Chakraborty 2019; Prasad and Chakravarty 2017) and distorted tetrahedral configurations respectively. Peaks corresponding to inside the pore are more pronounced and well defined compared to the outside due to more heterogeneous environment. Further, it is noticed that the charged nanotubes have more pronounced peak compared to its neutral analogue. As

tube length is decreased, the peak height is increased. Similar trend is found for water molecules in the outer pore. Here peak distributions are broader compared to inner pore.

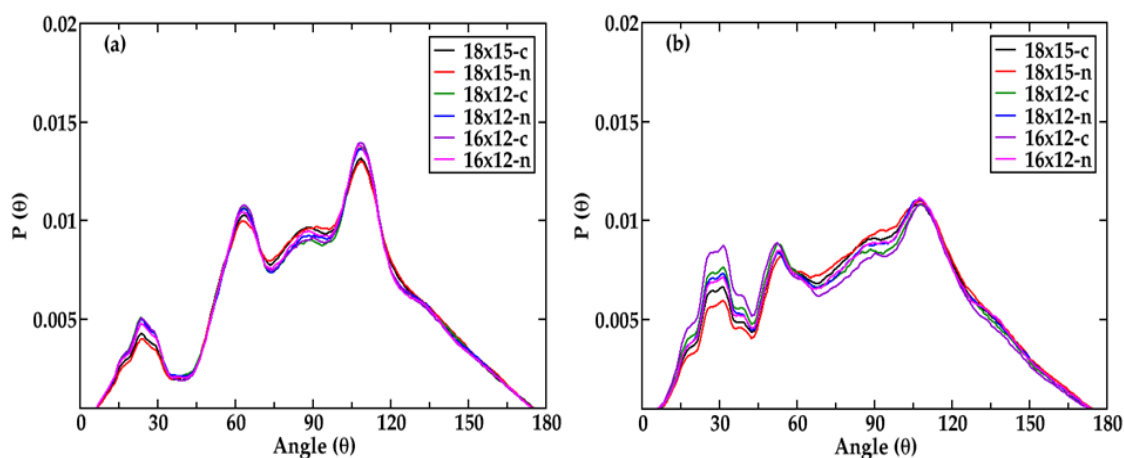


Figure 5.14: Normalized probability distribution of $\langle \text{O-O-O} \rangle$ angle of oxygen atoms of water molecules (a) within the pore and (b) outside the pore for different systems up to distance 5.6 Å of acetyl and N-methyl amide groups.

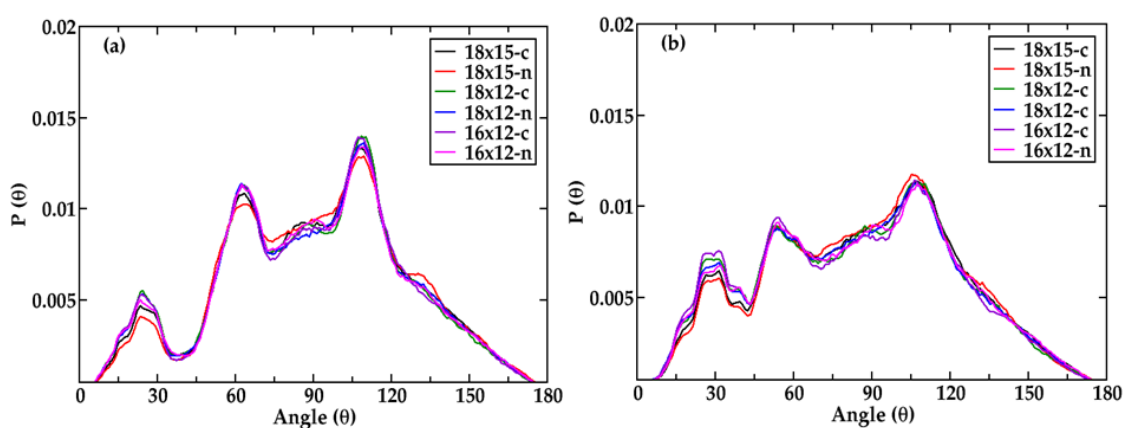


Figure 5.15: Normalized probability distribution of $\langle \text{O-O-O} \rangle$ angle of oxygen atoms of water molecules (a) within the pore and (b) outside the pore for different systems within distance 5.3-10.0 Å of acetyl and N-methyl amide groups.

The orientation profile of water molecules within the pore (left) and outside the pore (right) for system 5 and its bromine analogue are given in Figure 5.16.

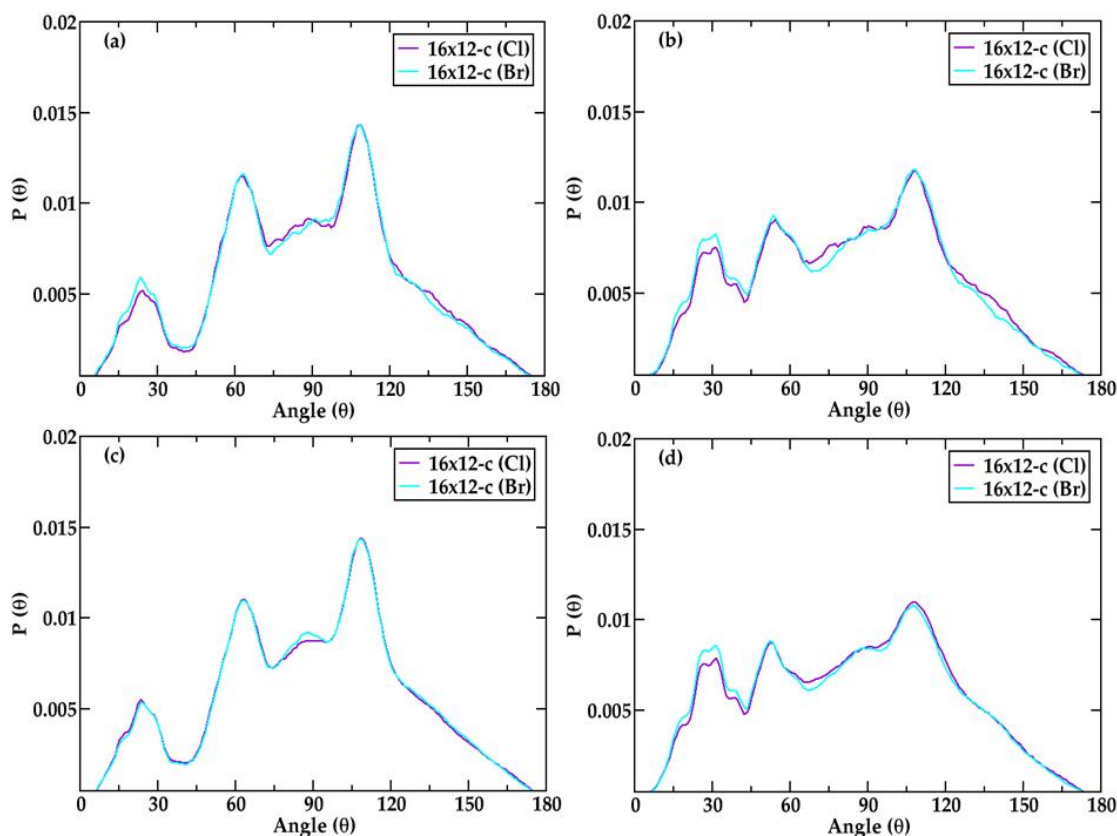


Figure 5.16: Normalized probability distribution of <O-O-O angle of oxygen atoms of water molecules within the pore (left) and outside the pore (right) for systems 5 and its bromine analogue up to distance 5.6 Å (a, b) and within distance 5.3-10.0 Å (c, d) of acetyl and N-methyl amide groups.

5.3.6 Hydrogen Bond Dynamics

In aqueous media, SLPs are capable of forming hydrogen bonds with water and they can also modify the regular water-water hydrogen bond network. The hydrogen bond dynamics of SLP-water and water-water molecules inside and outside the pore were characterized in terms of time correlation functions (TCF's), namely continuous hydrogen bond, $S_{HB}(t)$ and intermittent hydrogen bond, $C_{HB}(t)$ lifetimes (τ_{HB}) (Chandra 2000; Luzar and Chandler 1996; Rapaport 1983; Stillinger 1975, 1980). Two molecules are said to be hydrogen bonded if the interatomic distance between hydrogen bond donor and acceptor pairs are < 2.5 Å.

$$S_{HB}(t) = \frac{\langle h(0)H(t) \rangle}{\langle h(0)^2 \rangle} \quad (5.2)$$

$$C_{HB}(t) = \frac{\langle h(0)h(t) \rangle}{\langle h(0)^2 \rangle} \quad (5.3)$$

where $\langle \dots \rangle$ denotes the average over all pairs of a given type. The population parameter $h(t) = 1$, when a particular pair between two molecules is bonded at time t or zero otherwise. On the other hand, variable $H(t)=1$, when tagged pair of sites remain continuously hydrogen bonded from time $t=0$ to $t=t$ or zero otherwise. $S(t)$ provides a strict definition of a tagged hydrogen bond lifetime whereas $C(t)$ provides information of overall relaxation time scales of hydrogen bond.

Hydrogen bond lifetimes formed between water molecules and peptide-water are tabulated in Table 5.4 and 5.5 respectively. It is clearly visible from the table that hydrogen bond lifetime of water molecules inside the pore is greater than water molecules which are residing outside the pore. The reason is very obvious due to the availability of lesser number of water molecules inside the pore. Once the hydrogen bond is made, it is preserved for longer time due to lack of neighbouring water molecules. Further, the diffusivity of water is less inside the pore compared to the outer pore which also contributes to the higher lifetime inside the pore. It is also found that hydrogen bond lifetimes of charged systems are more compared to its neutral analogues due to the presence of ions, resulting in stronger bond formation between water molecules.

Table 5.4: The continuous and intermittent lifetime (τ_{HB}) of hydrogen bonds (in ps) formed by water-water inside the pore and outside the pore of nanotubes. *

Systems	$\langle \tau_s^{WW} \rangle$ (ps) (continuous)		$\langle \tau_c^{WW} \rangle$ (ps) (intermittent)	
	Inside the pore	Outside the pore	Inside the pore	Outside the pore
18x15-charged	1.542	1.310	15.093	11.256
18x15-neutral	1.289	1.247	10.450	10.080
18x12-charged	1.457	1.260	13.594	10.349
18x12-neutral	1.250	1.230	10.303	9.960
16x12-charged	1.590 (1.541)	1.240 (1.200)	15.934 (15.206)	9.997 (9.112)
16x12-neutral	1.542	1.164	14.812	8.831
Bulk water	0.842		3.825	

*The τ_s and τ_c values for pure bulk water are listed for comparison. The lifetime for bromine analogue of system 5 are given in parenthesis.

Maximum hydrogen bond lifetime was found for water molecules inside the pore of 16x12 system compared to 18x15 and 18x12 systems. This is because number of water molecules trapped inside the nanotube of 16x12 are less compared to other systems. Therefore, a bonded water molecule takes more time to find a new neighbour in order to make a new hydrogen bond which increases the hydrogen bond lifetime of 16x12 systems. In case of 18x12 system, number of water molecules trapped will be less due to lesser height and bigger pore size, hence hydrogen bond lifetime of this system is less. However, it is found that hydrogen bond lifetimes of water molecules present outside the pore of 18x15 system are more than 18x12 system and least in case of 16x12 system. The continuous and intermittent lifetimes of bulk water matches very well with reported literatures (Guàrdia et al. 2002, 2006b; Kumar et al. 2009).

This can be explained due to the fact that 18x15 system have bigger nanotube structure which makes the number of interfacial water molecules more in comparison to 18x12 system and 16x12 system and hence the trend. Similar trend is seen in the case of intermittent hydrogen bond lifetime. Hydrogen bond lifetime for bromine analogue of 16x12 charged system was also calculated and it was found to have lower hydrogen bond lifetime compared to the presence of chloride ions. This is due to the bigger size of bromide ion which results in lesser charge density than chloride ion and hence decreased electrostatic force of interactions with water molecules.

Table 5.5: The continuous lifetime (τ_{HB}) of hydrogen bonds (in ps) formed by peptide-water inside the pore and outside the pore of nanotubes. *

Systems	$\langle \tau_s^{PW} \rangle$ (ps) (continuous)	
	Inside the pore	Outside the pore
18x15-charged	1.422	0.760
18x15-neutral	1.346	0.796
18x12-charged	1.338	0.764
18x12-neutral	1.311	0.796
16x12-charged	1.456 (1.318)	0.723 (0.729)
16x12-neutral	1.394	0.795

*The lifetime for bromine analogue of system 5 are given in the parenthesis.

Further, peptide-water hydrogen bond lifetime inside and outside the pore have been calculated and the results are tabulated in Table 5.5. Here also, hydrogen bond

lifetimes inside the pore are more for all cases and enhanced in case of charged systems. In case of bromine, however, hydrogen bond lifetime is comparable with the neutral analogue. Outside the pore, since lysine part interacts with water molecules, which is less hydrophilic compared to its glycine counterpart, the hydrogen bond lifetime decreases significantly compared to inner pore. Interestingly, it is found that charged systems have less peptide-water hydrogen bond lifetime outside the pore compared to its neutral analogues. This can be attributed due to the presence of chloride ions in charged systems which are mutually attracted towards the positively charged nitrogen groups present towards outer pore of nanotube, which significantly reduces the probability of peptide-water interactions.

5.4. Conclusions

Structural and dynamic properties of water inside the pore and outside the nanotube were studied with the pre-assembled nanotubes of surfactant-like peptides with molecular structures G₆K (neutral and charged). The effect of increasing length, pore size and effect of charge on water structure near these SLP nanotubes have been focussed. Three different systems 18x15, 18x12 and 16x12 were considered. It is found that the density of water is more in case of charged systems along z-direction as compared to its neutral analogue. However, in the x/y axis, charged systems are found to be more inhomogeneous. Calculation of fraction of hydrogen bonds and orientation profile of water molecules suggests that structures of water molecules are more tetrahedral in neutral systems.

Tetrahedrality decreases as moved towards the smallest nanotube 16x12 which shows maximum hydrogen bond lifetime between water-water and water-peptide molecules in the inner pore. Lifetime increases for charged analogues due to the presence of trapped chloride ions inside the nanotube and maximum lifetime is found for 16x12 system. 18x12 systems show minimum hydrogen bond lifetime in the inner pore due to its larger pore size compared to smaller height. Outside the pore, 18x15 shows maximum water-water hydrogen bond lifetime. Hydrogen bond lifetimes of peptide-water molecules are lesser outside the pore due to favourable interactions between the negatively charged chloride ions and positively charged lysine groups which decreases the probability of interactions between peptide and water. Neutral analogues are found to have more peptide-water hydrogen bond lifetime compared to

the charged cases. Insights gained in this study have shown interesting features on the behaviour of water molecules in different nanotubes and effect of ions in it.



CHAPTER-6

CHAPTER 6

SUMMARY AND CONCLUSIONS

***Abstract:** This chapter bestows a summary of the whole research work. It also confers the major conclusions drawn from the research work.*

6.1 SUMMARY

- Molecular dynamics simulations of aqueous amino acids, amides and peptides in presence of osmolytes and ions as cosolvents with varying concentrations have been performed.
- The effects of cosolvents on the solvation structure of different moieties of amino acids, amides and peptides have been investigated.
- The structural properties of cosolvents and water molecules near the interface and bulk of these biomolecules have been investigated in terms of radial distribution functions (RDF), spatial distribution functions (SDF), number of hydrogen bonds and orientation profile calculations.
- Thermodynamic properties are calculated in terms of Potential Mean Force (PMF) and Kirkwood-Buff (KB) Integrals.
- Calculations pertaining to preferential binding coefficients of water and cosolvents with biomolecules have been carried out.
- Dynamic properties are calculated in terms of hydrogen bond autocorrelation functions.
- Structural and dynamic properties of water molecules inside and outside the pore of pre-assembled SLP nanotubes with varying core size and tube length have been carried out.
- The effect of charge and ions on the structural and dynamic properties of peptide-water and water-water interactions in the pre-assembled SLP nanotubes have been investigated.

6.2 CONCLUSIONS

The major conclusions of the present research work are listed below.

- Radial distribution functions and spatial distribution functions showed the presence of a protective hydration layer near the C_{α} of glycine amino acid in presence of TMAO which gets reduced in case of urea, KCl and minimum in case of LiCl.
- In ionic systems especially for LiCl, an increment in water density at higher distance from the hydrophobic unit of glycine is found due to the presence of first solvation shell of lithium-ion bounded to the carboxylate group of the glycine. This water density is also found to give extra stability to the glycine molecule.
- Changes in solvation shells near the carboxylate group of glycine in presence of KCl are found to be less pronounced as compared to LiCl. However, the second solvation shell near the carboxylate group of glycine in presence of KCl is seen to be disrupted.
- TMAO imparts stability to the biomolecules by increasing the hydration shell especially near the C_{α} carbon and strengthening the hydrogen bond network of the solution. In solutions of urea, this protective hydration shell is missing and less interaction between solvent molecules and biomolecules are found.
- The hydration shells near the hydrophobic unit were found to impart extra stability to the systems of aqueous biomolecules. This hydration shell results mainly from the strong hydration shell of the neighbouring polar groups i.e., the carbonyl carbon and the amine group of the biomolecule.
- The addition of cosolvents increases the hydrogen bond strength of water molecules compared to those aqueous biomolecular systems.
- Positions of the subgroups i.e., amine, carbonyl and hydrophobic groups in amino acids and peptides play a key role in imparting the stability of proteins in presence of osmolytes.
- In presence of TMAO, water molecules tend to preferentially bind with amino acids and amides. Strong hydrogen bonds and preferential binding affinity of water molecules towards biomolecules are found to be the key reasons for stability in presence of TMAO.
- In aqueous solutions of urea, amides are found to be less solvated with water in comparison to amino acids.

-
- Urea and TMAO were preferably excluded from the surface of amino acids but preferential exclusion of TMAO molecules was observed from the surface of amide molecules compared to urea.
 - In pre-assembled peptide nanotubes, density of water is found to be more in the inner pores in case of charged nanotubes compared to its neutral analogues.
 - Water molecules were found to be more tetrahedral in case of neutral nanotubes compared to their charged analogue. Further, the tetrahedrality decreases as the size of the nanotube decreases.
 - For neutral analogues, number of peptide-peptide hydrogen bonds are more and number of peptide-water hydrogen bonds are less when compared with their charged analogues.
 - Water molecules consisted of bent linear, icosahedral and distorted tetrahedral configurations around the peptide nanotubes.
 - Water molecules inside the pore have greater hydrogen bond strength compared to water molecules residing outside the pore.
 - Due to the presence of ions, hydrogen bond lifetimes of charged systems are more compared to its neutral analogues.
 - Hydrogen bond lifetimes of water molecules inside the pore increases with decrease in nanotube length and pore size due to decrease in number of water molecules available for making and breaking of hydrogen bonds.
 - Hydrogen bond life time of water molecules increases outside the pore for bigger length of nanotube due to more heterogeneity of the system.
 - Peptide-water hydrogen bond lifetime of charged analogues are lesser outside the pore due to favourable interactions between the negatively charged chloride ions and positively charged lysine groups which decreases the probability of interactions between peptide and water.

The present research work gives a glance at the effects of cosolvents on the hydration characteristics of amino acids, amides and peptides (along with SLP nanotubes) and its specific properties which can be tuned based on their applications. As much is to be explored, the future work will be devoted towards further understanding of the effects of other cosolvents on different biomolecular structures with varying functionalities and properties. Successively, greater insights can be obtained by the study of the effect of pH, temperature to understand the elementary

forces that are responsible for the stabilization or destabilization of biomolecules. Insights gained through this study gives some interesting features on the stability issue of proteins and the behaviour of water molecules in different nanotubes in presence of ions.



REFERENCES

-
- Adler-Abramovich, L., and Gazit, E. (2014). “The physical properties of supramolecular peptide assemblies: from building block association to technological applications.” *Chem Soc Rev*, 43(20), 6881–6893.
- Aggeli, A., Bell, M., Carrick, L. M., Fishwick, C. W. G., Harding, R., Mawer, P. J., Radford, S. E., Strong, A. E., and Boden, N. (2003). “pH as a Trigger of Peptide β -Sheet Self-Assembly and Reversible Switching between Nematic and Isotropic Phases.” *J. Am. Chem. Soc.*, 125(32), 9619–9628.
- Akiyama, M. (2002). “Study on hydration enthalpy of N-methylacetamide in water.” *Spectrochim. Acta A Mol. Biomol. Spectrosc.*, 58(9), 1943–1950.
- Albrecht, Gustav., and Corey, R. B. (1939). “The Crystal Structure of Glycine.” *J. Am. Chem. Soc.*, 61(5), 1087–1103.
- Alder, B. J., and Wainwright, T. E. (1959). “Studies in Molecular Dynamics. I. General Method.” *J. Chem. Phys.*, 31(2), 459–466.
- Alder, B. J., and Wainwright, T. E. (1960). “Studies in Molecular Dynamics. II. Behavior of a Small Number of Elastic Spheres.” *J. Chem. Phys.*, 33(5), 1439–1451.
- Allen, F. H., Bellard, S., Brice, M. D., Cartwright, B. A., Doubleday, A., Higgs, H., Hummelink, T., Hummelink-Peters, B. G., Kennard, O., Motherwell, W. D. S., Rodgers, J. R., and Watson, D. G. (1979). “The Cambridge Crystallographic Data Centre: computer-based search, retrieval, analysis and display of information.” *Acta Crystallogr. B*, 35(10), 2331–2339.
- Allen, M. P., and Tildesley, D. J. (1989). *Computer Simulation of Liquids: Second Edition*. Oxford University Press.
- Allison, S. K., Bates, S. P., Crain, J., and Martyna, G. J. (2006). “Solution Structure of the Aqueous Model Peptide N-Methylacetamide.” *J. Phys. Chem. B*, 110(42), 21319–21326.
- Andrade, D., and Colherinhas, G. (2020). “A6H polypeptide membranes: Molecular dynamics simulation, GIAO-DFT-NMR and TD-DFT spectroscopy analysis.” *J. Mol. Liq.*, 316, 113850.
- Andrade, D., Oliveira, L. B. A., and Colherinhas, G. (2019). “Elucidating NH₂-I3V3A3G3K3-COOH and NH₂-K3G3A3V3I3-COOH polypeptide membranes: A classical molecular dynamics study.” *J. Mol. Liq.*, 279, 740–749.
-

-
- Andrade, D., Oliveira, L. B. A., and Colherinhas, G. (2020). "Design and analysis of polypeptide nanofiber using full atomistic Molecular Dynamic." *J. Mol. Liq.*, 302, 112610.
- Andrew Mackay, J., and Chilkoti, A. (2008). "Temperature sensitive peptides: Engineering hyperthermia-directed therapeutics." *Int. J. Hyperthermia.*, 24(6), 483–495.
- Åqvist, J. (1990). "Ion-water interaction potentials derived from free energy perturbation simulations." *J. Phys. Chem.*, 94(21), 8021–8024.
- Arakawa, T., and Timasheff, S. N. (1985). "The stabilization of proteins by osmolytes." *Biophys. J.*, 47(3), 411–414.
- Assarsson, P., and Eirich, F. R. (1968). "Properties of amides in aqueous solution. I. Viscosity and density changes of amide-water systems. An analysis of volume deficiencies of mixtures based on molecular size differences (mixing of hard spheres)." *J. Phys. Chem.*, 72(8), 2710–2719.
- Athawale, M. V., Dordick, J. S., and Garde, S. (2005). "Osmolyte Trimethylamine-N-Oxide Does Not Affect the Strength of Hydrophobic Interactions: Origin of Osmolyte Compatibility." *Biophys. J.*, 89(2), 858–866.
- Auton, M., and Bolen, D. W. (2004). "Additive Transfer Free Energies of the Peptide Backbone Unit That Are Independent of the Model Compound and the Choice of Concentration Scale." *Biochemistry*, 43(5), 1329–1342.
- Auton, M., and Bolen, D. W. (2005). "Predicting the energetics of osmolyte-induced protein folding/unfolding." *Proc. Natl. Acad. Sci.*, 102(42), 15065–15068.
- Auton, M., Bolen, D. W., and Rösgen, J. (2008). "Structural thermodynamics of protein preferential solvation: Osmolyte solvation of proteins, aminoacids, and peptides." *Proteins Struct. Funct. Bioinforma.*, 73(4), 802–813.
- Auton, M., Holthauzen, L. M. F., and Bolen, D. W. (2007). "Anatomy of energetic changes accompanying urea-induced protein denaturation." *Proc. Natl. Acad. Sci.*, 104(39), 15317–15322.
- Auton, M., Rösgen, J., Sinev, M., Holthauzen, L. M. F., and Bolen, D. W. (2011). "Osmolyte effects on protein stability and solubility: A balancing act between backbone and side-chains." *Biophys. Chem.*, 159(1), 90–99.
- Ayad, S., Boot-Handford, R., Humphries, M., Kadler, K., and Shuttleworth, A. (1998). *The Extracellular Matrix Factsbook - 2nd Edition*.
-

-
- Baker, E. N., and Hubbard, R. E. (1984). "Hydrogen bonding in globular proteins." *Prog. Biophys. Mol. Biol.*, 44(2), 97–179.
- Baldwin, R. L. (1996). "How Hofmeister ion interactions affect protein stability." *Biophys. J.*, 71(4), 2056–2063.
- Barton, K. N., Buhr, M. M., and Ballantyne, J. S. (1999). "Effects of urea and trimethylamine N-oxide on fluidity of liposomes and membranes of an elasmobranch." *Am J Physiol Regul Integr Comp Physiol.*, 276(2), R397–R406.
- Baskakov, I., and Bolen, D. W. (1998). "Forcing Thermodynamically Unfolded Proteins to Fold." *J. Biol. Chem.*, 273(9), 4831–4834.
- Baudry, J., and Smith, J. C. (1994). "Molecular mechanics analysis of peptide group hydrogen bonding cooperativity and influence on Φ and Ψ rotational barriers." *J. Mol. Struct: THEOCHEM*, 308, 103–113.
- Baumann, M. K., Textor, M., and Reimhult, E. (2008). "Understanding Self-Assembled Amphiphilic Peptide Supramolecular Structures from Primary Structure Helix Propensity." *Langmuir*, 24(15), 7645–7647.
- Bennion, B. J., and Daggett, V. (2003). "The molecular basis for the chemical denaturation of proteins by urea." *Proc. Natl. Acad. Sci.*, 100(9), 5142–5147.
- Bennion, B. J., and Daggett, V. (2004). "Counteraction of urea-induced protein denaturation by trimethylamine N-oxide: A chemical chaperone at atomic resolution." *Proc. Natl. Acad. Sci.*, 101(17), 6433–6438.
- Berendsen, H. J. C. (1999). "Molecular Dynamics Simulations: The Limits and Beyond." Springer Berlin Heidelberg, 3–36.
- Berendsen, H. J. C., Grigera, J. R., and Straatsma, T. P. (1987). "The missing term in effective pair potentials." *J. Phys. Chem.*, 91(24), 6269–6271.
- Berendsen, H. J. C., Gunsteren, W. F. van, and Hermans, J. (1981). "Interaction Models for Water in Relation to Protein Hydration." *Intermolecular Forces*, 14, 331–342.
- Berendsen, H. J. C., Postma, J. P. M., Gunsteren, W. F. van, DiNola, A., and Haak, J. R. (1984). "Molecular dynamics with coupling to an external bath." *J. Chem. Phys.*, 81(8), 3684–3690.
- Berendsen, H. J. C., Spoel, D. van der, and Drunen, R. van. (1995). "GROMACS: A message-passing parallel molecular dynamics implementation." *Comput. Phys. Commun.*, 91(1–3), 43–56.
-

-
- Berteotti, A., Barducci, A., and Parrinello, M. (2011). “Effect of Urea on the β -Hairpin Conformational Ensemble and Protein Denaturation Mechanism.” *J. Am. Chem. Soc.*, 133(43), 17200–17206.
- Best, R. B., Zhu, X., Shim, J., Lopes, P. E. M., Mittal, J., Feig, M., and MacKerell, A. D. (2012). “Optimization of the Additive CHARMM All-Atom Protein Force Field Targeting Improved Sampling of the Backbone ϕ , ψ and Side-Chain χ_1 and χ_2 Dihedral Angles.” *J. Chem. Theory Comput.*, 8(9), 3257–3273.
- Biswas, S., Chakraborty, D., and Mallik, B. S. (2018). “Interstitial Voids and Resultant Density of Liquid Water: A First-Principles Molecular Dynamics Study.” *ACS Omega*, 3(2), 2010–2017.
- Bolen, D. W., and Baskakov, I. V. (2001). “The osmophobic effect: natural selection of a thermodynamic force in protein folding.” *J. Mol. Biol.*, 310(5), 955–963.
- Bolen, D. W., and Rose, G. D. (2008). “Structure and Energetics of the Hydrogen-Bonded Backbone in Protein Folding.” *Annu. Rev. Biochem.*, 77(1), 339–362.
- Bonaccorsi, R., Palla, P., and Tomasi, J. (1984). “Conformational energy of glycine in aqueous solutions and relative stability of the zwitterionic and neutral forms. An ab initio study.” *J. Am. Chem. Soc.*, 106(7), 1945–1950.
- Borghain, G., and Paul, S. (2016). “Model Dependency of TMAO’s Counteracting Effect Against Action of Urea: Kast Model versus Osmotic Model of TMAO.” *J. Phys. Chem. B*, 120(9), 2352–2361.
- Born, B., Kim, S. J., Ebbinghaus, S., Gruebele, M., and Havenith, M. (2009). “The terahertz dance of water with the proteins: the effect of protein flexibility on the dynamical hydration shell of ubiquitin.” *Faraday Discuss*, 141, 161–173.
- Brant, D. A., and Flory, P. J. (1965). “The Configuration of Random Polypeptide Chains. II. Theory.” *J. Am. Chem. Soc.*, 87(13), 2791–2800.
- Brehm, M., and Kirchner, B. (2011). “TRAVIS - A Free Analyzer and Visualizer for Monte Carlo and Molecular Dynamics Trajectories.” *J. Chem. Inf. Model.*, 51(8), 2007–2023.
- Brooks, C. L., and Nilsson, L. (1993). “Promotion of helix formation in peptides dissolved in alcohol and water-alcohol mixtures.” *J. Am. Chem. Soc.*, 115(23), 11034–11035.
- Brovchenko, I., and Oleinikova, A. (2008). “Multiple Phases of Liquid Water.” *ChemPhysChem*, 9(18), 2660–2675.
-

-
- Bryant, R. G. (1996). "The Dynamics of Water-Protein Interactions." *Annu. Rev. Biophys. Biomol. Struct.*, 25(1), 29–53.
- Bussi, G., Donadio, D., and Parrinello, M. (2007). "Canonical sampling through velocity rescaling." *J. Chem. Phys.*, 126(1), 014101.
- Caballero-Herrera, A., Nordstrand, K., Berndt, K. D., and Nilsson, L. (2005). "Effect of Urea on Peptide Conformation in Water: Molecular Dynamics and Experimental Characterization." *Biophys. J.*, 89(2), 842–857.
- Cacace, M. G., Landau, E. M., and Ramsden, J. J. (1997). "The Hofmeister series: salt and solvent effects on interfacial phenomena." *Q. Rev. Biophys.*, 30(3), 241–277.
- Cafilisch, A., and Karplus, M. (1999). "Structural details of urea binding to barnase: a molecular dynamics analysis." *Structure*, 7(5), 477-S2.
- Caló, E., and Khutoryanskiy, V. V. (2015). "Biomedical applications of hydrogels: A review of patents and commercial products." *Eur. Polym. J.*, 65, 252–267.
- Campo, M. G. (2006). "Molecular dynamics simulation of glycine zwitterion in aqueous solution." *J. Chem. Phys.*, 125(11), 114511.
- Canchi, D. R., and García, A. E. (2013). "Cosolvent Effects on Protein Stability." *Annu. Rev. Phys. Chem.*, 64(1), 273–293.
- Canchi, D. R., Jayasimha, P., Rau, D. C., Makhatadze, G. I., and Garcia, A. E. (2012). "Molecular Mechanism for the Preferential Exclusion of TMAO from Protein Surfaces." *J. Phys. Chem. B*, 116(40), 12095–12104.
- Cappa, C. D., Smith, J. D., Messer, B. M., Cohen, R. C., and Saykally, R. J. (2006). "The Electronic Structure of the Hydrated Proton: A Comparative X-ray Absorption Study of Aqueous HCl and NaCl Solutions." *J. Phys. Chem. B*, 110(3), 1166–1171.
- Carta, R., and Tola, G. (1996). "Solubilities of L-Cystine, L-Tyrosine, L-Leucine, and Glycine in Aqueous Solutions at Various pHs and NaCl Concentrations." *J. Chem. Eng. Data*, 41(3), 414–417.
- Cavalli, S., Albericio, F., and Kros, A. (2010). "Amphiphilic peptides and their cross-disciplinary role as building blocks for nanoscience." *Chem Soc Rev*, 39(1), 241–263.
- Chakraborty, D., and Chandra, A. (2011). "Diffusion of ions in supercritical water: Dependence on ion size and solvent density and roles of voids and necks." *J. Mol. Liq.*, 162(1), 12–19.
-

-
- Chakraborty, D., Taly, A., and Sterpone, F. (2015). “Stay Wet, Stay Stable? How Internal Water Helps the Stability of Thermophilic Proteins.” *J. Phys. Chem. B*, 119(40), 12760–12770.
- Chand, A., and Chowdhuri, S. (2016). “Effects of dimethyl sulfoxide on the hydrogen bonding structure and dynamics of aqueous N-methylacetamide solution.” *J. Chem. Sci.*, 128(6), 991–1001.
- Chandra, A. (2000). “Effects of Ion Atmosphere on Hydrogen-Bond Dynamics in Aqueous Electrolyte Solutions.” *Phys. Rev. Lett.*, 85(4), 768–771.
- Chandrasekhar, J., Spellmeyer, D. C., and Jorgensen, W. L. (1984). “Energy component analysis for dilute aqueous solutions of lithium(1+), sodium(1+), fluoride(1-), and chloride(1-) ions.” *J. Am. Chem. Soc.*, 106(4), 903–910.
- Chaplin, M. F. (2001). “Water: its importance to life.” *Biochem. Mol. Biol. Educ.*, 29(2), 54–59.
- Chau, P.-L., and Hardwick, A. J. (1998). “A new order parameter for tetrahedral configurations.” *Mol. Phys.*, 93(3), 511–518.
- Chaudhari, A., Sahu, P. K., and Lee, S.-L. (2004). “Many-body interaction in glycine–(water)₃ complex using density functional theory method.” *J. Chem. Phys.*, 120(1), 170–174.
- Chen, C., Pan, F., Zhang, S., Hu, J., Cao, M., Wang, J., Xu, H., Zhao, X., and Lu, J. R. (2010). “Antibacterial Activities of Short Designer Peptides: a Link between Propensity for Nanostructuring and Capacity for Membrane Destabilization.” *Biomacromolecules*, 11(2), 402–411.
- Chen, J., and Zou, X. (2019). “Self-assemble peptide biomaterials and their biomedical applications.” *Bioact. Mater.*, 4, 120–131.
- Chen, J.-X., Wang, H.-Y., Li, C., Han, K., Zhang, X.-Z., and Zhuo, R.-X. (2011). “Construction of surfactant-like tetra-tail amphiphilic peptide with RGD ligand for encapsulation of porphyrin for photodynamic therapy.” *Biomaterials*, 32(6), 1678–1684.
- Cho, S. S., Reddy, G., Straub, J. E., and Thirumalai, D. (2011). “Entropic Stabilization of Proteins by TMAO.” *J. Phys. Chem. B*, 115(45), 13401–13407.
- Chowdhuri, S., and Chandra, A. (2001). “Molecular dynamics simulations of aqueous NaCl and KCl solutions: Effects of ion concentration on the single-particle, pair, and

- collective dynamical properties of ions and water molecules.” *J. Chem. Phys.*, 115(8), 3732–3741.
- Chowdhuri, S., and Chandra, A. (2003). “Hydration structure and diffusion of ions in supercooled water: Ion size effects.” *J. Chem. Phys.*, 118(21), 9719–9725.
- Colherinhas, G., and Fileti, E. (2014a). “Molecular Description of Surfactant-like Peptide Based Membranes.” *J. Phys. Chem. C*, 118(18), 9598–9603.
- Colherinhas, G., and Fileti, E. (2014b). “Molecular Dynamics Study of Surfactant-Like Peptide Based Nanostructures.” *J. Phys. Chem. B*, 118(42), 12215–12222.
- Collins, K. (2004). “Ions from the Hofmeister series and osmolytes: effects on proteins in solution and in the crystallization process.” *Methods*, 34(3), 300–311.
- Collins, K. D. (1995). “Sticky ions in biological systems.” *Proc. Natl. Acad. Sci.*, 92(12), 5553–5557.
- Collins, K. D., Neilson, G. W., and Enderby, J. E. (2007). “Ions in water: Characterizing the forces that control chemical processes and biological structure.” *Biophys. Chem.*, 128(2–3), 95–104.
- Collins, K. D., and Washabaugh, M. W. (1985). “The Hofmeister effect and the behaviour of water at interfaces.” *Q. Rev. Biophys.*, 18(4), 323–422.
- Cordeiro, M. A. M., Santana, W. P., Cusinato, R., and Cordeiro, J. M. M. (2006). “Monte carlo investigations of intermolecular interactions in water–amide mixtures.” *J. Mol. Struct. THEOCHEM*, 759(1–3), 159–164.
- Cornell, W. D., Cieplak, P., Bayly, C. I., Gould, I. R., Merz, K. M., Ferguson, D. M., Spellmeyer, D. C., Fox, T., Caldwell, J. W., and Kollman, P. A. (1995). “A Second Generation Force Field for the Simulation of Proteins, Nucleic Acids, and Organic Molecules.” *J. Am. Chem. Soc.*, 117(19), 5179–5197.
- Cote, Y., Fu, I. W., Dobson, E. T., Goldberger, J. E., Nguyen, H. D., and Shen, J. K. (2014). “Mechanism of the pH-Controlled Self-Assembly of Nanofibers from Peptide Amphiphiles.” *J. Phys. Chem. C*, 118(29), 16272–16278.
- Courtenay, E. S., Capp, M. W., Anderson, C. F., and Record, M. T. (2000). “Vapor Pressure Osmometry Studies of Osmolyte–Protein Interactions: Implications for the Action of Osmoprotectants in Vivo and for the Interpretation of ‘Osmotic Stress’ Experiments in Vitro.” *Biochemistry*, 39(15), 4455–4471.
- Cui, H., Webber, M. J., and Stupp, S. I. (2010). “Self-assembly of peptide amphiphiles: From molecules to nanostructures to biomaterials.” *Biopolymers*, 94(1), 1–18.

-
- Daggett, V. (2006). "Protein Folding–Simulation." *Chem. Rev.*, 106(5), 1898–1916.
- Darden, T., York, D., and Pedersen, L. (1993). "Particle mesh Ewald: An $N \cdot \log(N)$ method for Ewald sums in large systems." *J. Chem. Phys.*, 98(12), 10089–10092.
- Debye, P., and Hückel, E. (1923). "De la theorie des electrolytes. I. abaissement du point de congelation et phenomenes associes." *Phys. Z.*, 24(9), 185–206.
- Dehsorkhi, A., Castelletto, V., Hamley, I. W., Seitsonen, J., and Ruokolainen, J. (2013). "Interaction between a Cationic Surfactant-like Peptide and Lipid Vesicles and Its Relationship to Antimicrobial Activity." *Langmuir*, 29(46), 14246–14253.
- Dexter, A. F. (2010). "Interfacial and Emulsifying Properties of Designed β -Strand Peptides." *Langmuir*, 26(23), 17997–18007.
- Dexter, A. F., and Middelberg, A. P. J. (2008). "Peptides As Functional Surfactants." *Ind. Eng. Chem. Res.*, 47(17), 6391–6398.
- Dilip.H.N., and Chakraborty, D. (2019). "Hydrophilicity of the hydrophobic group: Effect of cosolvents and ions." *J. Mol. Liq.*, 280, 389–398.
- Dilip.H.N., and Chakraborty, D. (2020). "Effect of cosolvents in the preferential binding affinity of water in aqueous solutions of amino acids and amides." *J. Mol. Liq.*, 300, 112375.
- Dill, K. A. (1990). "Dominant forces in protein folding." *Biochemistry*, 29(31), 7133–7155.
- Dill, K. A., and Shortle, D. (1991). "Denatured States of Proteins." *Annu. Rev. Biochem.*, 60, 795–825.
- Dill, K. A., Truskett, T. M., Vlachy, V., and Hribar-Lee, B. (2005). "Modeling Water, the Hydrophobic Effect, and Ion Solvation." *Annu. Rev. Biophys. Biomol. Struct.*, 34(1), 173–199.
- Ding, Y., and Krogh-Jespersen, K. (1992). "The glycine zwitterion does not exist in the gas phase: results from a detailed ab initio electronic structure study." *Chem. Phys. Lett.*, 199(3–4), 261–266.
- Dixon, D. A., Dobbs, K. D., and Valentini, J. J. (1994). "Amide-Water and Amide-Amide Hydrogen Bond Strengths." *J. Phys. Chem.*, 98(51), 13435–13439.
- Dobson, C. M. (2003). "Protein folding and misfolding." *Nature*, 426(6968), 884–890.
- Dolui, B. K., Bhattacharya, S. K., and Kundu, K. K. (2008). "Solvent Effect on Deprotonation Equilibria of Acids of Various Charge Types in Non-aqueous

- Isodielectric Mixtures of Protic Ethylene Glycol and Dipolar Aprotic N,N-Dimethylformamide at 298.15 K.” *J. Solut. Chem.*, 37(7), 987–1003.
- Drabik, P., Liwo, A., Czaplewski, C., and Ciarkowski, J. (2001). “The investigation of the effects of counterions in protein dynamics simulations.” *Protein Eng. Des. Sel.*, 14(10), 747–752.
- Drakenberg, T., and Forsén, S. (1971). “The barrier to internal rotation in monosubstituted amides.” *J Chem Soc D*, 0(21), 1404–1405.
- Du, H., Rasaiah, J. C., and Miller, J. D. (2007). “Structural and Dynamic Properties of Concentrated Alkali Halide Solutions: A Molecular Dynamics Simulation Study.” *J. Phys. Chem. B*, 111(1), 209–217.
- Dunshee, L. C., Sullivan, M. O., and Kiick, K. L. (2020). “Manipulation of the dually thermoresponsive behavior of peptide-based vesicles through modification of collagen-like peptide domains.” *Bioeng. Transl. Med.*, 5(1).
- Eberhardt, E. S., and Raines, R. T. (1994). “Amide-Amide and Amide-Water Hydrogen Bonds: Implications for Protein Folding and Stability.” *J. Am. Chem. Soc.*, 116(5), 2149–2150.
- Elstner, M., Frauenheim, T., and Suhai, S. (2003). “An approximate DFT method for QM/MM simulations of biological structures and processes.” *J. Mol. Struct. THEOCHEM*, 632(1–3), 29–41.
- Engels, M., Bashford, D., and Ghadiri, M. R. (1995). “Structure and Dynamics of Self-Assembling Peptide Nanotubes and the Channel-Mediated Water Organization and Self-Diffusion. A Molecular Dynamics Study.” *J. Am. Chem. Soc.*, 117(36), 9151–9158.
- Essmann, U., Perera, L., Berkowitz, M. L., Darden, T., Lee, H., and Pedersen, L. G. (1995). “A smooth particle mesh Ewald method.” *J. Chem. Phys.*, 103(19), 8577–8593.
- Ewald, P. P. (1921). “Die Berechnung optischer und elektrostatischer Gitterpotentiale.” *Ann. Phys.*, 369(3), 253–287.
- Fan, T., Yu, X., Shen, B., and Sun, L. (2017). “Peptide Self-Assembled Nanostructures for Drug Delivery Applications.” *J. Nanomater.*, 2017, 1–16.
- Fenimore, P. W., Frauenfelder, H., McMahon, B. H., and Young, R. D. (2004). “Bulk-solvent and hydration-shell fluctuations, similar to and fluctuations in glasses, control protein motions and functions.” *Proc. Natl. Acad. Sci.*, 101(40), 14408–14413.

-
- Ferreira, L. A., Macedo, E. A., and Pinho, S. P. (2009). "The effect of ammonium sulfate on the solubility of amino acids in water at (298.15 and 323.15)K." *J. Chem. Thermodyn.*, 41(2), 193–196.
- Fichman, G., and Gazit, E. (2014). "Self-assembly of short peptides to form hydrogels: Design of building blocks, physical properties and technological applications." *Acta Biomater.*, 10(4), 1671–1682.
- Fillaux, F., and Baron, M. H. (1981). "Vibrational spectra and dynamics of conformation and hydrogen bonding of n-methylacetamide. I. Conformational dynamics of the CH₃CONHCH₃ molecule and NH out of plane band splitting." *Chem. Phys.*, 62(3), 275–285.
- Fogarty, J. C., Aktulga, H. M., Grama, A. Y., Duin, A. C. T. van, and Pandit, S. A. (2010). "A reactive molecular dynamics simulation of the silica-water interface." *J. Chem. Phys.*, 132(17), 174704.
- Frank, H. S., and Evans, M. W. (1945). "Free Volume and Entropy in Condensed Systems III. Entropy in Binary Liquid Mixtures; Partial Molal Entropy in Dilute Solutions; Structure and Thermodynamics in Aqueous Electrolytes." *J. Chem. Phys.*, 13(11), 507–532.
- Frank, H. S., and Franks, F. (1968). "Structural Approach to the Solvent Power of Water for Hydrocarbons; Urea as a Structure Breaker." *J. Chem. Phys.*, 48(10), 4746–4757.
- Friedman, R. (2011). "Ions and the Protein Surface Revisited: Extensive Molecular Dynamics Simulations and Analysis of Protein Structures in Alkali-Chloride Solutions." *J. Phys. Chem. B*, 115(29), 9213–9223.
- Friedman, R., Nachliel, E., and Gutman, M. (2005). "Molecular Dynamics of a Protein Surface: Ion-Residues Interactions." *Biophys. J.*, 89(2), 768–781.
- Fu, I. W., Markegard, C. B., Chu, B. K., and Nguyen, H. D. (2013). "The Role of Electrostatics and Temperature on Morphological Transitions of Hydrogel Nanostructures Self-Assembled by Peptide Amphiphiles Via Molecular Dynamics Simulations." *Adv. Healthc. Mater.*, 2(10), 1388–1400.
- Ganguly, P., Mukherji, D., Junghans, C., and Vegt, N. F. A. van der. (2012). "Kirkwood–Buff Coarse-Grained Force Fields for Aqueous Solutions." *J. Chem. Theory Comput.*, 8(5), 1802–1807.
-

-
- Ganguly, P., and Vegt, N. F. A. van der. (2013). “Convergence of Sampling Kirkwood–Buff Integrals of Aqueous Solutions with Molecular Dynamics Simulations.” *J. Chem. Theory Comput.*, 9(3), 1347–1355.
- Ganguly, P., Vegt, N. F. A. van der, and Shea, J.-E. (2016). “Hydrophobic Association in Mixed Urea–TMAO Solutions.” *J. Phys. Chem. Lett.*, 7(15), 3052–3059.
- Gao, X., Fang, J., and Wang, H. (2016). “Sampling the isothermal-isobaric ensemble by Langevin dynamics.” *J. Chem. Phys.*, 144(12), 124113.
- Gazit, E. (2007). “Self-assembled peptide nanostructures: the design of molecular building blocks and their technological utilization.” *Chem. Soc. Rev.*, 36(8), 1263.
- Ghadiri, M. R., Granja, J. R., Milligan, R. A., McRee, D. E., and Khazanovich, N. (1993). “Self-assembling organic nanotubes based on a cyclic peptide architecture.” *Nature*, 366(6453), 324–327.
- Ghosh, A., Haverick, M., Stump, K., Yang, X., Tweedle, M. F., and Goldberger, J. E. (2012). “Fine-Tuning the pH Trigger of Self-Assembly.” *J. Am. Chem. Soc.*, 134(8), 3647–3650.
- Ghosh, T., Kalra, A., and Garde, S. (2005). “On the Salt-Induced Stabilization of Pair and Many-body Hydrophobic Interactions.” *J. Phys. Chem. B*, 109(1), 642–651.
- Goldberger, J. E., Berns, E. J., Bitton, R., Newcomb, C. J., and Stupp, S. I. (2011). “Electrostatic Control of Bioactivity.” *Angew. Chem. Int. Ed.*, 50(28), 6292–6295.
- Granata, V., Palladino, P., Tizzano, B., Negro, A., Berisio, R., and Zagari, A. (2006). “The effect of the osmolyte trimethylamine N-oxide on the stability of the prion protein at low pH.” *Biopolymers*, 82(3), 234–240.
- Greber, K. E., Dawgul, M., Kamysz, W., and Sawicki, W. (2017). “Cationic Net Charge and Counter Ion Type as Antimicrobial Activity Determinant Factors of Short Lipopeptides.” *Front. Microbiol.*, 8.
- Greenberg, A., Breneman, C. M., and Liebman, J. F. (2000). *The Amide Linkage: Structural Significance in Chemistry, Biochemistry, and Materials Science*.
- Grossfield, A. (2005). “Dependence of ion hydration on the sign of the ion’s charge.” *J. Chem. Phys.*, 122(2), 024506.
- Grossfield, A., Ren, P., and Ponder, J. W. (2003). “Ion Solvation Thermodynamics from Simulation with a Polarizable Force Field.” *J. Am. Chem. Soc.*, 125(50), 15671–15682.
-

-
- Guàrdia, E., Laria, D., and Martí, J. (2006a). “Hydrogen Bond Structure and Dynamics in Aqueous Electrolytes at Ambient and Supercritical Conditions.” *J. Phys. Chem. B*, 110(12), 6332–6338.
- Guàrdia, E., Laria, D., and Martí, J. (2006b). “Hydrogen Bond Structure and Dynamics in Aqueous Electrolytes at Ambient and Supercritical Conditions.” *J. Phys. Chem. B*, 110(12), 6332–6338.
- Guàrdia, E., Martí, J., Padró, J. A., Saiz, L., and Komolkin, A. V. (2002). “Dynamics in hydrogen bonded liquids: water and alcohols.” *J. Mol. Liq.*, 96–97, 3–17.
- Hagler, A. T., Huler, E., and Lifson, S. (1974). “Energy functions for peptides and proteins. I. Derivation of a consistent force field including the hydrogen bond from amide crystals.” *J. Am. Chem. Soc.*, 96(17), 5319–5327.
- Halle, B. (2004). “Protein hydration dynamics in solution: a critical survey.” *Philos. Trans. R. Soc. Lond. B. Biol. Sci.*, 359(1448), 1207–1224.
- Hamley, I. W. (2011). “Self-assembly of amphiphilic peptides.” *Soft Matter*, 7(9), 4122.
- Han, S., Cao, S., Wang, Y., Wang, J., Xia, D., Xu, H., Zhao, X., and Lu, J. R. (2011). “Self-Assembly of Short Peptide Amphiphiles: The Cooperative Effect of Hydrophobic Interaction and Hydrogen Bonding.” *Chem. - Eur. J.*, 17(46), 13095–13102.
- Hanasaki, I., and Nakatani, A. (2006). “Hydrogen bond dynamics and microscopic structure of confined water inside carbon nanotubes.” *J. Chem. Phys.*, 124(17), 174714.
- Hartgerink, J. D., Beniash, E., and Stupp, S. I. (2001). “Self-Assembly and Mineralization of Peptide-Amphiphile Nanofibers.” *Science*, 294(5547), 1684–1688.
- Hartgerink, J. D., Beniash, E., and Stupp, S. I. (2002). “Peptide-amphiphile nanofibers: A versatile scaffold for the preparation of self-assembling materials.” *Proc. Natl. Acad. Sci.*, 99(8), 5133–5138.
- Hassan, S. A. (2005). “Amino Acid Side Chain Interactions in the Presence of Salts.” *J. Phys. Chem. B*, 109(46), 21989–21996.
- Held, C., Cameretti, L. F., and Sadowski, G. (2011). “Measuring and Modeling Activity Coefficients in Aqueous Amino-Acid Solutions.” *Ind. Eng. Chem. Res.*, 50(1), 131–141.
- Hess, B., Bekker, H., Berendsen, H. J. C., and Fraaije, J. G. E. M. (1997). “LINCS: A linear constraint solver for molecular simulations.” *J. Comput. Chem.*, 18(12), 1463–1472.
-

-
- Heyda, J., Hrobárik, T., and Jungwirth, P. (2009). “Ion-Specific Interactions between Halides and Basic Amino Acids in Water.” *J. Phys. Chem. A*, 113(10), 1969–1975.
- Hofmeister, F. (1888a). “About the science of the effects of salts: About the water withdrawing effect of the salts.” *Arch Exp Pathol Pharmacol*, 24, 247–260.
- Hofmeister, F. (1888b). “Zur lehre von der wirkung der salze.” *Arch. Für Exp. Pathol. Pharmacol.*, 25(1), 1–30.
- Hoover, W. G. (1985). “Canonical dynamics: Equilibrium phase-space distributions.” *Phys. Rev. A*, 31(3), 1695–1697.
- Hosseinkhani, H., Hong, P.-D., and Yu, D.-S. (2013). “Self-Assembled Proteins and Peptides for Regenerative Medicine.” *Chem. Rev.*, 113(7), 4837–4861.
- Hribar, B., Southall, N. T., Vlachy, V., and Dill, K. A. (2002). “How Ions Affect the Structure of Water.” *J. Am. Chem. Soc.*, 124(41), 12302–12311.
- Hu, C. Y., Lynch, G. C., Kokubo, H., and Pettitt, B. M. (2009). “Trimethylamine N-oxide influence on the backbone of proteins: An oligoglycine model.” *Proteins Struct. Funct. Bioinforma.*, NA-NA.
- Hua, L., Zhou, R., Thirumalai, D., and Berne, B. J. (2008). “Urea denaturation by stronger dispersion interactions with proteins than water implies a 2-stage unfolding.” *Proc. Natl. Acad. Sci.*, 105(44), 16928–16933.
- Huang, R., Wang, Y., Qi, W., Su, R., and He, Z. (2014). “Temperature-induced reversible self-assembly of diphenylalanine peptide and the structural transition from organogel to crystalline nanowires.” *Nanoscale Res. Lett.*, 9(1), 653.
- Humphrey, W., Dalke, A., and Schulten, K. (1996). “VMD: visual molecular dynamics.” *J. Mol. Graph.*, 14(1), 33–38.
- Hunger, J., Tielrooij, K.-J., Buchner, R., Bonn, M., and Bakker, H. J. (2012). “Complex Formation in Aqueous Trimethylamine-N-oxide (TMAO) Solutions.” *J. Phys. Chem. B*, 116(16), 4783–4795.
- Hyde, A. M., Zultanski, S. L., Waldman, J. H., Zhong, Y.-L., Shevlin, M., and Peng, F. (2017). “General Principles and Strategies for Salting-Out Informed by the Hofmeister Series.” *Org. Process Res. Dev.*, 21(9), 1355–1370.
- Infante, M. R., Pérez, L., Pinazo, A., Clapés, P., Morán, M. C., Angelet, M., García, M. T., and Vinardell, M. P. (2004). “Amino acid-based surfactants.” *Comptes Rendus Chim.*, 7(6–7), 583–592.
-

-
- Jensen, F. (1992). "Structure and stability of complexes of glycine and glycine methyl analogs with H⁺, Li⁺, and Na⁺." *J. Am. Chem. Soc.*, 114(24), 9533–9537.
- Jensen, J. H., and Gordon, M. S. (1995). "On the Number of Water Molecules Necessary To Stabilize the Glycine Zwitterion." *J. Am. Chem. Soc.*, 117(31), 8159–8170.
- Jensen, K. P., and Jorgensen, W. L. (2006). "Halide, Ammonium, and Alkali Metal Ion Parameters for Modeling Aqueous Solutions." *J. Chem. Theory Comput.*, 2(6), 1499–1509.
- Jin, Q., Zhang, L., and Liu, M. (2013). "Solvent-Polarity-Tuned Morphology and Inversion of Supramolecular Chirality in a Self-Assembled Pyridylpyrazole-Linked Glutamide Derivative: Nanofibers, Nanotwists, Nanotubes, and Microtubes." *Chem. - Eur. J.*, 19(28), 9234–9241.
- Johnson, M. E., Malardier-Jugroot, C., and Head-Gordon, T. (2010). "Effects of co-solvents on peptide hydration water structure and dynamics." *Phys Chem Chem Phys*, 12(2), 393–405.
- Jönsson, M., Skepö, M., and Linse, P. (2006). "Monte Carlo Simulations of the Hydrophobic Effect in Aqueous Electrolyte Solutions." *J. Phys. Chem. B*, 110(17), 8782–8788.
- Jönsson, P. G., and Kvick, Å. ;. (1972). "Precision neutron diffraction structure determination of protein and nucleic acid components. III. The crystal and molecular structure of the amino acid α -glycine." *Acta Crystallogr. B*, 28, 1827–1833.
- Jorgensen, W. L., and Madura, J. D. (1983). "Quantum and statistical mechanical studies of liquids. 25. Solvation and conformation of methanol in water." *J. Am. Chem. Soc.*, 105(6), 1407–1413.
- Jorgensen, W. L., Maxwell, D. S., and Tirado-Rives, J. (1996). "Development and Testing of the OPLS All-Atom Force Field on Conformational Energetics and Properties of Organic Liquids." *J. Am. Chem. Soc.*, 118(45), 11225–11236.
- Jorgensen, W. L., and Tirado-Rives, J. (1988). "The OPLS [optimized potentials for liquid simulations] potential functions for proteins, energy minimizations for crystals of cyclic peptides and crambin." *J. Am. Chem. Soc.*, 110(6), 1657–1666.
- Kalra, A., Tugcu, N., Cramer, S. M., and Garde, S. (2001). "Salting-In and Salting-Out of Hydrophobic Solutes in Aqueous Salt Solutions." *J. Phys. Chem. B*, 105(27), 6380–6386.
-

- Kamali-Ardakani, M., Modarress, H., Taghikhani, V., and Khoshkbarchi, M. K. (2001). "Activity coefficients of glycine in aqueous electrolyte solutions: experimental data for (H₂O+ KCl + glycine) at T= 298.15 K and (H₂O + NaCl + glycine) at T= 308.15 K." *J. Chem. Thermodyn.*, 33(7), 821–836.
- Kang, Y. K. (2000). "Which Functional Form Is Appropriate for Hydrogen Bond of Amides?" *J. Phys. Chem. B*, 104(34), 8321–8326.
- Kar, K., and Kishore, N. (2007). "Enhancement of thermal stability and inhibition of protein aggregation by osmolytic effect of hydroxyproline." *Biopolymers*, 87(5–6), 339–351.
- Kast, K. M., Brickmann, J., Kast, S. M., and Berry, R. S. (2003). "Binary Phases of Aliphatic N-Oxides and Water: Force Field Development and Molecular Dynamics Simulation." *J. Phys. Chem. A*, 107(27), 5342–5351.
- Kayal, A., and Chandra, A. (2015). "Exploring the structure and dynamics of nano-confined water molecules using molecular dynamics simulations." *Mol. Simul.*, 41(5–6), 463–470.
- Keshri, S., and Tembe, B. L. (2017). "Thermodynamics of association of water soluble fullerene derivatives [C₆₀(OH)_n, n = 0, 2, 4, 8 and 12] in aqueous media." *J. Chem. Sci.*, 129(9), 1327–1340.
- Khan, S. H., Arnott, J. A., and Kumar, R. (2011). "Naturally Occurring Osmolyte, Trehalose Induces Functional Conformation in an Intrinsically Disordered Activation Domain of Glucocorticoid Receptor." *PLoS ONE*, (A. Mitraki, ed.), 6(5), e19689.
- Khandogin, J., Chen, J., and Brooks, C. L. (2006). "Exploring atomistic details of pH-dependent peptide folding." *Proc. Natl. Acad. Sci.*, 103(49), 18546–18550.
- Khoe, U., Yang, Y., and Zhang, S. (2009). "Self-Assembly of Nanodonut Structure from a Cone-Shaped Designer Lipid-like Peptide Surfactant." *Langmuir*, 25(7), 4111–4114.
- Kiley, P., Zhao, X., Vaughn, M., Baldo, M. A., Bruce, B. D., and Zhang, S. (2005). "Self-Assembling Peptide Detergents Stabilize Isolated Photosystem I on a Dry Surface for an Extended Time." *PLoS Biol.*, (G. Petsko, ed.), 3(7), e230.
- Kim, J., Han, T. H., Kim, Y.-I., Park, J. S., Choi, J., Churchill, D. G., Kim, S. O., and Ihee, H. (2010). "Role of Water in Directing Diphenylalanine Assembly into Nanotubes and Nanowires." *Adv. Mater.*, 22(5), 583–587.

-
- Klauda, J. B., Venable, R. M., Freites, J. A., O'Connor, J. W., Tobias, D. J., Mondragon-Ramirez, C., Vorobyov, I., MacKerell, A. D., and Pastor, R. W. (2010). "Update of the CHARMM All-Atom Additive Force Field for Lipids: Validation on Six Lipid Types." *J. Phys. Chem. B*, 114(23), 7830–7843.
- Kleinjung, J., and Fraternali, F. (2012). "Urea–Water Solvation Forces on Prion Structures." *J. Chem. Theory Comput.*, 8(10), 3977–3984.
- Kohn, W. D., Kay, C. M., and Hodges, R. S. (1997). "Salt effects on protein stability: two-stranded α -helical coiled-coils containing inter- or intrahelical ion pairs." *J. Mol. Biol.*, 267(4), 1039–1052.
- Koutsopoulos, S., Kaiser, L., Eriksson, H. M., and Zhang, S. (2012). "Designer peptidesurfactants stabilize diverse functional membrane proteins." *Chem Soc Rev*, 41(5), 1721–1728.
- Kumar, N., and Kishore, N. (2014). "Protein stabilization and counteraction of denaturing effect of urea by glycine betaine." *Biophys. Chem.*, 189, 16–24.
- Kumar, P. P., Kalinichev, A. G., and Kirkpatrick, R. J. (2009). "Hydrogen-Bonding Structure and Dynamics of Aqueous Carbonate Species from Car–Parrinello Molecular Dynamics Simulations." *J. Phys. Chem. B*, 113(3), 794–802.
- Kuntz, I. D., and Kauzmann, W. (1974). "Hydration of Proteins and Polypeptides." *Adv. Protein Chem.*, Elsevier, 239–345.
- Kusalik, P. G., and Svishchev, I. M. (1994). "The Spatial Structure in Liquid Water." *Science*, 265(5176), 1219–1221.
- Laage, D., Stirnemann, G., and Hynes, J. T. (2009). "Why Water Reorientation Slows without Iceberg Formation around Hydrophobic Solutes." *J. Phys. Chem. B*, 113(8), 2428–2435.
- Langley, C. H., and Allinger, N. L. (2003). "Molecular Mechanics (MM4) and ab Initio Study of Amide–Amide and Amide–Water Dimers." *J. Phys. Chem. A*, 107(26), 5208–5216.
- Larini, L., and Shea, J.-E. (2013). "Double Resolution Model for Studying TMAO/Water Effective Interactions." *J. Phys. Chem. B*, 117(42), 13268–13277.
- Lee, J., Cheng, X., Swails, J. M., Yeom, M. S., Eastman, P. K., Lemkul, J. A., Wei, S., Buckner, J., Jeong, J. C., Qi, Y., Jo, S., Pande, V. S., Case, D. A., Brooks, C. L., MacKerell, A. D., Klauda, J. B., and Im, W. (2016). "CHARMM-GUI Input Generator for NAMD, GROMACS, AMBER, OpenMM, and CHARMM/OpenMM Simulations

- Using the CHARMM36 Additive Force Field.” *J. Chem. Theory Comput.*, 12(1), 405–413.
- Lee, K. K., Fitch, C. A., Lecomte, J. T. J., and García-Moreno E. B. (2002). “Electrostatic Effects in Highly Charged Proteins: Salt Sensitivity of pKa Values of Histidines in Staphylococcal Nuclease.” *Biochemistry*, 41(17), 5656–5667.
- Lee, S., Shek, Y. L., and Chalikian, T. V. (2010). “Urea interactions with protein groups: A volumetric study.” *Biopolymers*, 93(10), 866–879.
- Lee, Trinh, Yoo, Shin, Lee, Kim, Hwang, Lim, and Ryou. (2019). “Self-Assembling Peptides and Their Application in the Treatment of Diseases.” *Int. J. Mol. Sci.*, 20(23), 5850.
- Lei, Y., Li, H., Pan, H., and Han, S. (2003). “Structures and Hydrogen Bonding Analysis of N,N-Dimethylformamide and N,N-Dimethylformamide–Water Mixtures by Molecular Dynamics Simulations.” *J. Phys. Chem. A*, 107(10), 1574–1583.
- Leung, K., and Rempe, S. B. (2005). “Ab initio molecular dynamics study of glycine intramolecular proton transfer in water.” *J. Chem. Phys.*, 122(18), 184506.
- Li, W., Qin, M., Tie, Z., and Wang, W. (2011). “Effects of solvents on the intrinsic propensity of peptide backbone conformations.” *Phys. Rev. E*, 84(4), 041933.
- Liao, Y.-T., Manson, A. C., DeLyser, M. R., Noid, W. G., and Cremer, P. S. (2017). “Trimethylamine N-oxide stabilizes proteins via a distinct mechanism compared with betaine and glycine.” *Proc. Natl. Acad. Sci.*, 114(10), 2479–2484.
- Lii, J.-H., and Allinger, N. L. (1998). “Directional hydrogen bonding in the MM3 force field: II.” *J. Comput. Chem.*, 19(9), 1001–1016.
- Lim, W. K., Rösgen, J., and Englander, S. W. (2009). “Urea, but not guanidinium, destabilizes proteins by forming hydrogen bonds to the peptide group.” *Proc. Natl. Acad. Sci.*, 106(8), 2595–2600.
- Lin, T.-Y., and Timasheff, S. N. (1994). “Why do some organisms use a urea-methylamine mixture as osmolyte? Thermodynamic compensation of urea and trimethylamine N-oxide interactions with protein.” *Biochemistry*, 33(42), 12695–12701.
- Liu, C., Jin, Q., Lv, K., Zhang, L., and Liu, M. (2014). “Water tuned the helical nanostructures and supramolecular chirality in organogels.” *Chem. Commun.*, 50(28), 3702.

-
- Liu, Y., and Bolen, D. W. (1995). "The Peptide Backbone Plays a Dominant Role in Protein Stabilization by Naturally Occurring Osmolytes." *Biochemistry*, 34(39), 12884–12891.
- Loo, Y., Zhang, S., and Hauser, C. A. E. (2012). "From short peptides to nanofibers to macromolecular assemblies in biomedicine." *Biotechnol. Adv.*, 30(3), 593–603.
- Lu, J., Wang, X.-J., Yang, X., and Ching, C.-B. (2006). "Solubilities of Glycine and Its Oligopeptides in Aqueous Solutions." *J. Chem. Eng. Data*, 51(5), 1593–1596.
- Ludwig, R. (2000). "Cooperative hydrogen bonding in amides and peptides." *J. Mol. Liq.*, 84(1), 65–75.
- Luzar, A., and Chandler, D. (1996). "Hydrogen-bond kinetics in liquid water." *Nature*, 379(6560), 55–57.
- Ma, J., Pazos, I. M., and Gai, F. (2014). "Microscopic insights into the protein-stabilizing effect of trimethylamine N-oxide (TMAO)." *Proc. Natl. Acad. Sci.*, 111(23), 8476–8481.
- Makovitzki, A., Baram, J., and Shai, Y. (2008). "Antimicrobial Lipopolypeptides Composed of Palmitoyl Di- and Tricationic Peptides: In Vitro and in Vivo Activities, Self-Assembly to Nanostructures, and a Plausible Mode of Action." *Biochemistry*, 47(40), 10630–10636.
- Maltzahn, G. von, Vauthey, S., Santoso, S., and Zhang, S. (2003). "Positively Charged Surfactant-like Peptides Self-assemble into Nanostructures." *Langmuir*, 19(10), 4332–4337.
- Mancera, R. L. (1999). "Influence of Salt on Hydrophobic Effects: A Molecular Dynamics Study Using the Modified Hydration-Shell Hydrogen-Bond Model." *J. Phys. Chem. B*, 103(18), 3774–3777.
- Mao, Y., Liu, K., Meng, L., Chen, L., Chen, L., and Yi, T. (2014). "Solvent induced helical aggregation in the self-assembly of cholesterol tailed platinum complexes." *Soft Matter*, 10(38), 7615–7622.
- Mason, P. E., Heyda, J., Fischer, H. E., and Jungwirth, P. (2010). "Specific Interactions of Ammonium Functionalities in Amino Acids with Aqueous Fluoride and Iodide." *J. Phys. Chem. B*, 114(43), 13853–13860.
- McCammion, J. A., and Karplus, M. (1977). "Internal motions of antibody molecules." *Nature*, 268(5622), 765–766.
-

- Meersman, F., Bowron, D., Soper, A. K., and Koch, M. H. J. (2009). “Counteraction of Urea by Trimethylamine N-Oxide Is Due to Direct Interaction.” *Biophys. J.*, 97(9), 2559–2566.
- Miller, W. G., Brant, D. A., and Flory, P. J. (1967). “Random coil configurations of polypeptide copolymers.” *J. Mol. Biol.*, 23(1), 67–80.
- Mirkin, N. G., and Krimm, S. (1991). “Ab initio vibrational analysis of hydrogen-bonded trans- and cis-N-methylacetamide.” *J. Am. Chem. Soc.*, 113(26), 9742–9747.
- Mishima, O., and Stanley, H. E. (1998). “Decompression-induced melting of ice IV and the liquid–liquid transition in water.” *Nature*, 392(6672), 164–168.
- Moeser, B., and Horinek, D. (2014). “Unified Description of Urea Denaturation: Backbone and Side Chains Contribute Equally in the Transfer Model.” *J. Phys. Chem. B*, 118(1), 107–114.
- Mondal, J., Stirnemann, G., and Berne, B. J. (2013). “When Does Trimethylamine-N-Oxide Fold a Polymer Chain and Urea Unfold It?” *J. Phys. Chem. B*, 117(29), 8723–8732.
- Morán, M. C., Pinazo, A., Pérez, L., Clapés, P., Angelet, M., García, M. T., Vinardell, M. P., and Infante, M. R. (2004). “‘Green’ amino acid-based surfactants.” *Green Chem.*, 6(5), 233–240.
- Mountain, R. D., and Thirumalai, D. (2003). “Molecular Dynamics Simulations of End-to-End Contact Formation in Hydrocarbon Chains in Water and Aqueous Urea Solution.” *J. Am. Chem. Soc.*, 125(7), 1950–1957.
- Musah, R. A., Jensen, G. M., Rosenfeld, R. J., McRee, D. E., Goodin, D. B., and Bunte, S. W. (1997). “Variation in Strength of an Unconventional C–H to O Hydrogen Bond in an Engineered Protein Cavity.” *J. Am. Chem. Soc.*, 119(38), 9083–9084.
- Nagai, A., Nagai, Y., Qu, H., and Zhang, S. (2007). “Dynamic Behaviors of Lipid-Like Self-Assembling Peptide A6D and A6K Nanotubes.” *J. Nanosci. Nanotechnol.*, 7(7), 2246–2252.
- Näslund, L.-Å., Edwards, D. C., Wernet, P., Bergmann, U., Ogasawara, H., Pettersson, L. G. M., Myneni, S., and Nilsson, A. (2005). “X-ray Absorption Spectroscopy Study of the Hydrogen Bond Network in the Bulk Water of Aqueous Solutions.” *J. Phys. Chem. A*, 109(27), 5995–6002.
- Newman, K. E. (1994). “Kirkwood–Buff solution theory: derivation and applications.” *Chem Soc Rev*, 23(1), 31–40.

-
- Niece, K. L., Hartgerink, J. D., Donners, J. J. J. M., and Stupp, S. I. (2003). “Self-Assembly Combining Two Bioactive Peptide-Amphiphile Molecules into Nanofibers by Electrostatic Attraction.” *J. Am. Chem. Soc.*, 125(24), 7146–7147.
- Nilsson, A., and Pettersson, L. G. M. (2015). “The structural origin of anomalous properties of liquid water.” *Nat. Commun.*, 6(1), 8998.
- Nosé, S. (1984). “A molecular dynamics method for simulations in the canonical ensemble.” *Mol. Phys.*, 52(2), 255–268.
- Nosé, S., and Klein, M. L. (1983). “Constant pressure molecular dynamics for molecular systems.” *Mol. Phys.*, 50(5), 1055–1076.
- Nucci, N. V., Pometun, M. S., and Wand, A. J. (2011). “Site-resolved measurement of water-protein interactions by solution NMR.” *Nat. Struct. Mol. Biol.*, 18(2), 245–249.
- Obst, S., and Bradaczek, H. (1996). “Molecular Dynamics Study of the Structure and Dynamics of the Hydration Shell of Alkaline and Alkaline-Earth Metal Cations.” *J. Phys. Chem.*, 100(39), 15677–15687.
- Pal, S. K., Peon, J., and Zewail, A. H. (2002). “Biological water at the protein surface: Dynamical solvation probed directly with femtosecond resolution.” *Proc. Natl. Acad. Sci.*, 99(4), 1763–1768.
- Panuszko, A., Bruździak, P., Zielkiewicz, J., Wyrzykowski, D., and Stangret, J. (2009). “Effects of Urea and Trimethylamine N-oxide on the Properties of Water and the Secondary Structure of Hen Egg White Lysozyme.” *J. Phys. Chem. B*, 113(44), 14797–14809.
- Panuszko, A., Gojło, E., Zielkiewicz, J., Śmiechowski, M., Krakowiak, J., and Stangret, J. (2008). “Hydration of Simple Amides. FTIR Spectra of HDO and Theoretical Studies.” *J. Phys. Chem. B*, 112(8), 2483–2493.
- Park, S., and Fayer, M. D. (2007). “Hydrogen bond dynamics in aqueous NaBr solutions.” *Proc. Natl. Acad. Sci.*, 104(43), 16731–16738.
- Parrinello, M., and Rahman, A. (1980). “Crystal Structure and Pair Potentials: A Molecular-Dynamics Study.” *Phys. Rev. Lett.*, 45(14), 1196–1199.
- Parrinello, M., and Rahman, A. (1981). “Polymorphic transitions in single crystals: A new molecular dynamics method.” *J. Appl. Phys.*, 52(12), 7182–7190.
- Pashuck, E. T., Cui, H., and Stupp, S. I. (2010). “Tuning Supramolecular Rigidity of Peptide Fibers through Molecular Structure.” *J. Am. Chem. Soc.*, 132(17), 6041–6046.
-

- Patra, M., and Karttunen, M. (2004). "Systematic comparison of force fields for microscopic simulations of NaCl in aqueous solutions: Diffusion, free energy of hydration, and structural properties." *J. Comput. Chem.*, 25(5), 678–689.
- Pattanayak, S. K., Chettiyankandy, P., and Chowdhuri, S. (2014). "Effects of co-solutes on the hydrogen bonding structure and dynamics in aqueous N-methylacetamide solution: a molecular dynamics simulations study." *Mol. Phys.*, 112(22), 2906–2919.
- Pattanayak, S. K., and Chowdhuri, S. (2011). "Effect of Water on Solvation Structure and Dynamics of Ions in the Peptide Bond Environment: Importance of Hydrogen Bonding and Dynamics of the Solvents." *J. Phys. Chem. B*, 115(45), 13241–13252.
- Pattanayak, S. K., and Chowdhuri, S. (2014). "Effects of methanol on the hydrogen bonding structure and dynamics in aqueous N-methylacetamide solution." *J. Mol. Liq.*, 194, 141–148.
- Paul, S., Abi, T. G., and Taraphder, S. (2014). "Structure and dynamics of water inside endohedrally functionalized carbon nanotubes." *J. Chem. Phys.*, 140(18), 184511.
- Paul, S., and Patey, G. N. (2007a). "Structure and Interaction in Aqueous Urea–Trimethylamine-N-oxide Solutions." *J. Am. Chem. Soc.*, 129(14), 4476–4482.
- Paul, S., and Patey, G. N. (2007b). "The Influence of Urea and Trimethylamine-N-oxide on Hydrophobic Interactions." *J. Phys. Chem. B*, 111(28), 7932–7933.
- Paul, S., and Patey, G. N. (2008). "Hydrophobic Interactions in Urea–Trimethylamine N-oxide Solutions." *J. Phys. Chem. B*, 112(35), 11106–11111.
- Pettitt, B. M., and Rossky, P. J. (1986). "Alkali halides in water: Ion–solvent correlations and ion–ion potentials of mean force at infinite dilution." *J. Chem. Phys.*, 84(10), 5836–5844.
- Pierce, V., Kang, M., Aburi, M., Weerasinghe, S., and Smith, P. E. (2008). "Recent Applications of Kirkwood–Buff Theory to Biological Systems." *Cell Biochem. Biophys.*, 50(1), 1–22.
- Pinazo, A., Manresa, M. A., Marques, A. M., Bustelo, M., Espuny, M. J., and Pérez, L. (2016). "Amino acid–based surfactants: New antimicrobial agents." *Adv. Colloid Interface Sci.*, 228, 17–39.
- Pinheiro, L., and Faustino, C. (2017). "Amino Acid-Based Surfactants for Biomedical Applications." *Appl. Charact. Surfactants*, R. Najjar, ed., InTech.

-
- Pizzitutti, F., Marchi, M., Sterpone, F., and Rossky, P. J. (2007). "How Protein Surfaces Induce Anomalous Dynamics of Hydration Water." *J. Phys. Chem. B*, 111(26), 7584–7590.
- Poole, P. H., Sciortino, F., Essmann, U., and Stanley, H. E. (1992). "Phase behaviour of metastable water." *Nature*, 360(6402), 324–328.
- Pradhan, A. A., and Vera, J. H. (1998). "Effect of acids and bases on the solubility of amino acids." *Fluid Phase Equilibria*, 152(1), 121–132.
- Prasad, S., and Chakravarty, C. (2017). "Solvation of LiCl in model liquids with high to low hydrogen bond strengths." *J. Chem. Phys.*, 146(18), 184503.
- Priyadarshini, A., Biswas, A., Chakraborty, D., and Mallik, B. S. (2020). "Structural and Thermophysical Anomalies of Liquid Water: A Tale of Molecules in the Instantaneous Low- and High-Density Regions." *J. Phys. Chem. B*, 124(6), 1071–1081.
- Qiu, F., Chen, Y., Tang, C., and Zhao, X. (2018). "Amphiphilic peptides as novel nanomaterials: design, self-assembly and application." *Int. J. Nanomedicine*, Volume 13, 5003–5022.
- Rad-Malekshahi, M., Lempsink, L., Amidi, M., Hennink, W. E., and Mastrobattista, E. (2016). "Biomedical Applications of Self-Assembling Peptides." *Bioconjug. Chem.*, 27(1), 3–18.
- Radom, L., and Riggs, N. (1982). "Ab initio studies on amides: acetamide, N-methylformamide and N-methylacetamide." *Aust. J. Chem.*, 35(6), 1071.
- Rahman, A. (1964). "Correlations in the Motion of Atoms in Liquid Argon." *Phys. Rev.*, 136(2A), A405–A411.
- Rajamani, S., Ghosh, T., and Garde, S. (2004). "Size dependent ion hydration, its asymmetry, and convergence to macroscopic behavior." *J. Chem. Phys.*, 120(9), 4457–4466.
- Rana, M., and Chandra, A. (2007). "Filled and empty states of carbon nanotubes in water: Dependence on nanotube diameter, wall thickness and dispersion interactions." *J. Chem. Sci.*, 119(5), 367–376.
- Rana, M. K., and Chandra, A. (2015). "Wetting behavior of nonpolar nanotubes in simple dipolar liquids for varying nanotube diameter and solute-solvent interactions." *J. Chem. Phys.*, 142(3), 034704.
-

-
- Randall, Merle., and Failey, C. Fairbanks. (1927). "The Activity Coefficient of Non-Electrolytes in Aqueous Salt Solutions from Solubility Measurements. The Salting-out Order of the Ions." *Chem. Rev.*, 4(3), 285–290.
- Rapaport, D. C. (1983). "Hydrogen bonds in water: Network organization and lifetimes." *Mol. Phys.*, 50(5), 1151–1162.
- Rashin, A. A., and Honig, B. (1985). "Reevaluation of the Born model of ion hydration." *J. Phys. Chem.*, 89(26), 5588–5593.
- Reches, M., and Gazit, E. (2003). "Casting Metal Nanowires Within Discrete Self-Assembled Peptide Nanotubes." *Science*, 300(5619), 625–627.
- Rezus, Y. L. A., and Bakker, H. J. (2007). "Observation of Immobilized Water Molecules around Hydrophobic Groups." *Phys. Rev. Lett.*, 99(14).
- Rezus, Y. L. A., and Bakker, H. J. (2009). "Destabilization of the Hydrogen-Bond Structure of Water by the Osmolyte Trimethylamine N-Oxide." *J. Phys. Chem. B*, 113(13), 4038–4044.
- Robinson, D. R., and Jencks, W. P. (1965). "The Effect of Concentrated Salt Solutions on the Activity Coefficient of Acetyltetraglycine Ethyl Ester." *J. Am. Chem. Soc.*, 87(11), 2470–2479.
- Rodríguez, H., Soto, A., Arce, A., and Khoshkbarchi, M. K. (2003). "Apparent Molar Volume, Isentropic Compressibility, Refractive Index, and Viscosity of DL-Alanine in Aqueous NaCl Solutions." *J. Solut. Chem.*, 32(1), 53–63.
- Rodríguez-Ropero, F., Röttscher, P., and Vegt, N. F. A. van der. (2016). "Comparison of Different TMAO Force Fields and Their Impact on the Folding Equilibrium of a Hydrophobic Polymer." *J. Phys. Chem. B*, 120(34), 8757–8767.
- Romero, C. M., and Oviedo, C. D. (2013). "Effect of Temperature on The Solubility of α -Amino Acids and α,ω -Amino Acids in Water." *J. Solut. Chem.*, 42(6), 1355–1362.
- Sahle, C. J., Schroer, M. A., Juurinen, I., and Niskanen, J. (2016). "Influence of TMAO and urea on the structure of water studied by inelastic X-ray scattering." *Phys. Chem. Chem. Phys.*, 18(24), 16518–16526.
- Samanta, N., Das Mahanta, D., and Kumar Mitra, R. (2014). "Does Urea Alter the Collective Hydrogen-Bond Dynamics in Water? A Dielectric Relaxation Study in the Terahertz-Frequency Region." *Chem. - Asian J.*, 9(12), 3457–3463.
-

-
- Sánchez, L., Mitjans, M., Infante, M. R., García, M. T., Manresa, M. A., and Vinardell, M. P. (2007). “The biological properties of lysine-derived surfactants.” *Amino Acids*, 32(1), 133–136.
- Sanchez, L., Mitjans, M., Infante, M. R., and Vinardell, M. P. (2006). “Potential irritation of lysine derivative surfactants by hemolysis and HaCaT cell viability.” *Toxicol. Lett.*, 161(1), 53–60.
- Santoso, S., Hwang, W., Hartman, H., and Zhang, S. (2002). “Self-assembly of Surfactant-like Peptides with Variable Glycine Tails to Form Nanotubes and Nanovesicles.” *Nano Lett.*, 2(7), 687–691.
- Schneck, E., Horinek, D., and Netz, R. R. (2013). “Insight into the Molecular Mechanisms of Protein Stabilizing Osmolytes from Global Force-Field Variations.” *J. Phys. Chem. B*, 117(28), 8310–8321.
- Schoenborn, B. (1995). “Hydration in protein crystallography.” *Prog. Biophys. Mol. Biol.*, 64(2–3), 105–119.
- Schröder, C., Rudas, T., Boresch, S., and Steinhauser, O. (2006). “Simulation studies of the protein-water interface. I. Properties at the molecular resolution.” *J. Chem. Phys.*, 124(23), 234907.
- Senes, A., Gerstein, M., and Engelman, D. M. (2000). “Statistical analysis of amino acid patterns in transmembrane helices: the GxxxG motif occurs frequently and in association with β -branched residues at neighboring positions.” *J. Mol. Biol.*, 296(3), 921–936.
- Senn, H. M., and Thiel, W. (2007a). “QM/MM Methods for Biological Systems.” *At. Approaches Mod. Biol.*, Topics in Current Chemistry, M. Reiher, ed., Springer Berlin Heidelberg, 173–290.
- Senn, H. M., and Thiel, W. (2007b). “QM/MM studies of enzymes.” *Curr. Opin. Chem. Biol.*, 11(2), 182–187.
- Seroski, D. T., and Hudalla, G. A. (2018). “Self-Assembled Peptide and Protein Nanofibers for Biomedical Applications.” *Biomed. Appl. Funct. Nanomater.*, Elsevier, 569–598.
- Shao, Q., He, Y., and Jiang, S. (2011). “Molecular Dynamics Simulation Study of Ion Interactions with Zwitterions.” *J. Phys. Chem. B*, 115(25), 8358–8363.
- Shinto, H., Morisada, S., and Higashitani, K. (2005). “Potentials of Mean Force for Hydrophilic–Hydrophobic Solute Pairs in Water.” *J. Chem. Eng. Jpn.*, 38(7), 465–477.
-

-
- Silva, R. M. P. da, Zwaag, D. van der, Albertazzi, L., Lee, S. S., Meijer, E. W., and Stupp, S. I. (2016). “Super-resolution microscopy reveals structural diversity in molecular exchange among peptide amphiphile nanofibres.” *Nat. Commun.*, 7(1), 11561.
- Singh, L. R., Dar, T. A., Rahman, S., Jamal, S., and Ahmad, F. (2009). “Glycine betaine may have opposite effects on protein stability at high and low pH values.” *Biochim. Biophys. Acta BBA - Proteins Proteomics*, 1794(6), 929–935.
- Sitkoff, D., and Case, D. A. (1997). “Density Functional Calculations of Proton Chemical Shifts in Model Peptides.” *J. Am. Chem. Soc.*, 119(50), 12262–12273.
- Smith, D. E., and Haymet, A. D. J. (1993). “Free energy, entropy, and internal energy of hydrophobic interactions: Computer simulations.” *J. Chem. Phys.*, 98(8), 6445–6454.
- Souza, N. R. de, Kolesnikov, A. I., Burnham, C. J., and Loong, C.-K. (2006). “Structure and dynamics of water confined in single-wall carbon nanotubes.” *J. Phys. Condens. Matter*, 18(36), S2321–S2334.
- Stillinger, F. H. (1975). “Theory and Molecular Models for Water.” *Adv. Chem. Phys.*, 31(1).
- Stillinger, F. H. (1980). “Water Revisited.” *Science*, 209(4455), 451–457.
- Stillinger, F. H., and Rahman, A. (1974a). “Improved simulation of liquid water by molecular dynamics.” *J. Chem. Phys.*, 60(4), 1545–1557.
- Stillinger, F. H., and Rahman, A. (1974b). “Molecular dynamics study of liquid water under high compression.” *J. Chem. Phys.*, 61(12), 4973–4980.
- Stirnemann, G., Hynes, J. T., and Laage, D. (2010). “Water Hydrogen Bond Dynamics in Aqueous Solutions of Amphiphiles.” *J. Phys. Chem. B*, 114(8), 3052–3059.
- Stumpe, M. C., and Grubmüller, H. (2007). “Interaction of Urea with Amino Acids: Implications for Urea-Induced Protein Denaturation.” *J. Am. Chem. Soc.*, 129(51), 16126–16131.
- Stumpe, M. C., and Grubmüller, H. (2008). “Polar or Apolar-The Role of Polarity for Urea-Induced Protein Denaturation.” *PLoS Comput. Biol.*, (V. S. Pande, ed.), 4(11), e1000221.
- Su, Z., Mahmoudinobar, F., and Dias, C. L. (2017). “Effects of Trimethylamine- N -oxide on the Conformation of Peptides and its Implications for Proteins.” *Phys. Rev. Lett.*, 119(10), 108102.
-

-
- Su, Z., Ravindhran, G., and Dias, C. L. (2018). “Effects of Trimethylamine-N-oxide (TMAO) on Hydrophobic and Charged Interactions.” *J. Phys. Chem. B*, 122(21), 5557–5566.
- Sun, J., Bousquet, D., Forbert, H., and Marx, D. (2010). “Glycine in aqueous solution: solvation shells, interfacial water, and vibrational spectroscopy from ab initio molecular dynamics.” *J. Chem. Phys.*, 133(11), 114508.
- Svergun, D. I., Richard, S., Koch, M. H. J., Sayers, Z., Kuprin, S., and Zaccai, G. (1998). “Protein hydration in solution: Experimental observation by x-ray and neutron scattering.” *Proc. Natl. Acad. Sci.*, 95(5), 2267–2272.
- Tanford, Charles. (1962). “Contribution of Hydrophobic Interactions to the Stability of the Globular Conformation of Proteins.” *J. Am. Chem. Soc.*, 84(22), 4240–4247.
- Tarek, M., and Tobias, D. J. (2000). “The Dynamics of Protein Hydration Water: A Quantitative Comparison of Molecular Dynamics Simulations and Neutron-scattering Experiments.” *Biophys. J.*, 79(6), 3244–3257.
- Teeter, M. M. (1991). “Water-Protein Interactions: Theory and Experiment.” *Annu. Rev. Biophys. Biophys. Chem.*, 20(1), 577–600.
- Teng, X., and Ichiye, T. (2019). “Dynamical Effects of Trimethylamine-N-Oxide on Aqueous Solutions of Urea.” *J. Phys. Chem. B*, 123(5), 1108–1115.
- Thomas, A. S., and Elcock, A. H. (2007). “Molecular Dynamics Simulations of Hydrophobic Associations in Aqueous Salt Solutions Indicate a Connection between Water Hydrogen Bonding and the Hofmeister Effect.” *J. Am. Chem. Soc.*, 129(48), 14887–14898.
- Timasheff, S. N., and Fasman, G. D. (1969). *Structure and stability of biological macromolecules*. Dekker New York.
- Toksoz, S., Mammadov, R., Tekinay, A. B., and Guler, M. O. (2011). “Electrostatic effects on nanofiber formation of self-assembling peptide amphiphiles.” *J. Colloid Interface Sci.*, 356(1), 131–137.
- Tomé, L. I. N., Domínguez-Pérez, M., Cláudio, A. F. M., Freire, M. G., Marrucho, I. M., Cabeza, O., and Coutinho, J. A. P. (2009). “On the Interactions between Amino Acids and Ionic Liquids in Aqueous Media.” *J. Phys. Chem. B*, 113(42), 13971–13979.
- Tomé, L. I. N., Jorge, M., Gomes, J. R. B., and Coutinho, J. A. P. (2010). “Toward an Understanding of the Aqueous Solubility of Amino Acids in the Presence of Salts: A Molecular Dynamics Simulation Study.” *J. Phys. Chem. B*, 114(49), 16450–16459.
-

-
- Tomé, L. I. N., Jorge, M., Gomes, J. R. B., and Coutinho, J. A. P. (2012). “Molecular Dynamics Simulation Studies of the Interactions between Ionic Liquids and Amino Acids in Aqueous Solution.” *J. Phys. Chem. B*, 116(6), 1831–1842.
- Tomé, L. I. N., Sousa, C. S. R., Gomes, J. R. B., Ferreira, O., Coutinho, J. A. P., and Pinho, S. P. (2015). “Understanding the cation specific effects on the aqueous solubility of amino acids: from mono to polyvalent cations.” *RSC Adv.*, 5(20), 15024–15034.
- Tortonda, F. R., Pascual-Ahuir, J. L., Silla, E., and Tuñón, I. (1996). “Why is glycine a zwitterion in aqueous solution? A theoretical study of solvent stabilising factors.” *Chem. Phys. Lett.*, 260(1–2), 21–26.
- Tuñón, I., Silla, E., and Ruiz-López, M. F. (2000). “On the tautomerization process of glycine in aqueous solution.” *Chem. Phys. Lett.*, 321(5–6), 433–437.
- Ulijn, R. V., and Smith, A. M. (2008). “Designing peptide based nanomaterials.” *Chem. Soc. Rev.*, 37(4), 664.
- Underwood, T. R., and Greenwell, H. C. (2018). “The Water-Alkane Interface at Various NaCl Salt Concentrations: A Molecular Dynamics Study of the Readily Available Force Fields.” *Sci. Rep.*, 8(1), 352.
- Urbic, T. (2014). “Ions increase strength of hydrogen bond in water.” *Chem. Phys. Lett.*, 610–611, 159–162.
- Vagenende, V., Yap, M. G. S., and Trout, B. L. (2009). “Mechanisms of Protein Stabilization and Prevention of Protein Aggregation by Glycerol.” *Biochemistry*, 48(46), 11084–11096.
- Van Der Spoel, D., Lindahl, E., Hess, B., Groenhof, G., Mark, A. E., and Berendsen, H. J. C. (2005). “GROMACS: Fast, flexible, and free.” *J. Comput. Chem.*, 26(16), 1701–1718.
- Vauthey, S., Santoso, S., Gong, H., Watson, N., and Zhang, S. (2002). “Molecular self-assembly of surfactant-like peptides to form nanotubes and nanovesicles.” *Proc. Natl. Acad. Sci.*, 99(8), 5355–5360.
- Vedamuthu, M., Singh, S., and Robinson, G. W. (1994). “Properties of Liquid Water: Origin of the Density Anomalies.” *J. Phys. Chem.*, 98(9), 2222–2230.
- Verlet, L. (1967). “Computer ‘Experiments’ on Classical Fluids. I. Thermodynamical Properties of Lennard-Jones Molecules.” *Phys. Rev.*, 159(1), 98–103.
- Verlet, L. (1968). “Computer ‘Experiments’ on Classical Fluids. II. Equilibrium Correlation Functions.” *Phys. Rev.*, 165(1), 201–214.
-

-
- Vidossich, P., and Magistrato, A. (2014). “QM/MM Molecular Dynamics Studies of Metal Binding Proteins.” *Biomolecules*, 4(3), 616–645.
- Vives, M. A., Infante, M. R., Garcia, E., Selve, C., Maugras, M., and Vinardell, M. P. (1999). “Erythrocyte hemolysis and shape changes induced by new lysine-derivate surfactants.” *Chem. Biol. Interact.*, 118(1), 1–18.
- Vives, M. A., Macián, M., Seguer, J., Infante, M. R., and Vinardell, M. P. (1997). “Hemolytic Action of Anionic Surfactants of the Diacyl Lysine Type.” *Comp. Biochem. Physiol. C Pharmacol. Toxicol. Endocrinol.*, 118(1), 71–74.
- Von Hippel, P. H. (1969). “Effects of neutral salts on the structure and conformational stability of macromolecules in solution.” *Struct. Stab. Biol. Macromol.*
- Wallqvist, A., and Åstrand, P. -O. (1995). “Liquid densities and structural properties of molecular models of water.” *J. Chem. Phys.*, 102(16), 6559–6565.
- Wang, A., and Bolen, D. W. (1996). “Effect of proline on lactate dehydrogenase activity: testing the generality and scope of the compatibility paradigm.” *Biophys. J.*, 71(4), 2117–2122.
- Wang, A., and Bolen, D. W. (1997). “A Naturally Occurring Protective System in Urea-Rich Cells: Mechanism of Osmolyte Protection of Proteins against Urea Denaturation.” *Biochemistry*, 36(30), 9101–9108.
- Wang, J., Han, S., Meng, G., Xu, H., Xia, D., Zhao, X., Schweins, R., and Lu, J. R. (2009). “Dynamic self-assembly of surfactant-like peptides A6K and A9K.” *Soft Matter*, 5(20), 3870.
- Wei, H., Fan, Y., and Gao, Y. Q. (2010). “Effects of Urea, Tetramethyl Urea, and Trimethylamine N-Oxide on Aqueous Solution Structure and Solvation of Protein Backbones: A Molecular Dynamics Simulation Study.” *J. Phys. Chem. B*, 114(1), 557–568.
- Wiradharma, N., Tong, Y. W., and Yang, Y.-Y. (2009). “Self-assembled oligopeptide nanostructures for co-delivery of drug and gene with synergistic therapeutic effect.” *Biomaterials*, 30(17), 3100–3109.
- Withers, P. C., Morrison, G., and Guppy, M. (1994). “Buoyancy Role of Urea and TMAO in an Elasmobranch Fish, the Port Jackson Shark, *Heterodontus portusjacksoni*.” *Physiol. Zool.*, 67(3), 693–705.
-

- Wong, C. H. S., Siu, F. M., Ma, N. L., and Tsang, C. W. (2002). "A theoretical study of potassium cation-glycine (K⁺-Gly) interactions." *J. Mol. Struct. THEOCHEM*, 588(1–3), 9–16.
- Woutersen, S. (1997). "Femtosecond Mid-IR Pump-Probe Spectroscopy of Liquid Water: Evidence for a Two-Component Structure." *Science*, 278(5338), 658–660.
- Xu, H., and Berne, B. J. (2001). "Hydrogen-Bond Kinetics in the Solvation Shell of a Polypeptide." *J. Phys. Chem. B*, 105(48), 11929–11932.
- Xu, H., Wang, J., Han, S., Wang, J., Yu, D., Zhang, H., Xia, D., Zhao, X., Waigh, T. A., and Lu, J. R. (2009). "Hydrophobic-Region-Induced Transitions in Self-Assembled Peptide Nanostructures." *Langmuir*, 25(7), 4115–4123.
- Xu, H., Wang, Y., Ge, X., Han, S., Wang, S., Zhou, P., Shan, H., Zhao, X., and Lu, J. R. (2010a). "Twisted Nanotubes Formed from Ultrashort Amphiphilic Peptide I3K and Their Templating for the Fabrication of Silica Nanotubes." *Chem. Mater.*, 22(18), 5165–5173.
- Xu, X.-D., Jin, Y., Liu, Y., Zhang, X.-Z., and Zhuo, R.-X. (2010b). "Self-assembly behavior of peptide amphiphiles (PAs) with different length of hydrophobic alkyl tails." *Colloids Surf. B Biointerfaces*, 81(1), 329–335.
- Yan, X., Zhu, P., and Li, J. (2010). "Self-assembly and application of diphenylalanine-based nanostructures." *Chem. Soc. Rev.*, 39(6), 1877.
- Yancey, P., Clark, M., Hand, S., Bowlus, R., and Somero, G. (1982a). "Living with water stress: evolution of osmolyte systems." *Science*, 217(4566), 1214–1222.
- Yancey, P., Clark, M., Hand, S., Bowlus, R., and Somero, G. (1982b). "Living with water stress: evolution of osmolyte systems." *Science*, 217(4566), 1214–1222.
- Yancey, P. H. (2001). "Water Stress, Osmolytes and Proteins." *Am. Zool.*, 41(4), 699–709.
- Yancey, P. H. (2005). "Organic osmolytes as compatible, metabolic and counteracting cytoprotectants in high osmolarity and other stresses." *J. Exp. Biol.*, 208(15), 2819–2830.
- Yancey, P. H., and Somero, G. N. (1979). "Counteraction of urea destabilization of protein structure by methylamine osmoregulatory compounds of elasmobranch fishes." *Biochem. J.*, 183(2), 317–323.

-
- Yancey, P. H., and Somero, G. N. (1980). "Methylamine osmoregulatory solutes of elasmobranch fishes counteract urea inhibition of enzymes." *J. Exp. Zool.*, 212(2), 205–213.
- Yang, C.-H., Brown, J. N., and Kopple, K. D. (2009). "Peptide-Water Association in Peptide Crystals." *Int. J. Pept. Protein Res.*, 14(1), 12–20.
- Yang, H., Tyagi, P., Kadam, R. S., Holden, C. A., and Kompella, U. B. (2012). "Hybrid Dendrimer Hydrogel/PLGA Nanoparticle Platform Sustains Drug Delivery for One Week and Antiglaucoma Effects for Four Days Following One-Time Topical Administration." *ACS Nano*, 6(9), 7595–7606.
- Zabicky, J. (1970). *The chemistry of amides*. London; New York: Interscience.
- Zaldivar, G., Vemulapalli, S., Udumula, V., Conda-Sheridan, M., and Tagliazucchi, M. (2019). "Self-Assembled Nanostructures of Peptide Amphiphiles: Charge Regulation by Size Regulation." *J. Phys. Chem. C*, 123(28), 17606–17615.
- Zaslhoff, M. (2002). "Antimicrobial peptides of multicellular organisms." *Nature*, 415(6870), 389–395.
- Zelenovskiy, P. S., Domingues, E. M., Slabov, V., Kopyl, S., Ugolkov, V. L., Figueiredo, F. M. L., and Kholkin, A. L. (2020). "Efficient Water Self-Diffusion in Diphenylalanine Peptide Nanotubes." *ACS Appl. Mater. Interfaces*, 12(24), 27485–27492.
- Zhang, L., Wang, L., Kao, Y.-T., Qiu, W., Yang, Y., Okobiah, O., and Zhong, D. (2007). "Mapping hydration dynamics around a protein surface." *Proc. Natl. Acad. Sci.*, 104(47), 18461–18466.
- Zhang, S. (2003). "Fabrication of novel biomaterials through molecular self-assembly." *Nat. Biotechnol.*, 21(10), 1171–1178.
- Zhang, S. (2012). "Lipid-like Self-Assembling Peptides." *Acc. Chem. Res.*, 45(12), 2142–2150.
- Zhang, S., Holmes, T., Lockshin, C., and Rich, A. (1993). "Spontaneous assembly of a self-complementary oligopeptide to form a stable macroscopic membrane." *Proc. Natl. Acad. Sci.*, 90(8), 3334–3338.
- Zhao, X. (2009). "Design of self-assembling surfactant-like peptides and their applications." *Curr. Opin. Colloid Interface Sci.*, 14(5), 340–348.

- Zhao, X., Pan, F., Xu, H., Yaseen, M., Shan, H., Hauser, C. A. E., Zhang, S., and Lu, J. R. (2010). "Molecular self-assembly and applications of designer peptide amphiphiles." *Chem. Soc. Rev.*, 39(9), 3480.
- Zhao, X., and Zhang, S. (2006). "Molecular designer self-assembling peptides." *Chem. Soc. Rev.*, 35(11), 1105.
- Zhao, Y., Wang, J., Deng, L., Zhou, P., Wang, S., Wang, Y., Xu, H., and Lu, J. R. (2013). "Tuning the Self-Assembly of Short Peptides via Sequence Variations." *Langmuir*, 29(44), 13457–13464.
- Zhu, P., Yan, X., Su, Y., Yang, Y., and Li, J. (2010). "Solvent-Induced Structural Transition of Self-Assembled Dipeptide: From Organogels to Microcrystals." *Chem. - Eur. J.*, 16(10), 3176–3183.
- Zou, Q., Bennion, B. J., Daggett, V., and Murphy, K. P. (2002). "The Molecular Mechanism of Stabilization of Proteins by TMAO and Its Ability to Counteract the Effects of Urea." *J. Am. Chem. Soc.*, 124(7), 1192–1202.



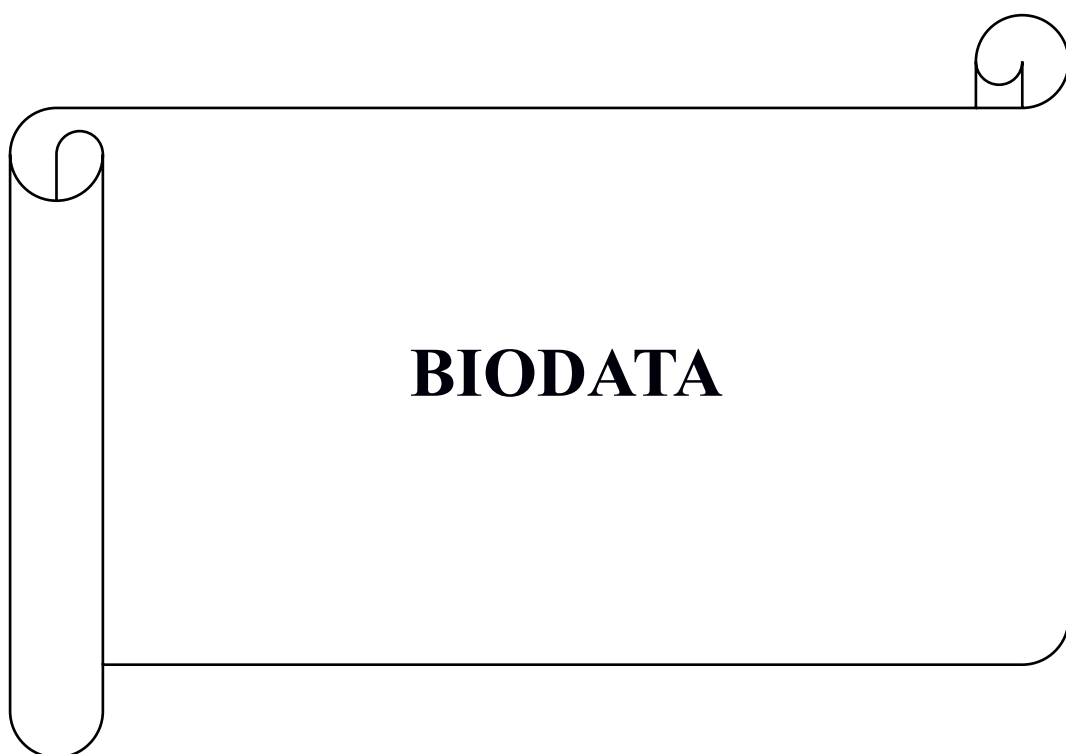
**LIST OF PUBLICATIONS
AND CONFERENCES**

LIST OF PUBLICATIONS

1. **Dilip, H. N.**, and Chakraborty, D. (2019). “Hydrophilicity of the hydrophobic group: Effect of cosolvents and ions.” *Journal of Molecular Liquids*, 280, 389–398.
2. **Dilip, H. N.**, and Chakraborty, D. (2020). “Effect of cosolvents in the preferential binding affinity of water in aqueous solutions of amino acids and amides” *Journal of Molecular Liquids*, 300, 112375.
3. **Dilip, H. N.**, and Chakraborty, D. (2021). “Structural and dynamical properties of water in surfactant-like peptide-based nanotubes: Effect of pore size, tube length and charge” *Journal of Molecular Liquids*, 323, 115033.

LIST OF CONFERENCES

1. Presented a poster on “Molecular Dynamics Simulations of Amino acids in co-solvents” International Conference on Emerging Trends in Chemical Sciences-2017, 14-16 September, 2017, Department of Chemistry, Manipal Institute of Technology, Manipal.
2. Attended Conference on Recent Advances in Dynamics at the Interface of Chemistry and Biology (DICB – 2019), 18-20 February, 2019, Department of Chemistry, IISc, Bengaluru.



Name: Dilip.H.N

Registration Number: 165025CY16F01

Email id: diliphn18@gmail.com

Academic Details:

Course	Name of the Institution/University	Year
Ph.D (Biophysical and Computational Chemistry)	NITK Surathkal, Mangaluru	2016-2020
Master of Science (Chemistry)	NITK Surathkal, Mangaluru	2014-2016
Bachelor of Science (CBZ)	MES Degree College, Bengaluru	2011-2014

Place: NITK Surathkal

Date: 11/08/2021